Book of Abstracts

Photosynthesis and Hydrogen Energy Research for Sustainability

GAETA, ITALY

5/17/26 - 5/20/26

Edited by

Suleyman Allakhverdiev, Barry Bruce,
Daniele Candelaresi and Giuseppe Spazzafumo

ORGANISED BY

EnTraT
Energy Transition Team

WITH THE PATRONAGE OF

Università degli Studi di Cassino e del Lazio Meridionale
Sol per Noctem

UNDER THE AUSPICES OF

iahe

ISPR

SPONSORS

AMBHER

ECOSEARCH
ENVIRONMENTAL MONITORING AND SAMPLING

LOMBARD & MAROZZINI
Instruments for our environment

PHOTON SYSTEMS INSTRUMENTS

WALZ
Photosynthesis Instruments

FuelSME

PHYTOAB

Agrisera
Antibodies

PUBLISHING PARTNERS

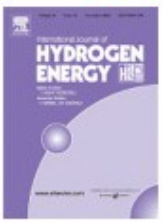

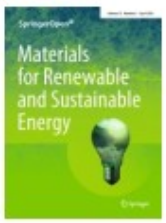

energies
an Open Access Journal by MDPI

PHRS Series Organising Committee

Suleyman I. Allakhverdiev (Russia)
Julian J. Eaton-Rye (New Zealand)
Bruce D. Barry (USA)
Tatsuya Tomo (Japan)

PHRS13 Organising committee

Salvatore P. Cicconardi (Honorary Chair)
Giuseppe Spazzafumo (Chair)
Daniele Candelaresi (Co-chair)
Romolo Di Bernardo
Gabriella Di Cicco
Vito Gallicchio
Antonio Gloria
Giorgio Grossi
Alessandra Perna
Matteo Tomasso

AMBHER H_2

www.ambherproject.eu

AMBHER project aims to develop short and long term hydrogen storage solutions:

- **Novel nanoporous Metal Organic Frameworks with high surface area included in a storage vessel.**
- **Advanced catalysts and membrane integrated into a Catalytic Membrane Reactor for green ammonia synthesis.**

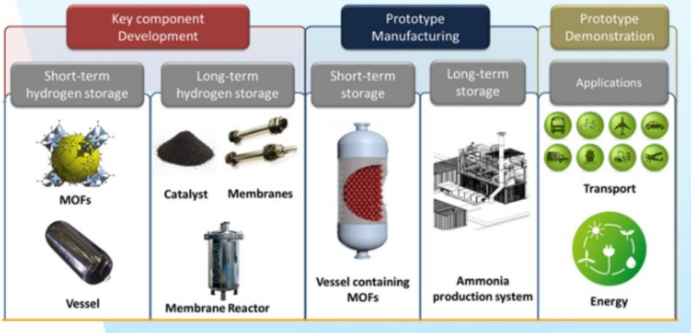

Project number: 101058565

Starting date: June 1st 2022

Duration: 48 months

EU funding: 4,915,870 Euro

Funded by the European Union

Funded by the European Union. Views and opinions expressed are however those of the author(s) only and do not necessarily reflect those of the European Union or European Health and Digital Executive Agency. Neither the European Union nor the granting authority can be held responsible for them

LOMBARD & MAROZZINI

Distributore WALZ per l'Italia

FuelSOME

Multifuel SOFC system

with Maritime Energy vectors

The FuelSOME project focuses on establishing the technological feasibility of a flexible, scalable, and multi-fuel capable energy generation system based on Solid Oxide Fuel Cells (SOFC) technology specially catered for long-distance maritime shipping.

Contents

Plenary lectures

R. Cogdell – How the modular construction of purple bacterial light harvesting complexes facilitates their ability to adapt to life in very different ecological niches

F. Barbir - Hydrogen role in energy future defined by new thermodynamic paradigm in energy value

W. Lubitz - Light-Induced Water Oxidation in Photosynthesis

I. Eroglu - Photobiological Hydrogen Production by Purple Nonsulfur Bacteria from Biomass

S.I. Allakhverdiev – Advanced Artificial Photosynthetic Systems for Efficient Hydrogen Generation

G. Torzillo, G. E. Lakatos, A. M. Silva Benavides, N. Jiménez-Conejo, E. Touloupakis, B. Cicchi, F. Balestra, G. Chini Zittelli, C. Faraloni – Opportunities and challenges in the photobiological hydrogen production with microalgae

G.E. Lakatos, B. Cicchi, F. Balestra, G. Chini Zittelli, G. Torzillo, C. Faraloni - Chemical oxygen absorber mediated direct photosynthetic hydrogen production by Synechocystis sp. PCC6803

F. Balestra, G. Torzillo, B. Cicchi, G. E. Lakatos, G. Chini Zittelli, C. Faraloni – Effect of light spectrum on growth, hydrogen production and biochemical composition of the cyanobacterium Synechocystis sp. PCC 6803

N. Jiménez Conejo, A. M. Silva Benavides, G. Torzillo - Hydrogen production by Synechocystis 6803 in seawater

R.M. Zampieri, I.C. Moia, and E. Touloupakis - Comparison of photofermentative hydrogen production in cylindrical photobioreactors

L. Gabrielyan, J. Manoyan, A. Petrosyan, A. Hambardzumyan, and L. Gabrielyan – Brewery spent grains as a potential substrate for growth and biohydrogen production by Rhodobacter sphaeroides and Parachlorella kessleri

B.D. Kossalbayev, A.K. Sadvakasova, and G.K. Kamshybayeva, D. Zaletova, M.O. Bauenova – Gas-phase optimization for long-term photobiological hydrogen production in heterocystous cyanobacteria

D.O. Dunikov, S.I. Allakhverdiev, D.V. Blinov, and A.M. Bozieva – Extraction of pure hydrogen from sources of natural origin

How the modular construction of purple bacterial light harvesting complexes facilitates their ability to adapt to life in very different ecological niches

Richard J. Cogdell
School of Molecular Biosciences, University of Glasgow, Glasgow G128QQ, UK
richard.cogdell@glasgow.ac.uk

In purple photosynthetic bacteria photosynthesis begins with the absorption of solar energy by the light harvesting system. Then rapidly and efficiently that excitation energy is transferred to the reaction centres where it is trapped. The light harvesting system usually consists of the peripheral LH2 complexes and the core RC-LH1 complexes. Both these antenna complexes are integral membrane proteins and are built by oligomerisation of pairs of alpha/beta apoproteins that bind, non-covalently, a small number of bacteriochlorophyll and carotenoid pigments. Their oligomerisation produces circular and elliptical holo-complexes. Recently, with the application of single particle cryo-EM there has been a flood of new structures of these LH complexes. Based on this new information it is now clear how this modular construction system can produce rings of different sizes and how incorporation of different alpha/beta dimers (modules) can allow holo-complexes with different absorption properties to be produced. It will be emphasised in this talk how the flexibility of this modular system facilitates the ability of these bacterial to control where their LH complexes absorb incoming solar energy, allowing them to optimise their light harvesting to match the available spectrum of the incident light in their particular niche and can respond to different light intensities.

Hydrogen role in energy future defined by new thermodynamic paradigm in energy value

Frano Barbir
University of Split, Croatia
fbarbir@fesb.hr

The present energy system is primarily based on combustion of fossil fuels. Useful energy is obtained through a series of energy conversion processes: chemical energy of fuels is converted to heat, heat to mechanical energy, and mechanical to electrical energy. There is an efficiency associated with each energy conversion process, resulting in degraded energy. The thermodynamic value of energy is measured to its ability to perform work, so called exergy. And it would be a thermodynamic sin to use electricity to generate heat for example. In a future energy system primarily based on renewable energy sources, electricity will be produced directly. However, because the renewable energy sources, primarily solar and wind, are intermittently available and with variable intensity there will be periods when the production would exceed the demand. This unusable energy in the form of electricity would have no value. Its value may be increased by converting it to something useful or something that can be stored. Electricity may be stored in chemical energy in batteries, but it also can be used to generate heat or to generate hydrogen (for example by water electrolysis). Both heat and hydrogen can be stored and used when needed. Storing electricity, or converting it to heat or hydrogen, degrades its value based on the current energy value paradigm, but it increases its usefulness. Therefore, a new paradigm in energy value is needed that will address its usefulness. A new measure of energy value i.e., its usefulness is here proposed called usergy. Unusable primary electricity from renewable energy has zero usergy, and its storage or conversion increases its usergy even if it is associated with energy conversion losses. Obviously, the overall efficiency of the future energy system should be maximized by increasing the use of both primary and secondary (stored) electricity. However, hydrogen will be needed in applications where the use of electricity is less practical or less economical, such as long-term, seasonal energy storage and then as a feedstock in industry (in production of ammonia and methanol), as a fuel in industry that requires high temperature heat (such as steel and cement), as fuel for transportation (where fast recharging or large energy storage is needed). In some cases hydrogen may also be used to produce synthetic fuels (so called e-fuels) and these fuels will be used in applications where they offer advantages over hydrogen. Hydrogen will have a role in the future energy system, but that will be a supporting role, so instead of Hydrogen Economy perhaps Hydricity economy, as suggested by prof. D.S. Scott, would be more appropriate.

Light-Induced Water Oxidation in Photosynthesis

W. Lubitz
Max Planck Institute for Chemical Energy Conversion, Mülheim/Ruhr, Germany
wolfgang.lubitz@cec.mpg.de

Understanding light-induced water oxidation in oxygenic photosynthesis is of great importance both for biology and (bio)technological applications. The process of water splitting and dioxygen release invented by early photosynthetic organisms led to the creation of our planet´s oxygen-rich atmosphere and the protective ozone layer in the stratosphere - both essential events for the development of higher life on earth. Photosynthesis stores the sun´s energy via CO_2 reduction in form of energy-rich organic compounds. It is the only basic source of food on earth, provides us with oxygen to breath, delivers many valuable biomaterials and it has generated all our fossil fuels.

Key to these chemical events is the catalytic water oxidation reaction. This difficult multi-electron/multi-step reaction takes place at a protein-bound Mn_4O_xCa cluster located in photosystem (PS) II whose structure has been determined by X-ray crystallography [1]. In the light-driven catalytic reaction the cluster passes through five intermediate redox states (S_n), in which the subscript indicates the number of stored oxidizing equivalents in the Mn cluster (n = 0-4) required to split two water molecules and release one O_2 (figure 1). A redox-active tyrosine residue (Y_Z) couples the fast light-induced single-electron charge separation to the slow catalytic four-electron water oxidation process in PSII. A detailed understanding of the intermediate steps requires information about the spatial *and* electronic structure of the Mn_4O_xCa complex. The latter is only available from spectroscopic studies.

Since all S-states are paramagnetic, electron paramagnetic resonance (EPR) is the spectroscopic method of choice to study the intermediates of the catalytic cycle. The S-states are trapped by light-flash/freeze-quench techniques and their electronic structure is studied by multifrequency EPR and advanced pulse EPR/NMR techniques (ENDOR, ESEEM, ELDOR-detected NMR) [2]. The experimental data are analyzed, interpreted and further exploited by quantum chemical calculations [3-4]. These results give information on the electronic structure (spin and oxidation states) of the four manganese ions, protonation/deprotonation events, the function of the Ca^{2+}, the effect of the amino acid surrounding as well as the binding, location, deprotonation and reaction dynamics of the two substrate water molecules in the cycle preceding O-O bond formation and the release of triplet dioxygen. Further information and leading references are found in [5-7]. Based on the experimental and theoretical data a robust model for the mechanism of biological water oxidation has been developed.

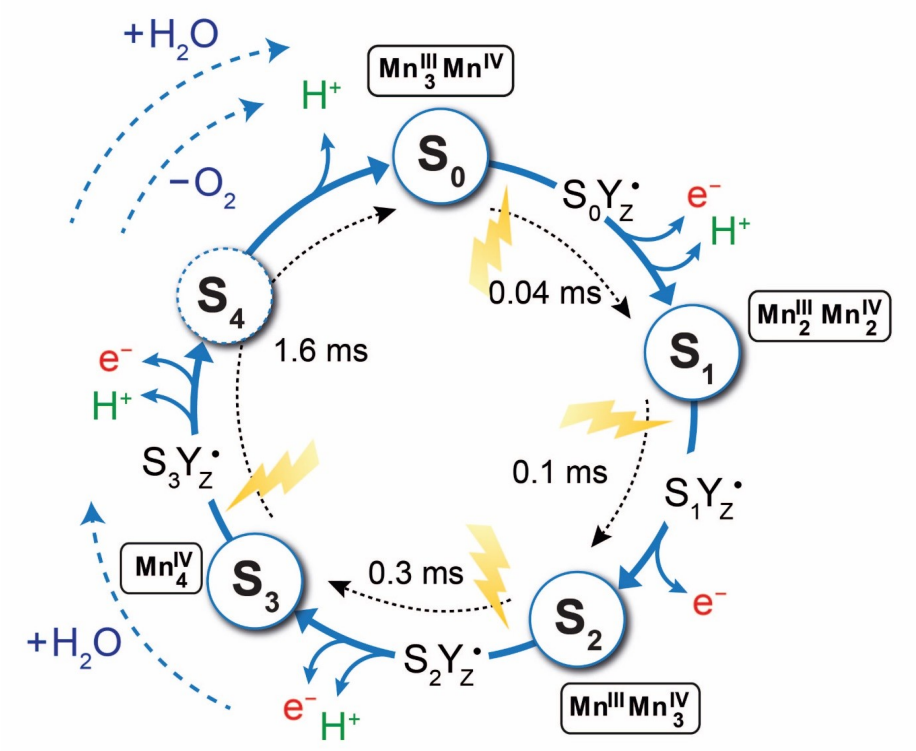

Figure 1: Water oxidation (Kok) cycle in PSII. The five basic S-states (S_0 to S_4), the light-induced one-electron oxidation steps (including the redox-active tyrosine Y_Z), and the reaction times are given (in ms). The oxidation states of the four Mn-ions for each S-state are shown, and the release of protons (H^+), the uptake of the 2 substrate water molecules (H_2O) and the loss of dioxygen (O_2) are indicated, for details see [5-7].

Acknowledgements
The work described in this contribution has been performed at the two Max Planck Institutes (Chemical Energy Conversion, CEC, and Coal Research, CR) in Mülheim/Ruhr, Germany. Continuous financial support of the Max Planck Society is gratefully acknowledged. Special thanks go to the group leaders Dimitrios Pantazis (Department Frank Neese, MPI CR) and to Johannes Messinger and Nicolas Cox (Department WL, CEC) and to all their coworkers who contributed to this work during the last two decades.

References

[1] Y. Umena et al. "Crystal structure of oxygen-evolving photosystem II at a resolution of 1.9 Å" Nature, 473, 2011, 55-60.
J. Kern et al. "Structures of the intermediates of Kok's photosynthetic water oxidation clock" Nature, 563, 2018, 421-425.
A. Bhowmick et al. "Structural evidence for intermediates during O2 formation in photosystem II" Nature, 617, 2023, 629-636.
H. Li et al. "Oxygen-evolving photosystem II structures during S1–S2–S3 transitions" Nature, 626, 2024, 670-677.

[2] N. Cox, A. Nalepa, M.E. Pandelia, W. Lubitz, A. Savitsky "Pulse double-resonance EPR techniques for the study of metallobiomolecules", Methods in Enzymology, 563, 2015, 211-249.

[3] D.A. Pantazis, M. Orio, T. Petrenko, S. Zein, E. Bill, W. Lubitz, J. Messinger, F. Neese "A new quantum chemical approach to the magnetic properties of oligonuclear transition-metal complexes: application to a model for the tetranuclear manganese cluster of photosystem II" Chem. Eur. J., 15, 2009, 5108-5123.

[4] V. Krewald, M. Retegan, N. Cox, J. Messinger, W. Lubitz, S. DeBeer, F. Neese, D.A. Pantazis "Metal oxidation states in biological water splitting" Chem. Sci., 6, 2015, 1676-1695.

[5] W. Lubitz, M. Chrysina, N. Cox "Water oxidation in photosystem II" Photosyn. Res.,142, 2019, 105-125.

[6] N. Cox, D.A. Pantazis, W. Lubitz "Current understanding of the mechanism of water oxidation in photosystem II and its relation to XFEL data" Ann. Rev. Biochem., 89, 2020, 795-820.

[7] W. Lubitz, D.A. Pantazis, N. Cox "Water oxidation in oxygenic photosynthesis studied by magnetic resonance techniques" FEBS Lett., 597, 2023, 6-29.

Photobiological Hydrogen Production by Purple Nonsulfur Bacteria from Biomass

I. Eroglu
[1] *Middle East Technical University Chemical Engineering Department, Ankara, Türkiye*
ieroglu@metu.edu.tr

Hydrogen is a critical energy vector in the future energy economy. Biohydrogen production is emerging as a promising option for sustainable, renewable energy. Biohydrogen production is among the most promising routes for future green hydrogen generation, offering an opportunity to utilize renewable feedstocks for sustainable hydrogen production. Biohydrogen is produced through light-driven processes that employ photosynthetic purple bacteria, microalgae, and cyanobacteria, or through light-independent processes utilizing dark fermentative bacteria. This presentation reviews the current state of biohydrogen production technologies, with a focus on metabolic processes and recent developments.

Two-step biohydrogen production, which involves dark fermentation in the first step and photofermentation in the second, is a highly efficient process that enables maximal substrate conversion to H2. During dark fermentation, biomass is converted to hydrogen, CO2, and organic acids by thermophilic or mesophilic fermentative bacteria. In photofermentation, the organic acids produced in dark fermentation are further converted to hydrogen by purple nonsulfur bacteria (PNSB). Biological hydrogen production can be enhanced through next-generation approaches, such as advanced bioreactors, nanoparticle incorporation, and integrated and hybrid systems, including combined dark and photofermentation, integration of dark fermentation with electrofermentation, and integration of inorganic nanoscale semiconductor materials with biological systems.

The METU Biological Hydrogen Production Research Team has been active for over three decades, advancing photofermentative hydrogen production from bench scale to pilot scale, with both indoor and outdoor applications. They also participated in designing a 2 MWe (50 kg/h) biological hydrogen production plant as part of an EU 6th Framework Integrated Project called "Non-thermal Pure Hydrogen Production from Biomass (HYVOLUTION)" [1].

Over the past decade, efforts have focused on improving hydrogen productivity and yield to reduce costs and land requirements by varying photobioreactor design, elucidating PNSB metabolism under light and dark conditions, and examining its responses to temperature stress, all of which are critical for outdoor applications. Studies continue on the immobilization of PNSB on promising novel supports.

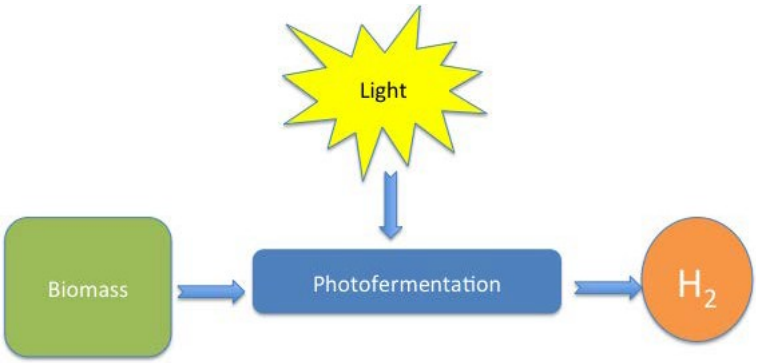

Figure 1: Photofermentation process

Two enzymes are especially critical for hydrogen production by photofermentation. Nitrogenase promotes hydrogen production, and the uptake hydrogenase consumes it. Though many substrates can be used for growth, only a portion is suitable for hydrogen production. The efficiency of a particular substrate depends on factors including the activity of the TCA cycle, the carbon-to-nitrogen ratio, the material's redox state, and its potential to be converted into valuable metabolites, such as polyhydroxybutyrate (PHB), carotenoids, Coenzyme Q10, etc. All these individual components of hydrogen production interact and are subject to strict regulatory controls. Practically all hydrogen production by PNSB (*R. sphareoides, R. capsulatus, Rd. rubrum, Rd. palustris*) species occurs under a photoheterotrophic metabolic mode [2]. Yet, results show that under certain conditions, alternative metabolic pathways (e.g., fermentation under light deficiency) are also possible and should be considered in photoreactor design.

The capability of *R. palustris* to produce hydrogen from sucrose was assessed using results from a metabolic model [3]. Their results indicated that acetic acid was the most effective and formic acid the least effective organic acid for hydrogen production. The flux distribution obtained showed that adding organic acids to sucrose increases H2 production. They compared their model results with experimental data [4]. The model-calculated efficiency was 56%, very close to the experimental efficiency of 53%.

One of the foremost challenges in biohydrogen production is low hydrogen productivity, a critical limitation. Despite the natural occurrence of microorganisms capable of biohydrogen production, their inherent efficiency is generally low. While productivity can be enhanced through genetic modifications or optimization of growth conditions, such improvements are difficult to achieve. Microorganism sensitivity is a significant issue, especially with hydrogenase enzymes, which are responsible for hydrogen production in dark fermentation. These enzymes are particularly sensitive to oxygen, which is present in the environment and inhibits activity and productivity. Scientists are actively seeking methods to either uncover O2-tolerant hydrogenases or protect the enzymes from oxygen.

Biohydrogen production from organic waste, particularly agricultural waste, has the potential to be economically and environmentally viable; there is also potential to utilize organic waste by-products [5]. However, the main challenge is securing suitable substrates year-round. Another significant challenge is developing efficient bioreactors for large-scale hydrogen production, which must address light penetration dynamics, mixing, and temperature control [6]. It remains difficult to set up experimental conditions with minimal energy input. When upscaling photobioreactors from the laboratory to industrial scale, issues related to optimal light distribution, biofilm growth, and engineering constraints may arise. Long-term stable operation is constrained by environmental factors, as photobiological hydrogen production must be conducted outdoors and relies on natural sunlight to be energy-efficient. Another significant challenge for large-scale, accessible hydrogen production is purifying hydrogen gas from culture media without resorting to energy-intensive methods.

The growing demand for hydrogen applications and the need for sustainable energy solutions are advancing rapidly. Notably, green hydrogen processes are poised to play a vital role in facilitating the transition to carbon-neutral bioenergy technologies. Beyond its natural decarbonization benefits as an energy source, hydrogen is increasingly favored as a fuel due to its zero-emission properties. Its gaseous and storable properties highlight its potential to become a leading bioenergy option in the future.

Acknowledgements
Prof. M. Yücel, Prof. U. Gündüz, Assoc. Prof. H. Koku, Prof. T. H. Ergüder-Bayramoğlu, and the other members of The METU Biological Hydrogen Production Research Team are acknowledged.

References

[1] P.A.M.Claassen et al., "Non-thermal production of pure hydrogen from biomass: HYVOLUTION", Journal of Cleaner Production, 18(1),2010, 4-8.
[2] H. Koku et al. "Aspects of the metabolism of hydrogen production by *Rhodobacter sphaeroides*", International Journal of Hydrogen Energy, 27(11), 2002,1315–1329.
[3] E.M. Doğan-Güner, H. Koku, "Analysis of the carbon metabolism of *Rhodopseudomonas palustris* for biohydrogen production". Biotech Studies, 31(1), 2022, 1-9.
[4] E. Sagir, et al. "Single-stage photofermentative biohydrogen production from beet molasses by different purple non-sulfur bacteria". Bioprocess Biosyst. Eng., 40(11), 2017,1589-1601.
[5] I. Eroglu et al. "Applications of Photofermentative Hydrogen Production", in "Microbial BioEnergy: Hydrogen Production, Editors: D. Zannoni, R. De Phillippis, Springer, Chapter 38, 2014, p.237-267. ISBN 978-94-017-8553-2
[6] D. D. Androga et al., "Dynamic modeling of temperature change in outdoor operated tubular photobioreactors", Bioprocess and Biosystems Engineering 40 (7), 2017,1017-1031.

Advanced Artificial Photosynthetic Systems for Efficient Hydrogen Generation

S. I. Allakhverdiev
K.A. Timiryazev Institute of Plant Physiology, Russian Academy of Sciences,
Botanicheskaya Street 35, Moscow 127276, Russia
suleyman.allakhverdiev@gmail.com

As the demand for clean energy increases, researchers are investigating methods to generate hydrogen harnessing sunlight. While natural photosynthesis demonstrates how plants capture light to produce fuel, replicating this process directly remains inefficient. Recent advancements involve integrating biological elements with engineered materials to enhance performance. This presentation explores the functioning of these interfaces, ranging from natural to artificial systems. We examine design strategies for connecting catalysts with light absorbers, key factors influencing charge transfer, and challenges such as durability and the use of cost-effective materials. Understanding these interfaces is essential for developing improved systems capable of producing hydrogen from sunlight efficiently.

Acknowledgements
This work was supported by the Russian Science Foundation (24-14-00033), and in particular (25-74-31001) and by the state contract of the Ministry of Science and Higher Education of the Russian Federation (theme No. 122050400128-1).

Opportunities and challenges in the photobiological hydrogen production with microalgae

G. Torzillo[1,2], G. E. Lakatos[1], A. M. Silva Benavides[2], N. Jiménez-Conejo[2], E. Touloupakis[3], B. Cicchi[1], F. Balestra[1], G. Chini Zittelli[1], C. Faraloni[1]

[1]Istituto per la Bioeconomia, CNR, Via Madonna del Piano, 10, 50019, Sesto F.no, Italy.
[2]Centro de Investigación en Ciencias del Mar y Limnología, Universidad de Costa Rica, San Pedro, San José 2060, Costa Rica.
[3]Istituto di Ricerca sugli Ecosistemi Terrestri, CNR, Via Madonna del Piano, 10, 50019, Sesto F.no, Italy.

giuseppe.torzillo@cnr.it

Hydrogen is currently mainly extracted from fossil fuels, resulting in a significant CO_2 emission which is considered the main responsible of global warming. Among the green options, photobiological hydrogen production by microalgae is one of the most environmentally friendly ways. Photobiological hydrogen production is based on two nanomachines, i.e., the photosystem II which splits H_2O in hydrogen and oxygen, and the enzyme hydrogenase which combines the protons and electrons to form H_2. The EU has gathered in his "Green Hydrogen portfolio" 9 projects called "Novel Routes to Green Hydrogen Production", launched in 2021 for the generation of green hydrogen, and extend for a period of up to 60 months. The total funding from the EIC (European Innovation Council) allocated for these projects is nearly 29 million. Among them *Photosynh2* was selected as a promising biological route to produce hydrogen based on the unicellular cyanobacterium *Synechocystis*. *Photosynh2* project is based on three fundamental pillars: (i) eliminate/reduce the sensibility of hydrogenase to oxygen; (ii) optimization of the electron transport to hydrogenase to reach a light conversion efficiency (LCE) close to the theoretical value, including the replacement of the Ni-Fe Hydrogenase with the Fe-Fe hydrogenase to increase the efficiency of the enzymatic process; (iii) the optimization of culture medium and an improved photobioreactor design for hydrogen production with *Synechocystis* outdoors**.** For the culture medium optimization, cultures of *Synechocystis* were grown in media prepared with seawater (SW) and with centrate in order to: 1) reduce/eliminate the dependence on fresh water and nutrients for the preparation of the culture medium thus improving the environmental sustainability and economy of the process.; 2) reduce the risk of contamination of the culture of *Synechocystis* with other competing microalgae and protozoa. Preparation of culture medium with SW in comparison to standard BG11 prepared with deionized water, caused a reduction in productivity by 25%, which, although significant, is still economically sustainable if we consider the increasing necessity, and thus cost, of fresh water for civil uses. An additional, not negligible, advantage of using SW was the protection of the *Synechosystis* cells by the grazing by the golden alga *Poterioochromonas malamensis* which can jeopardize the cultivation of *Synechocystis*. Therefore, the development of a *Synechocystis* strain fully resistant to SW salinity, that is, without incurring a reduction of productivity may be relevant to

further improve the economics of the process. Another important issue concerning the economic sustainability of photobiological hydrogen production with microalgae is represented by the still too low light conversion efficiency attained by cultures outdoors. According to [1] theoretical solar light conversion efficiency (light to H_2), *i.e*. the ratio between the hydrogen energy attained to solar light supplied, can reach as much as 13.5 %, which is higher than that for biomass as final product (about 10%). However, in outdoor cultures of microalgae the actual light conversion efficiency is still about a tenth of the theoretical value. Light saturation of photosynthesis is mostly responsible for this low efficiency. To address this issue, the performance of a vertical multiplate photobioreactor in which was possible to reduce the effect of light saturation of photosynthesis of *Synechocystis* outdoors was studied. The design was aimed to take advantage of the so called "*light dilution effect*", that is, a reduction of the incident light intensity on the surface of the bioreactor attained by increasing the illuminated surface of the reactor with respect of the ground area it occupied. The photobioreactor consisted of 20 vertical plates (1 m^2 each) connected by manifolds and a working volume of 1300 litres. The total area occupied (footprint) was 10 m^2, while the illuminated area was 40 m^2, therefore the ratio of illuminated area to volume ratio was about 30 m^{-1}, that is, more than 3 times higher than that normally achieved in open ponds. The performance of the photobioreactor was evaluated using a culture of *Synechocystis* PCC 6803. The results indicated that the amount of light captured by the photobioreactor at a plate spacing of 0.5m was 90.2% of the light incident on the horizontal surface, while at a plate spacing of 1.0 m, 50.3% was captured. The corresponding biomass yield, calculated based on the ground area occupied by the reactor, was 26.0 g m^{-2} day^{-1} and 7.2 g m^{-2} day^{-1}, when the plates were spaced at 0.5 m and 1.0 m respectively. Therefore, the light conversion efficiency calculated based on the ground area occupied by the reactor was significantly higher in the configuration with a plate spacing of 0.5 m, reaching 5.43% based on PAR (photosynthetically active radiation), and 2.44% based on solar radiation, giving a value 3.7 higher than when the plates were spaced 1.0 m apart [2]. Although the light conversion efficiency was significantly improved, further improvements in the design of the photobioreactor are still necessary. This issue is addressed within the ongoing *Photosynh2* project. Recently a new strain of *Chlorella* which can grow heterotrophically, photo-autotrophically and mixotrophically was studied for hydrogen production [3]. Of the most important features of this strain is its higher respiration rate and the higher level of saturation of photosynthesis compared to *Chlamydomonas* strain CC-124, both conditions are desirable for hydrogen production. The production of H_2 in the light reached a total 900 ml of H_2 per litre of culture in 8 days which is the highest production reached so far. The maximum output reached with this strain was 12mLH_2/L culture/h, corresponding to a maximum light conversion efficiency (light to H_2) of 7.7% (average 3.2%, over the 8-day period, PAR basis). Recently, with the *Chlorella* G-120 strain medium optimization the total hydrogen production has reached 1500 mlH_2/L of culture in 6 days. This high performance prompts us to further optimize the growth conditions of this strain. To improve the sustainability of

the process, the replacement of glucose with molasses is being studied. In conclusion, photobiological hydrogen production by using microalgae is very appealing but some important barriers need to be overcome. Among them, the high sensibility of hydrogenase to oxygen, and necessity to further improve the light conversion efficiency of the cultures outdoors. However, it worth to point out that photobiological hydrogen production presents unique advantages: 1) the process does not requires artificial catalysators; 2) the process is associated to products such as biomass, protein, pigments and high value substances for biorefinery purposes, plant stimulants; 3) potential use of seawater, wastewater and digestates and CO_2 fixation makes the process environmentally friendly; 4) use of natural catalysators, *i.e.*, the hydrogenase and PSII which are self-sustaining and no replacement is needed during the lifetime of the hydrogen production process. Further improvements are expected by exploiting the progress attained by synthetic biology, particularly with *Synechocystis*, a cyanobacterium more amenable to genetic manipulations, which could help to significantly increase its performance, and thus reduce the photobiological hydrogen production costs in the future.

Acknowledgements

This work was partially supported by the European Innovation Council (grant 101070948 [PhotoSynH2]), 2013-2017.

References

[1] G. Torzillo, M. Seibert (2013). Hydrogen production by *Chlamydomonas reinhardtii.* Handbook of Microalgal Cultures (Richmond A., Hu Q. Eds.). Blackwell Science Ltd. Oxford.

[2] G. Torzillo, G. Chini Zittelli, B. Cicchi, M. Diano *et al*. (2023). Effect of plate distance on light conversion efficiency of a *Synechocystis* culture grown outdoors in a multiplate photobioreactor. *Science of the Total Environment* 842,156840

[3] E. Touloupakis, C. Faraloni, A. M. Silva Benavides, J. Masojídek, G. Torzillo (2021). Sustained photobiological hydrogen production by *Chlorella vulgaris* G-120 without nutrient starvation. *Int. J. of Hydrogen Energy*. 3684-3694

Chemical oxygen absorber mediated direct photosynthetic hydrogen production by *Synechocystis* sp. PCC6803

***Gergely Ernő Lakatos*[1], Bernardo Cicchi[1], Francesco Balestra[1], Graziella Chini Zittelli[1], Giuseppe Torzillo[1,2], Cecilia Faraloni[1]**

[1] *Institute of BioEconomy, Biology, Agriculture and Food Sciences Department, National Research Council of Italy, Sesto Fiorentino, Italy*

[2] *Centro de Investigación en Ciencias del Mar y Limnologia, Universidad de Costa Rica, San Pedro, San José 2060, Costa Rica*

gergelylakatos@cnr.it

Hydrogen is pivotal for several industrial processes, yet 99% of current production relies on fossil-based grey hydrogen, responsible for approximately 920 million tonnes (Mt) of annual CO_2 emissions in 2024. Biological hydrogen from microalgae offers a carbon-negative alternative, but its long-term stable usage struggles with boundaries. The cyanobacterium *Synechocystis* sp. PCC6803 (hereafter *Synechocystis*) possesses a bidirectional NiFe-hydrogenase, which is strongly sensitive to the presence oxygen, thus hydrogen evolution is possible under dark conditions by fermentation [1]. However, at the onset of photosynthesis in dark-adapted cells, hydrogenase catalyses hydrogen production during the brief anaerobic phase of growth [2].

Based on these findings, we assumed that if the anaerobiosis under light conditions is maintained by using an artificial oxygen absorber, the hydrogen production may last longer. To test this assumption, *Synechocystis* was grown on BG11 supplemented with marine salt at in 35 g L^{-1} concentration to suppress the risk of contamination. Interrupting the growth, the culture was directly transferred into an illuminated and sealed, horizontally placed Roux bottle, into whose headspace bags of oxygen absorbers were placed. Both oxygen, pH and conductivity sensors were used to monitor the culture conditions. Hydrogen accumulation in the headspace was monitored on a daily basis. Besides, physiological status of the culture was followed by photosynthesis measurements, carbohydrate, protein and pigment analysis.

As a result, we observed a three-week long continuous hydrogen evolution. The average accumulated hydrogen yield was 14.23 mL g^{-1} dry matter. The hydrogen production rate stepwise declined along the time.

Acknowledgements
This activity is supported by the PhotosynH2 project: EIC Pathfinder grant #101070948

References
[1] Touloupakis, E., Rontogiannis, G., Benavides, A. M. S., Cicchi, B., Ghanotakis, D. F., & Torzillo, G. (2016). Hydrogen production by immobilized

Synechocystis sp. PCC 6803. international journal of hydrogen energy, 41(34), 15181-15186.
[2] Appel, J., Phunpruch, S., Steinmüller, K., & Schulz, R. (2000). The bidirectional hydrogenase of Synechocystis sp. PCC 6803 works as an electron valve during photosynthesis. Archives of microbiology, 173(5), 333-338.

Effect of light spectrum on growth, hydrogen production and biochemical composition of the cyanobacterium *Synechocystis* sp. PCC 6803

***Francesco Balestra*[1], *Giuseppe Torzillo*[1,2] *Bernardo Cicchi*[1], *Gergely Ernő Lakatos*[1], *Graziella Chini Zittelli*[1], *Cecilia Faraloni*[1]**

[1] *Institute of BioEconomy, Biology, Agriculture and Food Sciences Department, National Research Council of Italy, Sesto Fiorentino, Italy*
[2] *Centro de Investigación en Ciencias del Mar y Limnología, Universidad de Costa Rica, San Pedro, San José 2060, Costa Rica*
corresponding.author@emailaddress.eu

The influence of light spectrum on the growth and biochemical composition of the cyanobacterium *Synechocystis* is a key research area in both microbiology and biochemistry. *Synechocystis* sp. PCC 6803 is a model organism, and it is frequently used in scientific investigations to understand photosynthesis, metabolic regulation, and bioproduct synthesis [1, 2]. Recently, this cyanobacterium has been the focus of extensive research on hydrogen photoproduction, a sustainable method of producing H2 [3]. The photobiological generation of hydrogen relies on two natural catalysts: hydrogenase enzyme, which combines protons ($H^{+)}$ and electrons from the photosynthetic process, and photosystem II (PSII), which ~~divides~~ splits water into H_2 and O_2.
In this study, white, orange and blue lights were used to test their effect on growth, metabolism and hydrogen production, while also evaluating pigment composition and photosynthetic performance. Culture growth was carried out in vertical glass tube photobioreactors using BG11 medium supplemented with marine salts (35 g L^{-1}) under controlled temperature, pH, and light intensity (200 µmoles photons m^{-2} s^{-1}). For hydrogen production, cultures were placed in Roux bottles under continuous LED illumination (200 µmol photons m^{-2} s^{-1}) with O_2 absorbers, monitoring redox potential, O_2, pH and H_2 production. Orange light enhanced biomass accumulation (doubling-that observed under white light), while under blue light it was reduced by half compared to the one under white light, corresponding to increased carotenoid accumulation. Hydrogen accumulation occurred only under orbital agitation, highlighting the importance of effective mixing and oxygen depletion. Among the tested wavelength, the orange and blue light promoted the highest hydrogen production, which was 97% and 7% higher than the production under withe light, respectively. These results show that different light spectra drive distinct physiological responses in *Synechocystis* sp. PCC 6803,influencing growth yield. Moreover, optimization of light quality combined with proper culture mixing and O_2

removal during the H_2 production phase is essential for efficient photobiological hydrogen production.

Acknowledgements
This activity is supported by the PhotosynH2 project: EIC Pathfinder grant #101070948

Literature

[1] Zavřel, T., Segečová, A., Kovács, L., Lukeš, M., Novák, Z., Pohland, A.C., Szabó, M., Somogyi, B., Prášil, O., Červený, J. & Bernát, G. (2024). A Comprehensive Study of Light Quality Acclimation in *Synechocystis* Sp. PCC 6803, Plant and Cell Physiology, 65(8), 1285–1297, https://doi.org/10.1093/pcp/pcae062

[2] Chini Zittelli, G., Mugnai, G., Milia, M., Cicchi, B., Silva Benavides, A.M., Angioni, A., Addis, P. & Torzillo, G. (2022). Effects of blue, orange and white lights on growth, chlorophyll fluorescence, and phycocyanin production of *Arthrospira platensis* cultures, Algal Research, Volume 61,102583, ISSN 2211-9264, https://doi.org/10.1016/j.algal.2021.102583.

[3] Jaramillo, A.; Satta, A.; Pinto, F.; Faraloni, C.; Chini Zittelli, G.; Silva Benavides, A.M.; Torzillo, G.; Schumann, C.; Mendez, J.F.; Berggren, G.; Lindblad, P.; Parente, M.; Esposito, S.; Diano, M. (2025). Outlook on synthetic biology-driven hydrogen production: Lessons from algal photosynthesis applied to cyanobacteria. Energy Fuel. 39, 4987−5006.

Hydrogen production by *Synechocystis* 6803 in seawater

N. Jiménez Conejo[1,2], A. M. Silva Benavides[2,3], G. Torzillo [2,4]

[1] Sistema de Estudios de Posgrado, Universidad de Costa Rica,
[2]Centro de Investigación en Ciencias del Mar y Limnología (CIMAR), Universidad de Costa Rica;
[3]Escuela de Biología, Universidad de Costa Rica;
[4]CNR-Istituto per la Bioeconomia, Via Madonna del Piano 10, 5019 Sesto Fiorentino, I-50019 Florence, Italy
Corresponding author : natalia.jimenezconejo@ucr.ac.cr

Synechocystis spp. PCC 6803 is a promising cyanobacterium for hydrogen production due to its rapid growth and a known genome, which facilitates genetic modifications [1]. However, the optimization culture medium for hydrogen production is still incomplete. The necessity to reduce the use of freshwater necessary for civil purposes prompted us to formulate a culture medium in which deionized water was replaced with seawater. For this purpose, *Synechocystis* spp. 6803 cultures were grown in seawater enriched with BG11 nutrients. Once the cultures had reached about 1 g/L of dry weight, were centrifuged and resuspended in fresh medium and placed in a homemade fully controlled flat bioreactor with constant stirring. Cultures were exposed to 120 µmol photons m^{-2} s^{-1}, temperature 32°C, pH 7.4. Hydrogen concentration was quantified daily for 8 days by gas chromatography using argon as the carrier gas. The dry weight of the cultures at the start of the hydrogen experiments ranged from 4.0 g/L and 8 g/L, while the hydrogen produced reached a total of 12.5 µL/L culture/day and 8.75 µL/L culture/day, respectively. At the end of experiments, the total protein and carbohydrate contents in the biomass were 56% and 16%, respectively. This study demonstrated the feasibility of hydrogen production of *Synechocystis* spp. 6803 in seawater with some important advantages, that is, a reduction of the production cost and an improvement of the environmental sustainability of the process. The high protein content recorded in the biomass at the end of each cycle underscores the need to valorize the leftover biomass for feed in aquaculture, and for use in agriculture as plant growth biostimulants. By this way the economy of the process may further improved.

Acknowledgements
This work was supported by University of Costa Rica, project number C6081

References
K. Bolatkhan, B. D. Kossalbayev, B. K. Zayadan, T. Tomo, T. N. Veziroglu, S. I. Alahverdian (2019). Hydrogen production from phototrophic microorganisms: Reality and perspectives. J. Hydrogen Energy, 44, 5799-5811.

Comparison of photofermentative hydrogen production in cylindrical photobioreactors

R.M. Zampieri[1,2], I.C. Moia[2], and E. Touloupakis[2]
[1] *Department of Agriculture, Food, Environment and Forestry, University of Florence, Via San Bonaventura 13, 50145 Firenze, Italy*
[2] *Research Institute on Terrestrial Ecosystems, National Research Council, Via Madonna del Piano 10, 50019 Sesto Fiorentino, Italy*
eleftherios.touloupakis@cnr.it

Purple Non-Sulphur Bacteria (PNSB) are Gram-negative photosynthetic bacteria that grow under anaerobic or microaerobic conditions, typically observed as red colonies. PNSB convert organic substrates anaerobically into molecular H_2 in a process known as photofermentation [1] (Figure 1). For example, *Rhodobacter sphaeroides* and *Rhodospirillum rubrum* can utilise organic acids for H_2 production with the nitrogenase enzyme [2,3]. Photofermentative H_2 production requires oxygen-free and ammonia-limited conditions, as nitrogenase is inhibited by the presence of oxygen and ammonium salts [4].

In this study, the ability of the PNSB *Rhodopseudomonas sp. S16-VOGS3* (hereafter *Rhodopseudomonas*) to produce H_2 was investigated in two cylindrical photobioreactors (PBRs) with different working volumes: 0.2 L (referred to as 0.2-PBR) and 4.0 L (referred to as 4.0-PBR) (Figure 1). Two mixing methods were tested in the 4.0-PBR: the first used a rotor with four paddles, and the second used a spiral rotor. Light conversion efficiency (LCE) was assessed for all three conditions. The culture in the 0.2-PBR produced 142.15 mL of H_2, with an average H_2 production rate of 0.74 mL/h, an average productivity of 3.70 mL/L/h, and an LCE of 0.59% (Figure 2) [5].

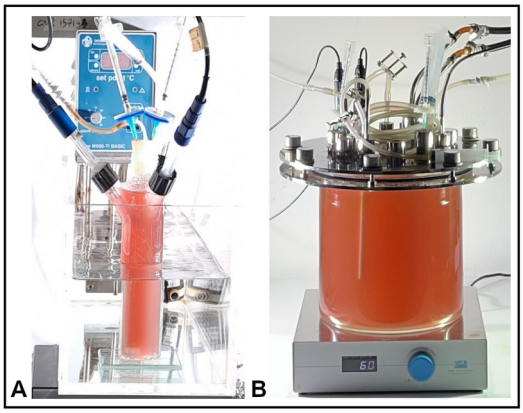

Figure 1: The 0.2-PBR and the 4.0-PBR used for the cultivation of *Rhodopseudomonas*.

The culture in the 4.0-PBR produced a total of 806.05 mL and 1642 mL of H_2 with the paddle rotor and the spiral rotor, respectively (Figure 2). The average

H_2 production rate and LCE were 2.29 mL/h and 0.58% for the paddle rotor, and 2.87 mL/h and 0.72% for the spiral rotor.

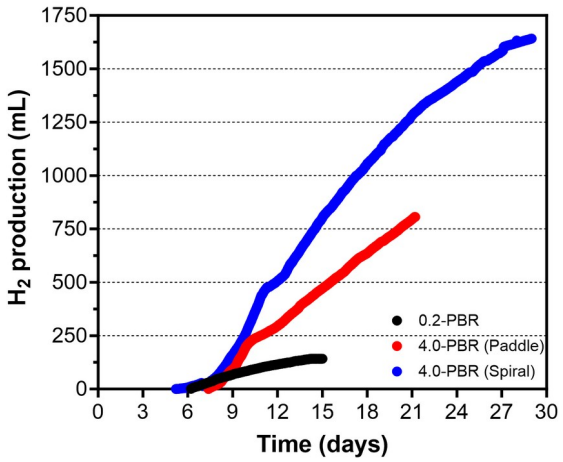

Figure 2: Cumulative H_2 production by *Rhodopseudomonas* cells grown in the 0.2-PBR (black dots), in the 4.0-PBR using the 4-paddle rotor (red dots) and in the 4.0-PBR using the spiral rotor (blue dots).

The more uniform and efficient mixing achieved with the spiral rotor played an important role compared to the paddle rotor, resulting in a higher LCE. This study reports a scale-up of the photofermentation process from 0.2 L to 4.0 L using the PNSB *Rhodopseudomonas sp* S16-VOGS3.

Acknowledgements
This research was funded by the European Union's Horizon Europe—the Framework Programme for Research and Innovation [grant number 101093150], project LIBRA (Light Based Multisensing Device for Screening of Pathogens and Nutrients in Bioreactors).

References
[1] Y. Verma, J. Iqbal, M. Naushad, A. Bhaskaralingam, A. Kumar, P. Dhiman, C.W. Lai, G. Sharma. "Recent developments in photo-fermentative hydrogen evolution: Fundamental biochemistry and influencing factors a review", Journal of Environmental Management, 374, 2025, 123976.
[2] Y. Zhang, X. Wang, J. Yuan, L. Guo. "Multidimensional engineering of *Rhodobacter sphaeroides* for enhanced photo-fermentative hydrogen production", Chemical Engineering Journal, 488, 2024, 150852.
[3] N. Hernández-Herreros, A. Rodríguez, B. Galán, M. Auxiliadora Prieto. "Boosting hydrogen production in *Rhodospirillum rubrum* by syngas-driven photoheterotrophic adaptive evolution", Bioresource Technology, 406, 2024, 130972.
[4] I.C. Moia, A. Kanaropoulou, D.F. Ghanotakis, P. Carlozzi, E. Touloupakis. "Photofermentative hydrogen production by immobilized *Rhodopseudomonas* sp. S16-VOGS3 cells in photobioreactors", Energy Reviews 3, 2024, 100055.
[5] R.M. Zampieri, E. Touloupakis, C. Faraloni, I.C. Moia. "Comparison of photofermentative hydrogen production in cylindrical photobioreactors using different mixing systems", Microorganisms, 13, 2025, 1386.

Brewery spent grains as a potential substrate for growth and biohydrogen production by *Rhodobacter sphaeroides* and *Parachlorella kessleri*

***L. Gabrielyan*[1], J. Manoyan[1], A. Petrosyan[1], A. Hambardzumyan[1], and L. Gabrielyan[2]**

[1] *Department of Biochemistry, Microbiology and Biotechnology, Yerevan State University, Yerevan, Armenia*

[2] *Department of Physical and Colloids Chemistry, Yerevan State University, Yerevan, Armenia*

lgabrielyan@ysu.am

The importance of clean and renewable energy sources has become vital in the search for sustainable energy solutions. One promising approach involves using of photosynthetic organisms, such as purple bacteria and green algae, for biohydrogen (H_2) production [1]. H_2 represents a viable alternative energy source due to its high energy density and low environmental impact when used as a fuel. Purple bacteria and green algae are photosynthetic microorganisms abundant in various ecosystems and have long been recognized for their potential in renewable energy production [1,2]. Moreover, strains of these microorganisms isolated in Armenia represent an unexploited resource for sustainable energy production.

This study aims to investigate the potential of brewery spent grains as a substrate for growth and H_2 production by purple bacterium *Rhodobacter sphaeroides* MDC6509 and green alga *Parachlorella kessleri* MDC6524, isolated in Armenia.

The brewery industry is considered one of the most polluting due to the diverse and large volumes of waste generated during production. Worldwide, it is estimated that the brewing sector produces approximately 40 million tons of waste annually with brewery spent grains (BSG) as the main byproduct [3,4]. Using microorganisms to convert such wastes presents a promising approach to reducing waste and promoting sustainability in this pollution-prone industry [2,3]. By converting these wastes into useful products, such as biofuels and secondary metabolites, photosynthetic microorganisms not only reduce the environmental impact of brewery production but also generate valuable products for a range of industries [2-4].

BSG were chosen as cultivation media for *Rhodobacter sphaeroides* and *Parachlorella kessleri* due to their availability, high carbon and nutrient content, and low cost. The chemical oxygen demand (COD) and total nitrogen concentration of BSG were determined, yielding values of 4.40 g O_2 L^{-1} and 42 mg L^{-1}, respectively. During cultivation of *R. sphaeroides* and *P. kessleri*, the nitrogen concentration in BSG-containing media decreased by approximately 70% and 40%, respectively.

The specific growth rate of *P. kessleri* and *R. sphaeroides* increased during cultivation in BSG-containing media. The highest growth rates for both *P. kessleri* and *R. sphaeroides* were observed in 2-fold diluted BSG media, with increases of 1.3- and 2-fold, respectively, compared to the control cultures

grown in Tamiya and Ormerod media. In contrast, cultivation in undiluted BSG-containing media resulted in a decrease in the specific growth rate of both microorganisms due to the high concentration of organic compounds in the BSG.

The highest H_2 yield in *R. sphaeroides* and *P. kessleri* was observed in 2-fold diluted BSG-containing media. H_2 production by both microorganisms began at 24 h and continued for at least 120-144 h. The highest H_2 production by *P. kessleri* was recorded in 2-fold diluted BSG-containing media, which was ~4-fold higher than the control grown in standard Tamiya medium. In *R. sphaeroides*, H_2 production was 2-fold higher compared to the control cultivated in Ormerod medium. No H_2 production was observed when *R. sphaeroides* was grown in undiluted BSG-containing medium, while *P. kessleri* showed minimal H_2 production, which may be due to the high organic compounds content in the BSG. The results highlight the importance of waste dilution to optimize the concentration of organic compounds for both biomass and H_2 production.

Thus, brewery spent grains represent a promising and sustainable feedstock for biomass and biohydrogen production. The use of *R. sphaeroides* and *P. kessleri* for H_2 production from BSG highlights the potential of these microorganisms for the effectively convertion of this waste into valuable biofuel. The results demonstrate that BSG in optimal dilution can serve as an efficient substrate for microorganisms growth and H_2 production. This approach not only provides an innovative method of waste valorization but also promotes the development of clean energy sources, supporting the transition to a circular economy in the brewing industry.

Acknowledgements
This work was supported by the Higher Education and Science Committee of Armenia, in the frames of the research project 25RG-1F098.

References

[1] C. Faraloni, G. Torzillo, F. Balestra, IC. Moia, RM. Zampieri, N. Jiménez-Conejo, E. Touloupakis "Advances and Challenges in Biohydrogen Production by Photosynthetic Microorganisms", Energies 18(9), 2025, 2319.
[2] L. Hakobyan, L. Gabrielyan "Phototrophic microorganisms as the future of green biotechnology", in: Microbial essentialism: An industrial perspective. Singh et al. (eds.). Elsevier: Academic Press, 2024, 181-205, ISBN: 978-0-443-13932-1.
[3] JI. Arranz, FJ. Sepúlveda, I. Montero, P. Romero, MT. Miranda "Feasibility analysis of brewers' spent grain for energy use: Waste and experimental pellets", Appl. Sci. 11, 2021, 2740.
[4] SAL. Bachmann, T. Calvete, LA. Feris "Potential applications of brewery spent grain: Critical an overview" J. Environ. Chem. Eng. 10(1), 2022, 106951.

Extraction of pure hydrogen from sources of natural origin

***D.O. Dunikov*[1], *S.I. Allakhverdiev*[2], *D.V. Blinov*[1], *and A.M. Bozieva*[2]**
[1] *Joint Institute for High Temperatures of RAS, Moscow, Russia*
[2] *K.A. Timiryazev Institute of Plant Physiology of RAS, Moscow, Russia*
ddo@mail.ru

In 2024 global hydrogen production has reached almost 100 Mt, nevertheless, less than 1% of hydrogen is produced by low-carbon paths, mostly by water electrolysis [1]. Some alternative natural sources of hydrogen, such as hydrogen of biological origin (biohydrogen) and geological origin (natural hydrogen), have great potential, but stay mostly unused. These sources have a low carbon footprint and their reserves are potentially huge, and their advantage over solar and wind energy lies in their constant generation over time. Biohydrogen is actively investigated since the 2010s, though the wide commercial use is still uncertain. From the 1950-1960s, it had become clear that molecular hydrogen (natural H_2) is present in almost all mineral occurrences but its use in energy production has not been considered until recently.

The main barrier to the use of these natural sources of hydrogen is that their feedstocks are low-pressure (less than 1 MPa) gas mixtures based on methane (natural gas), carbon dioxide or even helium with a low concentration of hydrogen (up to 10 mol.% or less). The extraction of such hydrogen by traditional methods is currently difficult and economically unjustified, thus there are currently no effective and affordable ways for practical use of hydrogen from mixtures of natural origin.

We propose to increase the partial pressure of hydrogen in biologically produced source gas by the use of dark fermentation at elevated hydrostatic pressures. These possibly can be achieved by the use of well-known hydrogen producing microorganisms and by the use of new extremophiles, which potentially can produce hydrogen at elevated pressures. Moreover, production of biohydrogen and natural hydrogen can be combined. Recently a US company Gold H2 has demonstrated a biologically stimulated hydrogen generation at commercial field scale with 40% of H_2 in the gas stream [1].

Commercial technologies (adsorption, membrane and cryogenic) for hydrogen purification have been developed to extract hydrogen from mixtures with an increased hydrogen content (more than 70%) and operate at pressures above 1 MPa. It is possible to solve the problem of hydrogen separation from low quality mixtures using substances that selectively absorb hydrogen even at low pressures, for example, metal hydrides. Purification, compression and storage of hydrogen by reversible metal hydrides is the safest and most compact option [2].

We present results of hydrogen production by *Synechocystis sp. PCC 6803 GT-L* in a 120 mL reactor at pressures up to 1 MPa, generated by the excess Ar pressure, successful hydrogen generation was demonstrated in first 24 h, up to 7% of hydrogen in the produced H2-CH4-CO2 mixture (excluding Ar) was detected by gas chromatography. Such a mixture could be purified using metal hydrides, though scale up in biohydrogen production (bigger reactor) is still needed to conduct joint experiments on hydrogen production and extraction.

Successful extraction of hydrogen by metal hydride was demonstrated from the concentrated natural gas probe (ca. 4% mol. H_2). The probe was delivered by the "Gazprom Hydrogen LLC" and produced by the membrane separation using the raw gas from the Kovyktinskoye gas and condensate field (0.07% mol. H_2) [3].

Practical implementation of the technologies for hydrogen production and extraction from natural sources could be done within the framework of the Russian Roadmap for "The development of high-tech direction Hydrogen energy up to 2030", in which PJSC Gazprom is the leading company in natural hydrogen.

Acknowledgements
The investigation was supported by the Russian Science Foundation project 25-19-00696.

References
[1] IEA. Global Hydrogen Review 2025. Typeset in France by IEA - September 2025. 2025.
[2] Lototskyy M.V., Tarasov B.P., Yartys V.A. Gas-phase applications of metal hydrides. Journal of Energy Storage, vol. 72, 108165 (2023)
[3] Dunikov D.O., Bezdudny A.V., Blinov D.V., Eronin A.A., Kazakov A.N., Romanov I.A., et al. Extraction of natural hydrogen from a natural gas probe by LaNi4.8Al0.2 metal hydride. International Journal of Hydrogen Energy, vol. 134, 84–91 (2025)

Gas-phase optimization for long-term photobiological hydrogen production in heterocystous cyanobacteria

***B.D. Kossalbayev*, A.K. Sadvakasova, and G.K. Kamshybayeva, D. Zaletova, M.O. Bauenova**
Faculty of Biology and Biotechnology, Al-Farabi Kazakh National University, Almaty, Kazakhstan
kossalbayev.bekzhan@gmail.com

Photobiological H_2 production by cyanobacteria is attractive for sustainable energy conversion, but practical rates and stability are often limited by the O_2 sensitivity of nitrogenase and hydrogenases. Heterocystous cyanobacteria partially mitigate this constraint via microoxic heterocysts, yet the surrounding gas composition can still strongly modulate long-term H_2 evolution.

Here we evaluated the impact of headspace O_2 (0–8%), N_2 (0–20%) and CO_2 (0–8%) on H_2 photoproduction by four N_2-fixing filamentous strains (*Anabaena variabilis* BTA-1047, *Nostoc punctiforme* SSP-01, *Anabaena* sp. ZTB-1 and *Calothrix* sp. BUY-14.2) and a non-heterocystous control (*Synechocystis* sp. PCC 6803). H_2 evolution was monitored over time and normalized to chlorophyll a.

The response to O_2 was strain dependent. In A. variabilis BTA-1047 and *N. punctiforme* SSP-01, moderate O_2 (>~6%) increased short-term H_2 rates, while O_2 <6% reduced H_2 evolution. In contrast, Anabaena sp. ZTB-1 and *Calothrix* sp. BUY-14.2 showed a monotonic decline with increasing O_2, with 8% O_2 decreasing H_2 production by up to ~90% in BUY-14.2. The *Synechocystis* control was highly O_2 sensitive, with inhibition evident already at 1% O_2.

Adding N_2 to the headspace consistently suppressed H_2 evolution in all N_2-fixing strains, consistent with competition for reductant and ATP through N_2 fixation. CO_2 supplementation at 2% enhanced H_2 production by ~25–46% (strain dependent), whereas higher CO_2 (6–8%) decreased H_2 rates and negatively affected culture fitness during prolonged incubations.

When O_2 and CO_2 were varied together, the best performance was observed at low but non-zero O_2 combined with modest CO_2; for example, 1% O_2 : 2% CO_2 yielded ~110% of the anaerobic control in BTA-1047. Overall, these results highlight that optimizing gas-phase composition is a practical lever to improve sustained H_2 photoproduction and to identify robust cyanobacterial candidates for scale-up.

Acknowledgements

This research has been funded by the Committee of Science of the Ministry of Science and Higher Education of the Republic of Kazakhstan (Grant No. AP26193911, AP23490113).

References

[1] Dutta D, De D, Chaudhuri S, Bhattacharya SK "Hydrogen production by Cyanobacteria", Microbial Cell Factories, 4, 2005, 36.

[2] Bandyopadhyay A, Stöckel J, Min H, Sherman LA, Pakrasi HB "High rates of photobiological H_2 production by a cyanobacterium under aerobic conditions", Nat Commun, 1, 2010, 139.

[3] Kosourov S, Leino H, Murukesan G, et al. "Hydrogen photoproduction by immobilized N_2-fixing cyanobacteria: understanding the role of the uptake hydrogenase in the long-term process", Appl Environ Microbiol, 80(18), 2014, 5807–5817.

Hydrogen Storage & Power to X

S. Scoppa and F. Gallucci - Intensified ammonia production: AMBHER project

C. Italiano, D.Maccarrone, G.Marino, M.Thomas, H.Brahim, and A.Vita – Boosting ammonia decomposition on pyrochlore – based catalysts

A. Iulianelli, P. F. Zito, S. Scognamiglio, A. Di Nardo, M. Musone, and G. Landi – A novel approach to Power-to-bioSNG by sequential membrane biogas separation and CO2 methanation

M. Tomasso, F. Arpino, G. Cortellessa, E. Caracci, G. Ficco, G. Grossi – Analysis of the effects of hydrogen blending on methane emissions localization and quantification techniques

R. Di Bernardo, V. Gallicchio, V. Spinelli, G. Spazzafumo, A. Gloria – Multi-objective optimization of lattice heat exchanger designs in metal hydride storage systems

V. Gallicchio, V. Spinelli, R. Di Bernardo, M. Martorelli, A. Gloria – Generative design for additive manufacturing of novel hydrogen storage systems based on metal-organic frameworks

Intensified ammonia production: AMBHER project

***S. Scoppa*[1] *and F. Gallucci*[1]**
[1] *1 Cube BV, Kastanjelaan 400 5616 LZ Eindhoven, The Netherlands*

f.gallucci@1cube.eu

The AMBHER project aims at providing a quantum leap in the development of hydrogen storage technologies. For that purpose, it develops its main activities around ammonia synthesis for the long-term storage and around novel nanoporous Metal Organic Frameworks (MOFs) for the short-time storage (Figure 1). For longterm storage, advanced catalysts and membranes and their combination in an intensified 3D-printed periodic open cell structured reactor will be developed to allow hydrogen storage in the form of ammonia in a cost-efficient and resource effective process at lower temperatures and pressures compared to conventional systems. For shortterm hydrogen storage, novel nanoporous MOFs of high surface area and low-cost synthesis will be developed following an original shaping process (3D printing). Conformable cryo-vessel to accommodate stacks of MOF bodies of tailored-made shape will be also developed.

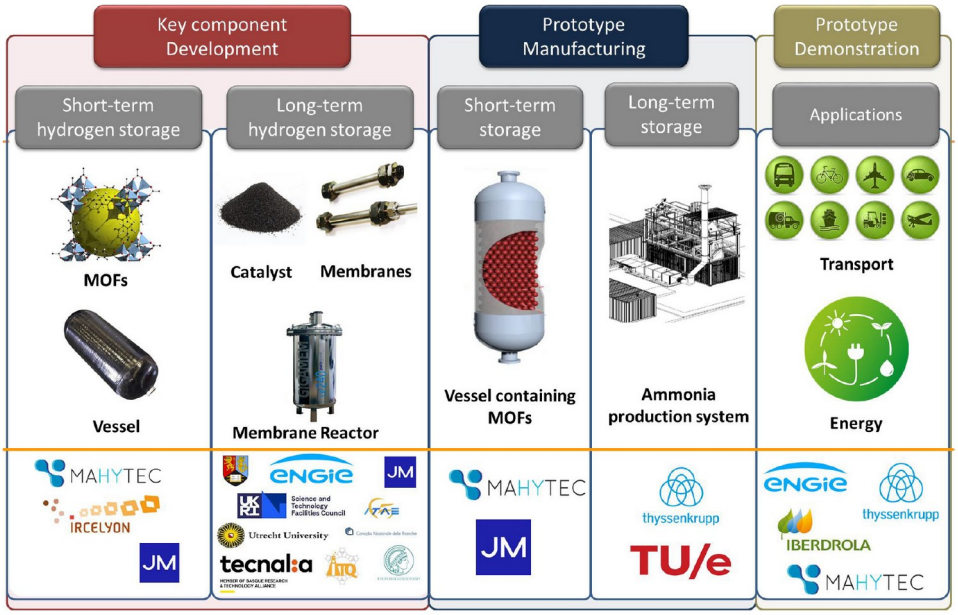

Figure 1. AMBHER project value chain

AMBHER project is validating both short term and long-term solutions at TRL 5. The main technical objectives on material and system level are the following:

➢To design and develop a MOF container for a storage hydrogen capacity of 40 g/L at 100 bar whilst at competitive cost (600-1.000 euros/kgH2).

➢To develop innovative conformable cryo-vessel operating up to 100 bars to be used in Hydrogen Refuel Station for Heavy Duty Vehicles.
➢ To develop Haber-Bosch process operating at pressures below 20 bar and temperatures below 250 °C with NH3 production rates 4 times higher than conventional reactors operated at the same conditions.
➢To develop innovative membranes for selective separation of ammonia during the gas phase production process with selectivities of NH3/N2> 50 and NH3/H2> 10.
➢To design and manufacture highly conductive Periodic Open Cellular Structures with optimized heat and mass transfer and thin struts.
➢To develop a full LCA, LCC and Health and Safety Analysis (HSE) of AMBHER.
➢To pave the way for future exploitation of AMBHER Key Exploitable results.

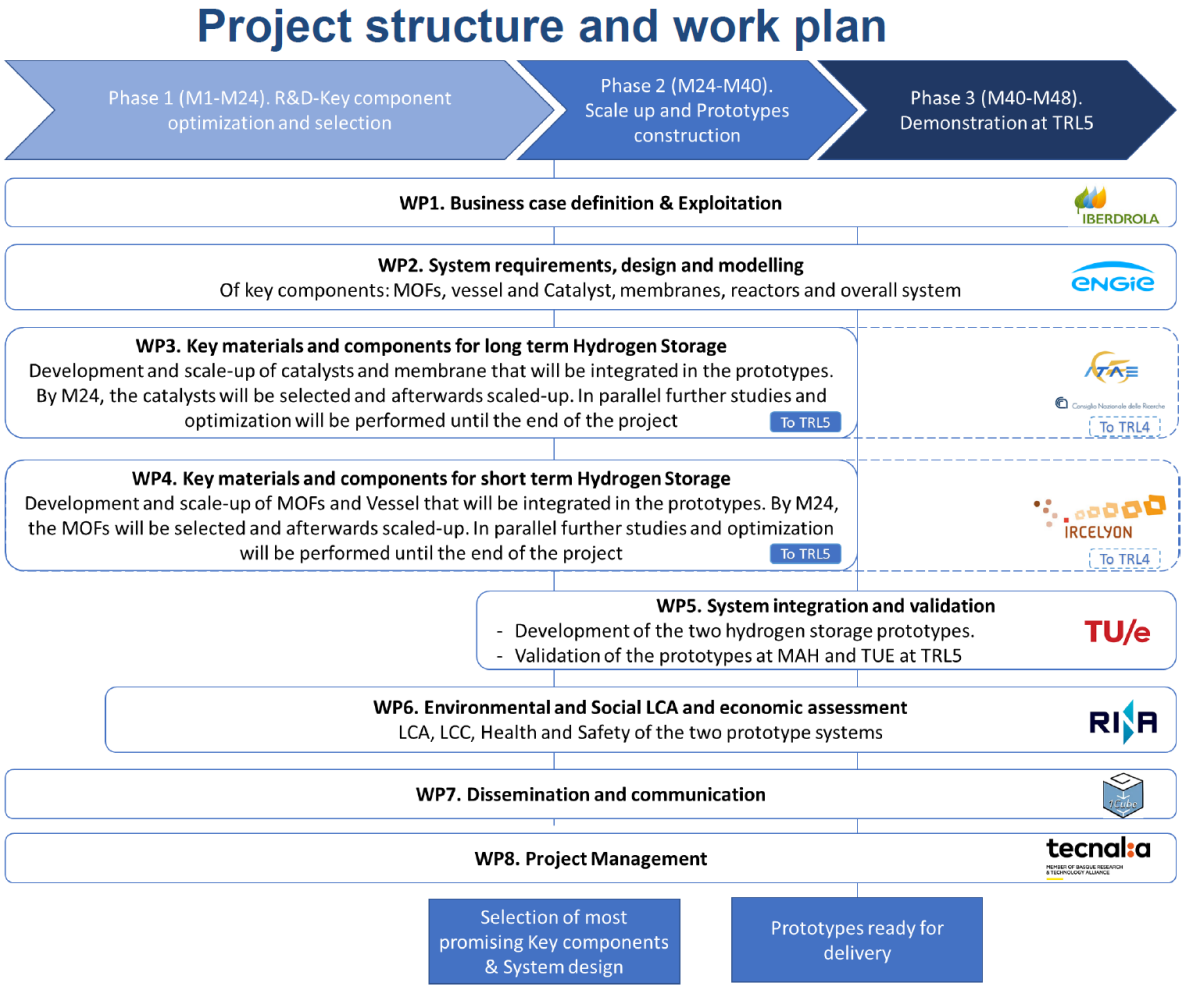

Acknowledgments
Funded by the European Union under the grant agreement 101058565 (AMBHER project). Views and opinions expressed are however those of the author(s) only and do not necessarily reflect those of the European Union or European Health and Digital Executive Agency. Neither the European Union nor the granting authority can be held responsible for them.

Boosting ammonia decomposition on pyrochlore – based catalysts

C.Italiano[1], D.Maccarrone[1], G.Marino[1], M.Thomas[1], H.Brahim[1], and A.Vita[1]

[1] *Institute of Advanced Energy Technologies of the National Research Council of Italy (CNR-ITAE), Via S. Lucia Sopra Contesse 5, 98126, Messina (ME), Italy*
cristina.italiano@cnr.it
domenico.maccarrone@cnr.it

Rising energy demand and fossil fuel depletion gained interest in renewables to supplant traditional fossil-based systems. Hydrogen emerges as a key future energy carrier, pivotal for a low-carbon economy transition. Ammonia serves as an effective hydrogen vector for long-term storage, facilitating long-distance transport and broad renewable energy applications.

Catalytic ammonia cracking offers a promising pathway for improving H2 – based economy, but synthetizing efficient, economical catalysts from non-noble metals continues to pose significant hurdles. This study explores pyrochlore-type oxides ($A_2B_2O_7$ structure) as promising support for ammonia decomposition catalysts (1,2). Their adaptable crystal framework, excellent thermal stability, and tunable redox and acid-base characteristics make pyrochlores well-suited for improving metal – support interaction and facilitating critical surface reactions.

Different $La_2Ce_xZr_{\{1-x\}}O_7$ ($0 \leq x \leq 1.5$) pyrochlores using sol-gel combustion were synthetized, followed by a wetness impregnation of Ru (2wt%) and characterized them via N_2 physisorption, XRD, H_2-TPR, CO_2–TPD , CO chemisorption, TEM, and XPS. In-situ DRIFT spectroscopy enabled NH_3 temperature-programmed desorption (TPD) to probe the reaction mechanism. Kinetic studies at 375 °C varied NH_3, N_2, and H_2 partial pressures under 60,000 NmL g^{-1} h^{-1} flow, applying power law and Temkin-Pyzhev models to derive kinetic parameters.

Catalytic activity (**Figure 1**) demonstrates that the Ce-Zr combination in the structure (particularly at 1:1 ratio) outperforms other compositions. Catalysts based solely on Ce or Zr exhibit inferior performance compared to those incorporating both cations at the B-site of the $A_2B_2O_7$ pyrochlore framework.

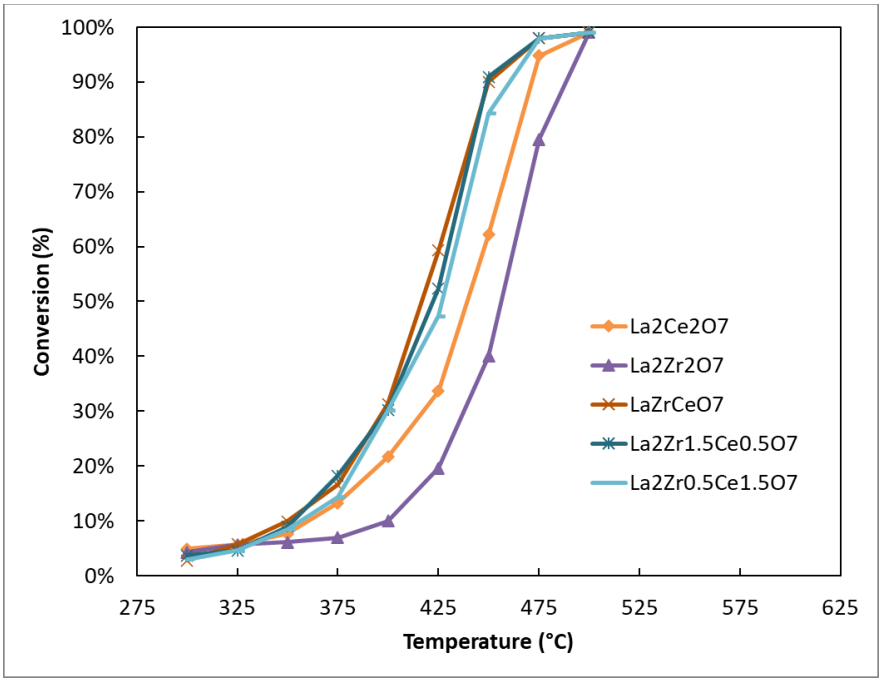

Figure 1: Catalysts screening (P = 1 atm, T = 300 – 500 °C, Ammonia Feed yNH_3 = 25%, 60,000 $NmL^3\ g^{-1}\ h^{-1}$, 200 mg catalyst – 400 mg Qz)

The Ce-Zr pairing distorts the fluorite-type structure observed in $La_2Zr_2O_7$ or $La_2Ce_2O_7$, forming a solid solution due to comparable ionic radii of Ce and Zr relative to La. Post-reduction, the emergence of metallic Ru phase confirms its exsolution and effective internalization within the pyrochlore lattice, with average Ru crystallite size ~2 nm indicating highly dispersed, nanosized particles. H_2-TPR peaks shift to higher temperatures, signifying enhanced structural stability and reduced reducibility, primarily from increased separation between active phase and oxygen vacancies in the pyrochlore(3). CO chemisorption and XPS analyses further verify well-dispersed Ni particles. Kinetic studies on the optimal La_2ZrCeO_7 catalyst reveal good agreement between experimental and Temkin-Pyzhev-predicted reaction rates, while in-situ NH_3-TPD validates the proposed mechanism.

Acknowledgements
This work has received funding from the European Union's Horizon 2020 research and innovation program under grant agreement No. 101112118 (ANDREAH project) and from national innovation program (PNRR Accordo di Programma MASE-ENEA/CNR – AdP POR H2 "Ricerca e sviluppo sull' idrogeno"). Views and opinions expressed are, however, those of the authors only and do not necessarily reflect those of the European Union or CHJU.

References

[1] Wu Q et al. « Highly effective ruthenium catalyst support on La2Zr2O7 for ammonia decomposition to COx-free hydrogen ». Fuel. 2025;379(July 2024):133106.

[2] Xu J et al. « Zhang Y, Xu X, Fang X, Xi R, Liu Y, et al. Constructing La2B2O7 (B = Ti, Zr, Ce) Compounds with Three Typical Crystalline Phases for the Oxidative Coupling of Methane: The Effect of Phase Structures, Superoxide Anions, and Alkalinity on the Reactivity ». ACS Catal. 2019;9(5):4030–45.

[3] Napolitano ES et al. « Enhanced ammonia decomposition using a Pd-Ag membrane reactor for high-purity hydrogen production ». Fuel Process Technol [Internet]. 2025;272(March):108203. Available from: https://doi.org/10.1016/j.fuproc.2025.108203

A novel approach to Power-to-bioSNG by sequential membrane biogas separation and CO_2 methanation

A. Iulianelli[1], P. F. Zito[1], S. Scognamiglio[2], A. Di Nardo[2], M. Musone[2], and G. Landi[2]
[1] *CNR-ITM, Rende (Cs), Italy*
[2] *CNR-STEMS, Naples, Italy*
gianluca.landi@cnr.it

In the last World Energy Outlook [1], biogas was reported to be the fastest growing form of bioenergy, whose production could reach 95 billion cubic metres of natural gas equivalent (bcme) in 2035. At the same time, biomethane production would rise proportionally and would reach 160 bcme in 2050. In this context, a key valorisation method is the hydrogenation of CO_2 with green hydrogen to produce synthetic natural gas (bioSNG), allowing conversion of CO_2 into methane suitable for injection in the gas grid. According to IEA, this could be a good opportunity to substitute the natural gas and to improve the EU energy security. This process also serves as a chemical storage for renewable hydrogen, fully fitting into the concept of power-to-gas. Several processes have been proposed, commonly presenting a post-methanation upgrading to achieve the high methane purity standards (>95%) for grid injection [2-4]. For instance, Italian regulations require CO_2 and H_2 concentrations ≤ 2.5 and 2.0 vol.% respectively. Membranes dominate industrial-scale separation due to their cost-effectiveness and performance in multi-stage systems designed to enhance purity and recovery [5] In this work, we propose a novel approach: biogas is preliminary separated into CH_4-rich and CO_2-rich streams by membrane separation and the latter is catalytically converted into methane with green hydrogen. Due to the use of kinetically driven reactor simulations, no assumption on the effectiveness of the methanation process were required. The proposed process for power-to-bioSNG using biogas as feedstock was modelled in AspenPlus© (AspenTech). The biogas flowrate and composition were set at 1 kmol/h and CH_4/CO_2=1.5 without further components. With respect to real biogas, the used mixture can be considered as a pre-treated biogas after the removal of contaminants. Membrane separation was modelled as a yield separator, while the methanator was modelled as an isothermal catalytic PFR with detailed kinetics, as proposed by Xu and Froment [6], including potential carbon monoxide formation. Condensation and water separation was carried out at 25 °C and reactor operating pressure; water/gas composition at the separation outlet was calculated according to thermodynamic equilibrium. By a design specification, H_2 supply was calculated to satisfy the constraint «y_{H2} in SNG = 2 vol.%».

The preliminary evaluation of the proposed process was carried out on the process flow diagram (PFD-1) reported in Figure 1. The selected membranes were ceramic and, thus, required high pressure to efficiently operate the separation between methane and carbon dioxide. Biogas is isothermally compressed up to 25 bar and sent to a membrane separation system; the

flowrates and compositions of the exiting streams were calculated by setting the recovery of CO_2 and CH_4 used as degrees of freedom. The permeate pressure was set at 5 bar. Carbon dioxide was mixed with a hydrogen flowrate; the so-obtained stream is pre-heated at the reactor inlet temperature (HEX1) and sent to the methanation reactor (REAC). The reactor was assumed isothermal at 280 °C; preliminary reactor dimensions were arbitrarily set at 6 m length and 1 m diameter, corresponding to about 4.7 m^3 and 4.2 ton of catalyst. Reacted stream was cooled down to room temperature without pressure change (HEX2), leading to water condensation. Liquid and gaseous streams were separated (SEP). The retentate stream is heated up (HEX3) to increase its enthalpy content and then expanded into a turbine (TURB) down to the final plant pressure (5 bar). The so-produced work is used to partially sustain biogas compression. The biomethane temperature at the turbine inlet is calculated to ensure that the exiting temperature is about 25 °C. The so-obtained biomethane stream is mixed with the methane-rich stream coming from the separator at the same temperature and pressure, thus leading to the synthetic natural gas stream (SNG).

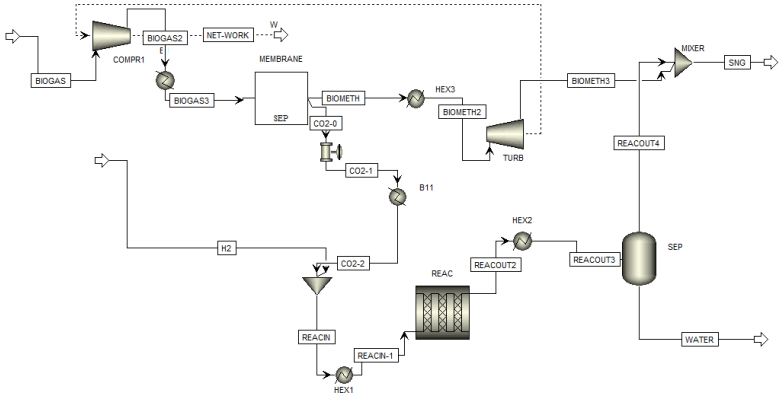

Figure 1: Process flow diagram #1 (PFD-1)

Preliminary evaluation of the feasibility of the proposed process was carried out by changing both methane and carbon dioxide recovery in the separation stage. The CO_2 fraction in SNG (not reported) was mainly affected by CO_2 rather than CH_4 recovery. The target 2.5 vol.% CO_2 in SNG is attained at CO_2 recovery slightly lower than 96%. Calculated CO concentration in SNG is lower than 10 ppm for any CH_4/CO_2 recovery pair. The required hydrogen (not reported) linearly increases by decreasing the CO_2 concentration in SNG. In the investigated range of operating conditions, H_2/biogas is between 1.5 and 1.55. Carbon recovery in SNG (not reported) was in a very narrow range (about 98.9%). It is lower than 1 due to absorption of CH_4 and CO_2 in the water stream. The process presented above was compared with a standard process of biogas methanation, i.e. without CO_2 separation by selective membranes, at three temperatures (250, 260, and 280 °C) and selected CO_2 and CH_4 recoveries (97.5 and 98.5% respectively). Figure 2 shows the combined effect of the PFD type and reactor temperature on the CO_2 concentration in SNG as a function of the reactor volume. Regardless of the process scheme, larger reactor volumes, i.e. higher catalyst weights, were required to achieve the same CO_2 concentration in SNG due to slower reaction rates; on the other hand, thermodynamic constraints

are more favourable at lower temperatures, allowing for lower final CO_2 concentrations in SNG. Comparing the PFDs, preliminary separation by membranes allows for a reduction in the maximum achievable CO_2 concentration in SNG due to more favourable thermodynamic conversions after methane removal from the reacting mixture. Moreover, due to faster kinetics (lower CH_4 partial pressures) and lower flowrates (CH_4 has been separated), lower catalyst weights were required. For instance, at 260 °C, 2.5 vol.% CO_2 in SNG can be obtained with a catalyst weight 4 times lower.

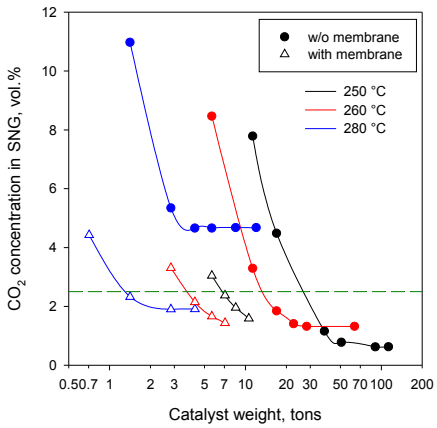

Figure 2: CO_2 concentration in SNG as a function of the reactor volume in the presence (△) and in the absence (●) of membrane separation at different reactor temperatures.

In conclusion, the proposed process including biogas membrane separation followed by CO_2 methanation allows for sustainable Power-to-bioSNG production with the following benefits: i) lower catalyst weight, ii) lower CO_2 concentrations in the SNG without further separation and recycling, iii) reuse of carbon dioxide, iv) bioSNG ready for injection in the gas grid.

References

[1] International Energy Agency. World Energy Outlook 2025.
[2] Witte J, Settino J, Biollaz SMA, Schildhauer TJ. "Direct catalytic methanation of biogas – Part I: New insights into biomethane production using rate-based modelling and detailed process analysis", Energy Convers Manag, 171, 2018, 750–68.
[3] Götz M, Lefebvre J, Mörs F, McDaniel Koch A, Graf F, Bajohr S, et al. "Renewable Power-to-Gas: A technological and economic review", Renew Energy, 85, 2016, 1371–90.
[4] Collet P, Flottes E, Favre A, Raynal L, Pierre H, Capela S, et al. "Techno-economic and Life Cycle Assessment of methane production via biogas upgrading and power to gas technology", Appl Energy, 192, 2016, 282–95.
[5] Marsico L, Brunetti A, Catizzone E, Migliori M, Barbieri G. "Integrated membrane gas separation process for the valorisation of H2 and CO2 to biomethane", Renew Energy, 254, 2025, 123693.
[6] Xu J, Froment GF. "Methane steam reforming, methanation and water-gas shift: I. Intrinsic kinetics", AIChE Journal, 35, 1989, 88–96.

Analysis of the effects of hydrogen blending on methane emissions localization and quantification techniques

M. Tomasso, ***F. Arpino, G. Cortellessa, E. Caracci, G. Ficco, G. Grossi***
University of Cassino and Southern Lazio, Cassino, Italy
matteo.tomasso@unicas.it

As is known, methane shows a greenhouse gas (GHG) potential much higher than carbon dioxide and, for this reason, the recent EU Regulation 2024/1787 [1] imposes stringent standards and measures to reduce methane emissions along the entire natural gas supply chain, from extraction to distribution. Among the most relevant measures, [1] requires monitoring, identifying and eliminating/reducing methane emissions through advanced monitoring and measurement technologies. On the other hand, to achieve environmental objectives, limiting methane emissions is not enough; the injection of natural gas and increasing content of green hydrogen produced from water by electrolysis using renewable energy (e.g., solar and wind) allows the exploitation of the current gas infrastructure for the storage and transport of green hydrogen.. Looking ahead, the percentage of hydrogen permitted in natural gas could increase from the current regulatory limit of 2% to 10-20% in the medium term, without need to substantially modify the components in the network (e.g. valves, compressors, meters, boilers and burners). In Italy, the new requirements of [1], aimed at containing the environmental impact of methane emissions, are integrated with the corresponding requirements of the current Regulation in force [2, 3], which have been introduced mainly aiming at guaranteeing the safety of the infrastructure and the continuity of the service.

In this scenario, several techniques are in use for the localization and quantification of methane emissions, and extensive scientific literature is available on their reliability in the natural gas transportation and distribution sectors [4]. However, it is still unknown to what extent the metrological performance (e.g., minumum detection limit, accuracy, etc.) of these techniques are affected by the presence of increasing amounts of hydrogen in the mixture (e.g., up to 20% by volume) and, in the long term, by hydrogen alone as an energy carrier.

This work is aimed at presenting and discussing the effects of hydrogen blending on the reliability and accuracy of methane emission measurement techniques in the natural gas infrastructure. Currently, the most widely used technologies for detecting and quantifying methane emissions from the gas infrastructure are listed below:

- Flame Ionization Detectors (FID) [4] which are among the most commonly used detectors in gas chromatography thanks to its high sensitivity, wide linear range, and excellent response to organic compounds; it uses a hydrogen flame to ionize gas molecules;
- catalytic sensors [4] which operating principle is based on gas combustion, which heats the catalyst and leads changes in its resistance, allowing

subsequent detection; they show an almost linear response in a wide measuring range;;
- semiconductor sensors [4], relying on the semiconductor resistance which decreases due to oxidation or reduction of the gas on the surface of the metal oxide; they are suitable only for low gas concentrations, but their low selectivity for methane represents a major limitation; nevertheless, they are widely used due to their low cost;
- thermal conductivity sensors, which rely on the principle that different gases show different thermal conductivities; these are very common because they are inexpensive and can detect methane concentrations above the flammability limit;
- Infrared sensors [5] are undoubtedly the most common, thanks to the wide range of configurations available on the market, which make them effective both in the proximity of the leak and from long distances, as well as their high selectivity and rapid response times. These sensors are based on the physical principle that certain gases absorb light at specific wavelengths or bands; this property allows to develop sensors tailored to a specific gas, such as methane.

Table 1 provides a brief summary of the characteristics of the above-mentioned technologies in terms of measuring range, advantages and disadvantages, and reference to the direct effects of hydrogen in the mixture.

Table 1 - Most common sensors for methane emissions localization and quantification

Type of Sensor	Measuring range	Advantages	Disadvantages	H_2 influence
FID	1 – 10000 ppm	– high sensitivity (10^{-13} g/s) – linearity	– low selectivity – safety	– none
Catalytic	0,5 – 10000 ppm	– linearity – simplicity	– only for low concentrations – poisoning – high response times	– possible false posi-tives – saturation
Semi-conductors	0 – 2000 ppm	– reliable at low concentrations – cheap	– influenced by contaminants and humidity	– possible over-esti-mation
Thermal conductivity	5 – 100%	– reliable for high concentrations (up to 100%) – cheap	– not reliable at low concentr. (under LFL)	– possible high over-estimation
Infrared	0 – 100%	– wide range – high selectivity – low influence from external parameters (e.g. temp., humidity, contaminants)	– sunlight or arti-ficial light can influence the measurement – expensive	– none

In some sensor types (e.g., catalytic and semiconductor), hydrogen can cause significant interference, leading to poor discrimination from methane or false positives [7]. Infrared sensors are generally not affected, since hydrogen does not absorb infrared radiation in the relevant wavelength bands. However, indirect effects related to methane dilution and changes in partial pressures may occur, potentially affecting the minimum detection threshold (LEL), particularly in sniffing-based instruments. Given the diversity of infrared technologies, each must be individually experimentally evaluated for methane detection in the presence of specific contents of hydrogen.

Acknowledgements
This research was funded by the European Union - NextGenerationEU from the Italian Ministry of Environment and Energy Security, POR H2 AdP MEES/ENEA with involvement of CNR and RSE, PNRR - Mission 2, Component 2, Investment 3.5 "Ricerca e sviluppo sull'idrogeno", LA2.2.9 CUP: I83C22001170006.

References
[1] Official Journal of the European Union "REGULATION (EU) 2024/1787 OF THE EUROPEAN PARLIAMENT AND OF THE COUNCIL of 13 June 2024 on the reduction of methane emissions in the energy sector and amending Regulation (EU) 2019/942";
[2] Autorità di Regolazione per Energia Reti e Ambiente "Regolazione della qualità del servizio di trasporto del gas naturale per il sesto periodo di regolazione 2024-2027 (RQTG) ", 12 december 2023, 589/2023/R/GAS;
[3] Autorità di Regolazione per Energia Reti e Ambiente "Regolazione della qualità del servizio di distribuzione e misura del gas naturale per il periodo di regolazione 2020-2025 (RQDG) ", 7 december 2019, 569/2019/R/GAS;
[4] Interstate Technology Regulation Council "Evaluation of Innovative Methane Detection Technologies ";
[5] J.I. Connolly, R.A. Robinson, T.D. Gardiner "Assessment of the Bacharach Hi Flow Sampler characteristics and potential failure modes when measuring methane emissions", Department of Chemical, Medical and Environmental Science, National Physical Laboratory, Teddington, Middlesex, United Kingdom;
[6] Mirosław Kwa´sny and Aneta Bombalska, "Optical Methods of Methane Detection", Sensors 2023, 23, 2834;
[7] Andy Connor et al., "Methods for detecting and quantifying hydrogen emissions over a wide range of temporal and spatial scales: a state-of-the-art review", Environmental Emissions Metrology Group, National Physical Laboratory, Teddington, TW11 0LW, United Kingdom.

Multi-objective optimization of lattice heat exchanger designs in metal hydride storage systems

***R. Di Bernardo*[1], *V. Gallicchio*[1], *V. Spinelli*[1], *G. Spazzafumo*[2,3], *and A. Gloria*[4]**

[1] *CeSMA, University of Naples Federico II, Naples, Italy*
[2] *Department of Civil and Industrial Engineering, University of Cassino and Southern Lazio, Cassino, Italy*
[3] *Energy Transition Team (EnTRaT), Cassino, Italy*
[4] *Department of Industrial Engineering, University of Naples Federico II, Naples, Italy*

romolo.dibernardo@unina.it

The future of transportation demands innovative solutions to power vehicles sustainably, and hydrogen stands out as one of the most promising energy carriers. On-board storage remains a critical challenge, typically addressed through pressurized gas, liquid hydrogen, or solid-state storage in Metal Hydrides (MH).

While each method presents distinct challenges, MH systems offer high volumetric density and safety. These systems utilize pressurized cylinders filled with hydride powders, where hydrogen is stored or released from the crystal lattice depending on pressure and temperature conditions. This process is governed by thermodynamics: the charging phase (absorption) is strongly exothermic, while the discharging phase (desorption) is endothermic. Consequently, effective thermal management is one of the challenges to guarantee maximum system performance [1, 2].

Current MH tanks rely on traditional heat exchangers to manage these thermal loads. However, system performance is strictly limited by the heat transfer efficiency of these components. In this context, research is shifting towards novel heat exchangers exploiting Lattice structures, specifically Triply Periodic Minimal Surfaces (TPMS) Gyroids. These complex geometries, manufacturable exclusively via Additive Manufacturing (AM), offer an exceptionally high surface-area-to-volume ratio, making them ideal for thermal applications while also providing superior structural properties [3, 4].

This work investigates the Conjugate Heat Transfer (CHT) performance of a Gyroid-based heat exchanger, aiming to provide a comprehensive development framework for this technology in MH applications.

The study is structured as a multi-objective optimization to analyse the trade-offs between competing physical phenomena. The analysis varies the characteristic dimensions of the TPMS unit cell (e.g., thickness, offset, typical materials) with the goal of:

1. maximizing heat transfer capabilities;

2. minimizing pressure drops;

3. assessing the structural integrity of the lattice under standard operating pressures found in MH literature [5].

The test geometry (Fig.1) was generated using nTop software, defining a cylindrical domain with the diameter of 60 mm, and a total length of 360 mm. This geometry was divided into three functional zones with the same length: an inlet flow straightener, the active Gyroid heat-exchange core, and an outlet recovery zone. Both CHT and mechanical stress analyses were performed using a dedicated software (Fig.2).

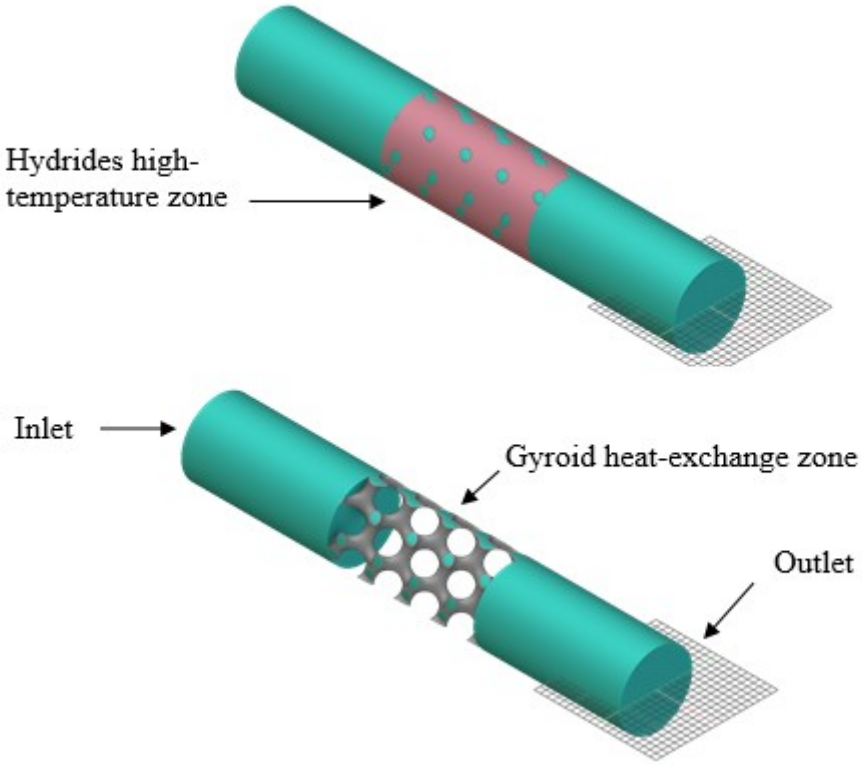

Figure 1: The geometry used for the analyses.

Finally, the results were analysed through the Pareto Frontier to identify the non-dominated solutions, offering a set of optimal design configurations that may balance thermal efficiency with hydraulic and structural performance.

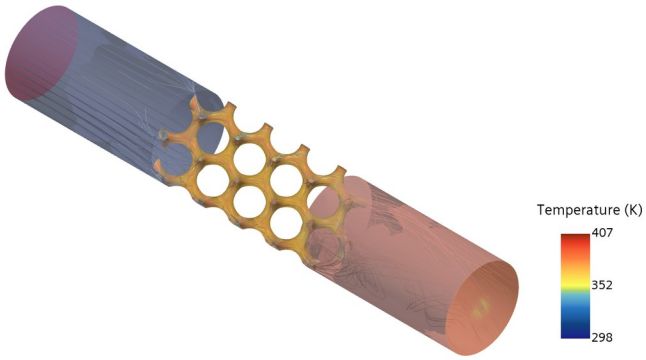

Figure 2: A preliminary result using an inlet fluid speed of 0.01 m/s, the temperature of the cold fluid and hydrides were properly set.

Acknowledgments
The research was partially carried out in the framework of the INVITALIA R&D&I Project NEMESI "New Engineering & Manufacturing Enhanced System Innovation", CUP C67G22000420008. The research was also partially supported by the European Research Executive Agency (REA) project SENS4CORN No 101086364.

References
[1] Ornelas-Ramón Luis G., Gómez-Ortega A., Pérez-Barrera J., Piedra S., "Computational analysis and engineering modeling for the heat transfer and fluid flow through the gyroid TPMS structure", Applied Thermal Engineering, 268, 2025.
[2] Ambrosino A., Chabane D., Hissel D., Djerdir A., Elkedim O., Sorrentino M., Lebaal N., "Thermal management of metal hydride hydrogen tank using lattice structures", Journal of Energy Storage, 131, 2025.
[3] Malfroy J., Van Bavel B., Steelant J., Vandepitte D., "Thin-walled tapered conformable low-pressure tanks: Concept and principles", Thin-Walled Structures, 197, 2024.
[4] Beer M., Rybar R. "Optimisation of Heat Exchanger Performance Using Modified Gyroid-Based TPMS Structures", Processes, 12, 2024.
[5] Atalmis Sari G., Kaplan R.N., Diler F., Ecmel Ece R., Toros S., Kaplan Y. "Investigation of hydrogen storage performance of reactors with different lattice structures manufactured by additive manufacturing method" International Journal of Hydrogen Energy, 182, 2025.
[6] Dassi L., Chatterton S., Parenti P., Pennacchi P. "Gyroid Lattice Heat Exchangers: Comparative Analysis on Thermo-Fluid Dynamic Performances" Machines, 12, 2024.

Generative design for additive manufacturing of novel hydrogen storage systems based on metal-organic frameworks

***V. Gallicchio*[1], *V. Spinelli*[1], *R. Di Bernardo*[1], *M. Martorelli*[2], *A. Gloria*[2]**
[1] *CeSMA, University of Naples Federico II, Italy*
[2] *Department of Industrial Engineering, University of Naples Federico II, Naples, Italy*

vito.gallicchio@unina.it

In the future, transportation will involve creative ways for powering cars responsibly, and hydrogen represents one of the most promising energy sources. Pressurized gas, liquid hydrogen, or solid-state storage in metal hydrides are commonly employed for handling the crucial problem of on-board storage [1,2].

In this context, it is also frequently reported how additive manufacturing technologies allow for the direct fabrication of smart and lightweight devices with specific external shape and architectural features as well as with tailored and improved structural/functional properties. In the context, integrated design methods lead to product reimagination from a new standpoint, improving the performance of critical components in well-defined applications (e.g., biomedical, automotive, aerospace, and further industrial) [3,4].

The introduction of additive manufacturing technologies provided the greatest contribution in developing 3D structures with precise and controlled architectural features. Moreover, bioinspired design aims to create innovative solutions for engineering problems benefiting from the knowledge evolved in biological systems. Engineers and designers can extract working principles from a biological strategy and adopt them for generating novel conceptual engineering solutions [3,4].

A new research era is characterised by the development of functional devices with tailored and improved properties, benefiting from suitable design methodologies (i.e., design for additive manufacturing) [3,4].

The research activities were focused on generative design for additive manufacturing of novel hydrogen storage systems based on metal-organic frameworks (MOFs). The processability of MOFs and materials used to benchmark hydrogen uptake capacity was first considered. This research step was then focused on novel routes towards the design of 3D additive manufactured hydrogen storage devices based on different kinds of materials.

Differently from the topology optimization process, the generative design approach does not remove the unnecessary material, but it builds up the

geometry connecting the preserved design areas, however avoiding prohibited areas [4].
The current research especially reported considerations on the role of generative design as a fundamental support to the ideation process through the development of design alternatives according to the designer's criteria. In particular, technical features and differences concerning design solutions were analysed.

Acknowledgments
The research was partially carried out in the framework of the INVITALIA R&D&I Project NEMESI "New Engineering & Manufacturing Enhanced System Innovation", CUP C67G22000420008. The research was also partially supported by the European Research Executive Agency (REA) project SENS4CORN No 101086364.

References
[1] Ornelas-Ramón Luis G., Gómez-Ortega A., Pérez-Barrera J., Piedra S., "Computational analysis and engineering modeling for the heat transfer and fluid flow through the gyroid TPMS structure", Applied Thermal Engineering, 268, 2025.
[2] Ambrosino A., Chabane D., Hissel D., Djerdir A., Elkedim O., Sorrentino M., Lebaal N., "Thermal management of metal hydride hydrogen tank using lattice structures", Journal of Energy Storage, 131, 2025.
[3] Martorelli M., Gallicchio V., Gloria A., Lanzotti A., "A Preliminary Analysis of the Effects of Process Parameters on the Impact Resistance of 3D Printed PETG and HIPS", Lecture Notes in Mechanical Engineering, 524-534, 2022.
[4] Papallo I., Martorelli M., Lamonaca F., Gloria A., "Generative design and insights in strategies for the development of innovative products with tailored mechanical and/or functional properties", Acta IMEKO, 12(4), 2023.

Photosystem architecture

B.D. Bruce, F. Ali, and M. Rao – Evolution of PSI- Symmetry, Serendipity, and Speculation

G. Han - Structural insights into the regulation and assembly of photosynthetic supercomplexes

A. Amelii, S. Capaldi, M. Russo, Z. Guardini, G. Sanità, E. Esposito, I. Olivé, M. Maiuri, L. Dall'Osto, G. Cerullo, G. Procaccini and R. Bassi – Back to the Seabed: The Unique Photosystem I Architecture of the Seagrass Posidonia oceanica

G. Hastings, H. Makita, F. Ali, B.D. Bruce, H. Liu, L. Luo, W. Xu, K. Redding, S.M. Mäusle and D.J. Nürnberg – Structural Conservation of the A1 Binding Site in Photosystem I Across Cyanobacteria and Green Algae

F. Ali, S. K. Penneru, M. Rao, B.D. Bruce - High-Resolution Cryo-EM Structure of Trimeric Photosystem I Solubilized by SMA-Copolymers

L. Cornet – On the non-oxygenic origins of thylakoids

Photosystem I: Serendipity, Symmetry, and Speculation

Barry D. Bruce, Fidaa Ali, and Mahipal Rao
University of Tennessee at Knoxville
bbruce@utk.edu

For decades, Photosystem I (PSI) in cyanobacteria was regarded as structurally "solved": a trimeric reaction center embedded in quasi-lamellar thylakoids, with plant and algal PSI as a monomeric descendant. Our work unintentionally disrupted this view through a combination of collaboration and serendipity. While searching for a more thermotolerant PSI, we were provided with a robust cyanobacterium from hot springs in northern Thailand by Professor Peerapornpisal at Chiang Mai University, initially named Chroococcidiopsis TS-821. This extremophile grows across wide ranges of temperature, salinity, and light, and biochemical analysis of its thylakoids revealed high–molecular–weight PSI complexes that did not conform to the canonical trimeric structure. Biochemical and structural studies demonstrated that these complexes correspond to a tetrameric form of PSI. Parallel work by others, together with our bioinformatic survey in collaboration with the Pasteur Culture Collection, showed that this architecture is not an oddity of TS-821 but is widely conserved across heterocyst-forming filamentous cyanobacteria, implying a widespread and evolutionarily significant PSI oligomeric transition.

We have now determined cryo-EM structures of both the dimeric and tetrameric PSI from TS-821 and shown that the tetrameric state is favored under high-light growth, where it accumulates ketocarotenoids. Cryo-EM reveals that the tetramer is a true "dimer of dimers," with extensive pigment–lipid–protein interfaces and mobility in one plane of the dimer. Detergent-free, polymer-extracted preparations further resolve additional chlorophylls, carotenoids, and lipids at these interfaces, indicating that oligomerization, local lipid composition, and membrane curvature are tightly coupled. Complementary in vivo time-resolved small-angle neutron scattering (SANS) shows an abrupt shift in thylakoid repeat distance and Q values during high-light adaptation, consistent with a light-induced reorganization of membrane architecture. We propose that the transition toward ketocarotenoid-rich tetrameric PSI induces thylakoid curvature, thereby contributing to photoprotection. Ongoing transcriptional and proteomic analyses aim to define the regulatory pathways and molecular components underlying this adaptation.

Viewed in a broader evolutionary context, these findings suggest that tetrameric PSI in extremophilic cyanobacteria such as TS-821 is a tunable photoprotective state that may have enabled early cyanobacteria to cope with intense, fluctuating irradiance in marginal or emerging terrestrial niches. The coupling of PSI oligomerization, specialized carotenoid binding, and membrane remodeling provides a mechanistic framework for how early photosynthetic organisms could buffer excitation pressure without abandoning high quantum efficiency. This tetrameric architecture may thus represent an intermediate along the trajectory from cyanobacterial PSI–phycobilisome assemblies to the monomeric, LHC-associated PSI of modern chloroplasts, linking stress,

membrane biophysics, and reaction-center evolution and underscoring that PSI architecture is more dynamic and evolutionarily plastic than the dogmatic trimer–monomer narrative suggests.

Structural insights into the regulation and assembly of photosynthetic supercomplexes

Guangye Han*
Key Laboratory of Photobiology, Institute of Botany, Chinese Academy of Sciences, Beijing, China.
hanguangye@ibcas.ac.cn

Oxygenic photosynthesis is the process by which photosynthetic organisms such as plants and algae utilize solar energy to drive oxidation of water and reduction of carbon dioxide (CO_2), which generates molecular oxygen and carbohydrates indispensable for sustaining almost all life forms on Earth. The initial light energy absorption, transfer and conversion reactions (light reactions) of photosynthesis take place in a series of supramolecular protein machines embedded in the thylakoid membranes of oxygenic photosynthetic organisms. The light reactions convert light energy into chemical energy in the form of ATP and NADPH, which is used for CO_2 fixation in the Calvin-Benson-Bassham cycle in the chloroplast stroma. Two types of photosynthetic electron transport pathways, linear and cyclic electron transport (LET and CET), operate in the thylakoid membranes. The CET is essential for balancing the changing demands of ATP/NADPH under various physiological conditions. We have analyzed the structures of photosynthetic supercomplexes in cyanobacteria, cryptophyte algae, green algae, moss and higher plants by cryo-electron microscopy (cryo-EM). The regulation and assembly of the photosystem I (PSI), photosystem II (PSII) and NADH dehydrogenase-like complex (NDH) were revealed. The research results not only help to understand the mechanism of energy conversion and utilization in photosynthesis, but also provide new ideas for designing new photosystems, constructing efficient photosynthetic membrane electron transfer circuits, and developing high photosynthetic efficiency and high carbon fixation components and modules by using synthetic biology techniques.

Acknowledgements
I would like to express my gratitude to students and collaborators for their contributions to these studies.

References
[1] Z Mao, X Li, Z Li, L Shen, X Li, Y Yang, W Wang, T Kuang, J-R Shen, G Han. Structure and distinct supramolecular organization of a PSII-ACPII dimer from a cryptophyte alga *Chroomonas placoidea*. Nature Communications, 15, 2024, 4535.

[2] L Shen, Y Gao, K Tang, R Qi, L Fu, J-H Chen, W Wang, X Ma, P Li, M Chen, T Kuang, X Zhang, J-R Shen, P Wang, G Han. Structure of a unique PSII-Pcb tetrameric megacomplex in a chlorophyll d-containing cyanobacterium. Science Advances, 10, 2024.eadk7140.

[3] S Zhang, K Tang, Q Yan, X Li，L Shen, W Wang, Y-K He, T Kuang, G Han, J-R Shen, X Zhang. Structural insights into a unique PSI-LHCI-LHCII-Lhcb9 supercomplex from moss *Physcomitrium patens*. Nature Plants, 9, 2023, 832-846.

[4] L Shen, K Tang, W Wang, C Wang, H Wu, Z Mao, S An, S Chang, T Kuang, J-R Shen, G Han, X Zhang. Architecture of the chloroplast PSI-NDH supercomplex in *Hordeum vulgare*. Nature, 601, 2022, 649-654.

[5] Z Huang, L Shen, W Wang, Z Mao, X Yi, T Kuang, J-R Shen, X Zhang, G Han. Structure of photosystem I-LHCI-LHCII from the green alga *Chlamydomonas reinhardtii* in State 2. Nature Communications, 12, 2021, 1100.

Back to the Seabed: The Unique Photosystem I Architecture of the Seagrass *Posidonia oceanica*

Antonello Amelii[1], Stefano Capaldi[1], Mattia Russo[2], Zeno Guardini[1], Gennaro Sanità[3], Emanuela Esposito[3], Irene Olivé[4], Margherita Maiuri[2], Luca Dall'Osto[1], Giulio Cerullo[2,5], Gabriele Procaccini[4] and Roberto Bassi[1,4,5].

[1] University of Verona, Verona, Italy.
[2] Politecnico di Milano, Milano, Italy.
[3] Institute of Applied Sciences and Intelligent Systems Unit, CNR, Naples, Italy.
[4] Stazione Zoologica Anton Dohrn, Naples, Italy.
[5] Accademia Nazionale dei Lincei, Rome, Italy.
roberto.bassi@univr.it

Seagrasses are marine flowering plants re-adapted for underwater life, creating highly productive ecosystems and long-term carbon sinks. Originating from monocots that returned to the sea 100–70 million years ago, about 80 species now cover 0.6–1.6 million km² of coastal seabed, storing organic carbon for millennia [1-2]. *Posidonia oceanica*, an endemic Mediterranean seagrass, forms dense meadows extending to depths of up to 50 m, where irradiance is strongly reduced and spectrally shifted toward blue-green wavelengths due to the rapid attenuation of red and far-red light by water. Additional shading from the canopy and epiphytic growth further limits light availability [1]. Despite these constraints, *P. oceanica* maintains high photosynthetic efficiency, yet the molecular mechanisms underlying its adaptation to dim, spectrally restricted light remain poorly understood.

To uncover the molecular mechanisms underlying these adaptations, we investigated the structural and functional features that enable *P. oceanica* to thrive underwater [3]. Plants collected from 4 and 22 m depth revealed distinctive characteristics of the photosynthetic apparatus compared with land plants, including enhanced Photosystem II (PSII) efficiency under low irradiance, markedly reduced non-photochemical quenching, enhancement of both PSI and PSII antenna size, and increased Chl b content in Lhcb proteins, enhancing blue-light absorption. Notably, *P. oceanica* also displayed a stable association of phosphorylated LHCII with PSI, suggesting a constitutive structural adaptation for efficient light-use efficiency under dim light.

Using single-particle cryo-electron microscopy, we determined the structure of *P. oceanica* PSI supercomplexes, whose excitation becomes increasingly limited with depth. The PSI-LHCI supercomplex was resolved at 2.83 Å resolution, and, for the first time in higher plants, a PSI-LHCI with an expanded antenna system—comprising a trimeric phosphorylated LHCII and an additional LHCI heterodimer—termed PSI-LHCI-mega, was resolved at 3.3 Å. Pigment mapping revealed excitation energy transfer (EET) pathways from peripheral antennae to the reaction center (RC). Low-energy chlorophyll (Chl) forms associated with LHCI, typical of land plants, which modulate antenna-to-RC energy transfer [4], were lost. Two-dimensional electronic spectroscopy (2DES) showed that *P. oceanica* PSI-LHCI had faster EET kinetics and shorter

trapping time at the RC than land plant PSI-LHCI. PSI-LHCI-mega retained efficient EET kinetics and comparable trapping times, indicating that antenna expansion is compensated for by the loss of low-energy Chl, achieving a potential trade-off between antenna size and quantum efficiency, which enables an increased absorption cross-section without losing efficiency.
Finally, by integrating structural and functional data, we identified the molecular determinants underlying the loss of low-energy Chl. Structural comparison identified amino acid substitutions underlying the spectral shift, which was validated by recombinant *Po*Lhca4 variants in which replacement with land-plant residues restored low-energy Chl, thereby pinpointing the structural basis of spectral tuning. In conclusion, our findings provide evidence for structural, functional, and spectral adaptations that enable *P. oceanica*, and likely other seagrasses, to optimize photosynthesis under marine light regimes, offering a proof-of-concept for engineering LHCs to tune their light absorption properties for crop synthetic biology [5].

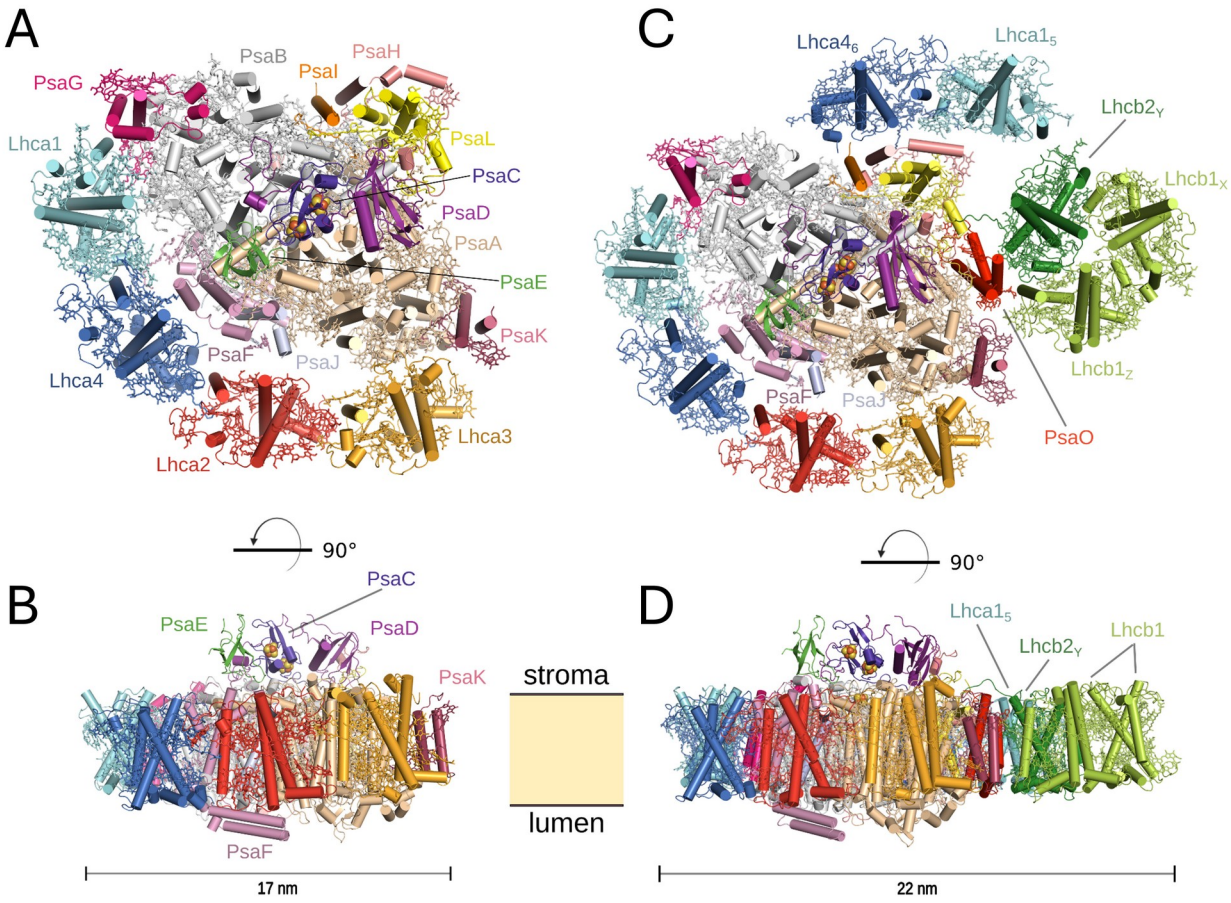

Figure 1: Overall structures of *P. oceanica* PSI-LHCI supercomplexes. (A, B) PSI-LHCI, (C, D) PSI-LHCI-mega. (A, C) Stromal views. (B, D) Side views (membrane orientation indicated).

Acknowledgements
This work was funded by European Research Council (ERC Advanced Grant 101053983-GrInSun) and the European Marine Biological Resource Centre (EMBRC-IT Grant 3097-PhotoSEA).

References

[1] Larkum, A. W., Pernice, M., Schliep, M., Davey, P., Szabo, M., Raven, J. A., Lichtenberg, M., Brodersen, K., Kendrick, G., & Ralph, P. J. "Photosynthesis and metabolism of seagrasses. In Seagrasses of Australia: structure, ecology and conservation", Cham: Springer International Publishing, 2018, 315-342.

[2] Fourqurean, J. W., Duarte, C. M., Kennedy, H., Marbà, N., Holmer, M., Mateo, M. A., Apostolaki, E., Kendrick, G., Krause-Jensen, D., McGlathery, K. & Serrano, O. "Seagrass ecosystems as a globally significant carbon stock", Nature Geoscience, 5, 7, 2012, 505–509.

[3] Charras-Ferroussier, Q., Mathiot, C., Semchonok, D. A., Elias, E., Bhatti, A. F., Lebrun, R., Guillemain, D., Siponen, M., Croce, R. & Jungas, C. "Thriving across seawater depths: How blue light shapes a large PSI supercomplex and specific photosynthetic traits in the seagrass *Posidonia oceanica*." Plant Communications, 7, 1, 2025.

[4] Russo, M., Casazza, A. P., Cerullo, G., Santabarbara, S., & Maiuri, M. "Direct evidence for excitation energy transfer limitations imposed by low-energy chlorophylls in photosystem I–light harvesting complex I of land plants", The Journal of Physical Chemistry B, *125*, 14, 2021, 3566-3573.

[5] Amelii, A., Cutolo, E. A., Montepietra, D., Battarra, C., Caferri, R., Capaldi, S., Guardini, Z., Dall'Osto, L., & Bassi, R. "Photosynthesis under far-red light—evolutionary adaptations and bioengineering of light-harvesting complexes." FEBS letters, 2025.

Structural Conservation of the A_1 Binding Site in Photosystem I Across Cyanobacteria and Green Algae

Gary Hastings[1], *Hiroki Makita*[2], *Fedaa Ali*[3], *Barry D. Bruce*[3, 4], *Haijun Liu*[5], *Lujun Luo*[6], *Wu Xu*[6], *Kevin Redding*[7], *Sarah M. Mäusle*[8] *and Dennis J. Nürnberg*[8, 9]

[1]*Department of Physics and Astronomy, Georgia State University, Atlanta, GA, USA*
[2]*Molecular Biophysics and Integrated Bioimaging Division, Lawrence Berkeley National Laboratory. Berkeley, CA, USA*
[3]*Department of Biochemistry & Cellular and Molecular Biology, University of Tennessee, Knoxville. Knoxville, TN, USA*
[4]*Program in Genome Science and Technology, Bredeson Center, University of Tennessee, Knoxville. Knoxville, TN, USA*
[5]*Department of Biology, Saint Louis University, St. Louis, MO, USA*
[6]*Department of Chemistry, University of Louisiana at Lafayette, LA, USA*
[7]*School of Molecular Sciences, Arizona State University, Tempe, AZ, USA*
[8]*Department of Physics, Freie Universität Berlin, Germany.*
[9]*Dahlem Centre of Plant Sciences, Freie Universität, Berlin, Germany.*
Corresponding Author Email: ghastings@gsu.edu

Time-resolved step-scan Fourier transform infrared (FTIR) difference spectroscopy was used to obtain (A_1^- – A_1) FTIR difference spectra from photosystem I (PSI) samples isolated from eight phylogenetically diverse cyanobacterial strains and one green alga, totaling thirteen PSI preparations. These included samples from cells grown under far-red light and PSI in monomeric, dimeric, trimeric, and tetrameric states. Spectral profiles were shown to be independent of oligomeric state.

Remarkably, all (A_1^- – A_1) FTIR difference spectra exhibited high similarity, underscoring the robustness of the technique and indicating minimal experimental variability. This congruence reveals a highly conserved environment for the phylloquinone cofactor at the A_1 binding site across diverse taxa. Conserved bands associated with the A_0 pigment further suggest structural continuity from A_0 to A_1.

To leverage this consistency, we constructed a composite (A_1^- – A_1) FTIR difference spectrum by averaging all thirteen spectra. This composite spectrum provides enhanced resolution, enabling unambiguous identification of previously unresolved bands. The fact that a highly resolved composite spectrum can be obtained by averaging demonstrates the similarity in the spectra from the different types of samples. Band assignments were refined using prior studies, yielding an improved spectral framework for future investigations of PSI electron transfer cofactors.

Acknowledgements
This work was supported by Department of Energy, (award number DE-SC-0017937, to GH).

High-Resolution Cryo-EM Structure of Trimeric Photosystem I Solubilized by SMA-Copolymers

***Fedaa Ali*[1], Sree Kavya Penneru[2], Mahipal Rao[2], Barry D. Bruce[1,2,3]**
[1]Genome Science and Technology Program, University of Tennessee, Knoxville
[2]Department of Biochemistry, Cellular and Molecular Biology
[3]Department of Microbiology
fali5@vols.utk.edu

Photosystem I (PSI) is the largest member of the photosynthetic type I reaction-center family and plays a central role in oxygenic photosynthesis by driving light-induced electron transfer. In cyanobacteria, PSI commonly assembles as a trimer, an architecture that promotes structural stability, efficient excitation-energy transfer, and conserved organization within the thylakoid membrane. Here, we present a 2.18 Å cryo-EM structure of trimeric PSI from the thermophilic cyanobacterium Thermosynechococcus elongatus (Thermosynechococcus vestitus) isolated using non-detergent SMA-like copolymers. Unlike conventional detergent-based purification, SMA-copolymer solubilization preserves PSI within a native-like lipid environment. The resulting PSI-SMALP complex is substantially larger than detergent-solubilized PSI and retains an extensive annular lipid shell containing approximately 800 lipid molecules. This lipid population is notably enriched in the anionic sulfolipid sulfoquinovosyldiacylglycerol, suggesting that specific lipid–protein interactions may contribute to PSI stability, trimer organization, and functional tuning. Additional lipid and cofactor densities are especially prominent at monomer–monomer interfaces, where they may stabilize the trimer and help maintain the pigment geometry required for efficient photochemistry. Comparison with detergent-solubilized PSI reveals a richer complement of boundary lipids, pigments, and cofactors in the detergent-free complex. Prior spectroscopic studies further indicate that excitation-energy transfer in PSI-SMALPs is faster than in detergent-isolated PSI, supporting the idea that retained native lipids influence PSI function as well as structure. We are therefore seeking to elucidate how these preserved lipids, particularly anionic sulfolipids, modulate PSI architecture, cofactor organization, and energy-transfer dynamics. This work provides, for the first time, a high-resolution structural comparison of a photosystem isolated without detergents, offering new insight into how the native membrane environment shapes photosynthetic reaction-center function.

On the non-oxygenic origins of thylakoids

Luc Cornet[1,2]

[1] BCCM/ULC, InBioS–Molecular Diversity and Ecology of Cyanobacteria, University of Liège, Liège, Belgium

[2] InBioS–PhytoSYSTEMS, Eukaryotic Phylogenomics, University of Liège, Liège, Belgium

Thylakoid membranes are the site of oxygenic photosynthesis. They emerged within cyanobacteria approximately 2.4 billion years ago, and the increase in membrane surface area they provided is thought to have played a major role in the Great Oxidation Event. Within cyanobacteria, the transition between the earliest-diverging taxa, the Gloeobacterales, and the *Thermostichales* that follow them in the phylogeny marks the emergence of these membranes. *Gloeobacterales* indeed lack thylakoid membranes and perform oxygenic photosynthesis in their cytoplasmic membrane, a condition that represents the ancestral state of the linear electron transfer chain of oxygenic photosynthesis. How this ancestral state evolved into the thylakoid membranes observed today, which were later transferred to plastids, remains a major biological enigma.

Using recent knowledge—largely derived from structural and biochemical studies—on thylakoid biogenesis and alternative electron flows, I propose an evolutionary theory in which the origin of thylakoid membranes is not linked to oxygenic photosynthesis, but rather to alternative electron flows, notably anoxygenic photosynthesis [1]. This evolutionary scenario is supported by the recent discovery of an ancestral version of sulfide quinone reductase in Antarctic *Gloeobacterales* [2]. The evolution of basal cyanobacteria, the biogeochemical context—especially the euxinic conditions of the Archean–Proterozoic transition—and the biogenesis of photosynthetic complexes in cyanobacteria, with a particular focus on photosystem II, will be discussed from an evolutionary perspective.

References

1 Cornet L. On the non-oxygenic origins of thylakoids. Commun Biol. Nature Publishing Group; 2025;8:1697. https://doi.org/10.1038/s42003-025-09100-w
2 Hambücken L, Sudianto E, Saw JH, Baurain D, Cornet L. Early-Diverging SQR Enzyme in Antarctic Gloeobacterales Indicates Sulfide Tolerance in Thylakoid-Lacking Cyanobacteria [Internet]. bioRxiv; 2025 [cited 2025 Dec 19]. p. 2025.10.24.684318. https://doi.org/10.1101/2025.10.24.684318

Hydrogen production I

M.V. Contreras-Martínez, F. Espinosa Lagunes, A. Arenillas, N Rey-Raap, I. Gatto, J. Ledesma-García, V. Baglio, L.G. Arriaga - Lanthanum base electrocatalysis for hydrogen production system

D. Pivetta, G. Volpato, F. Del Mondo, M. Russo Cirillo, M. Bogar, R. De Souza, A. Lazzaretto, R. Taccani – Stochastic Optimization Framework for Reliable Hydrogen Cost Predictions: A Case Study in North-East Italy

E.X. Dias, Aruna P.T., C.J. Tseng, M. Bhavanari – Urea-thiourea mediated sulfur incorporation into CoMnTi-based electrocatalyst on nickel foam for alkaline water splitting at high current density

V. La Ferrara, R. Viscardi, M. Martino, A. Marino, G. Landi, S. Del Gobbo, N. Lisi and A. Giaconia – Bridging Photovoltaics and Photoelectrochemistry: Perovskite Photoanodes for Solar-Driven Water Splitting

M. Minutillo, A. Cappiello, F. Romano, S. Di Micco, and G. Di Ilio - On-site hydrogen refueling stations as a strategy to integrate renewables and reduce power curtailment

S. Ozgul, H.G. Ozcan, G. Soykan and B.Caglar - Techno-Economic Evaluation of Biohydrogen Production System Utilizing Wastewater Treatment Plant Powered by Floating Photovoltaic

Lanthanum base electrocatalysis for hydrogen production system

M.V. Contreras-Martínez[1], F. Espinosa Lagunes[2], A. Arenillas[3], N Rey-Raap[3], I. Gatto[4], J. Ledesma-García[5], V. Baglio[4], L.G. Arriaga[2,]

[1]Centro de Investigación y Desarrollo Tecnológico en Electroquímica, 76703, Santiago de Querétaro, México.
[2]Tecnológico de Monterrey, Institute of Advanced Materials for Sustainable Manufacturing, 76130, Santiago de Querétaro, México.
[3]Instituto de Ciencia y Tecnología del Carbono, INCAR-CSIC, Francisco Pintado Fe, 26. 33011 Oviedo, Spain.
[4]Istituto di Tecnologie Avanzate per l'Energia "Nicola Giordano", CNR-ITAE, Salita Santa Lucia sopra Contesse, 5, 98126, Messina, Italy.
[5]División de Investigación y Posgrado, Facultad de Ingeniería, Universidad Autónoma de Querétaro, 76010, Santiago de Querétaro, México.

*Corresponding author: * lg.arriaga@tec.mx*

The transition to sustainable energy relies heavily on green hydrogen production through water electrolysis [1]. Anion Exchange Membrane Water Electrolyzers (AEMWEs) are a promising technology, yet their widespread adoption is limited by the high overpotentials required for the oxygen evolution reaction (OER). Therefore, there is a critical need to develop efficient, durable, and cost-effective electrocatalysts from earth-abundant materials. Mixed metal oxides with perovskite ($LaCoMnO_3$) and spinel ($MnCo_2O_4$) structures are leading candidates for catalysis free of Platinum Group Metals (PGMs), which are non-precious and cost-effective alternatives for OER catalysis. Aerogels, characterized by their high porosity and large surface area, offer an ideal morphology to maximize active sites [2]. In this work, we report the synthesis of novel $LaCoMnO_3$ and $MnCo_2O_4$ aerogels via a microwave-assisted sol-gel method and evaluate their enhanced performance as electrocatalysts for the OER in AEMWEs.

X-ray Diffraction (XRD) confirmed the successful synthesis of both phases. As shown in Figure 1a, $MnCo_2O_4$ crystallized in a single-phase cubic spinel structure (crystallite size 5.9 nm), while $LaCoMnO_3$ formed a single-phase perovskite structure (crystallite size 4.4 nm). BET analysis (Figure 1b) confirmed that both aerogels are mesoporous. LaCoMnO3 showed a narrow and uniform pore size distribution (3.5–4 nm), which is beneficial for mass transport, while MnCo2O4 exhibited a broader distribution (4–10 nm). This structural control and optimal mesoporosity are key factors for catalytic performance [3].

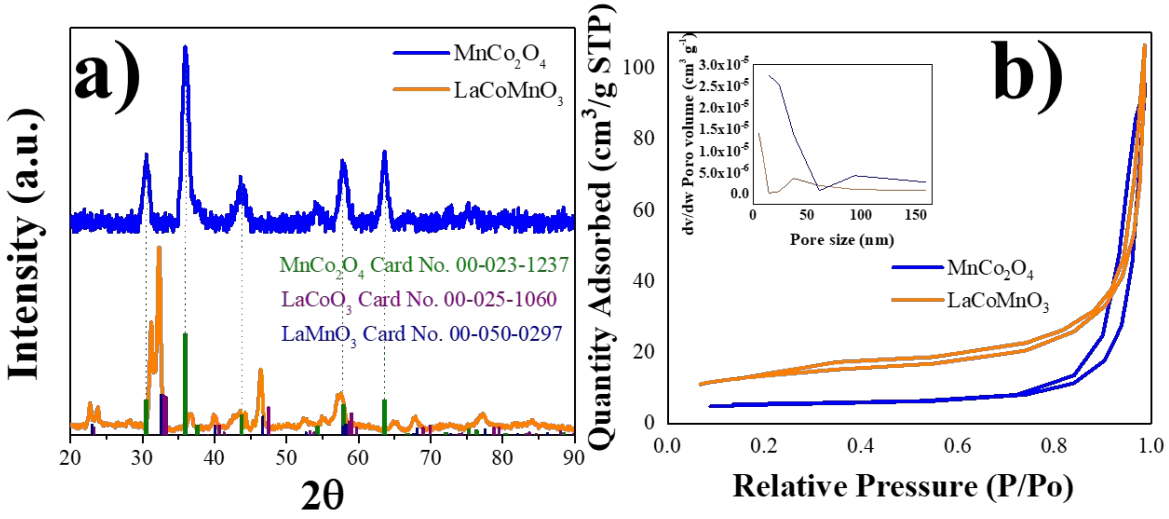

Figure 1: XRD patterns (a) showing the spinel and perovskite phases, N_2 Adsorption-Desorption Isotherms b) and Pore Size Distribution (c) confirming the mesoporosity.

The structural advantages demonstrated by XRD and BET analysis directly translated into superior electrochemical performance. The $LaCoMnO_3$ perovskite exhibited superior activity, requiring only approx. 1.7 V to reach 1 A cm^{-2} and achieved 5.65 A cm^{-2} at 2.2 V. Electrochemical Impedance Spectroscopy confirmed $LaCoMnO_3$ displaying the lowest Charge Transfer Resistance (Rct) at 0.14 Ω·cm^2. This performance is largely due to the unique perovskite structure and optimal mesoporosity demonstrated by the characterization. Both aerogels demonstrated excellent stability, maintaining performance at 1 A cm^{-2} for 100 hours.

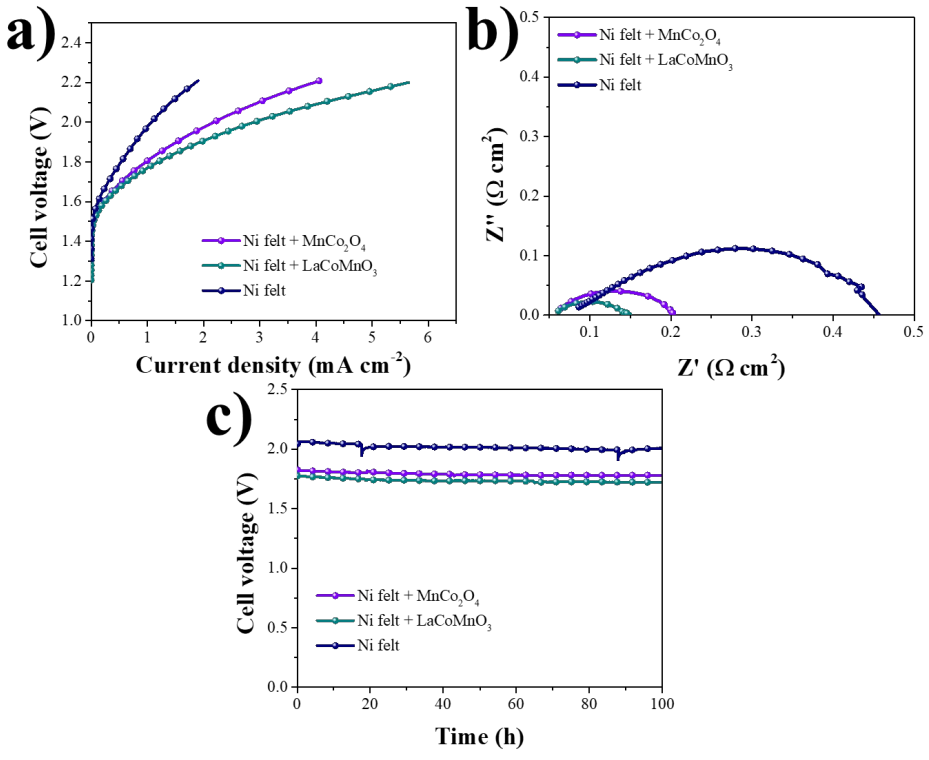

Figure 2: a) Linear sweep voltammetric curves, (b) electrochemical impedance spectroscopy plots (Nyquist); recorded at 1.8 V at 80°C, and c) stability aerogels at 1 A cm^{-2} for 100 h.

Conclusions

We successfully synthesized $LaCoMnO_3$ (perovskite) and $MnCo_2O_4$ (spinel) aerogels via a microwave-assisted sol-gel method. The structural characterization (XRD and BET) confirmed the formation of the desired phases and the superior uniform mesoporosity of LaCoMnO3. This catalyst showed superior OER electrocatalytic activity, reaching 5.65 A cm^{-2} at 2.2 V and exhibiting the lowest charge transfer resistance (0.14 $\Omega \cdot cm^2$). The outstanding performance is linked to the structural advantages of the perovskite phase. Both aerogels demonstrated exceptional long-term stability, proving them to be highly competitive, cost-effective PGM-free catalysts for AEMWEs [4].

Acknowledgements

CNR-ITAE authors acknowledge the financial support of Ministero degli Affari Esteri e della Cooperazione Internazionale and Ministero dell'Università e della Ricerca for the project "DURAble, Scalable, and Recyclable Components and Cell Designs for Next Generation Alkaline Exchange Membrane Water ElectroLYSis (DURALYS)". The authors thank the Secretaría de Ciencia, Humanidades, Tecnología e Innovación (Secihti) for financial support through the Ciencia de Frontera 2023 projects, grants 416 and 567.

References

[1] C. Santoro et al., "What is Next in Anion-Exchange Membrane Water Electrolyzers? Bottlenecks, Benefits, and Future," ChemSusChem, vol. 15, no. 8, Apr. 2022.
[2] C. Triolo et al., "Spinel-Structured High-Entropy Oxide Nanofibers as Electrocatalysts for Oxygen Evolution in Alkaline Solution: Effect of Metal Combination and Calcination Temperature," Adv Funct Mater, vol. 34, no. 6, Feb. 2024.
[3] J. Y. Loh et al., "Unleashing the versatility of porous nanoarchitectures: A voyage for sustainable electrocatalytic water splitting," Chinese Journal of Catalysis, vol. 58, Mar. 2024.
[4] A. Badreldin et al., "Oxygen-deficient perovskites for oxygen evolution reaction in alkaline media: a review," Emergent Mater, vol. 3, no. 5, Oct. 2020.

Stochastic Optimization Framework for Reliable Hydrogen Cost Predictions: A Case Study in North-East Italy

D. Pivetta[1], G. Volpato[1,2], F. Del Mondo[1], M. Russo Cirillo[1], M. Bogar[1], R. De Souza[1], A. Lazzaretto[2], R. Taccani[1]

[1] Department of Architecture and Engineering, University of Trieste, Trieste, Italy
[2] Department of Industrial Engineering, University of Padova, Padova, Italy
taccani@units.it

Hydrogen produced from renewable electricity has emerged as one of the key enablers of industrial decarbonization. Accurately predicting its production costs under technological and economic uncertainty becomes essential for robust investment planning. Although numerous works have assessed Hydrogen Supply Chains (HSCs), most rely on single-point estimates or narrow sensitivity ranges for electrolyzer capital expenditures (CAPEX) and efficiencies, potentially underestimating the true variability of future costs. Recent literature has addressed HSC design optimization [1], electrolyser cost projections [2], and uncertainty quantification using Monte Carlo approaches [3,4]. However, the systematic integration of these approaches within a unified framework for local HSC design has received limited attention.

This study presents a four-step stochastic optimization procedure for reliable Levelized Cost of Hydrogen (LCOH) and Levelized Cost of Electricity (LCOE) predictions in local HSCs. The methodology integrates: 1) systematic collection of electrolyzer CAPEX scenarios from literature, categorized by technology (Alkaline – ALK, Proton Exchange Membrane – PEM) and size range; 2) statistical analysis and Probability Density Function (PDF) fitting to identify distributions that best represent CAPEX uncertainty; 3) Linear Programming optimization of HSC design and operation using PyPSA, solved across a 19-year historical dataset (2005–2023) of solar irradiance, grid prices, and energy demands; 4) LCOH and LCOE distribution estimation by random sampling from best-fitting PDFs and Kernel Density Estimation (KDE).

The framework is applied to a grid-connected HSC located in Trieste (North-East Italy), designed to meet both hydrogen and electricity demands of an industrial end-user. The system comprises a photovoltaic plant and a 5 MW electrolyzer (ALK or PEM), with an annual hydrogen production of 300 t H_2/year. Two configurations are analysed: HSC1 with Electrical Energy Storage (EES) only, and HSC2 incorporating both EES and Hydrogen Storage (HS). Three electrolyzer efficiency scenarios (minimum, mean, maximum) reflect potential technological improvements toward 2030.

Statistical analysis reveals that gamma and beta distributions best fit the CAPEX scenarios for ALK and PEM electrolyzers, respectively. Distribution fitting confirms median CAPEX values around 730 €/kW for small-scale systems (with sizes smaller than 20 MW), with significant variability (500–1200 €/kW for ALK, 400–1300 €/kW for PEM). Table I presents the key performance indicators for the Trieste case study across different configurations and electrolyzer technologies with mean efficiency scenarios.

Table I: LCOH and LCOE results for the Trieste HSC (5 MW electrolyser, 300 t H_2/year) with mean efficiency scenarios.

Config.	Tech.	LCOH (€/kgH_2)	LCOE (€/MWh)	HS (kgH_2)
HSC1	ALK	11.7–12.5	39.2–41.8	–
HSC1	PEM	11.2–12.1	39.8–43.1	–
HSC2	ALK	9.5–10.9	39.6–46.3	494–609
HSC2	PEM	9–10.7	39.8–48.1	487–606

Results demonstrate that improving electrolyzer efficiency from minimum to maximum scenarios reduces LCOH by 33–38% (HSC1) and up to 44% (HSC2). Hydrogen storage in HSC2 decreases LCOH by approximately 2 €/kg H_2 compared to HSC1, due to enhanced electrolyzer utilization and temporal decoupling between production and demand. However, this benefit comes at the cost of increased LCOE, as the system prioritizes hydrogen production over grid exports. PEM electrolyzers achieve lower LCOH values than ALK units owing to their higher efficiency, despite comparable CAPEX ranges at medium scale. The KDE-derived distributions reveal that the greatest uncertainty in LCOH predictions is for small-scale PEM systems (standard deviation up to 0.6 €/kg H_2), while medium-scale ALK configurations exhibit the most stable cost projections.
This work demonstrates that integrating statistical uncertainty analysis with design-operation optimization provides a robust basis for evaluating hydrogen investment strategies under cost variability. Future developments will extend the procedure to include different hydrogen distribution technologies, additional HSC configurations (e.g., ammonia-based storage), alternative renewable sources, and a comparative assessment across multiple European locations.

Acknowledgements

The authors acknowledge the financial support from the NAHV project. (North Adriatic Hydrogen Valley, HORIZON-JTI-CLEANH2-2022-2, Project ID: 101111927)

References

[1] D. Pivetta, G. Volpato, G. Carraro, C. Dall'Armi, L. Da Lio, A. Lazzaretto, R. Taccani, Optimal Decarbonization Strategies for an Industrial Port Area by Using Hydrogen as Energy Carrier, International Journal of Hydrogen Energy 52 (2024) 1084-1103.
[2] F. Frieden, J. Leker, Future costs of hydrogen: a quantitative review, Sustainable Energy & Fuels 8(9) (2024) 1806-1822.
[3] N. Wolf, M.A. Tanneberger, M. Höck, Levelized cost of hydrogen production in Northern Africa and Europe in 2050: A Monte Carlo simulation for Germany, Norway, Spain, Algeria, Morocco, and Egypt, International Journal of Hydrogen Energy 69 (2024) 184-194.
[4] J. Collis, R. Schomäcker, Determining the Production and Transport Cost for H2 on a Global Scale, Frontiers in Energy Research Volume 10 (2022).

Urea-thiourea mediated sulfur incorporation into CoMnTi-based electrocatalyst on nickel foam for alkaline water splitting at high current density

E.X. Dias[1], Aruna P.T.[2], C.J. Tseng[3,4,5], M. Bhavanari[6,7]
[1] *Department of Chemistry, Manipal Institute of Technology, Manipal Academy of Higher Education, Manipal 576104, India*
[2] *Department of Physics, Manipal Institute of Technology, Manipal Academy of Higher Education, Manipal 576104, India*
[3] *Hydrogen Energy Research Center, National Central University, Taoyuan 320317, Taiwan*
[4] *Institute of Energy Engineering, National Central University, Taoyuan 320317, Taiwan*
[5] *Research Center for Critical Issues, Academia Sinica, Tainan 711010, Taiwan*
[6] *Research Laboratory for Bioplasmonics and Energy Technology, Department of Electronics and Communication Engineering, Manipal Institute of Technology, Manipal Academy of Higher Education, Manipal 576104, India*
[7] *Center for Renewable Energy, Manipal Academy of Higher Education, Manipal 576104, India*
bhavanari.m@manipal.edu

The quest for cost-effective and durable electrocatalysts for water splitting holds great promise in achieving a green hydrogen economy. The use of benchmark PGM-based materials for water electrolysis hinders widespread deployment of electrolyzers because of the limited availability and high cost of these metals, in addition to their low durability at high current densities [1]. To address this limitation, noble metal-free electrocatalysts have emerged as a promising alternative due to their natural abundance, redox nature, and tunable oxidation states. This work presents a novel strategy for the solvothermal synthesis of a trimetallic oxide/sulfide electrocatalyst ($CoMnTiO_xS_y$) over Ni foam by optimizing the precursor ratio of urea to thiourea (U:TU). Different samples were prepared by varying the U:TU ratios. Towards HER, $CoMnTiO_xS_y$/NF with a U:TU ratio of 0.1:0.9 exhibited better performance by achieving current densities of −20, −100, and −1000 $mA \cdot cm^{-2}$, at overpotentials of −138 mV, −230 mV and −315 mV, respectively (Figure 1a). A Tafel slope of 112.9 $mV \cdot dec^{-1}$ highlighted the Volmer–Heyrovsky mechanism with the Volmer step as the RDS (Figure 1b). The improved charge transfer was reflected in its low charge transfer resistance (R_{ct}) of 1.97 Ω (Figure 1c). The bifunctional nature of this electrocatalyst facilitated the OER to operate at 50, 100 and 1000 $mA \cdot cm^{-2}$, requiring overpotentials of 348 mV, 367 mV and 447 mV, respectively (Figure 1d). The Tafel slope of 64 $mV \cdot dec^{-1}$ and R_{ct} of 0.34 Ω complemented the fast reaction kinetics and efficient charge transfer (Figure 1e, f). Towards OWS in a two-electrode setup, the electrocatalyst achieved 50, 100 and 1000 $mA \cdot cm^{-2}$ at *i*R-compensated cell potentials of 1.78 V, 1.85 V and 2.25 V, respectively, with a resistance of 8.86 Ω. At 2.25 V, the electrocatalyst exhibited durability of 64 hours at 1050 $mA \cdot cm^{-2}$. The I-V and EIS characterizations after the durability test revealed no increase in the cell potential and R_{ct} (Figure 1g, h, i). HR-XRD

analysis revealed the formation of spinel sulfide structure in the CoMnTi electrocatalyst (Figure 2a). The SEM analysis of the electrocatalyst with U:TU ratio of 0.1:0.9 portrayed vertical nanorods with nanospheres at the base, providing a high surface area that facilitates efficient H^+/OH^- adsorption, electrolyte transfer and bubble diffusion (Figure 2b). FT–IR spectroscopy highlighted the presence of metal sulfides with additional vibrational peaks relating to sulfate species due to the partial oxidation of surface sulfides (Figure 2c). These results were also complemented by Raman spectroscopy analysis (Figure 2d). In contrast, the urea-rich samples formed metal carbonate hydroxides. The post-durability SEM images revealed that the cathode maintained the vertical nanorod morphology, while the anode surface underwent structural reconstruction. This could be due to the ready conversion of sulfides to oxyhydroxides, which is the RDS of the OER. The improved HER in metal sulfides compared with metal carbonates can be attributed to the lower hydrogen binding energy of metal sulfides which facilitates efficient H^+ adsorption [2]. Due to the lower electronegativity of S than O, a covalent bond exists between M and S, which easily dissociates to form M–OOH intermediate during the OER [3]. This work underscores that synergistic electron modulation due to Co, Mn and Ti, along with the excellent charge transfer capabilities of sulfide species, collectively contribute to the enhanced bifunctionality and durability of the $CoMnTiO_xS_y$/NF electrocatalyst towards alkaline water electrolysis.

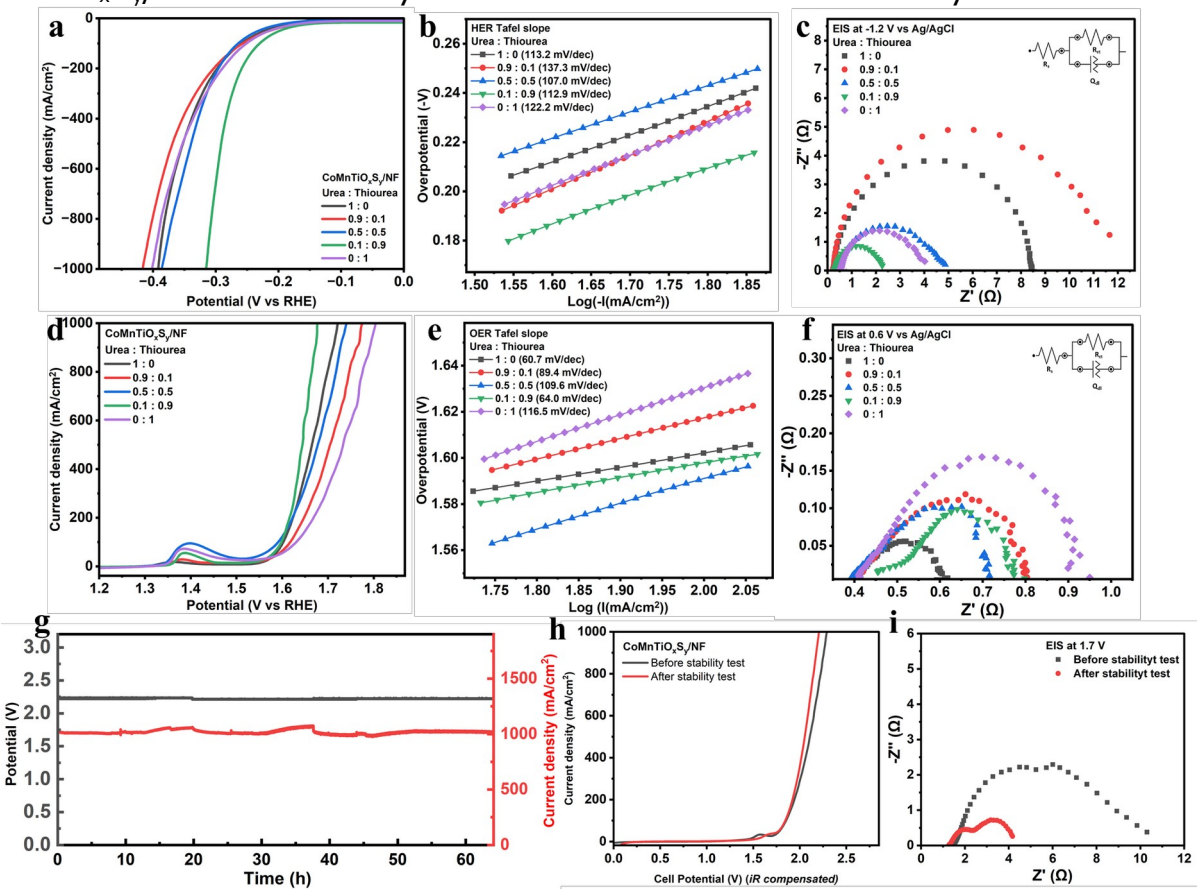

Figure 1: (a) HER polarization curve, (b) HER Tafel slope, (c) EIS at −1.2 V vs Ag/AgCl, (d) OER polarization curve, (e) OER Tafel slope, (f) EIS at 0.6 V vs Ag/AgCl, (g) Chronoamperometry test at 2.25 V, (h) Post-stability OWS polarization curve, (i) Post-stability EIS at 1.7 V

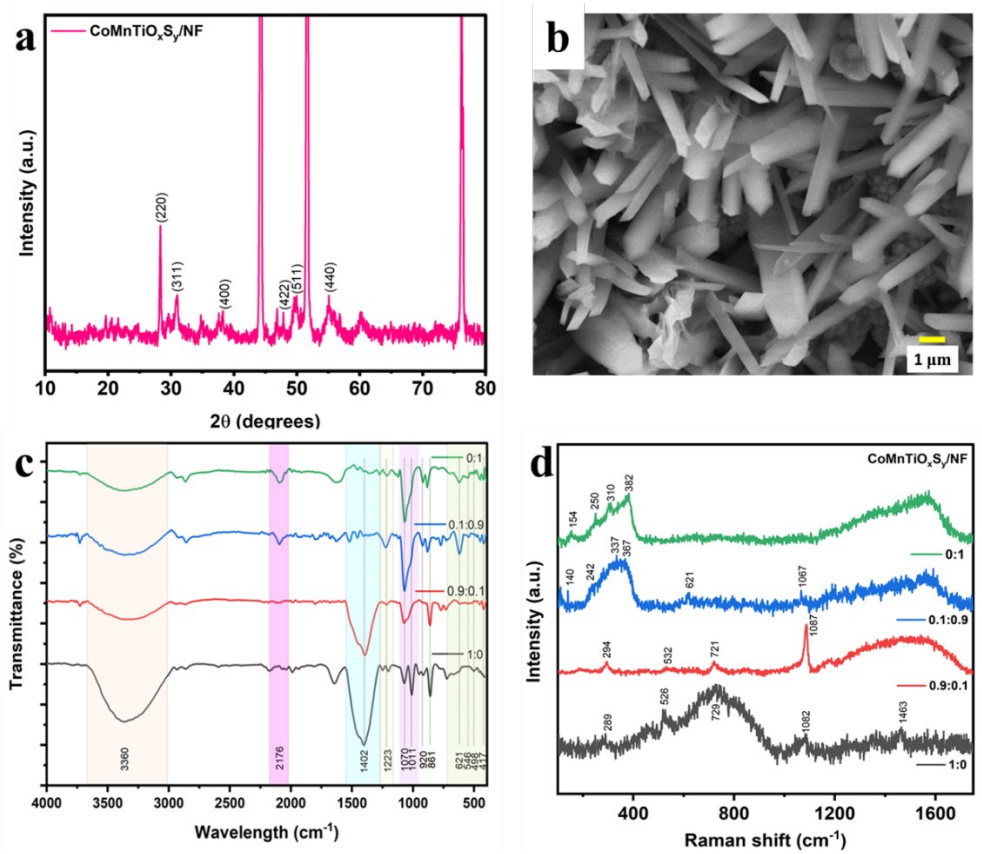

Figure 2: (a) HR-XRD analysis, (b) SEM image, (c) FT–IR spectroscopy analysis, (d) Raman spectroscopy analysis

Acknowledgements

The authors acknowledge the Directorate of Research (DoR) and Centre for Doctoral Studies (CDS), Manipal Academy of Higher Education (MAHE), Manipal, India, for the Intramural Fund and Dr. TMA Pai Scholarship. The authors are grateful to the Director and Administration of Manipal Institute of Technology (MIT), Manipal, for their support and encouragement. We thank the Central Analytical Instrumentation Facility (CAIF) at MIT and the Central Research Facility (CRF) at the National Institute of Technology, Karnataka (NITK) for their support in the characterization studies.

References

[1] S. V. Chauhan, K. K. Joshi, P. M. Pataniya, and C. K. Sumesh, "Advancing industrial rate current density in water electrolysis for green hydrogen production: catalyst development, benchmarking, and best practices," *Sustainable Energy Fuels*, vol. 9, no. 13, pp. 3550–3576, 2025.

[2] Y. Wu *et al.*, "Electron density modulation of $NiCo_2S_4$ nanowires by nitrogen incorporation for highly efficient hydrogen evolution catalysis," *Nat Commun*, vol. 9, no. 1, p. 1425, 2018.

[3] A. Naderi, M. Jourshabani, M. Razi Asrami, and B. Lee, "Bottom-up reconstruction and phase change over nickel–iron layered double hydroxides for boosted electrocatalytic oxygen evolution reaction," *Chemical Engineering Journal*, vol. 484, p. 149111, 2024.

Bridging Photovoltaics and Photoelectrochemistry: Perovskite Photoanodes for Solar-Driven Water Splitting

Vera La Ferrara[1], Rosanna Viscardi[2*], Marco Martino[1], Antonio Marino[1], Giovanni Landi[3], Silvano Del Gobbo[2], Nicola Lisi[2] and Alberto Giaconia[2]

[1] *Energy Technologies and Renewable Sources Department, ENEA Portici Research Center, Portici, (Italy)*
[2] *Energy Technologies and Renewable Sources Department, ENEA Casaccia Research Center, Rome, (Italy)*
[3] *Energy Efficiency Unit Department, ENEA Portici Research Center, Portici (Italy)*

corresponding author: rosanna.viscardi@enea.it

In this study we explore the pathway for integrating halide perovskites into photoelectrochemical (PEC) systems by transforming a photovoltaic-inspired architecture into a self-standing photoanode for solar-driven hydrogen production [1-2]. The work is framed within the broader context where the direct conversion of sunlight into chemical fuels represents a key technological route toward long-term sustainability. While halide perovskites have revolutionized the field of photovoltaics due to their exceptional optoelectronic properties, their translation into photoelectrochemical environments remains challenging, primarily because of interfacial instability and the mismatch between photovoltaic and electrochemical operating conditions. Here, we study that these limitations can be addressed through architectural and interfacial engineering, enabling perovskites to operate as active photoelectrodes for water splitting. Starting from a conventional glass/ITO/SnO_2/perovskite stack, widely used in n–i–p perovskite solar cells, the device is re-engineered to operate directly in alkaline electrolyte, allowing light absorption and water oxidation to occur within the same monolithic structure. In contrast to tandem or photovoltaic-assisted PEC configurations, where a solar cell is externally wired to an electrochemical electrode, this approach exploits the intrinsic photovoltage generated by the perovskite absorber to directly drive anodic reactions at the solid–liquid interface. The elimination of external wiring, separate electrodes and additional power management components significantly simplifies the system, reducing both structural complexity and energetic losses. Such monolithic integration represents an important step toward compact, scalable, and efficient solar fuel devices. The role of interfacial design in governing the transition from photovoltaic to electrochemical functionality will be studied. In a PEC photoanode, the interface between the semiconductor, the conductive substrate, and the electrolyte is not merely a contact region, but where photogenerated charge carriers and catalytic processes converge. Conductive and catalytic interlayers are introduced as functional bridges between the perovskite absorber and the aqueous environment. These interlayers serve multiple purposes: they provide a physical barrier that mitigates direct chemical attack on the perovskite, they facilitate selective hole extraction toward the electrolyte, and they offer catalytic sites for the oxygen evolution reaction (OER). By carefully tuning their composition and thickness, it becomes possible to maintain favorable energetic

alignment with the perovskite valence band while suppressing interfacial recombination pathways. This strategy enables a modular design, in which the perovskite bulk can be optimized primarily for optical absorption, bandgap tuning and carrier transport, while the surface layers are tailored for electrochemical stability and reaction kinetics. The performance of the resulting monolithic photoanodes is evaluated through photoelectrochemical measurements under simulated solar illumination, and by structural, optical, and morphological characterization. The results demonstrate that appropriate interfacial design leads to a substantial enhancement in photocurrent density and a marked reduction in the onset potential for water oxidation. These improvements directly reflect more efficient hole transfer across the solid–liquid interface and reduced recombination losses within the device. Microscopic and spectroscopic analyses reveal that engineered interfaces promote uniform coverage, improved adhesion and more favorable charge transport pathways, all of which contribute to the observed macroscopic performance gains. The study shows that the high photovoltage characteristic of perovskite absorbers can be preserved in a liquid environment when the architecture is properly designed. By bridging the conceptual and technological gap between solar cells and photoelectrodes, this approach contributes to a vision of solar energy conversion, in which light harvesting and chemical transformation are integrated. Such integration is essential for the realization of compact, efficient, and sustainable systems for green hydrogen generation.

Acknowledgements
This research was funded by the European Union – NextGeneration EU from the Italian Ministry of Environment and Energy Security, POR H2 AdP MEES/ENEA with involvement of CNR and RSE, PNRR - Mission 2, Component 2, Investment 3.5 "Ricerca e sviluppo sull'idrogeno", CUP: I83C22001170006

References
[1] A.M.K Fehr, A. Agrawal, F. Mandani, C. L. Conrad, Q. Jiang, S. Y. Park, O. Alley, B. Li, S. Sidhik, I. Metcalf, C. Botello, J. L. Young, J. Even, J. C. Blancon, T. G. Deutsch, K. Zhu, S. Albrecht, F. M. Toma, M. Wong and A. D. Mohite "Integrated halide perovskite photoelectrochemical cells with solar-driven water-splitting efficiency of 20.8%" Nature Communications 14 (2023): 3797.
[2] D. Hansora, J.W. Yoo, R. Mehrotra, W. J. Byun, D. Lim, Y. K. Kim, E. Noh, H. Lim, J. W. Jang, S. I. Seok and J. S. Lee "All-perovskite-based unassisted photoelectrochemical water splitting system for efficient, stable and scalable solar hydrogen production", Nat Energy, 9 (2024): 272–284

On-site hydrogen refueling stations as a strategy to integrate renewables and reduce power curtailment

M. Minutillo[1], A. Cappiello[2], F. Romano[1], S. Di Micco[2], and G. Di Ilio[2]
[1] *University of Salerno, Fisciano, Italy*
[2] *University of Naples Parthenope, Naples, Italy*
simona.dimicco@uniparthenope.it

The rapid deployment of renewable energy sources (RES), particularly solar photovoltaic (PV) and wind power, is a cornerstone of the European Union's decarbonization strategy under initiatives such as REPowerEU [1]. While the increasing penetration of RES contributes to reducing greenhouse gas emissions and dependency on fossil fuels, it also give rises to challenges related to grid management, notably electricity curtailment caused by supply–demand imbalances and network constraints. At the same time, green hydrogen produced via water electrolysis is widely recognized as a key energy vector for decarbonizing the transport sector, especially in applications where battery-electric solutions face limitations. However, the widespread adoption of hydrogen-based mobility critically depends on the availability, sizing, and cost-effectiveness of hydrogen refueling infrastructure.
In this context, the present study investigates the potential synergy between renewable energy curtailment mitigation and hydrogen mobility by assessing the use of curtailed electricity from large-scale PV plants to produce hydrogen directly at on-site hydrogen refueling stations (HRSs). The analysis focuses on passenger fuel cell electric vehicles (FCEVs) in Europe and is framed within the regulatory context defined by Directive 2014/94/EU. Building upon previous work on hydrogen demand and refueling infrastructure planning [2], the study provides a comprehensive assessment combining infrastructure sizing, station-level system design, and renewable energy integration.

The methodology is structured around three main pillars. First, the number of HRSs required to satisfy the hydrogen demand of the European passenger FCEV fleet registered in 2024 is estimated. A reference fleet of approximately 5000 FCEVs is considered [3], assuming an onboard hydrogen storage capacity of 5 kg. Three representative HRS typologies are then analyzed: small (S), medium (M), and large (L), characterized by 1, 2, and 4 dispensers, respectively. These configurations differ in maximum refueling throughput, allowable waiting times, and daily hydrogen dispensing capacity. Based on standardized refueling times and typical operating conditions, the required number of stations is determined for each scenario. Results indicate that, to meet the considered hydrogen demand of passenger vehicles alone, approximately 139 small, 69 medium, or 21 large HRSs would be sufficient, which is in line with the existing European infrastructure (167 publicly accessible HRSs in 2024 [4]).
The second pillar of the study concerns the preliminary design and dynamic modeling of the HRSs. For each station size, a cascade storage system

composed of low-, medium-, and high-pressure banks (400, 650, and 900 bar, respectively) is defined. The stations are designed to refuel the target number of vehicles consecutively without intermediate compression between refueling events, with storage replenishment occurring outside peak operating hours. This design choice aims to minimize system complexity, energy consumption, and capital costs associated with high-power booster compressors.

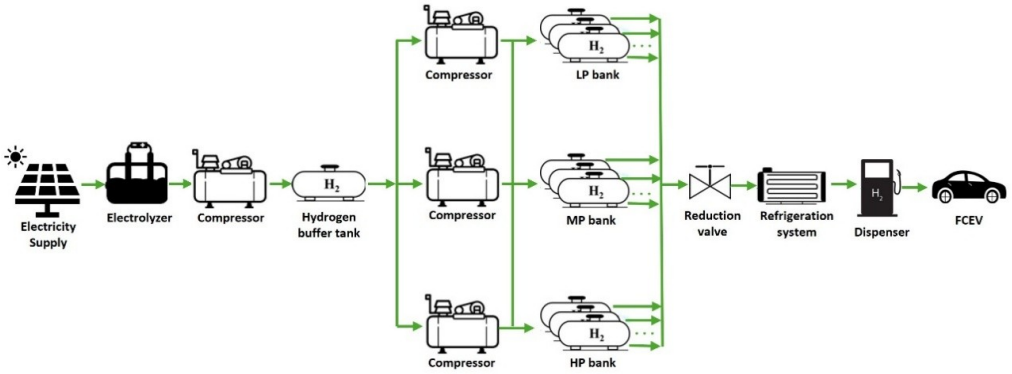

Figure 1. Schematic of the HRS layout with cascade system.

A simplified model of the refueling process is implemented in MATLAB environment. The model is based on mass balance equations and real-gas thermodynamic properties for hydrogen. The refueling dynamics are governed by a prescribed mass flow rate and an average pressure ramp rate compliant with SAE J2601 recommendations, assuming pre-cooled hydrogen delivery. Simulation results provide the required storage volumes, number of storage units, and total hydrogen mass delivered for each HRS configuration. The analysis shows that the selected cascade layouts achieve relatively high hydrogen utilization factors (approximately 0.37–0.39), indicating an effective trade-off between storage capacity and operational flexibility.

The third pillar evaluates the feasibility of supplying the hydrogen demand of the designed HRSs using curtailed renewable electricity. Curtailment is assumed to account for 5% of total PV electricity production, in line with values reported in the literature. A sensitivity analysis is performed considering utility-scale PV plants with nominal capacities ranging from 30 to 300 MW. Two representative European locations—Rome (Italy) and Berlin (Germany)—are selected to capture the impact of different solar irradiance conditions. Monthly PV electricity production is obtained using the PVGIS tool, and the corresponding curtailed energy is converted into hydrogen via electrolysis, assuming a specific electricity consumption of 55 kWh/kg.

The results highlight a strong dependence of hydrogen availability on both PV plant size and geographical location. For small HRSs, a PV plant with a capacity of around 120 MW is generally sufficient to fully cover the annual hydrogen demand using curtailed electricity, particularly in high-irradiance regions such as Southern Europe. In contrast, a 30 MW PV plant can only partially meet the demand, with coverage levels varying seasonally and dropping significantly during winter months. Medium-sized HRSs exhibit similar trends, though requiring larger PV capacities for full coverage. Large HRSs represent the most challenging case: even with a 300 MW PV plant, curtailed energy is typically

insufficient to satisfy the annual hydrogen demand, achieving full coverage only during peak summer periods and primarily in favorable locations.

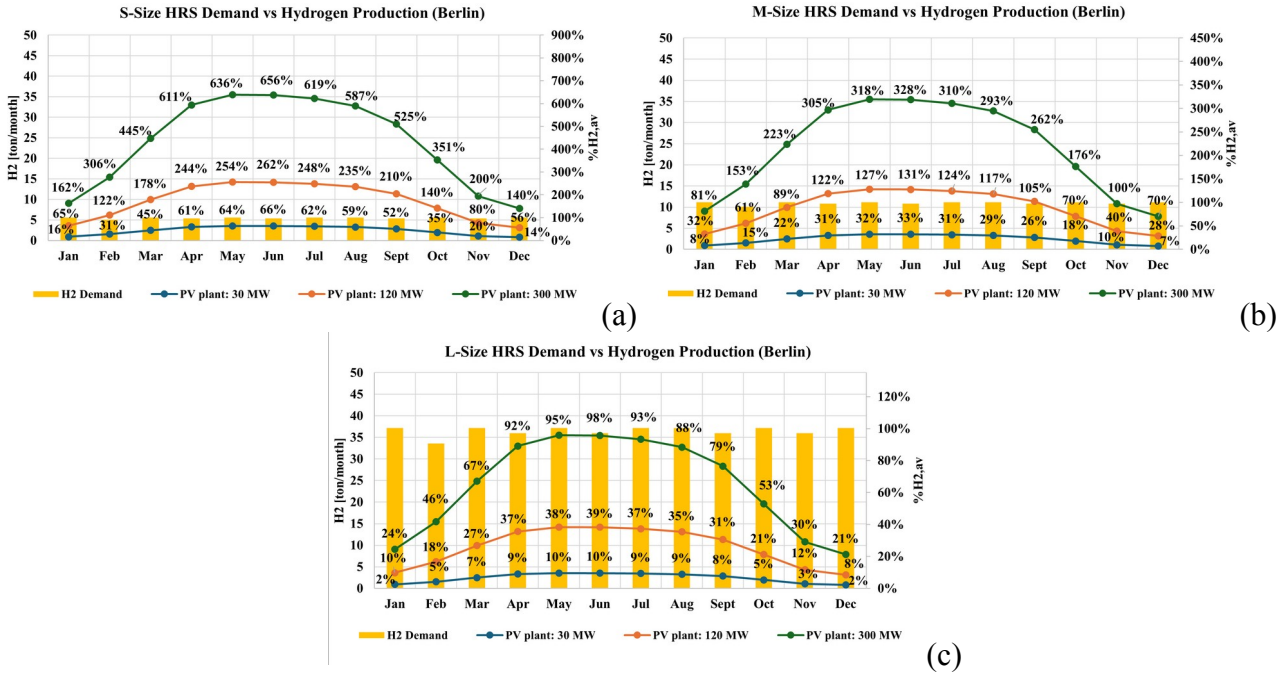

Figure 2. H2 demand vs H2 production in Berlin.

Comparative results between Rome and Berlin show systematically lower hydrogen coverage in the latter due to reduced solar resource availability, emphasizing the importance of site-specific assessments when coupling renewable generation with hydrogen production.

Overall, the study demonstrates that using curtailed renewable electricity for on-site hydrogen production at HRSs can contribute to both mitigating RES curtailment and supporting sustainable mobility. However, the technical viability of this approach strongly depends on the scale of the renewable power plants and is currently more suitable for small- and medium-sized HRSs. For large stations, curtailed energy can only provide a supplementary contribution to hydrogen supply. These findings underline the need for integrated planning of renewable generation, hydrogen infrastructure, and grid management to fully exploit the potential of power-to-hydrogen solutions in future energy systems.

References

[1] M. Siddi, "*Assessing the European Union's REPowerEU plan: energy transition meets geopolitics*". Finnish Institute of International Affairs, 2022.

[2] M. Minutillo, et al., "Analysis of Hydrogen Demand and Refueling Infrastructure in the Road Transportation Sector in Europe" in *Proceedings of 24th EEEIC International Conference on Environment and Electrical Engineering - EEEIC2024*.

[3] European Hydrogen Observatory, "The European hydrogen market landscape" November 2024. https://observatory.clean-hydrogen.europa.eu/.

[4] European Hydrogen Observatory, *"Hydrogen Refuelling Stations". https://observatory.clean-hydrogen.europa.eu/*

Techno-Economic Evaluation of Biohydrogen Production System Utilizing Wastewater Treatment Plant Powered by Floating Photovoltaic

S. Ozgul[1,*], H.G. Ozcan[1], G. Soykan[1] and B.Caglar[2]
[1]Bahcesehir University, Istanbul, Türkiye
[2]Izmir Institute of Technology, Izmir, Türkiye
[*]Corresponding author: sevim.ozgul@bau.edu.tr

Considering the increasing global energy demand, the depletion of fossil fuel resources, and the growing concerns over global warming and environmental pollution, biohydrogen has emerged as a promising alternative energy carrier. Several biohydrogen production technologies have been developed, including bio photolysis, photo fermentation, dark fermentation, and microbial electrolysis cells. Among these, dark fermentation (DF) stands out due to its higher hydrogen production rate, process simplicity, lower net energy input, and ability to utilize low-value wastes as raw materials. According to the literature, most DF studies have been conducted at the laboratory scale, whereas only a limited number of studies have addressed in a pilot-scale industrial applications [1–3]. This gap between laboratory findings and large-scale implementation highlights the need for process modelling and simulation to identify technical and fundamental limitations in biohydrogen production. Nevertheless, research specifically focused on DF-based biohydrogen process modelling remains scarce [4,5]. The aim of this study is to develop a comprehensive process numerical model of biohydrogen production from wastewater treatment plant via dark fermentation to better understand process dynamics and optimize operating conditions for maximum hydrogen yield. Key process parameters, such as pH, temperature, microorganism selection, and hydraulic retention time, affecting hydrogen yield are examined. Additionally, a sensitivity analysis is performed to investigate the influence of critical variables on the overall process. The modelling framework provides insight into the primary technical challenges limiting hydrogen production and establishes a foundation for process optimization.

Building on this process-level understanding, the study further analyzes system-level integration by considering wastewater treatment plants, typically located adjacent to lakes, rivers, or coastal areas, as potential hubs for renewable energy coupling. Given their substantial electricity demand, an integrated DF–floating photovoltaic (FPV) system is considered and evaluated by a comprehensive techno-economic analysis. As land availability constraints drive increasing interest toward offshore and water-based solar deployment, FPV systems provides advantages such as reduced shading and higher effective solar irradiance. However, large-scale implementation faces significant challenges, , including high initial capital expenditure, complex water desalination needs, and demanding marine logistics. Therefore, for

field-scale applications, it is crucial to improve technological components and develop system-level integration and logistics solutions adapted to local conditions.

Keywords: Dark fermentation; hydrogen production; numerical work; waste water treatment plant; floating solar photovoltaics

References

[1] Cavinato, C.; Giuliano, A.; Bolzonella, D.; Pavan, P.; Cecchi, F. Bio-hythane production from food waste by dark fermentation coupled with anaerobic digestion process: A long-term pilot scale experience. Int. J. Hydrogen Energy 2012, 37, 11549–11555.

[2] Ren, N.; Li, J.; Li, B.; Wang, Y.; Liu, S. Biohydrogen production from molasses by anaerobic fermentation with a pilot-scale bioreactor system. Int. J. Hydrogen Energy 2006, 31, 2147–2157.

[3] Jayalakshmi, S.; Joseph, K.; Sukumaran, V. Bio hydrogen generation from kitchen waste in an inclined plug flow reactor. Int. J. Hydrogen Energy 2009, 34, 8854–8858.

[4] Mokhtarani, B.; Zanganeh, J.; Moghtaderi, B**.** A Review on Biohydrogen Production Through Dark Fermentation, Process Parameters and Simulation. Energies 2025, 18, 1092.

[5] Alam, M.; Nayan, N.F., Techno-Economic Assessment of Biohydrogen Production from Dark Fermentation of Wastewater Sludge. 2024, PREPRINT (Version 1) available at Research Square [https://doi.org/10.21203/rs.3.rs-3891939/v1]

Bioengineering and Applied Photosynthesis

A. Freiberg – From UV to IR: Strategies for Complete Solar Energy Capture in Photosynthesis

N. Brady, A. Greenaway, C. Lubner and P. King – Wiring PSI-SMALP thin films to electrodes for light to electricity conversion

T. D. Kim, S. Bhattacharjee, D. Pretorius, J. W. Murray, D. A. Pantazis, and T. Cardona – Evolutionary engineering of photosystem II: From directed evolution to data-driven design

I. Vunderink, A. Cutillas Farray, N. Claassens, M. Barbosa, S. D'Adamo – Artificial Light Harvesting and Metabolic Reprogramming for Enhanced Microalgae-Derived Fuel Production: The SUN-PERFORM Approach.

R. Caferri, E. A. Cutolo, C. Battarra, A. Amelii, L. Dall'Osto and R. Bassi - Spectral re-design of Lhc proteins for engineering photosynthetic light use efficiency

R.Y. Pishchalnikov, D.D. Chesalin, V.A. Kurkov, N.N. Reutskii, A.P. Razjivin - Numerical evaluation of the impact of protein on the optical properties of carotenoids in photosynthetic pigment-protein complexes

From UV to IR: Strategies for Complete Solar Energy Capture in Photosynthesis

***A. Freiberg*[1,2]**
[1] *Institute of Physics, University of Tartu: W. Ostwaldi 1, Tartu, 50411, Estonia*
[2] *Estonian Academy of Sciences: Kohtu 6, Tallinn, 10130, Estonia*
arvi.freiberg@ut.ee

Photosynthesis powers nearly all life on Earth, yet optimizing light energy utilization across the entire solar spectrum remains a key scientific challenge with far-reaching implications for sustainability [1]. While canonical systems capture primarily visible light, a large fraction of solar energy lies in the infrared, and ultraviolet photons—though scarce—can profoundly affect pigment–protein architectures. Here, we investigate how photosynthetic bacteria extend light harvesting across an extraordinary range (200–1100 nm) through a combination of native adaptations and engineered modifications [2]. By resolving the dynamic interplay between pigments [3] and their protein scaffolds, we reveal strategies that push the theoretical limits of photosynthetic efficiency. These insights chart a path toward bioinspired energy technologies capable of leveraging the full breadth of solar radiation.

References

[1] K. Timpmann, M. Rätsep, and A. Freiberg "Enhancing solar spectrum utilization in photosynthesis: exploring exciton and site energy shifts as key mechanisms", Scientific Reports, 13, 2023, 22299.
[2] K. Timpmann, M. Rätsep, E. Jalviste, and A. Freiberg "Tuning by Hydrogen Bonding in Photosynthesis", The Journal of Physical Chemistry B, 128, 2024, 9120-9131.
[3] J. R. Reimers, M. Rätsep, J. M. Linnanto, and A. Freiberg "Chlorophyll spectroscopy: conceptual basis, modern high-resolution approaches, and current challenges", Proceedings of the Estonian Academy of Sciences, 71, 2, 2022, 127-164.

Wiring PSI-SMALP thin films to electrodes for light to electricity conversion

***N. Brady*[1], *A. Greenaway*[1], *C. Lubner*[1] *and P. King*[1]**
[1] *National Laboratory of the Rockies, Golden, Colorado, USA*
Nate.brady@nlr.gov

The extraction of cyanobacterial trimeric Photosystem I (PSI) using amphiphilic copolymers such as styrene maleic acid (SMA) has demonstrated numerous advantages over the typical detergent solubilization approach [1]. The resulting SMA lipid particles (SMALPs) retain ~1,400 native thylakoid lipids (compared to ~30 lipids) and ~16% more antennae chlorophyll compared to the detergent-solubilized complex [2]. This preservation of the native environment of the trimeric PSI complex within SMALPs has demonstrated an ~1,000X faster charge separation event that is lost during detergent solubilization [3]. The work presented here takes this innovation a step further to compress these PSI-SMALPs into oriented and uniform thin-films for incorporation onto electrode surfaces to make biohybrid solar devices. These results will elucidate whether the biophysical enhancements previously reported for PSI-SMALPs translate into higher efficiencies *in fabrica*. PSI-SMALPs were compressed into thin-films using a Langmuir-Blodgett trough, transferred and covalently linked onto gold-coated silicon electrodes for electrochemical analysis. Upon radiation with the equivalent of 1 sun (total irradiance of 86.6 mW/cm2), chronoamperometry of the PSI-SMALP functionalized photoanodes show considerably higher photocurrent generation compared to those incorporating detergent solubilized PSI. This reconstitution of the thylakoid membrane into proteo-lipid thin films *in vitro* also offers a more natural biomimetic system from which we can study yet unresolved phenomena such as: supercomplex formation, changes in PSI oligomeric state, near-field effects arising from the architecture of the uniform PSI array, and interaction dynamics between PSI and the phycobilisome antennae complex.

References

[1] N. G. Brady, M. Li, Y. Ma, J. C. Gumbart, and B. D. Bruce. "Non-detergent isolation of a cyanobacterial photosystem I using styrene maleic acid alternating copolymers", *RSC Advances*, 9, 2019, 31781-31796.
[2] N. G. Brady, S. Qian, J. Nguyen, H. M. O'Neill, and B. D. Bruce. "Small angle neutron scattering and lipidomic analysis of a native, trimeric PSI-SMALP from a thermophilic cyanobacteria", *Biochimica et Biophysica Acta* (*BBA) - Bioenergetics*, 1863, 7, 2022.
[3] D. A. Cherepanov, N. G. Brady, I. V. Shelaev, J. Nguyen, F. E. Gostev, M. D. Mamedov, V. A. Nadtochenko, and B. D. Bruce. " PSI-SMALP, a detergent-free cyanobacterial photosystem I, reveals faster femtosecond Photochemistry", *Biophysical Journal*, 118, 2, 2019, 337-351.

Evolutionary engineering of photosystem II: From directed evolution to data-driven design

***T. D. Kim*[1], *Sinjini Bhattacharjee*[2], *D. Pretorius*[3], *J. W. Murray*[3], *D. A. Pantazis*[2], *and T. Cardona*[1]**

[1] *School of Biological and Behavioural Sciences, Queen Mary University of London, London, United Kingdom*

[2] *Max Planck Institut für Kohlenforschung, Mülheim, Germany*

[3] *Department of Life Sciences, Imperial College London, London, United Kingdom*

t.kim@qmul.ac.uk

Photosynthesis underpins nearly all life on Earth by converting solar energy into chemical potential. At the heart of this process lies photosystem II (PSII), a remarkably complex photochemical engine that catalyses light-driven charge separation and water oxidation, supplying electrons to the photosynthetic electron transport chain (1). Beyond its central biological role, PSII has long been viewed as a blueprint for improving crop productivity, enabling sustainable photochemistry, and powering emerging biohybrid systems (2). Yet, despite decades of mechanistic insight, PSII remains difficult to engineer, owing to its deep integration with cellular viability and its finely tuned evolutionary optimisation.

In the first phase of my work, I established the first directed evolution platform for PSII in a cyanobacterial system, using *Synechocystis* sp. PCC 6803 as a genetically tractable model. Focusing on the D1 reaction centre protein, which provides most ligands for charge separation and water oxidation, I developed an error-prone PCR based platform paired with enhanced natural transformation through a pre-methylation step in *Escherichia coli*, expressing *Synechocystis*-innate methyltransferases. These efforts demonstrated that the applicability of directed evolution to PSII, but also revealed fundamental constraints: because PSII function is hard-wired to growth and survival hence many variants are not very stable.

To overcome these limits, the project geared up towards data-assisted evolutionary engineering. First, D1 protein was used as a test case to evaluate the applicability of high-confidence structure prediction in photosynthesis research. By combining AlphaFold-predicted models with structural phylogenetics, it was shown that evolutionary relationships and functionally relevant variation can be recovered from predicted structures, partially bridging the gap between extensive sequence diversity and the limited availability of experimental PSII structures (3). Building on this, current work combines AlphaFold3-based structure prediction with molecular dynamics simulations to generate synthetic, physics-informed data that map how evolutionary variation reshapes PSII structure, dynamics, and charge separation properties. Starting from a curated set of PSII variants and scaling towards hundreds to thousands of models, this approach aims to create a

sufficiently rich dataset to support future AI and machine learning based design of de novo photosystem II.

Looking ahead, my vision is to integrate these computational designs with targeted directed evolution, closing a loop between evolution, structural dynamics, and experimental validation and optimisation. Rather than promising complete redesign of PSII, this framework seeks to probe the accessible engineering space of one of nature's most sophisticated molecular machines, and to establish general principles for the data-driven engineering of photosynthetic energy conversion.

References

[1] Y. Umena, K. Kawakami, J. R. Shen, N. Kamiya, "Crystal structure of oxygen-evolving photosystem II at 1.9 Å resolution", *Nature*, 473, 7345, 2011, 55–60.
[2] M. Xuan, J. Li. "Photosystem II-based biomimetic assembly for enhanced photosynthesis", *National Science Review*, 8, 8, 2021, nwab051.
[3] T.D. Kim, D. Pretorius, J.W. Murray, T. Cardona, "Exploring the Structural Diversity and Evolution of the D1 Subunit of Photosystem II Using AlphaFold and Foldtree", *Physiologia Plantarum*, 177, 3, 2025, e70284.

Artificial Light Harvesting and Metabolic Reprogramming for Enhanced Microalgae-Derived Fuel Production: The SUN-PERFORM Approach.

Vunderink I[1], Cutillas Farray A[1], Claassens N[1], Barbosa M[1], D'Adamo S[1]*.

[1] *Wageningen University and Research, The Netherlands*

**corresponding author: sarah.dadamo@wur.nl*

Achieving climate neutrality in sectors with intrinsically high energy demands, such as aviation and ocean-going transport, requires transformative advances in the production of sustainable, energy-dense liquid fuels. However, the technological landscape remains fragmented: natural biological routes are constrained by modest biomass productivities and unfavorable energy balances [1, 2], whereas many synthetic and electrochemical approaches have yet to demonstrate robustness at scale. These persistent limitations underscore the need for hybridized systems capable of integrating biological adaptability with engineered photonic efficiency.

The Horizon Europe **SUN-PERFORM** project (https://sunperform.eu) addresses this challenge by developing a biohybrid photoconversion platform that couples nanotechnology-enabled light management with comprehensive metabolic rewiring of microalgal chassis organisms. The overarching research hypothesis is that merging artificial light-harvesting materials with precision synthetic biology can circumvent the fundamental photosynthetic inefficiencies that cap microalgal productivity, thereby enabling markedly elevated fluxes toward lipid biosynthesis. The platform leverages tunable nanomaterials engineered to convert otherwise underexploited segments of the solar spectrum into photosynthetically active radiation, enhancing photon capture and distribution at the reactor scale. In parallel, multi-layered cellular reprogramming strategies introduce a non-native, synthetic, carbon-fixation cycle to complement the canonical Calvin–Benson–Bassham pathway, implement ATP-stabilizing energy-buffering modules to mitigate light-induced energetic fluctuations, and redirect carbon metabolism to favor the accumulation of triacylglycerols [3, 4], the principal molecular precursors for sustainable aviation and maritime fuels. This presentation will outline SUN-PERFORM conceptual foundations, interdisciplinary framework, and initial experimental progress, providing insight into the feasibility and system-level performance of this biohybrid platform.

Acknowledgements

This project research is funded by the European Union (Grant Agreement ID 101172946).

References

[1] Ruiz, J., Olivieri, G., de Vree, J., Bosma, R., Willems, P., Reith, J. H., Eppink, M. H. M., Kleinegris, D. M. M., Wijffels, R. H., Barbosa, M. J. (2016). Towards industrial products from microalgae. *Energy & Environmental Science*, *9*(10), 3036-3043. https://doi.org/10.1039/c6ee01493c
[2] Work, V. H., D'Adamo, S., Radakovits, R., Jinkerson, R. E., Posewitz, M. C. (2012). Improving photosynthesis and metabolic networks for the competitive production of phototroph-derived biofuels. *Curr Opin Biotechnol*, *23*(3), 290-297. https://doi.org/10.1016/j.copbio.2011.11.022
[3] Munoz, C. F., Sudfeld, C., Naduthodi, M. I. S., Weusthuis, R. A., Barbosa, M. J., Wijffels, R. H., D'Adamo, S. (2021). Genetic engineering of microalgae for enhanced lipid production. *Biotechnol Adv*, *52*, 107836. https://doi.org/10.1016/j.biotechadv.2021.107836
[4] Sudfeld, C., Kiyani, A., Wefelmeier, K., Wijffels, R. H., Barbosa, M. J., D'Adamo, S. (2023). Expression of glycerol-3-phosphate acyltransferase increases non-polar lipid accumulation in Nannochloropsis oceanica. *Microb Cell Fact*, *22*(1), 12. https://doi.org/10.1186/s12934-022-01987-y

Spectral re-design of Lhc proteins for engineering photosynthetic light use efficiency

R. Caferri[1], E. A. Cutolo[2], C. Battarra[1], A. Amelii[1], L. Dall'Osto[1] & R. Bassi[3,4]

[1] *University of Verona, Verona, Italy*
[2] *University Federico II, Naples, Italy*
[3] *Stazione Zoologica Anton Dohrn, Naples, Italy*
[4] *Accademia Nazionale dei Lincei, Rome, Italy*
roberto.caferri@univr.it

Traditional crop breeding has reached its maximum potential for increasing plant yield. Modern genetic engineering offers additional opportunities to enhance productivity by the rational optimization of photosynthesis. Light availability and spectral distribution are the primary evolutionary constraint for photosynthetic organisms and has driven the diversification of their light-harvesting antenna systems. However, modern agricultural practices impose highly specific light environments to which crop species have not yet fully adapted their photosynthetic machinery. In high-density crop systems, light distribution is heterogeneous, with both spectral quality and intensity varying across canopy depth, thereby reducing overall light-use efficiency. Improving sunlight-to-biomass conversion may therefore be achieved by genetically tuning the photosynthetic apparatus to efficiently absorb a broader spectrum of photons.

Previous studies have identified the structural and biophysical determinants underlying long-wavelength light absorption in a subset of eukaryotic photosystem I antenna proteins, where nature of chromophore ligand favours the formation of low-energy chlorophyll clusters[1,2]. In this work, we focused on photosystem II antenna proteins, specifically the monomeric CP29 and the trimer-forming Lhcb1/LhcbM1, from the higher plant *Arabidopsis thaliana* and the unicellular alga *Chlamydomonas reinhardtii*. Starting from knockout lines[3,4], we complemented the corresponding genotypes with either the wild-type (WT) gene or single-point mutants targeting candidate residues. Specifically, histidine or asparagine axial ligands coordinating two chlorophyll *a* molecules (a609/a5 and a612/a2) were reciprocally exchanged.

We report the *in vivo* expression and *ex vivo* spectroscopic characterization of plant and algal CP29 and LHCII trimers harbouring novel chlorophyll–chlorophyll interactions generated through the modulation of excitonic coupling within two distinct, symmetrically arranged pigment dimers. Results show that: (1) these mutations do not compromise protein stability, allowing WT-like accumulation levels; (2) absorption spectra in the Q_y region are shifted either toward shorter (blue) or longer (far-red) wavelengths, depending on the specific mutation; (3) the effect of the H→N substitution on the a603/a5 pigment cluster is conserved across species, indicating strong intra- and interspecific conservation; (4) the spectral effects of individual mutations are additive; (5) in Lhcb1 mutants, absorption shifts are detectable directly in

intact leaves, with a 2 nm blue shift or a 1 nm far-red shift of the Q_y maximum relative to WT, depending on the mutation considered (Figure 1); and (6) fluorescence lifetimes are markedly shortened in the a5 H→N mutant, likely reflecting altered chlorophyll–carotenoid distance and/or orientation within this pigment cluster.

Although the magnitude of the spectral shifts is limited, these results demonstrate the feasibility of extending the absorption range of plant and algal antenna systems through targeted mutagenesis. Moreover, the conserved response of the a603/a5 cluster suggests that H→N substitutions at homologous sites could be applied to antenna proteins from other organisms with similar results. Finally, the additive nature of the observed effects indicates that by combining multiple mutations may further enhance the spectral tuning, as long as the protein stability is maintained.

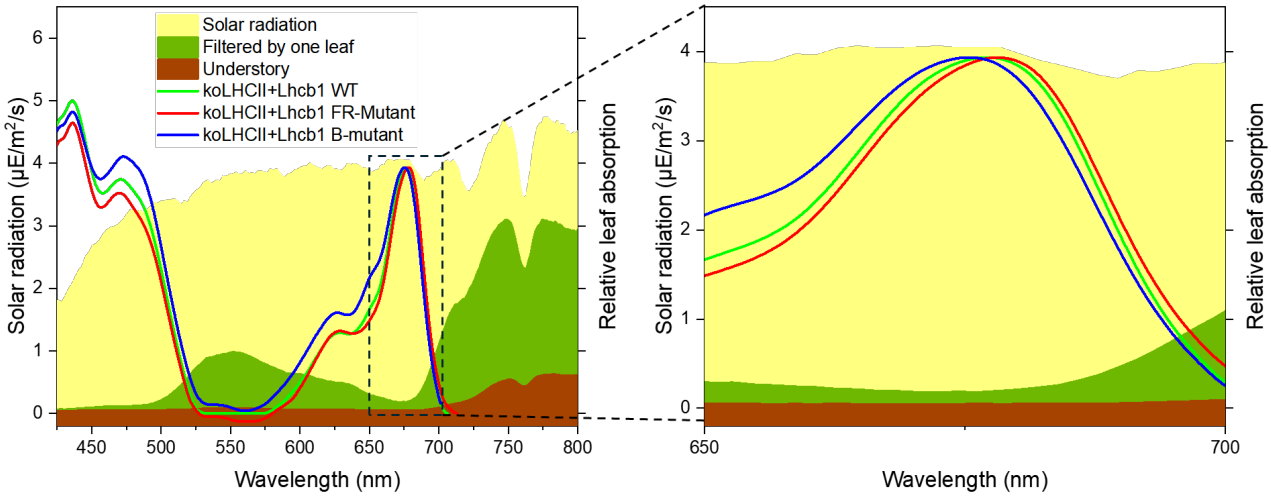

Figure 1: Light spectra in three different environments (full sun solar spectrum in yellow, solar radiation filtered by one leaf in green, and the understory spectrum in brown) are overlaid on the leaf absorption spectra of koLHCII complemented with the Lhcb1 WT sequence or with Lhcb1 mutated to shift absorbance toward the blue or far-red regions (represented by light green, blue, and red, respectively).

Acknowledgements

This work was funded by the European Commission, ERC Advanced Grant, Project GrInSun, grant agreement No 101053983.

References

[1] T. Morosinotto, J. Breton, R. Bassi, & R. Croce. The nature of a chlorophyll ligand in Lhca proteins determines the far red fluorescence emission typical of photosystem I. Journal of Biological Chemistry, 278(49), 2003, 49223-49229.

[2] S. Capaldi, Z. Guardini, D. Montepietra, V. F. Pagliuca, A. Amelii, E. Betti, C. John, L. Pedraza-Gonzalàlez, L. Cupellini, B. Mennucci, D. M. V. Bonnet, A. Chaves-Sanjuan, L. Dall'Osto & R. Bassi. Structural determinants for red-

shifted absorption in higher-plants Photosystem I. *New Phytologist*, *248*(5), 2025, 2331-2346.
[3] S. de Bianchi, N. Betterle, R. Kouril, S. Cazzaniga, E. Boekema, R. Bassi & L. Dall'Osto, L. Arabidopsis mutants deleted in the light-harvesting protein Lhcb4 have a disrupted photosystem II macrostructure and are defective in photoprotection. *The Plant Cell*, *23*(7), 2011, 2659-2679.
[4] Z. Guardini, L. Dall'Osto, R. L. Gomez, R. Caferri, P. Joliot, & R. Bassi. Mapping light-harvesting and photoprotection responses in the Photosystem II antenna system of higher plants. *Plant Physiology*, *199*(4), 2025, kiaf588.

Numerical evaluation of the impact of protein on the optical properties of carotenoids in photosynthetic pigment-protein complexes

***R.Y. Pishchalnikov*[1], *D.D. Chesalin*[2], *V.A. Kurkov*[1], *N.N. Reutskii*[3], *A.P. Razjivin*[4]**

[1] *Prokhorov General Physics Institute of the Russian Academy of Sciences, Moscow, Russia*

[2] *Lomonosov Moscow State University, Faculty of Biology, Moscow, Russia*

[3] *Lomonosov Moscow State University, Faculty of Physics, Moscow, Russia*

[4] *Belozersky Research Institute of Physico-Chemical Biology, Moscow State University, Moscow, Russia*

rpishchal@kapella.gpi.ru

The photosynthetic pigment-protein complexes contain cofactors whose physical and chemical properties are strongly dependent on the local protein environment. One way to model their quantum behavior, is to perform *ab initio* simulations that consider the spatial arrangement of atoms and molecules within the complex and variety of interactions between them. However, these calculations can be resource-intensive and may not always provide an accurate assessment of the processes. We propose a combined approach to estimate the optical properties of these pigment-protein complexes, based on semiclassical theory and evolutionary optimization [1-4]. The key element of this approach is the spectral density function (SDF), which is modeled by fitting of the experimental data based on the multimode Brownian oscillator model. The SDF contains information about the vibrational modes of the molecule and their effective interaction energy with electronic transition. Each mode can be associated with either a particular chemical bond or a residual.

To study the properties of the electronic transitions of a pigment in the visible range, polar and nonpolar solvents are often used to perform the spectroscopy measurements. Carotenoids are very sensitive to the local surrounding and this effect can be estimated by determining the Huang-Rhys factor for the modes of different frequencies. As the result, the obtained SDF can be regarded as a characteristic function describing the degree of electron-phonon interaction for each vibronic mode with an electronic transition.

To demonstrate our methodology, we used the spectra of light-harvesting complexes (LH1) of *Rh. rubrum* (wildtype) containing the carotenoid spirilloxanthin and a carotenoid-free mutant (G9). Comparing the spectra, we obtained the absorption of spirilloxanthin in the LH1 protein. Thus, by simulating the absorption of this carotenoid in solvent (benzene) and in the light-harvesting complex, we can analyze the features of the electron-phonon interaction specific to different carotenoid environments.

The simulation results are shown in Figures 1 and 2. The thin lines in the figures are carotenoid absorption spectra after the first generations of the evolutionary algorithm. The thick black line represents experimental data, and the blue line with round markers represents the final calculated spectrum,

which has the smallest discrepancy from the experimental one. Thus, by comparing the quantum parameters, particularly the Huang-Rhys factors, we can evaluate the degree of activity of the vibrational modes of the molecule for a given environment.

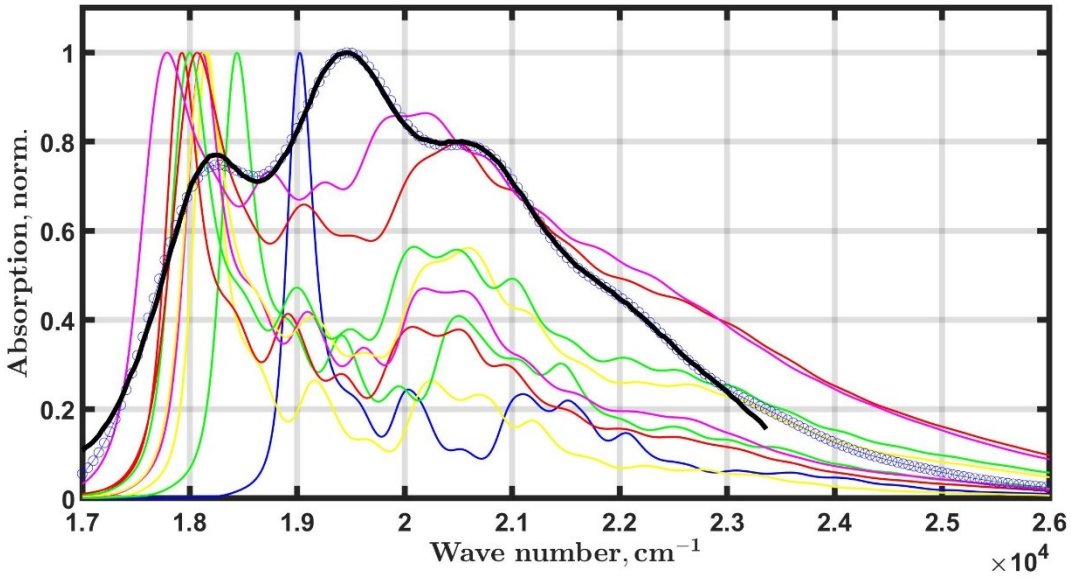

Figure 1: Spirilloxanthin in LH1 from *Rh. rubrum*

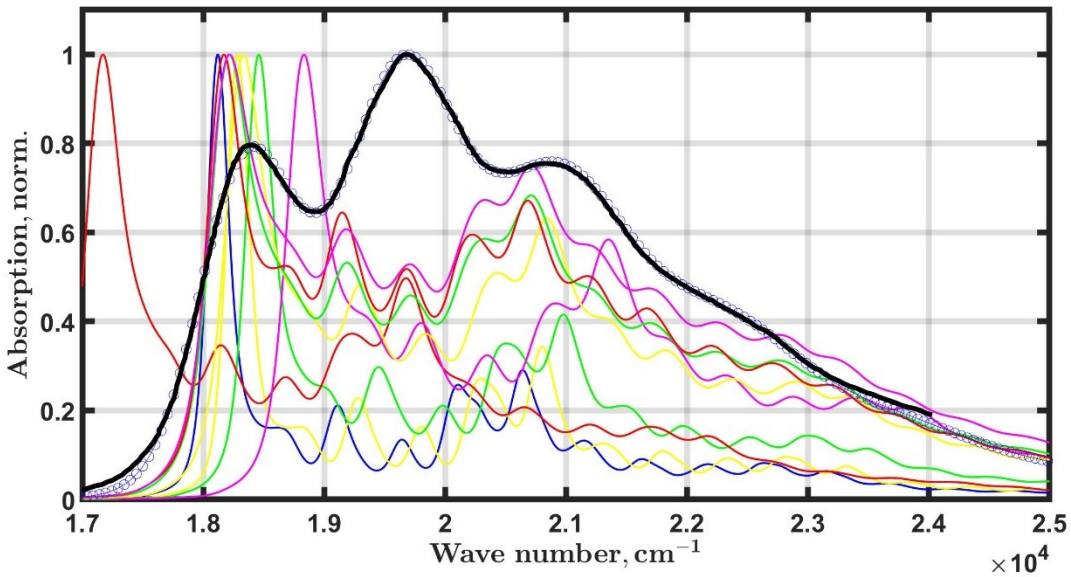

Figure 2: Spirilloxanthin in benzene.

Acknowledgements
This research was supported by the Russian Science Foundation (RSF no. 25-21-00375, https://rscf.ru/en/project/25-21-00375/)

References

[1] D.D. Chesalin, E.A. Kulikov, I.A. Yaroshevich, E.G. Maksimov, A.A. Selishcheva, R.Y. Pishchalnikov, "Differential evolution reveals the effect of polar and nonpolar solvents on carotenoids: A case study of astaxanthin optical response modeling", *Swarm and Evolutionary Computation*, 75, 2022, 101210, doi: 10.1016/j.swevo.2022.101210
[2] R.Y. Pishchalnikov, I.A. Yaroshevich, D.V. Zlenko, G.V. Tsoraev, E.M. Osipov, V.A. Lazarenko, E.Y. Parshina, D.D. Chesalin, N.N. Sluchanko, E.G. Maksimov, "The role of the local environment on the structural heterogeneity of carotenoid β-ionone rings", *Photosynthesis research*, 156, 1, 2023, 3-17, doi: 10.1007/s11120-022-00955-2
[3] R.Y. Pishchalnikov, D.D. Chesalin, V.A. Kurkov, A.P. Razjivin, S.V. Gudkov, A.A. Grishin, A.S. Dorokhov, A.Y. Izmailov, "Classification of Fungal Pigments by Simulating Their Optical Properties Using Evolutionary Optimization", *Mathematics*, 12, 23, 2024, 3844, doi: 10.3390/math12233844
[4] D.D. Chesalin, R.Y. Pishchalnikov, "A local minima escape procedure to improve the convergence of differential evolution", *Applied Soft Computing*, 171, 2025, 112753, doi: 10.1016/j.asoc.2025.11275

Fuel Cells

P.K. Lan, P.Y. Lin, and C.J. Tseng – Ultrasonically refined NiCuO as a thin decomposition layer for enhanced ammonia cracking and fuel-tolerant PCFC performance

D.F.M. Santos, D.S. Falcão, A.M.F.R. Pinto, and R.B. Ferreira - Development and characterization of a hydrogen proton exchange membrane fuel cell system designed for use in unmanned aerial vehicles

V. Monfreda, L. Spiridigliozzi, A. Vendittelli, F. Milano, L. Ferrigno and G. Dell'Agli – A new bixbyite-structured high entropy oxide as possible electrolyte in Solid Oxide Cells (SOC)

G. Grossi, F. Arpino, E. Caracci, G. Cortellessa, G. Ficco, and M. Tomasso – Numerical modelling of a Solid Oxide Fuel Cell with anode degradation effects

Ultrasonically refined NiCuO as a thin decomposition layer for enhanced ammonia cracking and fuel-tolerant PCFC performance

P.K. Lan[1], P.Y. Lin[1], and C.J. Tseng[2,3,4]
[1] *Department of Mechanical Engineering, National Central University, Taoyuan, Taiwan*
[2] *Institute of Energy Engineering, National Central University, Taoyuan, Taiwan*
[3] *Hydrogen Energy Research Center, National Central University, Taoyuan, Taiwan*
[4] *Research Center for Critical Issues, Academia Sinica, Tainan, Taiwan*
cjtseng@ncu.edu.tw

This study employs an ultrasonic process to refine NiCuO particles and applies the resulting fine powder as an additional anode decomposition layer (ADL) on top of a coarse-particle NiCu ADL, thereby constructing a hierarchical bilayer ADL architecture to enhance ammonia cracking and interfacial reaction kinetics on the fuel side. Electrochemical measurements were conducted at 800 °C using H_2/NH_3 mixed fuels with varying NH_3 fractions (0, 25, 50, 75, and 100%) to evaluate performance and impedance characteristics. As shown in Fig. 1, the peak power density decreased only slightly from 2350 to 2190 mW cm^{-2} with increasing NH_3 content, demonstrating that the refined-particle NiCu ADL effectively mitigates the impact of fuel-composition variations on overall output. Impedance analysis further reveals that increasing NH_3 content increases the impedance contributions in both the high frequency and low frequency ranges, while a mid frequency relaxation initially indistinct progressively separates and becomes more pronounced. This behavior implies that ammonia cracking and hydrogen-supply processes introduce additional time constants and polarization components. Nevertheless, within the bilayer ADL configuration, the amplified impedance does not lead to abrupt performance collapse, indicating that the fine-particle layer provides a higher density of catalytically active sites, thereby improving in situ NH_3 to H_2 conversion and stabilizing fuel-side interfacial reactions. Overall, the thin ADL derived from ultrasonically refined NiCuO offers an effective and scalable fuel-side interfacial engineering strategy for maintaining robust power stability in PCFCs operated with H_2/NH_3 mixed fuels, while also establishing a basis for frequency-resolved analysis of ammonia-related polarization mechanisms.

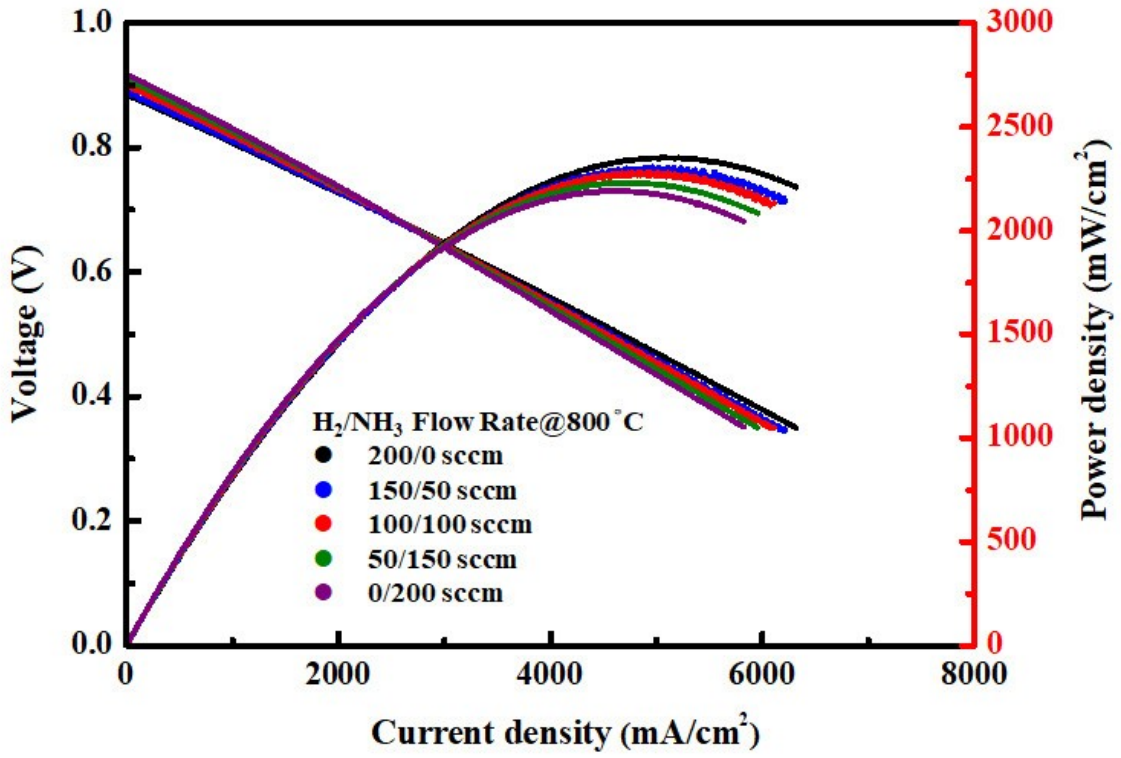

Figure 1: I–V and power-density characteristics of the PCFC measured at 800 °C under H_2/NH_3 mixed fuels with a total flow rate of 200 sccm.

Acknowledgements
The authors thank National Science and Technology Council of Taiwan for supporting this research work.

Development and characterization of a hydrogen proton exchange membrane fuel cell system designed for use in unmanned aerial vehicles

***D.F.M. Santos*[1], D.S. Falcão[1], A.M.F.R. Pinto[1], and R.B. Ferreira[1]**
[1] *CEFT-Transport Phenomena Research Center, ALiCE – Associate Laboratory in Chemical Engineering, Faculty of Engineering, University of Porto, Rua Dr. Roberto Frias, 4200-465 Porto, Portugal*
diogosantos@fe.up.pt

Unmanned aerial vehicles (UAVs) are autonomously or remotely controlled flying vehicles [1] that, due to their mobility and detection capabilities, can be used in several applications such as medical supply delivery, mapping, structure inspection, military missions, and others.
UAVs are generally powered by internal combustion engines (ICEs) or electric motors using batteries. However, ICEs have a high thermal and noise signatures and are environmentally harmful [2], while batteries have low energy density, resulting in limited flight time, and slow charging [3].
Hydrogen proton exchange membrane fuel cells (PEMFCs) have emerged as an alternative, offering high energy density, fast refuelling, low environmental impact, high efficiency and low weight [4].
Due to the strict weight and size constraints of UAV applications, the design and operation of the PEMFC system are of particular importance. In this work, a 30-cell PEMFC system was designed, manufactured and characterized envisioning UAV application.

The developed 30-cell PEMFC has an active area of 25 cm^2 per cell, weights around 1.3 kg, and has overall dimensions of 17 × 12 × 8 cm. This PEMFC operates with an open-cathode and dead-end anode configuration to minimize weight and ensure compactness. In addition to the PEMFC, the balance of plant (BOP), including the auxiliary components and the electronic controller, was also developed in-house to provide a ready-to-use power supply system.
The system was comprehensively evaluated, including an analysis of its electrical, thermal and efficiency characteristics, the integration of a small auxiliary battery for peak-power demands, and a flight simulation based on real UAV load data to assess applicability in a realistic scenario.

The system performance was first evaluated using polarization curves. The PEMFC delivered a power output of around 180 W, which translated into about 160 W of usable system power after accounting for BOP consumption.
To evaluate the PEMFC operationality for longer periods of time, the system was operated continuously at fixed voltages for 20 min. If no significant drop in the current was observed, the voltage was reduced and the stability reassessed.

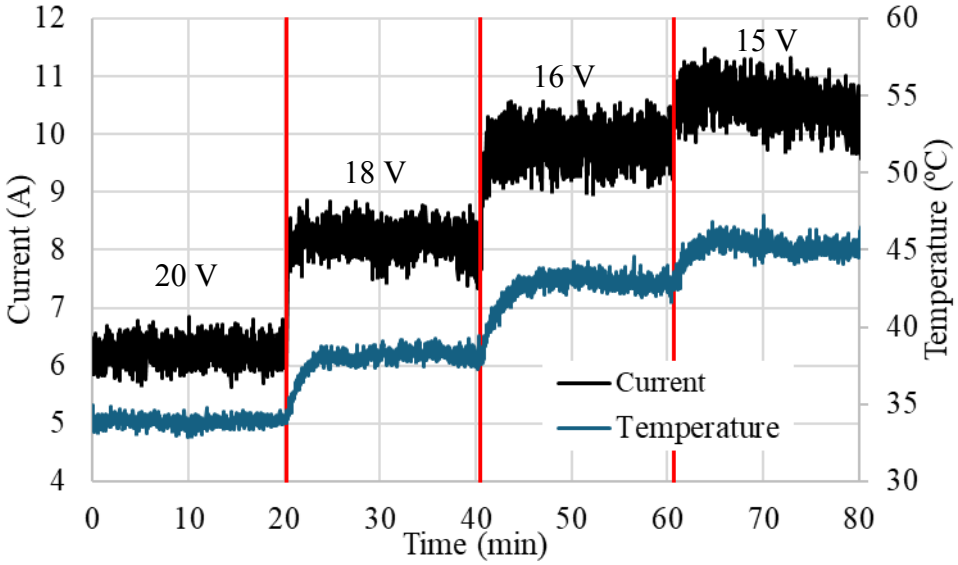

Figure 1: PEMFC current and temperature stability at different operating voltages.

As shown in Figure 1, the PEMFC operated stably until 16 V (around 10 A). However, at 15 V, a decrease in the produced current was observed, from 10.1-11.0 A to 9.7-10.6 A during the 20 min test, indicating that continuous operation below 16 V is not feasible. This performance drop appears to be related to the elevated temperatures reached (around 45 ºC) which caused membrane drying, increasing ohmic losses.

The system exhibited a maximum efficiency of 39 %, lower than expected due to the excessive temperatures, which reduced performance at high loads. At maximum efficiency, 47 % of the input hydrogen energy was lost as heat, 8 % as unreacted hydrogen and 6% due to BOP consumption.

An auxiliary battery was successfully integrated into the system to provide additional power during high-demand phases of a UAV flight. When the system current was suddenly increased from 0 to 15 A (simulating UAV take-off), the PEMFC initially supplied only 55 % of the required power, with the rest being supplied by the battery. During this step, the PEMFC current gradually increased and reached 70 % by the end of the phase. This demonstrated that the auxiliary battery is essential not only for peak-power support but also for improving system responsiveness.

To evaluate system operability under realistic conditions, a power profile based on an actual UAV flight was applied. The system successfully met the power requirements, and the current response during this test can be seen in Figure 2. During this dynamic test the PEMFC performance was generally higher than during the polarization curves, likely due to more favourable temperature and humidification conditions.

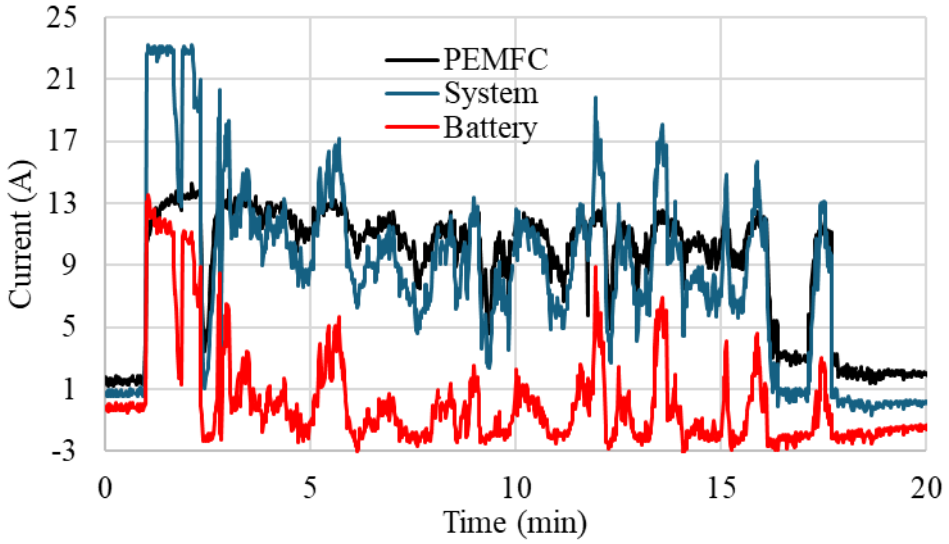

Figure 2: Current variation of the PEMFC, battery and global system during the flight simulation test.

Acknowledgements
This work is a result of Agenda "Aero.Next Portugal", nr. C645727867-00000066, investment project nr. 31, financed by the Recovery and Resilience Plan (PRR) and by European Union - NextGeneration EU. This work was supported by national funds through FCT/MECI: CEFT, UID/00532/2025 (https://doi.org/10.54499/UID/00532/2025) and UID/PRR/00532/2025 (https://doi.org/10.54499/UID/PRR/00532/2025) and ALiCE, LA/P/0045/2020 (https://doi.org/10.54499/LA/P/0045/2020).

References
[1] M.N. Boukoberine, Z. Zhou, M. Benbouzid, "A critical review on unmanned aerial vehicles power supply and energy management: Solutions, strategies, and prospects", Applied Energy, 255, 2019, 113823.
[2] B. Wang, D. Zhao, W. Li, Z. Wang, Y. Huang, Y. You, S. Becker, "Current technologies and challenges of applying fuel cell hybrid propulsion systems in unmanned aerial vehicles", Progress in Aerospace Sciences, 116, 2020, 100620.
[3] C. Zhang, Y. Qiu, J. Chen, Y. Li, Z. Liu, Y. Liu, J. Zhang, C.S. Hwa, "A comprehensive review of electrochemical hybrid power supply systems and intelligent energy managements for unmanned aerial vehicles in public services", Energy and AI, 9, 2022, 100175.
[4] Y. Wang, D.F. Ruiz Diaz, K.S. Chen, Z. Wang, X.C. Adroher, "Materials, technological status, and fundamentals of PEM fuel cells – A review", Materials Today, 32, 2020, 178-203.

A new bixbyite-structured high entropy oxide as possible electrolyte in Solid Oxide Cells (SOC)

***V. Monfreda*[1], *L. Spiridigliozzi*[1], *A. Vendittelli*[2], *F. Milano*[2], *L. Ferrigno*[2] *and G. Dell'Agli*[1]**

[1] *Department of Civil and Mechanical Engineering, University of Cassino and Southern Lazio, Cassino (FR), Italy*

[2] *Department of Electrical and Information Engineering, University of Cassino and Southern Lazio, Cassino (FR), Italy*

viviana.monfreda@unicas.it

The recently discovered class of high-entropy oxides (HEOs) [1] is receiving considerable attention from researchers worldwide for a wide range of potential applications, including catalysis [2], lithium-ion batteries electrodes [3], etc. In this context, one of the most interesting areas explored is the application of HEOs as possible materials for SOCs, as a result of their electrical behaviour, recently investigated for example in high-entropy bixbyites and fluorites [5]. In the present study, a Rare-Earth based high entropy bixbyite, whose composition is $(Ce_{0.2}Zr_{0.2}Yb_{0.2}Er_{0.2}Nd_{0.2})_2O_{3+\delta}$ was synthesized via a simple coprecipitation route, followed by calcination at 1250 °C to stabilize the single bixbyite phase and subsequently its electrochemical behaviour was investigated by Electrochemical Impedance Spectroscopy (EIS).

The raw materials used for the preparation of the material were $RE(NO_3)_3 \cdot xH_2O$ (where RE = Ce, Yb, Er, Nd and x = 5 or 6) and $ZrO(NO_3)_2$; the coprecipitation synthesis cycle was carried out as follows: (i) two aqueous solutions containing stoichiometric amounts of the selected nitrate salts and a proper amount of ammonium carbonate granting a molar ratio [anions]/[total cations] equal to 2.5 were prepared; (ii) the solutions were mixed together to let co-precipitation occur (magnetic stirring was applied upon precipitation); (iii) the obtained precipitate was recovered by vacuum filtration and dried overnight at 60 °C. The as-synthesized powder is amorphous in nature (see Fig. 1) and, by calcination at 1250 °C for 1 h, the formation of the single bixbyite phase was achieved (see Fig. 1), according to the predictor proposed by the authors in [6], as all the reflections present in Fig. 1 can be associated to a pure bixbyite-like crystal structure (strongest peaks are marked with Miller Indices in Fig. 1). The lattice parameter of the bixbyite unit cell, extracted from diffraction data, is equal to 1.073 nm, which results in a theoretical density equal to 7.33 g/cm^3.

Pellets obtained by uniaxial pressing of the powders were then sintered in air at 1300 °C for 3 hours, i.e. relatively mild sintering conditions. The bulk density of the pellets, measured by using the Archimedes method, was found to be essentially identical to the theoretical density, indicating a nearly complete densification. Consistently, the microstructure of the sintered body observed by SEM fully supports this conclusion, being characterized by the absence of porosity and by limited grain growth resulting in an average grain size on the order of 0.5 µm.

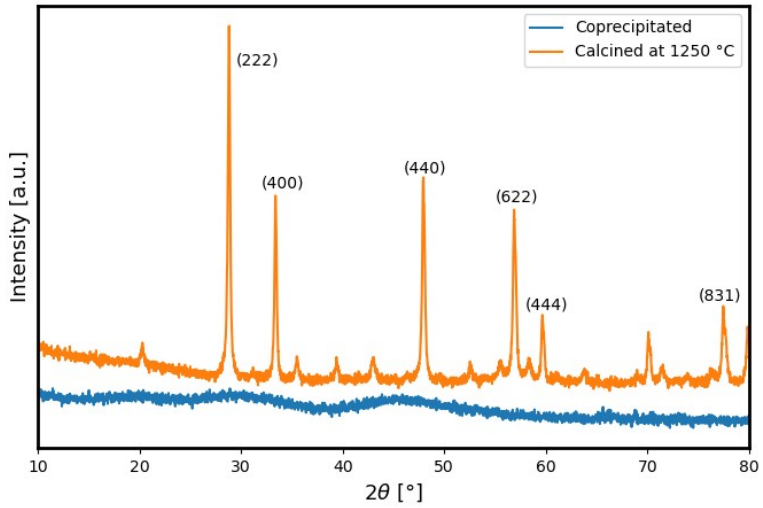

Figure 1 XRD patterns of samples coprecipitated and calcined at 1250 °C

Finally, the electrochemical behaviour of the sintered pellet was investigated through EIS, to evaluate its total conductivity at temperatures ranging from 400 °C to 800 °C, i.e. the typical intermediate temperature range for SOC. The impedance responses, presented as Nyquist plots at different temperatures, are displayed in Fig. 2. The shape of the plots suggests the presence of an electronic contribution in the electrical conductivity, in addition to a ionic contribution. Bixbyite structure can be considered as a defective fluorite, with a large amount of oxygen vacancies but characterized by a limited mobility due to their ordering. Actually, the ionic conductivity in bixbyite structure is due to the motion of oxygen anions in interstitial position, a phenomenon well established [6]; indeed, the doping of ZrO_2 in a bixbyite lattice introduces such interstitial anions according to the following defect equation:

$$2ZrO_2 \xrightarrow{RE_2O_3} 2Zr'_{RE} + 3O_O^x + O_i''$$

The electronic conductivity, instead, may be attributed to p-type transport arising from small-polaron formation. This behaviour results from the interaction with atmospheric oxygen, which oxidises Ce^{3+} to Ce^{4+}, as illustrated by the following defect reaction:

$$\frac{1}{2}O_2(g) + V_O^{\cdot\cdot} + 2Ce_{Ce}^x \rightarrow 2Ce'_{Ce} + O_O^x$$

where Ce'_{Ce} represents the small polaron characterized by the defect of a negative charge. Based on that, and considering the presence of a non-blocking electrode, the semicircles displayed in Fig. 2 fully refer to the behaviour of the electrolyte. Indeed, analysing them by fitting the experimental data using an equivalent electrical model based on the well-known Randles circuit, the values of the associated capacitance (around 115 pF for all the temperatures) confirms that. The total electrical conductivity has been calculated for all the investigated temperatures, ranging between 8.4×10^{-3} S/m at 400 °C and 3.5×10^{-2} S/m at 800 °C. The conductivity data are all well aligned in an Arrhenius plot (not shown here) and the corresponding slope, i.e.

the activation energy of the electrical conduction, is around 0.35 eV, a rather low value consistent with the mechanism of small-polaron transport.
In conclusion, $(Ce_{0.2}Zr_{0.2}Yb_{0.2}Er_{0.2}Nd_{0.2})_2O_{3+\delta}$ exhibiting bixbyite structure was synthesized and sintered at a nearly full densification at mild sintering conditions. The presence of Zr and Ce in the system introduces specific point defects able to increase in a great extent the total electrical conductivity of the material, resulting in a product potentially interesting for SOC electrolytes. In view of potential applications of this material, it needs to determine both the ionic and electronic transport numbers, and this is currently an ongoing research activity.

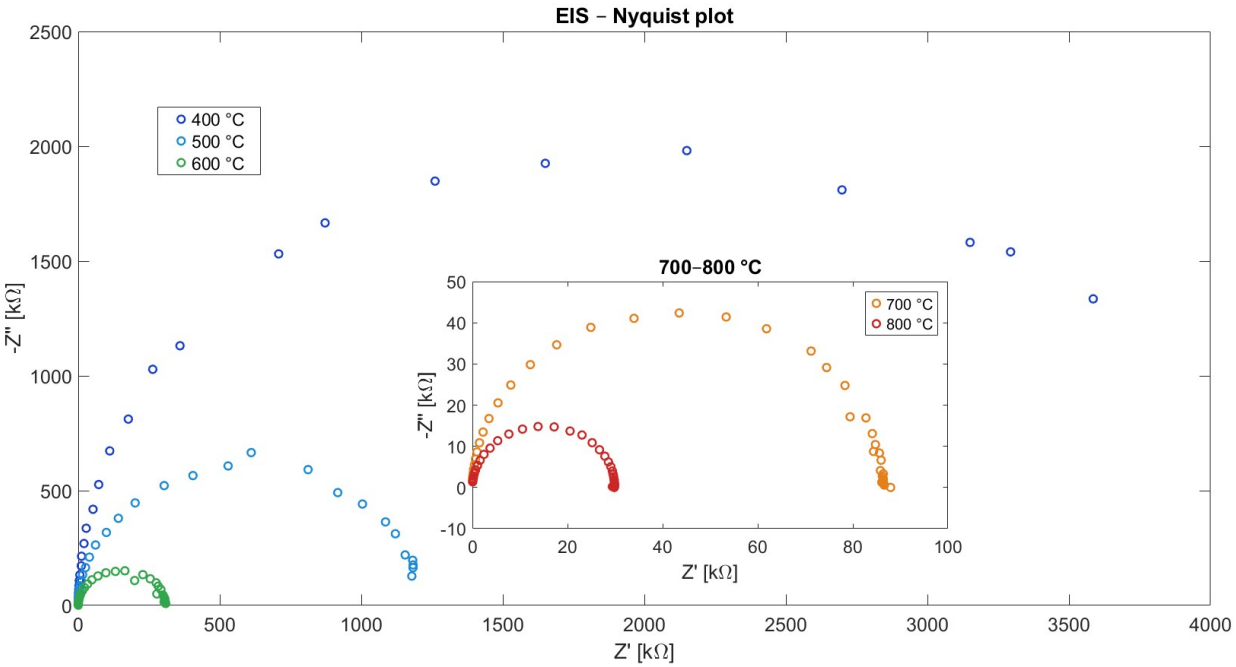

Figure 2: Nyquist plot at various temperature (A).

References

[1] C.M. Rost, et al. Entropy-stabilized oxides. *Nat. Commun.*, 6(1), 8485, 2015.
[2] A. Mancuso, et al. Engineered synthesis of a novel bixbyite-structured high-entropy oxide $(Ce_{0.2}Zr_{0.2}Yb_{0.2}Er_{0.2}Gd_{0.2})_2O_{3.4}$ as a stable and high-performing visible-light-active photocatalyst for multifunctional pollutant degradation, *J. Alloys Compd.*, 1026, 180435, 2025.
[3] N. Qiu, et al. A high entropy oxide $(Mg_{0.2}Co_{0.2}Ni_{0.2}Cu_{0.2}Zn_{0.2}O)$ with superior lithium storage performance, *J. Alloys Compd.*, 777, 2019, 767-774.
[4] K. Hou, et al. The effects of configuration-entropy and aliovalent-doping on the electrical and stability properties of bixbyite oxides, *J. Eur. Ceram. Soc.*, 45(11), 117378, 2025.
[5] L. Spiridigliozzi, et al. A simple and effective predictor to design novel fluorite-structured High Entropy Oxides (HEOs). *Acta Mater* 202, 2021, 181-189.
[6] M.R. Levy et al. Defect chemistry of doped bixbyite oxides. *Solid State Sci.*, 9(7), 2007, 588-593.

Numerical modelling of a Solid Oxide Fuel Cell with anode degradation effects

***G. Grossi*[1,2], *F. Arpino*[1,2], *E. Caracci*[1,2], *G. Cortellessa*[1,2], *G. Ficco*[1,2], *and M. Tomasso*[1,2]**

[1] *Department of Civil and Mechanical Engineering, University of Cassino and Southern Lazio, Cassino, FR, Italy*

[2] *European University of Technology EUt+, European Union*

giorgio.grossi@unicas.it

The increasing global energy demand, together with the need to mitigate associated greenhouse gas emissions, calls for intensive research efforts aimed at improving the efficiency of existing energy conversion systems. In this context, fuel cells (FCs) represent a promising technology, as they enable the direct conversion of the chemical energy of fuels into electrical energy, thereby avoiding the efficiency limitations and environmental drawbacks typical of conventional thermochemical conversion systems. Among the different FC technologies, solid oxide fuel cells (SOFCs) are particularly attractive due to their high operating temperatures, which (i) allow the use of less expensive catalyst materials, (ii) enable fuel flexibility, including hydrogen-enriched natural gas (H_2NG), and (iii) offer cogeneration capabilities [1–3]. Moreover, reversible solid oxide cells (rSOCs), operating alternately in fuel cell and steam electrolysis modes and employing green H_2 as both a fuel and a storage medium, represent a highly promising solution for energy storage and conversion.

Despite the significant progress achieved in recent years, SOFCs still face major challenges related to performance degradation and long-term durability [4]. For economic viability and large-scale industrial deployment, degradation rates should be below 0.5%/kh, whereas current values typically range between 1 and 3%/kh. These large values are ascribed to different aging phenomena promoted by the high operating temperature, mostly related to atoms self-diffusion or inter-diffusion between the cell constituents [4–6].

A comprehensive understanding of SOFC degradation mechanisms requires detailed insight into the coupled mass, momentum, heat, chemical species, and electric charge transport, as well as into the electrochemical reactions occurring within the cell. Achieving such a level of detail through experimental approaches alone is challenging. Advanced numerical simulation techniques, and in particular Computational Fluid Dynamics (CFD), enable a detailed analysis of the spatial distribution of relevant variables not only within the gas channels, but also across the porous electrodes and the electrolyte. When properly validated against experimental data, these models represent a powerful tool for investigating local phenomena and supporting the design of more efficient and reliable SOFC systems.

Building on the above context, the present study focuses on the mathematical and numerical modelling of an anode-supported SOFC. Experimental data available for a commercial cell, operated at 1023 K and fed with 3000 ml/min

of air and 500 ml/min of a H_2–N_2 (60/40 composition) fuel mixture in co-flow configuration, were adopted to calibrate and validate the models.
The analysed cell, experimentally characterized in terms of polarization curve and anode species concentration, has an active area of 9 × 9 cm² and consists of: a Ni-YSZ anode with a thickness of 258.64 µm, a YSZ electrolyte of 8.35 µm, and a LSCF-LSC cathode of 42.45 µm, separated from the electrolyte by an intermediate GDC layer. The current collector is made of a nickel mesh.
Based on the available experimental data, a 0D electrochemical model was developed to simulate the current–voltage (i–V) characteristic of the cell, accounting for both electrochemical reactions and gaseous species transport. This model enabled the calibration of the electrode kinetic parameters (i.e., charge transfer coefficients and exchange current densities), by fitting the polarization curve.
The calibrated parameters were subsequently implemented in a 3D CFD model of the cell, developed using the finite volume-based Ansys Fluent 2024 R2 software and the SOFC addon module for the resolution of electrochemical phenomena [7]. The CFD model was validated in terms of global performance by comparison with the experimental polarization curve, and in terms of hydrogen mole fraction in the anode channel, showing average deviations of 0.28% and 5.41%, respectively.
Finally, the 0D model was employed to perform preliminary analyses of the impact of Ni coarsening on cell performance. Microstructural evolution of the Ni–YSZ cermet is indeed recognized as one of the main factors responsible for the overall performance degradation of SOFCs: the coarsening of the Ni phase, which occurs during high-temperature operation, leads to a reduction in the TPB length density, significantly affecting cell performance. In this study, the anode degradation was analysed using the model developed within the framework of the AD-ASTRA project (H2020, FCH2-JU, G.A. No. 825027) [8].
Simulations were carried out at three different temperatures (i.e., 973 K, 1023 K, and 1073 K), and for 10000 and 20000 hours of operation. Results show a decrease of the voltage drop with increasing operating temperature, in agreement with data reported in the scientific literature [4].
The outcomes of this work provide a solid foundation for future developments, which will focus on integrating the degradation model into the validated CFD tool. This integrated approach will enable detailed investigations of local degradation effects and allow the extension of numerical simulations to transient operating conditions.

References

[1] Arpino F, Massarotti N. Numerical simulation of mass and energy transport phenomena in solid oxide fuel cells. Energy 2009;34:2033–41. https://doi.org/10.1016/j.energy.2008.08.025.
[2] Mauro A, Arpino F, Massarotti N. Three-dimensional simulation of heat and mass transport phenomena in planar SOFCs. International Journal of Hydrogen Energy 2011;36:10288–301. https://doi.org/10.1016/j.ijhydene.2010.10.023.

[3] Arpino F, Massarotti N, Mauro A, Vanoli L. Metrological analysis of the measurement system for a micro-cogenerative SOFC module. International Journal of Hydrogen Energy 2011;36:10228–34. https://doi.org/10.1016/j.ijhydene.2010.11.016.
[4] Hubert M, Laurencin J, Cloetens P, Morel B, Montinaro D, Lefebvre-Joud F. Impact of Nickel agglomeration on Solid Oxide Cell operated in fuel cell and electrolysis modes. Journal of Power Sources 2018;397:240–51. https://doi.org/10.1016/j.jpowsour.2018.06.097.
[5] Lay-Grindler E, Laurencin J, Villanova J, Cloetens P, Bleuet P, Mansuy A, et al. Degradation study by 3D reconstruction of a nickel–yttria stabilized zirconia cathode after high temperature steam electrolysis operation. Journal of Power Sources 2014;269:927–36. https://doi.org/10.1016/j.jpowsour.2014.07.066.
[6] Monaco F, Hubert M, Vulliet J, Ouweltjes JP, Montinaro D, Cloetens P, et al. Degradation of Ni-YSZ Electrodes in Solid Oxide Cells: Impact of Polarization and Initial Microstructure on the Ni Evolution. J Electrochem Soc 2019;166:F1229–42. https://doi.org/10.1149/2.1261915jes.
[7] Ghorbani B, Vijayaraghavan K. 3D and simplified pseudo-2D modeling of single cell of a high temperature solid oxide fuel cell to be used for online control strategies. International Journal of Hydrogen Energy 2018;43:9733–48. https://doi.org/10.1016/j.ijhydene.2018.03.211.
[8] Laurencin J, Bianchi F, Polverino P, Pianese C, Pandolfi A, Leon A, et al. AD ASTRA Deliverable D5.3 "Final version of performance and RUL prediction models including Probabilistic degradation functions with validated accelerating factors and multiple model prognosis". 2022.

Crop stress physiology

L. Ferroni, E. Aliprandi, A. Aquilano, R. Tassinari, M. Živčak, M. Brestič, and E. Marrocchino - Altered leaf elementome in chlorophyll-deficient wheat mutants

A. Pashayeva, I. Zulfugarov, C-H Lee, and I. Huseynova - Thylakoid protein phosphorylation drives photosystem plasticity and stress acclimation in crop plants

M.S. Shabanova, S.K.Zharmukhamedov, S.I. Allakhverdiev - Effects of a newly synthesized copper complex $[CuL_2]Br_2$ on the functional activity of photosystem II (online)

Altered leaf elementome in chlorophyll-deficient wheat mutants

L. Ferroni[1], E. Aliprandi[1], A. Aquilano[1], R. Tassinari[2], M. Živčak[3], M. Brestič[3,4], and E. Marrocchino[1]

[1] *Department of Environmental and Prevention Sciences, University of Ferrara, Ferrara, Italy*

[2] *Department of Physics and Earth Sciences, University of Ferrara, Ferrara, Italy*

[3] *Institute of Plant and Environmental Sciences, Faculty of Agrobiology and Food Resources, Slovak University of Agriculture, Nitra, Slovakia*

[4] *College of Life Science, State Key Laboratory of Wheat Improvement, Shandong Agricultural University, Taian, China*

lorenzo.ferroni@unife.it

Synthesis of chlorophylls and assembly of the photosynthetic machinery require a set of metal ions, which are classified as macro- and micronutrients for the plant and are available in the soil for the plant absorption. Beside Mg included in the chlorophyll ring, Ca, Fe, Cu and Mn are structural constituents or cofactors of enzymes or photosynthetic proteins. Their deficiency unavoidably affects plant metabolism and results invariably in a chlorotic phenotype. If elemental deficiencies lead to complex and not completely understood (dys)regulation of chlorophyll synthesis and photosynthesis, the same could be conceivably valid on the opposite sense: does deregulation of chlorophyll synthesis and/or photosynthesis bring about alterations of a leaf's elementomic profile? Actually, global changes in leaf elemental profile following an altered photosynthetic metabolism are probable, but hardly predictable.

This work investigates if a partially impaired chlorophyll synthesis due to genetic mutations results in an imbalanced elemental composition of leaves. To test this hypothesis, eight well-characterized lines of bread (wild-type NS-67 and its mutants ANBW-4A, ANBW-4B, ANK-32A) or durum wheat (wild-type LD-222 and its mutants ANDW-7A, ANDW-7B, ANDW-8A), which differ in their chlorophyll accumulation were analysed [1-3]. The experiment was conducted in plants cultivated at the Botanical Garden of the University of Ferrara, Italy. After the tillering phase, the youngest mature leaves were analysed. The photosynthetic phenotype was characterised by means of chlorophyll quantification, fast chlorophyll *a* fluorimetry and multiparametric MultiSpeQ spectrometry. The same leaves were sampled and analysed for the high-throughput elemental profile by Triple Quadrupole Inductively Coupled Plasma Mass Spectrometry (ICP-MS QQQ). For reference, the geochemical composition of soil samples was also analysed combining ICP-MS QQQ and X-ray fluorescence (XRF).

The photosynthetic phenotyping confirmed already reported features of the mutants, i.e., beside lower levels of chlorophylls, also smaller trans-thylakoidal proton-motive force and NPQ but enlarged pool size of electron carriers [1-3]. The set of photosynthetic parameters was treated with principal component analysis to order the phenotypes of the wheat lines and compare the phenotype severity with the global leaf elementome. Although the leaf

elemental profile was species-specific of either bread or durum wheat, a negative correlation linked photosynthetic phenotype severity and Mg content across all lines. Analysing separately the leaf elementome of bread and durum wheat lines, an enrichment in Mg, Al, P and rare earth elements (REEs) was found in the mutants. For a more straightforward comparison, REEs concentrations in leaves were normalized to the corresponding concentrations in soil. In general, the abundance of REEs in the wild-type lines closely matched the relative concentrations in soil, with a bioconcentration factor in the order of 10^{-3}. Only exceptions were a selective enrichment in europium (Eu) and, conversely, a depletion in thulium (Tm). Fractionation of REEs leading to a positive Eu anomaly was already reported for wheat [4]. However, interestingly, in the leaves of the mutants, REEs were more concentrated and the uptake selectivity, positive for Eu and negative for Tm, got lost.
Collectively, we have obtained evidence that a deregulation of chlorophyll synthesis, particularly a chlorophyll deficiency accompanied by functional alterations of the photosynthetic membrane, results in adjustments of the global leaf elementomic profile, including the pattern of REEs.

References

[1] M. Živčak, M. Brestič, L. Botyanszka, Y.E. Chen, S.I. Allakhverdiev "Phenotyping of isogenic chlorophyll-less bread and durum wheat mutant lines in relation to photoprotection and photosynthetic capacity", Photosynthesis research, 139(1), 2019, 239-251.
[2] L. Ferroni, M. Živčak, O. Sytar, M. Kovár, N. Watanabe, S. Pancaldi, C. Baldisserotto, M. Brestič "Chlorophyll-depleted wheat mutants are disturbed in photosynthetic electron flow regulation but can retain an acclimation ability to a fluctuating light regime", Environmental and Experimental Botany, 178, 2020, 104156.
[3] L. Ferroni, M. Živčak, M. Kovár, A. Colpo, S. Pancaldi, S.I. Allakhverdiev, M. Brestič "Fast chlorophyll *a* fluorescence induction (OJIP) phenotyping of chlorophyll-deficient wheat suggests that an enlarged acceptor pool size of Photosystem I helps compensate for a deregulated photosynthetic electron flow", Journal of Photochemistry and Photobiology B: Biology, 234, 2022, 112549.
[4] D.I.N.G. Shi-Ming, T. Liang, C.S. Zhang, W.A.N.G. Li-Jin, S.U.N. Qin "Accumulation and fractionation of rare earth elements in a soil-wheat system", Pedosphere, 16(1), 2006, 82-90.

Thylakoid protein phosphorylation drives photosystem plasticity and stress acclimation in crop plants

Aynura Pashayeva[1], Ismayil Zulfugarov[1], Choon-Hwan Lee[2], and Irada Huseynova[1]

[1] Institute of Molecular Biology, Ministry of Science and Education of the Republic of Azerbaijan, Baku, Azerbaijan

[2] Department of Molecular Biology, Pusan National University, Busan, Republic of Korea

aynurapashayeva@gmail.com, i_guseinova@mail.ru

Photosynthetic performance in plants is continually challenged by fluctuating environmental conditions, such as excessive light and salinity, which disrupt excitation energy balance and compromise photosystem stability. To prevent photodamage and maintain efficiency, plants rely on rapid acclimation mechanisms involving reversible modification of thylakoid membrane proteins and dynamic reorganization of photosynthetic complexes. While phosphorylation-dependent thylakoid plasticity has been well characterized in model species and rice [1], its conservation or diversification across major crop lineages remains unclear.

In this study, we conducted a comparative investigation of thylakoid phosphorylation dynamics and photosystem remodeling in two staple cereals, rice (*Oryza sativa*) and wheat (*Triticum aestivum*), exposed to abiotic stress. Using physiological assays, native gel electrophoresis, and phosphoprotein profiling, we examined stress-induced changes in phosphorylation patterns, photosystem supercomplex stability, and photoprotective responses. Both species displayed increased phosphorylation of PSII core and LHCII proteins, accompanied by rearrangements in thylakoid supercomplex organization. However, wheat exhibited distinct kinetic profiles, including prolonged retention of phosphorylated LHCII assemblies under sustained stress conditions. These modifications correlated closely with species-specific adjustments in non-photochemical quenching and energy distribution between photosystems. Notably, differential accumulation of phospho-proteins within specific LHCII populations in wheat suggests a fine-tuned mechanism for maintaining photosynthetic connectivity under adverse conditions, differing from the more transient response observed in rice.

Together, our findings highlight thylakoid protein phosphorylation as a central mechanism integrating photosystem organization, energy dissipation, and stress adaptation. This comparative perspective advances our understanding of photosynthetic resilience in crops and provides insight into species-specific strategies that may be exploited for improving stress tolerance.

Reference

[1] Pashayeva, A., Wu, G., Huseynova, I., Lee, C.H., Zulfugarov, I. S. "Role of thylakoid protein phosphorylation in energy-dependent quenching of chlorophyll fluorescence in rice plants". International journal of molecular sciences, 22(15), 2021, 7978.

Effects of a newly synthesized copper complex $[CuL_2]Br_2$ on the functional activity of photosystem II

***M.S. Shabanova*[1*] , S.K.Zharmukhamedov[2], S.I. Allakhverdiev[1,3,4]**
[1]Ministry of Science and Education of the Republic of Azerbaijan Institute of Molecular Biology Public Legal Entity of the, Baku AZ1073, Azerbaijan
[3] Institute of Basic Biological Problems, FRC PSCBR Russian Academy of Sciences, Pushchino 142290, Russia
[4] Controlled Photobiosynthesis Laboratory, K.A. Timiryazev Institute of Plant Physiology, Russian Academy of Sciences, Botanicheskaya Str. 35, Moscow 127276, Russia
mehriban_shabanova@mail.ru

Herbicides continue to play a key role in ensuring sustainable agricultural production, remaining the most effective tool for weed control. At the same time, the widespread and prolonged use of a limited range of active substances is accompanied by an increase in weed resistance, as well as the accumulation of chemical compounds in soil and aquatic ecosystems, which leads to a serious environmental problem (Dayan & Duke, 2020).

Photosynthesis is a complex biological process in which solar energy is converted into the energy of chemical bonds. As an essential process for the survival of all photosynthetic organisms, photosynthesis represents an important target for inhibitory compounds (Karacan et al., 2021).To date, numerous chemical substances have been identified that can inhibit key stages of photosynthesis. However, compounds that affect only specific metabolic pathways in plants often prove to be insufficiently effective due to the development of resistance. Therefore, the development of universal inhibitors capable of simultaneously targeting multiple vital processes represents a promising strategy for overcoming resistance. In addition, chemical compounds are widely used as tools for studying the mechanisms of photosynthetic reactions.

Various chemical compounds have been investigated as inhibitors of the photosynthetic electron transport chain, including organic ligand complexes with metals and semimetals (Fe, Pb, Co, Ni, Cr, Zn). Many of these metals and semimetals, as well as their free ions, exhibit high reactivity and can participate in diverse chemical interactions. However, their application is limited by low solubility in hydrophobic media, which may prevent them from effectively reaching their biological targets and exerting inhibitory effects on plant growth.

Copper is an essential trace element involved in a number of physiological processes in plants, including electron transfer reactions, photosynthetic metabolism, and antioxidant protection. However, exceeding physiologically permissible concentrations of copper leads to toxic effects

accompanied by impaired photosynthetic activity, generation of reactive oxygen species, and damage to photosystem II protein complexes. According to current data, photosystem II exhibits significantly higher sensitivity to Cu(II) ions compared to photosystem I, which is associated with disruption of the oxygen-evolving complex, the reaction center, and the processes involved in the reduction of primary electron acceptors (Sharma et al., 2020).

In this study, the newly synthesized copper-based complex $[CuL_2]Br_2$ was investigated to evaluate its potential inhibitory effects on the photosynthetic apparatus. These effects were examined using photosystem II–enriched thylakoid membranes isolated from spinach leaves (*Spinacia oleracea* L.) according to a method similar to the one described previously (Khorobrykh & Ivanov, 2002). For the experiment, solution with photosystem II were incubated in the presence of Cu(II) complex before measurements. Then, changes in chlorophyll fluorescence yield were measured by using a pulse-amplitude modulated fluorimeter (XE-PAM, Heinz Walz, Germany) equipped with Power Graph Professional 3.3 software (DiSoft). In parallel, the rate of oxygen evolution was determined using a Clark-type oxygen electrode (Hansatech Instruments Ltd., Norfolk, UK).

During the experiments, it was found that the $[CuL_2]Br_2$ complex (1) suppresses the rate of photoinduced oxygen evolution; (2) does not act as an artificial electron acceptor on the acceptor side of photosystem II (Q_A); and (3) under steady-state conditions, lowers the F_M level due to a decrease in the variable fluorescence (Fv) of photosystem II.

Based on the results obtained, it was suggested that the main effect on the photochemical activity of photosystem II is probably due to the interaction of the inhibitory agent with the reaction center, leading to some conformational changes in its structure. Further research using other methods is needed to obtain a more accurate answer.

References.

1. Dayan, F. E., & Duke, S. O. (2020). Natural compounds as next-generation herbicides. *Plant Physiology, 184*(2), 483–499.
2. Sharma, A., Shahzad, B., Rehman, A., Bhardwaj, R., Landi, M., & Zheng, B. (2020). Response of phenylpropanoid pathway and the role of polyphenols in plants under abiotic stress. *Molecules, 25*(11), 2452.
3. Khorobrykh, S. A., & Ivanov, B. N. (2002). Oxygen reduction in a plastoquinone pool of isolated pea thylakoids. *Photosynthesis Research, 71*(3), 209–219.

Life Cycle Assessment

S. Sofi, R. Albanese, A. Nicita, G. Maggio, S. Trocino, M. Giorgianni – Life Cycle Thinking of a Photoelectrolysis Cell for Green Hydrogen Production

S.K.R. Maddula, J. Dufour, and D. Iribarren – A framework for micro-to-macro decision support in hydrogen-based transport systems

Life Cycle Thinking of a Photoelectrolysis Cell for Green Hydrogen Production

***S. Sofi*, R. Albanese, A. Nicita, G. Maggio, S. Trocino, M. Giorgianni**
CNR - ITAE, Messina, Italy
soniasofi@cnr.it

Objectives

Our multi-stakeholder engagement research, conducted at a territorial level in the Nebrodi region (North-East of Sicily), revealed several factors influencing the acceptance of hydrogen technologies within the potential realisation of a local hydrogen economy. As resulted, the reduction of economic costs and the possible environmental benefits are considered to be fundamental drivers of this acceptance. For this reason, we decided to conduct in-depth research into these two dimensions in the context of a novel photoelectrolysis cell — a technology that could play a significant role in the deployment of green hydrogen.
This analysis includes the results of research carried out within the framework of the "Piano Triennale di realizzazione 2022-2024 della Ricerca di Sistema Elettrico Nazionale". It consists of a Life Cycle Assessment (LCA), performed according to ISO 14040/44 standards [1-2] and an Environmental LCC (eLCC) [3] analysis of a novel photoelectrolysis cell, using a cradle-to-gate approach to help designers make environmentally sustainable and economically viable choices.
The calculations were performed on a laboratory prototype cell having an area of 10 cm^2, and then scaled up to a commercial cell of 80 cm^2.

Methods

The aforementioned local multi-stakeholder engagement research involved conducting eleven semi-structured interviews with actors from academia, government, industry and civil society (Quadruple Helix Model) [4]. This research was useful in identifying two key aspects of hydrogen social acceptance to investigate: economic costs and environmental benefits.
The LCA was conducted using SimaPro 9.6 [5] with Ecoinvent 3 data [6] and the ReCiPe 2016 Midpoint (H) method [7]. The functional unit comprised a single assembled cell, incorporating an anode on FTO glass, a cathode, a polymer membrane and a PVDF casing.
The LCC analysis encompassed the calculation of capital expenditures (CAPEX) and operating expenditures (OPEX). In particular, the Net Present Value (NPV) was calculated to assess the economic viability of the investment.
The eLCC was based on the "Environmental Price" (EP) approach, which expresses the willingness to pay for less pollution in euros per kilogram of pollutant [8] considering Climate change category.

Results

The results indicate that climate change, human toxicity and terrestrial ecotoxicity are the most relevant impact categories (see Fig. 1). The primary areas of concern relate to the anode process and fluoropolymer materials, due

to the high energy consumption and production of fluorinated compounds. Membrane, casing and assembly stages contribute less significantly. In order to enhance the environmental performance of the cell, it is recommended that energy use during thermal treatments be reduced and that low-impact materials be adopted. Despite the low technology readiness level (TRL), the study simulated a realistic production and commercialisation process.
The analysis assumed a semi-artisanal production, with production volumes not exceeding 4,000 units per year. The target market includes not only industry, but also research institutions commissioning cells for experiments. The NPV calculation showed that the break-even point is reached within 3.5 years (see Fig. 2).
Considering externalities as additional costs affecting the production value of the photoelectrolysis cell, the incidence of each cost category is as follows:

- Capex 91.98%
- Opex 7.94%
- Climate change (EP) 0.08%.

Conclusions

The study highlights the need to reduce the energy intensity of anode fabrication and to replace fluoropolymers with lower-impact materials, steering the development of photoelectrolytic cells toward more sustainable and scalable technologies.
The product and production process under investigation can be defined as virtuous and sustainable in terms of environmental impact, representing an investment with a good potential return in purely economic terms.

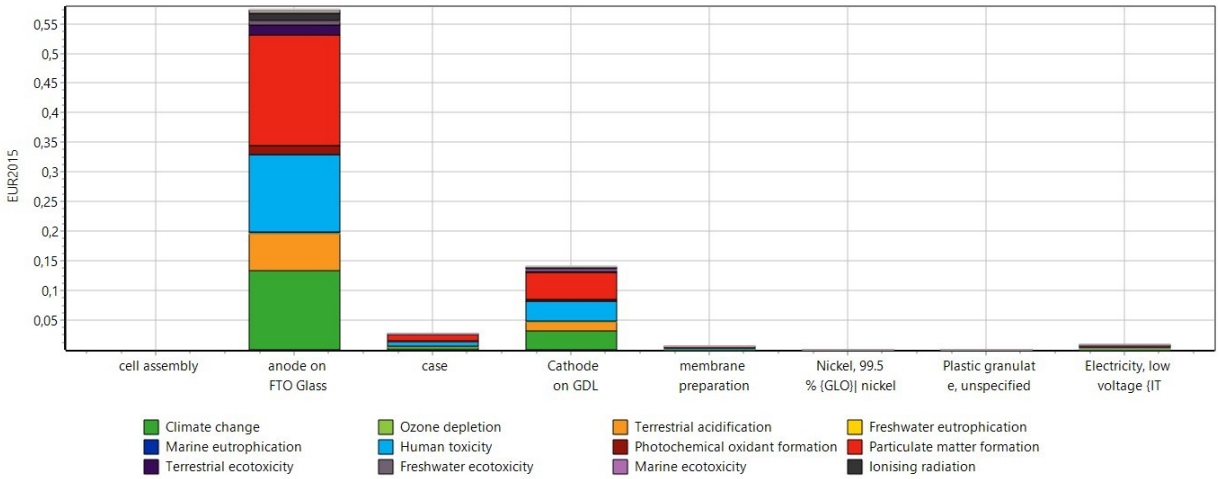

Figure 1: Environmental Price Method results of the photoelectrolysis cell.

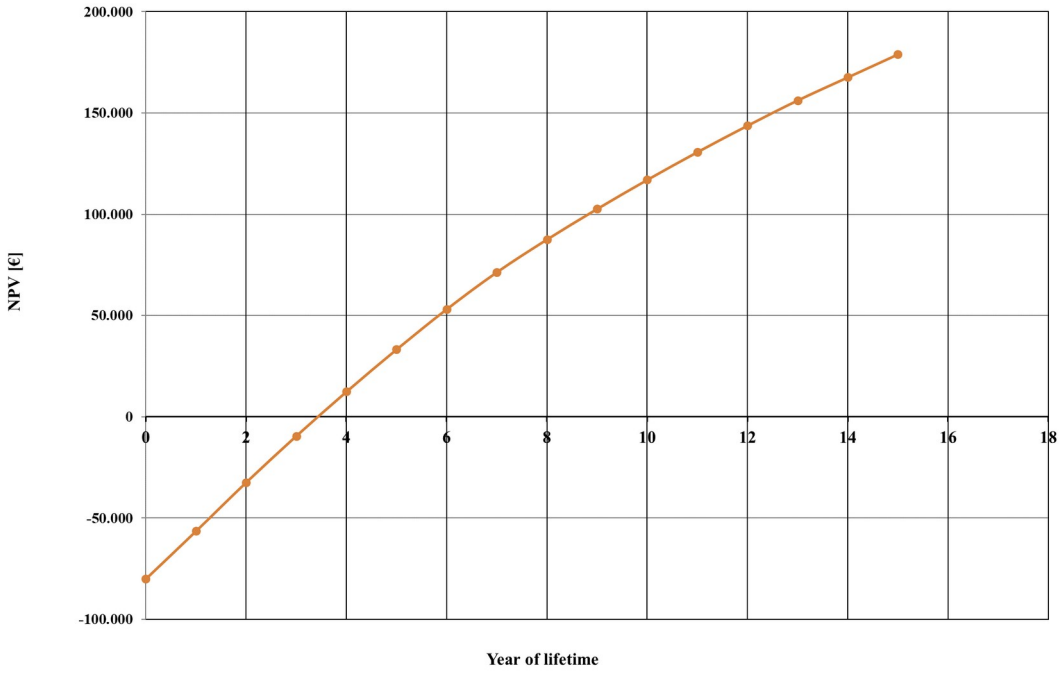

Figure 2: NPV results of the photoelectrolysis cell.

References

[1] ISO (2006a). ISO 14040: Life cycle assessment — Principles and framework. International Organization for Standardization, Geneva, Switzerland.
[2] ISO (2006b). ISO 14044: Environmental management — Life cycle assessment — Requirements and guidelines. International Organization for Standardization, Geneva, Switzerland.
[3] PRé Sustainability, 2022. SimaPro LCA software for informed change markets. Available at: https://Simapro.com/ (accessed on March 16, 2022).
[4] Grundel, I. & Dahlström, M. (2016). A Quadruple and Quintuple Helix Approach to Regional Innovation Systems in the Transformation to a Forestry-Based Bioeconomy. Journal of the Knowledge Economy, Springer, Portland Interna-tional Center for Management of Engineering and Technology (PICMET), vol. 7(4), 963-983, December 2016.
[5] Frischknecht R., Jungbluth N., Althaus H.-J., et al. (2007), Implementation of Life Cycle Impact Assessment Methods. Ecoinvent Report No. 3, v2.0. Swiss Centre for Life Cycle Inventories, Dübendorf.
[6] Huijbregts M.A.J., Steinmann Z.J.N., Elshout P.M.F., et al. (2017). ReCiPe 2016: a harmonised life cycle impact assessment method at midpoint and endpoint level, Int. J. Life Cycle Assess. 22, 138-147.
[7] D. Hunkeler, K. Lichtenvort, G. Rebitzer, Environmental Life Cycle Costing. CRC Press, Boca Ranton, 2008.
[8] S. De Bruyn, M. Bijleveld, L. de Graaff, et al., Environmental Prices Handbook EU28 Version, CE Delft, Delft, The Netherlands, October 2018.

A framework for micro-to-macro decision support in hydrogen-based transport systems

***S.K.R. Maddula*[1,2], *J. Dufour*[1,2], *and D. Iribarren*[1]**
[1] *IMDEA Energy, Systems Analysis Unit, 28935 Móstoles, Spain*
[2] *Rey Juan Carlos University, Chemical and Environmental Engineering Group, 28933 Móstoles, Spain*
sumanth.maddula@imdea.org

1. Introduction

Mitigating climate change is a critical global challenge, with the transportation sector contributing a significant and growing share of greenhouse gas emissions. Due to aspects such as long infrastructure lifetimes and rapid technological development, transport decarbonisation decisions have long-term implications for climate targets, public health, economic development, and social equity. In particular, hydrogen-based mobility has emerged as a promising option offering potential emission reductions [1].

Most existing sustainability assessments in the field of hydrogen transport focus on product-level or process-based attributional life cycle assessment (A-LCA). Though valuable, such approaches are insufficient for informing large-scale deployment decisions, as they do not capture system interactions. In hydrogen-based transport, such decisions typically involve large-scale substitution of conventional transport technologies and a system-wide increase in hydrogen demand. In this sense, there is a lack of structured pathways to move from A-LCA to consequential life cycle assessment (C-LCA) approaches that reflect macro-decision contexts [2].

This work addresses this gap by developing a structured framework that enables the transition from A-LCA to C-LCA for hydrogen-based mobility systems. The framework supports decision-oriented assessment by linking process-level sustainability information with system-wide responses, allowing the evaluation of net impacts associated with large-scale deployment. The framework provides a foundation for future illustrative case studies across transport modes to assess the consequences of scaling hydrogen technologies from individual to collective entities.

2. Methodology

The development of the proposed framework followed a structured methodological approach. A focused literature review was conducted to examine existing frameworks in transport decarbonisation, hydrogen mobility, and life cycle assessment (LCA), with particular attention to A-LCA and C-LCA approaches. This review aimed to identify conceptual foundations and existing attempts to integrate different LCA perspectives while tracing hydrogen across its value chain.

The review revealed a lack of frameworks capable of moving from process-level technology and operational decisions to macro-decision contexts relevant to climate change mitigation strategies. In response to this gap, a structured methodological framework was developed to enable such a transition, explicitly accounting for scale effects and system-wide interactions along the hydrogen value chain. The framework was designed to support decision-oriented assessment by linking process-level sustainability information with fleet-level technology substitution and the resulting system-level consequences, allowing the evaluation of net impacts.

3. Results

Figure 1 illustrates the proposed framework, showing how technology selection, operational choices, and performance-based considerations in hydrogen mobility translate into system-level outcomes. The results highlight the relevance of technology-level decisions for national hydrogen strategies, transportation decarbonisation targets, and climate change mitigation pathways, including net-zero objectives, by explicitly linking hydrogen mobility deployment to broader energy-system responses. A-LCA provides process-level sustainability information for technology assessment. These attributional results are translated into decision-oriented inputs through deployment scenarios, technology substitution, and service demand expansion with quantified changes in hydrogen demand and associated energy and material requirements. C-LCA is applied to evaluate system-wide consequences associated with large-scale deployment.

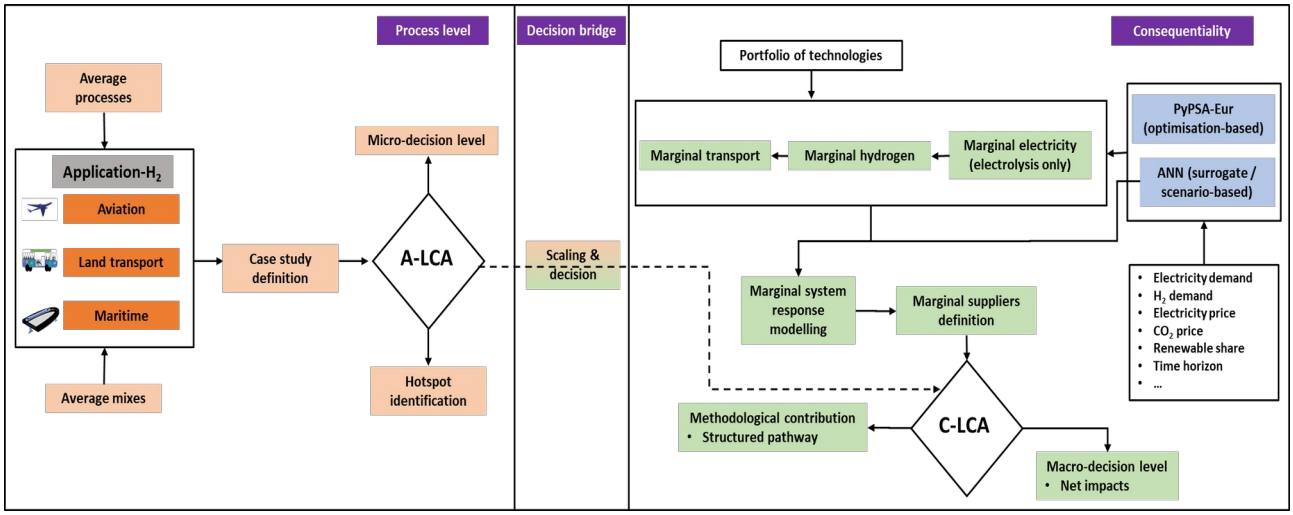

Figure 1: Micro-to-macro decision support framework for hydrogen mobility.

In addition to conventional transport technology substitution, consequential assessment requires the identification of marginal aspects associated with the increased deployment of hydrogen technologies. This deployment induces additional hydrogen demand, affecting hydrogen production pathways. In the case of electrolysis, marginal influence further propagates upstream by increasing electricity demand and requiring the identification of marginal

electricity supply. To capture these effects, the framework incorporates a marginal system-response modelling step, implemented using either optimisation-based energy system modelling (PyPSA-Eur) or data-driven surrogate modelling through artificial neural networks (ANN). The resulting marginal actors are integrated with case-specific life cycle inventories for hydrogen-based products and substituted technologies, enabling the assessment of net impacts and scenario sensitivity.

4. Conclusions

A framework that addresses the methodological gap between A-LCA and C-LCA in hydrogen-based mobility was developed, enabling micro-to-macro decision support through structured decision translation and system-response modelling. The framework enables the assessment of net impacts associated with large-scale hydrogen mobility deployment, accounting for scale effects and marginal actors, thus supporting transport decarbonisation and national hydrogen strategies. While the present study focuses on framework development, future work will apply the approach to illustrative multi-modal case studies, establishing a foundation for integrated, decision-oriented sustainability assessment of emerging transport technologies.

Acknowledgements
This work has been carried out in the context of the project PID2024-157951OB-I00 (ProsConsHy), funded by MICIU/AEI/10.13039/501100011033 and by ERDF/EU.

References
[1] International Energy Agency “Tracking Clean Energy Progress 2023”, IEA, Paris, 2025.
[2] E. Bargiacchi, G. Puig-Samper, F. Campos-Carriedo, D. Iribarren, J. Dufour, A. Ciroth et al. “Definition of FCH-LCA guidelines”, SH2E Project, 2024.

Primary photochemistry & Regulatory acclimation

G. Di Stefano, G. Rigano, A. Chirico, C.M. Martella, A. D'Agostino, F. Colini and D. Billi – Far-red light acclimation supports cyanobacterial life in extreme deserts and its possibility beyond Earth

D. Vetoshkina, N. Balashov, T. Abramova, A. Frolova, I. Pozdnyakova-Filatova, M. Borisova-Mubarakshina - Reversible Stress-Induced Inhibition of State Transitions in Arabidopsis thaliana

A. Petrova, G. Milanovsky, M. Kozuleva, D. Cherepanov and A. Semenov - Internal back reaction vs electron transfer to the exogenous acceptors in Photosystem I interacting with Ascorbate and 2,6-dichlorophenolindophenol: revealing acceptor power of the old electron donors

D. Vetoshkina, N. Rudenko, T. Marenkova, A. Nikolaev, A. Ashikhmin, and M. Borisova-Mubarakshina – Increased plastoquinone biosynthesis improves redox balance and photosynthetic function of higher plants

Far-red light acclimation supports cyanobacterial life in extreme deserts and its possibility beyond Earth

***G. Di Stefano[1], G. Rigano[1,2], A. Chirico[1], C.M. Martella[1]*, A. D'Agostino[1], F. Colini[1] and D. Billi[1]**
[1] *University of Rome Tor Vergata, Dept Biology, Rome, Italy*
[2] *University of Trento, Trento, Italy*
Billi@uniroma2.it

The discovery of cyanobacteria capable of harvesting light beyond the visible spectrum, a process known as far-red light photoacclimation (FaRLiP) has changed the paradigm that oxygenic photosynthesis is only driven by visible light and chlorophyll *a* [1], and has highlighted the possibility for life on planets orbiting around M-stars with a light spectrum peaking in the far-red and infrared [2]. On Earth, far-red light photosynthesis occurs in cyanobacteria living in environments where visible light is strongly attenuated, for instance, by competing photosynthetic organisms or by physical conditions [3]. A recent screening of desert cyanobacteria identified *Chroococcidiopsis* sp. CCMEE 010 as capable of FaRLiP with a reduced genetic cluster of 15 genes as opposed to the 20 genes of FarLiP cyanobacteria described so far [4]. Since the FaRLiP process in rock-inhabitant cyanobacteria remains poorly deciphered, an investigation of the response of *Chroococcidiopsis* sp. CCMEE 010 to far-red light was attemped by performing transcriptomic and proteomic analyses. Desert strains capable of FarLiP acclimation are also suitable for laboratory-planetary simulations and real space exposure to investigate the adaptation potential of life as we know it to better define the boundary of habitability of other worlds [5, 6]. At the same time, the potential role of *Chroococcidiopsis* sp. CCMEE 010 in biological life support systems to support human outposts on the Moon and Mars is under evaluation by optimizing the experimental conditions for cultivation using Martian regolith simulants a nutrient source and biomass utilization for down-stream processes [7].

References

[1] Gan F, Zhang S, Rockwell NC, Martin SS, Lagarias JC, and Bryant D.A. "Extensive remodeling of a cyanobacterial photosynthetic apparatus in far-red light", Science 345, 2014, 1312–1317.
[2] Gan F., Shen G., and Bryant D.A. "Occurrence of far-red light photoacclimation (FaRLiP) in diverse cyanobacteria", Life 5, 2015, 4–24.
[3] Cockell CS, Kaltenegger L, and Raven J.A. "Cryptic photosynthesis – extrasolar planetary oxygen without a surface biological signature", Astrobiology 9, 2009, 623–636.
[4] Billi D, Napoli A, Mosca C, Fagliarone C, de Carolis R, Balbi A, Scanu M, Selinger VM, Antonaru LA, and Nürnberg D.J. "Identification of far-red light acclimation in an endolithic *Chroococcidiopsis* strain and associated genomic

features: Implications for oxygenic photosynthesis on exoplanets", Front Microbiol, 2022, 13.
[5] Billi D. "Desert cyanobacteria under non-Earth conditions: Implications for astrobiology and sustainable life support", Acta Astronautica 238, part A, 2025. 209–214.
[6] Di Stefano G, Baqué M, Garland S, Lorek A, de Vera JP, Gangi MEM, Bellucci M, Billi D. "Resilience of metabolically active biofilms of a desert cyanobacterium capable of far-red photosynthesis under Mars-like conditions", *Life (Basel)* 15, 2025, 622.
[7] Santos de Sousa I, Di Stefano G, D'Agostino A, Martella CM, Chirico A, Rigano G, Santo L, Billi D. "The potential of far-red light-acclimating cyanobacteria to support sustainable outposts on Mars", Front. Astron. Space Sci. 12, 2025, 1658632.

Reversible Stress-Induced Inhibition of State Transitions in Arabidopsis thaliana

***D. Vetoshkina*[1], N. Balashov[1], T. Abramova[2], A. Frolova[2], I. Pozdnyakova-Filatova[2], M. Borisova-Mubarakshina[1]**

[1]*Institute of Basic Biological Problems RAS, Federal Research Center Pushchino Scientific Center for Biological Research of RAS, 142290 Pushchino, Moscow Region, Russia*

[2]*G.K. Skryabin Institute of Biochemistry and Physiology of Microorganisms, Federal Research Center Pushchino Scientific Center for Biological Research of RAS, 142290 Pushchino, Moscow Region, Russia*

vetoshkinadv@gmail.com

State transitions (ST) represent a key short-term adaptive mechanism that enables photosynthetic organisms to balance excitation energy distribution between photosystem II (PSII) and photosystem I (PSI) in response to changing environmental conditions. This process is mediated by reversible phosphorylation of light-harvesting complex II (LHCII) proteins, Lhcb1 and Lhcb2, catalysed by the thylakoid membrane-associated kinase STN7. Inhibition of ST under high light (HL) conditions has been repeatedly reported in higher plants, the dynamics and regulatory basis of this response under different stress conditions remain insufficiently understood (Lemeille and Rochaix, 2010; Mekala et al., 2015).

In this study, we analyzed the regulation of state transitions in leaves of higher plants exposed to elevated light intensity, salinity, and altered CO_2 concentration. All tested stress conditions caused a rapid inhibition of Lhcb1 and Lhcb2 phosphorylation and, consequently, suppression of state transitions. Notably, immediately after stress onset, ST inhibition coincided with a sharp increase in cellular reactive oxygen species (ROS), particularly hydrogen peroxide, levels. However, several days after acclimation to the new conditions, state transitions were partially or fully restored. This recovery correlated with a decrease in hydrogen peroxide content, indicating that ST inhibition is a reversible process tightly linked to stress acclimation.

Based on the observed correlation between ROS accumulation and ST suppression, we hypothesized that increased hydrogen peroxide levels in chloroplasts may directly affect the activity of STN7 kinase. The state transitions were assessed using low-temperature (77 K) chlorophyll a fluorescence spectroscopy, which enables simultaneous monitoring of excitation energy redistribution between the two photosystems. The extent of ST was quantified by the F745/F685 fluorescence ratio, reflecting the relative excitation of PSI and PSII. Illumination of isolated thylakoids with low intensity red light induced a significant increase in the F745/F685 ratio, indicating the transition from state 1 to state 2. However, the presence of exogenous hydrogen peroxide at concentrations of 25–50 μM completely suppressed this increase, demonstrating inhibition of the ST process under conditions that normally promote LHCII migration to PSI (Balashov et al., 2025).

To identify the specific stage affected by hydrogen peroxide, we analyzed the accumulation of phosphorylated Lhcb1 and Lhcb2 proteins. Light-dependent phosphorylation of both proteins was markedly reduced in the presence of H_2O_2, with a more pronounced inhibitory effect observed for Lhcb2 phosphorylation. Importantly, inhibition persisted in the presence of NaF, a phosphatase inhibitor (), indicating that hydrogen peroxide specifically suppresses STN7 kinase activity rather than enhancing dephosphorylation by TAP38/PPH1 phosphatase. These findings demonstrate that hydrogen peroxide interferes with the initial stage of state transitions, namely the activation of STN7 kinase and phosphorylation of LHCII proteins.

To determine whether the observed effects were indirect consequences of impaired photosynthetic electron transport, we measured oxygen uptake rates as an indicator of electron transport activity. Hydrogen peroxide at the applied concentrations did not reduce electron transport rates, indicating that ST inhibition was not caused by suppression of the photosynthetic electron transport chain. Furthermore, the activity of STN8 kinase, a paralog of STN7 responsible for phosphorylation of the PSII core protein D1, was not inhibited by hydrogen peroxide. In contrast, D1 phosphorylation increased in the presence of H_2O_2, confirming the specificity of hydrogen peroxide action toward STN7 kinase.

High light illumination, which promotes endogenous production of reactive oxygen species in thylakoids, also resulted in reduced accumulation of phosphorylated Lhcb proteins. Importantly, removal of hydrogen peroxide by catalase under HL conditions restored Lhcb1 and Lhcb2 phosphorylation to levels comparable to those observed under low light, providing further evidence for the involvement of H_2O_2 in STN7 inhibition. These results suggest that hydrogen peroxide generated in close proximity to the thylakoid membrane and photosynthetic electron transport components plays a key role in regulating STN7 activity in vivo.

The accumulation of hydrogen peroxide under stress conditions, as well as the inhibition of STN7 kinase activity, may also be important for the development of other adaptive responses, such as the regulation of chloroplast gene expression. To explore a potential link between short-term regulation of state transitions and more longer-term adaptive responses, we analysed chloroplast gene expression in wild type Arabidopsis plants and mutants lacking STN7 kinase. Transcriptome analysis of chloroplast-encoded genes under control conditions and after 3 h of high light exposure revealed a coordinated and significant downregulation of chloroplast gene expression in wild type plants. In contrast, stn7-knokout mutants exhibited heterogeneous and non-coordinated expression changes, significantly differing from the wild type response.

Taken together, our findings provide direct experimental evidence that hydrogen peroxide acts as a specific inhibitor of STN7 kinase and, consequently, of state transitions in higher plant thylakoids. This mechanism offers a coherent explanation for the inhibition of ST under high light conditions and highlights hydrogen peroxide as an important redox signal linking light intensity, reactive oxygen species production, and adaptive regulation of the

photosynthetic apparatus. The H_2O_2-mediated suppression of STN7 activity may represent a general stress-responsive regulatory pathway that contributes to the long-term chloroplast gene regulation and photosynthetic performance in plants.

Acknowledgements
This work was supported by the Russian Science Foundation, grant number 23-14-00396 (extension), https://rscf.ru/project/23-14-00396/.

References

[1] S., Lemeille, and J.-D., Rochaix "State transitions at the crossroad of thylakoid signalling pathways", Photosynth Res., 106, 2010, 33-46.
[2] N. R., Mekala, M., Suorsa, M., Rantala, E.-M., Aro, and M., Tikkanen "Plants actively avoid state transitions upon changes in light intensity: role of light-harvesting complex II protein dephosphorylation in high light", Plant Physiol., 168, 2015, 721-734.
[3] N. V., Balashov, M. M., Borisova-Mubarakshina, D. V., Vetoshkina "The Effect of Hydrogen Peroxide on the Redistribution of Antenna Complexes Between Photosystems in Higher Plants", Biochemistry (Moscow), 90(7), 2025, 943-955.

Internal back reaction *vs* electron transfer to the exogenous acceptors in Photosystem I interacting with Ascorbate and 2,6-dichlorophenolindophenol: revealing acceptor power of the old electron donors

***A. Petrova*[1], *G. Milanovsky*[1], M. Kozuleva[2], D. Cherepanov[1] *and* *A. Semenov* [1]**

[1] *A.N. Belozersky Institute of Physical-Chemical Biology, Lomonosov Moscow State University, Moscow, Russia*

[2] *Institute of Basic Biological Problems, Pushchino Scientific Center for biological Research of the Russian Academy of Sciences, Pushchino, Russia*

draparnaldia@gmail.com

Pigment-protein supercomplex of Photosystem I (PSI) is one of the few natural molecular machines, performing light-dependent charge separation and subsequent reduction of the extremely low-potential exogenous acceptors. In the cells of the oxygenic phototrophs Ferredoxin (or Flavodoxin in cyanobacteria) being reduced by iron-sulfur clusters F_A/F_B at the acceptor side of PSI further serves as an electron donor for $NADP^+$ and downstream metabolic reactions, such as Calvin-Benson cycle, nitrogen and sulfur assimilation. In photovoltaic devices the reducing power of purified photosystem I is applied for photocurrent generation [1]. The photooxidized ultimate electron donor chlorophyll a dimer P_{700} under conditions *in vitro* is usually reduced by sodium ascorbate (Asc) in combination with redox-mediators 2,6-dichlorophenolindophenol (DCPIP) or *N,N,N′,N′*-tetramethyl-*p*-phemilemediamine (TMPD). The oxidized forms of all three compounds potentially may accept electrons from PSI [2]. Yet, the contribution of the redox-mediators to the outflow of electrons from PSI has not been studied well enough. In this study we investigated the reactions of Asc, DCPIP and TMPD with donor and acceptor sides of PSI and developed kinetic model.

The millisecond P_{700}^+ reduction kinetics were measured in trimeric PSI complexes from cyanobacteria *Synechocystis* sp. PCC 6803 by laser transient absorption spectroscopy. It was shown that charge recombination in PSI was efficiently suppressed by 5 μM DCPIP in the presence of 10 mM Asc, revealing DCPIP acceptor activity. Asc appeared to be a significantly less efficient acceptor: noticeable suppression of charge recombination was observed only at concentrations above 10 mM. TMPD at concentrations up to 50 μM in the presence of 10 mM Asc was unable to compete for electrons with backward electron transfer reactions. In contrast to the TMPD, both donor and acceptor reactions of DCPIP with PSI showed explicit dependence on the molecular oxygen presence in the medium and pH. Thus, oxidation of DCPIP to the semiquinone ($DCPIP^{\bullet -}$) and further to the fully oxidized form ($DCPIP^{OX}$) ensures high donor and acceptor efficiency of this mediator (Fig.1). At the same time TMPD in the presence of Asc is not accumulated in oxidized state and cannot provide an efficient oxidation of the terminal PSI cofactors.

The rate constants of the donor and acceptor reactions, k_d and k_a, correspondingly, were elucidated from the lifetimes and relative contributions of the slow sub-second kinetic phase of P_{700}^+ reduction using the kinetic model [2] (Table 1).

Table I: Estimated rates constants of DCPIP and TMPD redox forms interactions with PSI as donor (k_d) or acceptor (k_a)

	k_d ($M^{-1}s^{-1}$)	k_a ($M^{-1}s^{-1}$)
$DCPIP^{RED}$	$5.9 \bullet 10^4$	-
$DCPIP^{\bullet -}$	$>7.2 \bullet 10^6$	-
$DCPIP^{OX}$	-	$2.9 \bullet 10^7$
TMPD	$4.1 \bullet 10^4$	$>3.6 \bullet 10^6$

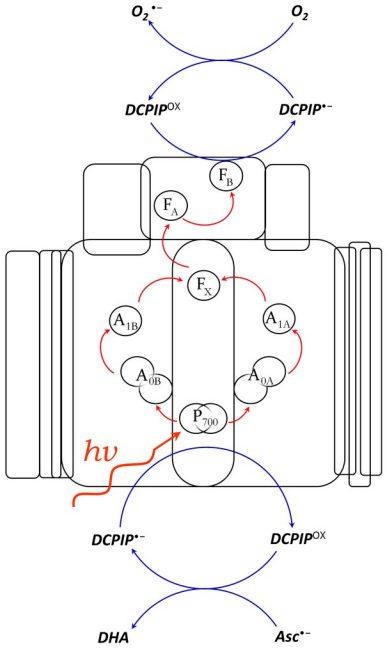

Figure 1: Scheme of the interaction of PS I with DCPIP under aerobic conditions.

Acknowledgements
This research was supported by the Russian Science Foundation Grant 23-74-00025

References
[1] A.H. Teodor and B.D. Bruce "Putting Photosystem I to Work: Truly Green Energy", Trends in Biotechnology, 38, 12, 2020, 1329-1342
[2] A.A. Petrova, G.E. Milanovsky, I.A. Volkhin, M.A. Kozuleva, D.A. Cherepanov, A.Yu. Semenov "The commonly used electron donor 2,6-dichlorophenolindophenol also serves as an efficient electron acceptor for Photosystem I", Photosynthesis Research, 164, 1, 2026

Increased plastoquinone biosynthesis improves redox balance and photosynthetic function of higher plants

D. Vetoshkina[1], N. Rudenko[1], T. Marenkova[2], A. Nikolaev[1], A. Ashikhmin[1], and M. Borisova-Mubarakshina[1]

[1]Institute of Basic Biological Problems RAS, Federal Research Center Pushchino Scientific Center for Biological Research of RAS, 142290 Pushchino, Russia

[2]Federal Research Center Institute of Cytology and Genetics, Siberian Branch of Russian Academy of Sciences, 630090, Novosibirsk, Russia

mubarakshinamm@gmail.com

Plastoquinone (PQ) plays a central role in higher plants as a multifunctional hub of photosynthetic and metabolic processes. The PQ pool is involved not only in linear electron transfer but also in alternative electron transfer pathways, including the Mehler reaction (photoreduction of O_2 to H_2O_2), cyclic electron flow around PS I, the short water–water cycle via plastid terminal oxidase, chlororespiration, and cyclic electron flow around PS II. Beyond its well-established function as a mobile electron carrier, PQ acts as an important antioxidant, directly or indirectly limiting reactive oxygen species formation and contributing to cellular redox homeostasis [for review see 1].

It is known that the redox state of the PQ pool reflects the functional status of the photosynthetic apparatus and provides a key signal for the chloroplast-to-nucleus retrograde regulation of nuclear genes associated with photosynthesis and stress responses [2]. It is assumed that not only the redox status of the PQ pool, but also the total content of PQ in chloroplasts is fundamentally important for plant adaptation [3], however, the relationship between the quantitative content of PQ in chloroplasts and signaling pathways in plants has not been sufficiently studied.

In order to evaluate the impact of changes in PQ biosynthesis on photosynthetic performance of higher plants, redox regulation, and plant sustainability, transgenic *Arabidopsis thaliana* lines with elevated PQ content were generated. The genetic construct was produced for Agrobacterium-mediated transformation based on the pCAMBIA1300 vector containing the fibrillin 5 (FBN5) gene. FBN5 was found to be essential for PQ biosynthesis, stimulating enzymatic activity of solanesyl diphosphate synthases through binding to its solanesyl moiety [4]. The PQ content in plants with FBN5 overexpression (oexFBN5 plants) was approximately 2 times higher than in wild type (WT) plants (21±3 vs. 10±2 nmol/g of fresh leaf weight) even under control conditions (120 μmol photons m^{-2} s^{-1}). When plants were transferred to high light conditions (light intensity of 550 μmol photons m^{-2} s^{-1}), the PQ content significantly increased in both WT and FBN5 plants: 5 days after being under in-

creased light intensity, the PQ content in WT plant leaves reached that one detected in mutants under control conditions and amounted to 18±2 nmol/g of fresh leaf weight, while in the oexFBN5 line, the PQ content under high light conditions raised to 27±1 nmol/g of fresh leaf weight.

WT and oexFBN5 plants exhibited similar photosynthetic characteristics under control conditions. However, following exposure to high light, low temperature, or drought stress, plants with increased PQ content displayed enhanced photosynthetic efficiency and stress tolerance. After prolonged high light treatment, oexFBN5 plants showed significantly higher maximum and effective quantum yields of PS II (Fv/Fm and Y(II). In addition, CO_2 assimilation rates were higher in oexFBN5 line in high light, indicating enhanced Calvin–Benson–Bassham cycle activity. The high CO_2 assimilation was accompanied by the increased stomatal conductance and transpiration.

Elevated PQ level in oexFBN5 plants were associated with metabolic and redox adjustments, including higher starch accumulation, altered light-harvesting antenna composition, and reduced oxidative status. These changes correlated with modified expression of other genes involved in PQ biosynthesis, as well as of genes coding components incorporated in chloroplast-to-nucleus retrograde signaling, photosynthetic regulation, and stress hormone pathways.

Overall, the obtained results demonstrate that altered PQ biosynthesis/ increased PQ content enhances the effectiveness of the photosynthetic machinery, improves redox homeostasis, and promotes metabolic stability of higher plants under stress conditions

Acknowledgements

This work was supported by the Russian Science Foundation, grant number 23-14-00396 (extension), https://rscf.ru/project/23-14-00396/.

References

1. Borisova-Mubarakshina M.M. (2025) Networking of plastoquinone pool and reactive oxygen species in higher plant signaling. Russian Journal of Plant Physiology, 72, p. 247.
2. Pfannschmidt, T., Nilsson, A., and Allen, J.F., (1999) Photosynthetic control of chloroplast gene expression. Nature, 397, no. 6720, pp. 625–628.
3. Vetoshkina, D.V., Nikolaev, A.A., and Borisova-Mubarakshina, M.M. (2024) Antioxidant properties of plant plastoquinone in vivo and in vitro. Biophysics, 69, no. 3, pp. 445–458.

4. Kim, E.-H., Lee, Y., Kim, H.U. (2015) Fibrillin 5 Is Essential for Plastoquinone-9 Biosynthesis by Binding to Solanesyl Diphosphate Synthases in Arabidopsis. Plant Cell, 27, pp. 2956–2971.

Hydrogen Economics

P. Marocco, M. Santarelli, and M. Gandiglio - Hydrogen as an Enabler for Complex Local Multi-Energy Microgrids

D. Lanni, G. Di Cicco, A. Perna, A. Agresta, M. Della Pietra, and V. Cigolotti# - On-site Hydrogen Refueling Stations with Electrolytic Hydrogen Production: Modelling and Techno-Economic Assessment

G. Di Cicco, D. Lanni , A. Perna , A. Agresta , M. Della Pietra , V. Cigolotti - Techno-economic assessment of off-grid on-site hydrogen refuelling stations based on biogas steam reforming at different production scales

F. Romano, V. Cigolotti, and M. Minutillo - Levelized Cost of Hydrogen from 1 MW Proton-Conducting Ceramic Electrolysis system: Techno-Economic Study in European scenario

S. Di Micco, A. Cappiello, and M. Minutillo - Economic Assessment of Multi-Fuel Solid Oxide Fuel Cells System for Shipping Under Alternative Hydrogen, Methanol, and Ammonia Supply Pathways

Hydrogen as an Enabler for Complex Local Multi-Energy Microgrids

P. Marocco[1], M. Santarelli[1], and M. Gandiglio[1]
[1] *Department of Energy, Politecnico di Torino, C.so Duca degli Abruzzi 24, 10129 Turin Italy*
marta.gandiglio@polito.it

Renewable Energy Communities (RECs) and local energy microgrids are emerging as key building blocks of the energy transition, enabling decentralised generation, increased self-consumption and active participation of end users. However, their operation is still strongly constrained by the variability of renewable energy sources, the difficulties in finding a perfect match between generation and consumption, which is the driver to maximise self-consumption. Moreover, multi-vector approaches and systems, capable of simultaneously addressing electrical, thermal and all energy needs could give further benefits to the community.
In this context, hydrogen technologies can play a strategic role as long-term energy storage and sector-coupling enablers, complementing short-term storage and demand-side flexibility. This contribution presents an integrated hydrogen-based architecture for community-scale applications, based on the H2SCORE project as a real-world demonstration framework, while addressing more generally the role of hydrogen in complex local multi-energy microgrids.
The proposed architecture relies on a dual hydrogen system, combining a low-temperature domain – based on a PEM electrolyser, metal hydride hydrogen storage and a PEM fuel cell – with a high-temperature domain centred on a reversible Solid Oxide Cell (rSOC), operating both in SOEC and SOFC modes. This hybrid configuration enables seasonal energy storage, fast response to renewable fluctuations and efficient cogeneration of electricity and heat. The integration of a biomass gasification unit supplying syngas to the SOFC further enhances system flexibility, enabling the valorisation of local biomass and supporting circular energy flows at community level.
The work is carried out within a strongly collaborative framework involving industrial technology providers, research institutions and local stakeholders: BluEnergy Revolution supplies electrolysis and hydrogen storage technologies; PowerCell Sweden and Zeppelin Power Systems provide PEM fuel cells; H2B2 and BIO2CHP contribute high-temperature rSOC and biomass gasifier respectively; Politecnico di Torino and CARTIF support system modelling, integration and optimisation connected with the demonstration site; VTT and NTNU address environmental assessment, social and safety aspects; while Environment Park, ENGREEN and the Municipality of Quarona support demonstration activities, regulatory aspects and stakeholder engagement, together with replication partners in Spain (University of Burgos), Switzerland (AEM) and Canada (Yukon University).

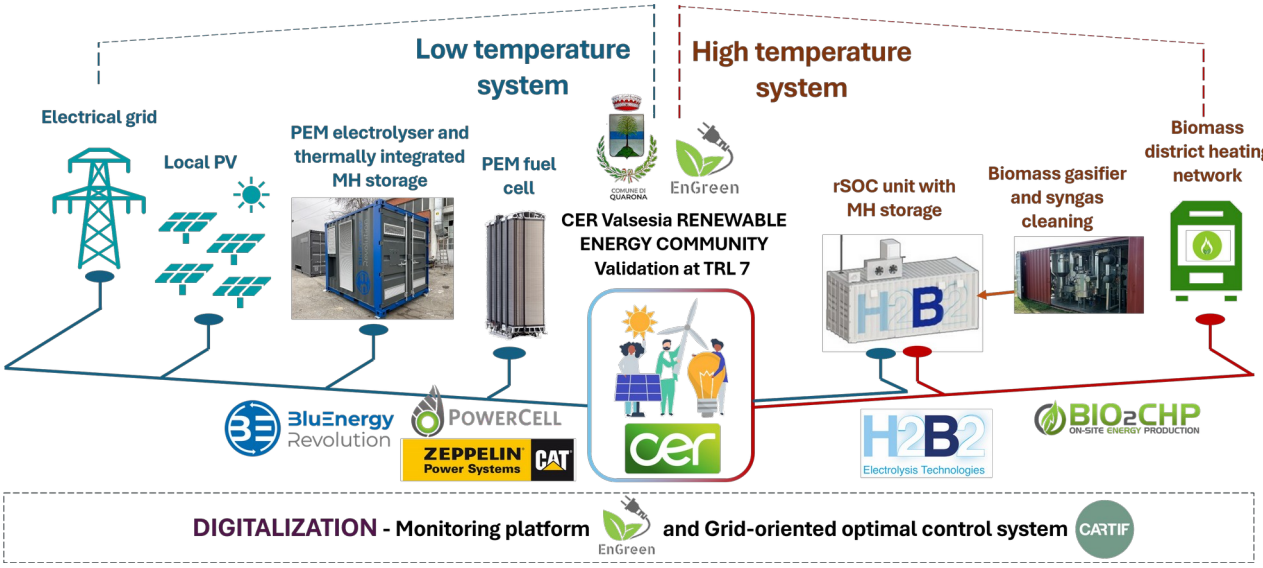

Figure 1: H2SCORE concept layout.

A key aspect of the proposed approach is its deep multi-vector integration. Hydrogen-based technologies are embedded within the local electrical grid and the district heating network, enabling sector coupling between electricity, hydrogen and heat, while also supporting the provision of flexibility and balancing services to the grid. In a broader perspective, the same architecture can be extended to additional energy vectors, such as mobility and transport applications, reinforcing the role of hydrogen as a cross-sector energy carrier.
Beyond the demonstration itself, the expected results include a systematic mapping of technology performance – at both component and system level – and an assessment of how different hydrogen technologies interact when integrated within complex local microgrids. This includes the analysis of efficiency, dynamic behaviour, operational strategies, and the impact on renewable self-consumption, grid interaction and overall system resilience. Modelling and techno-economic optimisation activities support the identification of optimal layouts and sizing rules under different boundary conditions.
The demonstration is being implemented in Valsesia (Italy), within a Renewable Energy Community characterised by photovoltaic and hydropower generation and an existing biomass-based district heating network. Launched on 1 December 2025, the project aims to reach TRL 7 during the demonstration phase.
Replication analyses in Spain, Switzerland and northern Canada will further explore the adaptability of the proposed hydrogen-enabled microgrid concept across different geographical, regulatory and socio-economic contexts. The Spanish case study represents an industrial-based community, mainly supplied by wind power, where hydrogen may play a dual role not only as a long-duration storage solution but also as a feedstock for industrial processes. The Swiss case focuses on a fully residential community characterised by extensive rooftop photovoltaic generation. Finally, remote off-grid communities in northern Canada represent a markedly different context, with extreme weather

conditions, significant logistical constraints and highly seasonal and variable energy demands. Within these diverse settings, the H2SCORE concept will be assessed and adapted to quantify the benefits that hydrogen can provide to different types of end users and energy system configurations.

Figure 2: H2SCORE replication studies.

Acknowledgements
The project is supported by the Clean Hydrogen Partnership and its members.

On-site Hydrogen Refueling Stations with Electrolytic Hydrogen Production: Modelling and Techno-Economic Assessment

***D. Lanni*[1], *G. Di Cicco*[1], *A. Perna*[1], *A. Agresta*[2], *M. Della Pietra*[2], *and V. Cigolotti*[3]**

[1] *Department of Civil and Mechanical Engineering, University of Cassino and Southern Lazio, Cassino, Italy*

[2] *DTE-PCU-SPCT, ENEA R. C. Casaccia, Rome, Italy*

[3] *TERIN-PSU-ABI, ENEA Portici, Portici, Italy*

davide.lanni@unicas.it

On-site hydrogen refueling stations are increasingly recognized as a key enabling infrastructure for hydrogen mobility, particularly when integrated with renewable electricity sources and advanced refueling architectures. In this framework, Power-to-Hydrogen (PtH) solutions based on water electrolysis enable the direct coupling of renewable electricity generation with on-site hydrogen production, while their overall energy and economic performance strongly depends on the coordinated design of the hydrogen production section and the refueling line, especially under realistic, time-varying refueling demand profiles [1–3]. In this context, this work presents the modelling approach and numerical sizing results for a PtH on-grid hydrogen refueling station equipped with a three-cascade refueling line, considering as a specific case study a station delivering approximately 500 kg/day of hydrogen, located in Central Italy. The analysis compares three renewable supply options for the production section, namely photovoltaic (PtH-PV), wind (PtH-Wind), and hybrid photovoltaic–wind (PtH-Hybrid), in order to assess their impact on system sizing, energy performance, and economic indicators.
The overall layout of the PtH on-grid hydrogen refueling station is shown in Figure 1.

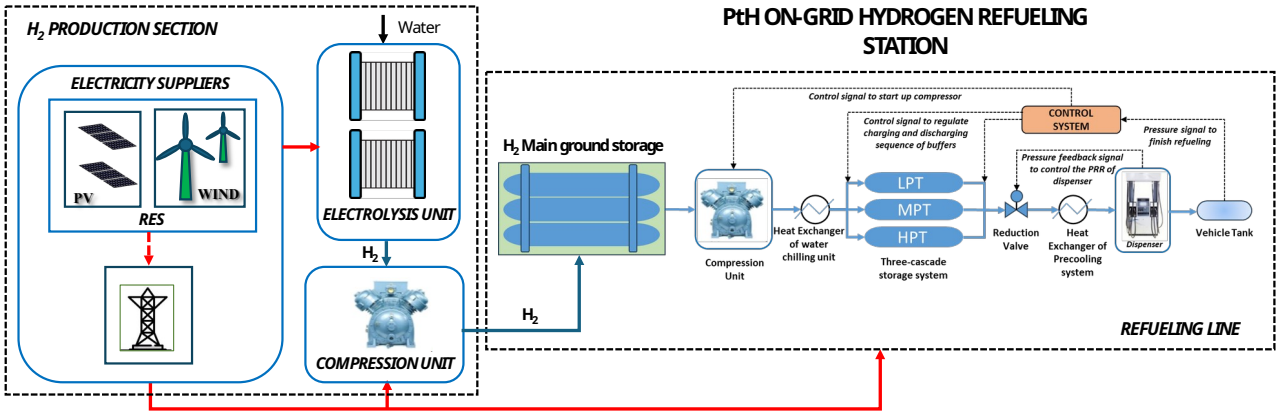

Figure 1: PtH on-grid hydrogen refueling station.

The station is composed of two main subsystems: the hydrogen production section and the refueling line. The hydrogen production section includes a renewable electricity generation system (PV, wind, or hybrid), an alkaline

water electrolyzer (AEL), and an intercooled (IC) hydrogen compression unit. The electrolyzer is based on a modular AEL stack architecture with a specific consumption of 64 kWh/kg. The refueling line includes a ground hydrogen storage tank operating at 200 bar, a three-cascade high-pressure storage system, a pre-cooling unit, and dispensers compliant with SAE J2601 refueling protocols.

The three-cascade storage system of the refueling line is composed of low-, medium-, and high-pressure storage banks operating at approximately 400 bar, 650 bar, and 900 bar, respectively. Hydrogen is dispensed sequentially from the lowest-pressure bank to the highest-pressure one, enabling efficient pressure equalization and limiting the use of active compression during refueling. The refueling line is modelled dynamically using mass balance equations applied to each storage tank and to the vehicle tank, coupled with a real-gas equation of state for hydrogen, with a simulation time step of 1 s. The refueling demand profile is generated through a stochastic algorithm reproducing the semi-random distribution of refueling events over a 24-hour period under a worst-case scenario, assuming all vehicles arrive with an initial state of charge equal to 10% and are refueled up to full capacity.

For light-duty vehicles and taxis, the refueling time is fixed at 5 min, corresponding to an average hydrogen mass flow rate of 0.918 kg/min, based on a delivered mass of 4.59 kg per event, while for heavy-duty vehicles the refueling time is 10 min with an average mass flow rate of 1.8 kg/min. The pressure ramp at the dispenser is controlled through an Average Pressure Ramp Rate equal to 159 bar/min for light-duty vehicles and taxis and 39 bar/min for heavy-duty vehicles, ensuring that the dispenser pressure does not exceed 125% of the nominal working pressure.

The sizing results of the refueling line show that a total cascade storage volume of 16.8 m^3 is required, assuming a single tank volume of 0.7 m^3 and a configuration composed of 4 low-pressure tanks, 8 medium-pressure tanks, and 12 high-pressure tanks. The maximum hydrogen mass stored in the cascade system is 685.9 kg, corresponding to a Hydrogen Utilization Factor of 72.1%. The cascade system is recharged from the 200-bar ground storage six times per day at regular intervals. The ground storage tank is sized at 950 kg of hydrogen, corresponding to a storage volume of 63.6 m^3 at 200 bar, providing adequate buffering capacity between production and refueling sections. The maximum electrical power absorbed by the refueling line is 137 kW, resulting from the combined operation of the pre-cooling unit (92 kW) and the main compression unit (45 kW). On an annual basis, the electricity consumption of the refueling line amounts to 127.6 MWh/year for compression and 243.5 MWh/year for pre-cooling, confirming that hydrogen thermal conditioning represents the dominant contribution to the refueling line energy demand.

The hydrogen production section is modelled dynamically in MATLAB in order to capture the interaction between the hydrogen demand imposed by the refueling line and the variability of renewable electricity generation. In all on-grid configurations, the electrolyzer operates at constant nominal load, while electricity deficits are covered by the grid, and surplus renewable electricity is

exported. The sizing results of the hydrogen production section are summarized in Table I.

Table I: Sizing results of the hydrogen production section

Parameter	Unit	PtH-PV	PtH-Wind	PtH-Hybrid
PV plant capacity	kW	7290	–	3570
Wind plant capacity	kW	–	5350	2730
Electrolysis unit size	kW	1400	1400	1400
IC compressor size	kW	23	23	23

The electrolyzer is sized at 1.4 MW for all three on-grid configurations, ensuring a hydrogen production consistent with the station demand. The PtH-PV configuration is based on a 7.29 MW photovoltaic plant, the PtH-Wind configuration on a 5.35 MW wind plant, while the PtH-Hybrid configuration includes 3.57 MW of photovoltaic capacity and 2.73 MW of wind capacity. In all cases, the IC hydrogen compressor power is fixed at 23 kW.
The techno-economic performance of the on-grid PtH configurations has been evaluated through a life-cycle costing approach, including capital expenditure, operation and maintenance costs, and component replacement. The levelized cost of hydrogen is equal to about 9.1 €/kg for the PtH-PV configuration and 9.8 €/kg for the PtH-Wind configuration, while the PtH-Hybrid configuration shows a lower LCOH of approximately 8.2 €/kg due to improved utilization of renewable electricity and reduced grid electricity purchases. The discounted payback period is equal to about 8 years for the PV-based system, increases to approximately 13 years for the wind-based option, and is reduced to around 9 years for the hybrid configuration, confirming the latter as a more economically balanced solution compared to the wind-only case.

Acknowledgements
This research was funded by the European Union - NextGenerationEU from the Italian Ministry of Environment and Energy Security, POR H2 AdP MEES/ENEA with involvement of CNR and RSE, PNRR - Mission 2, Component 2, Investment 3.5 "Ricerca e sviluppo sull'idrogeno", CUP: I83C22001170006.

References
[1] R. Atabay *et al.*, Design and techno-economic analysis of solar energy based on-site hydrogen refueling station, *Int. J. Hydrogen Energy*, 80, 2024, pp. 151–160.
[2] M. A. Mahmood *et al.*, Techno-economic evaluation of hydrogen refuelling station with on-site electrolysis production powered by photovoltaic solar energy for the railway sector, *Int. J. Hydrogen Energy*, 138, 2025, pp. 802–822.
[3] G. W. Kim *et al.*, Techno-economic optimal operation of an on-site hydrogen refueling station, *Appl. Sci.*, 15, 2025, 10999.

Techno-economic assessment of off-grid on-site hydrogen refuelling stations based on biogas steam reforming at different production scales

G. Di Cicco*[*1], D. Lanni [1], A. Perna [1], A. Agresta [2], M. Della Pietra [2], V. Cigolotti [3]
[1]*DICEM, University of Cassino and Southern Lazio, Cassino, Italy*
[2] *DTE-PCU-SPCT, ENEA R. C. Casaccia, Rome, Italy*
[3] *TERIN-PSU-ABI, ENEA Portici, Portici, Italy*
gabriella.dicicco@unicas.it

Hydrogen refuelling stations (HRSs) with on-site hydrogen production operating in off-grid configuration are widely regarded as a promising solution for the strengthening of hydrogen mobility, particularly in remote areas where centralized supply chains are still limited [1]. Among the available production pathways, biogas-based hydrogen production offers the opportunity to combine a renewable feedstock with mature thermochemical conversion technologies such as steam reforming, potentially reducing both greenhouse gas emissions and dependence on fossil fuels. A number of studies have examined HRSs from a technical or economic point of view. Nevertheless, comprehensive assessments that include refueling line dynamics, hydrogen production system modeling, and economic evaluations are still scarce. In this context, the present work focuses on a techno-economic assessment of small, medium and large size off-grid hydrogen refuelling stations (200, 500 and 1000 kgH_2/day respectively) based on biogas steam reforming (BtH_SR) and a three-cascade storage refuelling system, whose schematic layout is depicted in Figure 1.

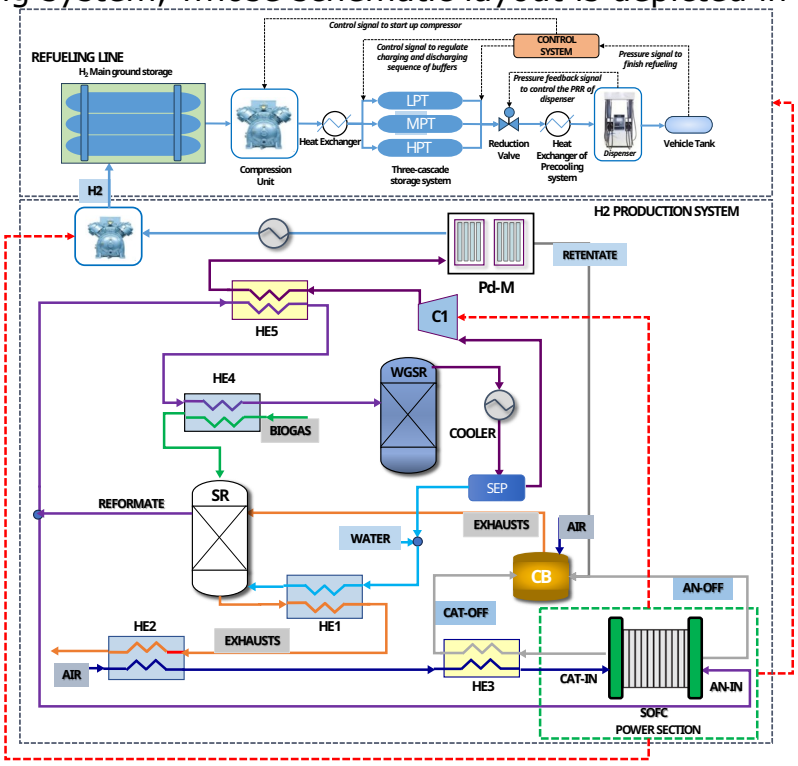

Figure 1: Schematic layout of the proposed hydrogen refuelling station

The electricity demand of both the hydrogen production plant and the refuelling line is fully supplied by a solid oxide fuel cell (SOFC) module, fuelled by the same biogas feedstock used for hydrogen production. The analysis aims to evaluate the technical feasibility, energy performance and economic competitiveness of the selected configuration.

The refueling line is modelled according to the three-cascade storage architecture, which enables the refueling of both heavy-duty and light-duty vehicles at pressures of 350 and 700 bar, respectively. The system comprises three storage banks operating at three different pressure levels (LPT, MPT, and HPT), which are sequentially connected to the dispenser during the refueling process. A dynamic MATLAB model is used to simulate hydrogen transfer from the cascade storage to the vehicle tank. The model is capable of solving mass and pressure balances for each storage bank and for the dispenser. It accounts for real-gas hydrogen properties and operational constraints (e.g. the SAE J2601 refueling protocol [2]).

The cascade system is sized based on daily hydrogen demand profiles corresponding to the three station sizes considered, generated using a stochastic algorithm representing a mix of light and heavy-duty vehicles. The model includes a 200-bar ground storage tank, compression units for the cascade system, and a pre-cooling unit for fast refueling.

The core of the hydrogen production system, modelled in the Aspen Plus environment, is the steam reformer reactor (SR), where hydrogen is obtained from biogas and water. This is followed by a water gas shift (WGS) section, aimed at increasing the hydrogen content of the reformate. A series of heat exchangers and a catalytic burner are employed to recover thermal energy from hot process streams, thus enabling the thermal self-sustainment of the plant under nominal operating conditions. After the reforming and water-gas shift sections, hydrogen is purified through a membrane-based separation unit to meet the purity requirements for refueling applications. A fraction of the reformate at the outlet of the steam reformer is directed to an on-site solid oxide fuel cell (SOFC), which satisfies the electrical demands of both the hydrogen production section and the refueling line, allowing the station to operate in a fully autonomous, off-grid configuration.

The economic assessment of the hydrogen refuelling station is performed using a life-cycle costing (LCC) approach. The model evaluates the economic performance of the system over its lifetime (equal to 20 years) by accounting for capital expenditures (CAPEX), operating and maintenance costs (OPEX) and component replacement costs (REPLEX). Capital costs are estimated by adding indirect costs related to installation, contingencies and owner’s costs to the bare equipment costs. Operating costs include fuel supply and routine operation and maintenance activities, while replacement costs account for the substitution of components characterised by a limited lifetime (such as compressors and fuel cell stacks). The economic performance is assessed through discounted cash flow analysis, from which the levelized cost of hydrogen (LCOH), and discounted payback period (DPBP) are derived.

The main technical and economic results of the techno-economic assessment of the proposed small, medium and large size BtH_SR hydrogen refuelling stations

operating in off-grid configuration are summarised in Table 1. Electricity demand of the refuelling line and biogas consumption are evaluated under average daily operating conditions.

Table I: Main technical and economic results for small, medium and large BtH_SR off-grid hydrogen refuelling stations

Parameter	Unit	Small	Medium	Large
Hydrogen production rate	(kg/h)	8.2	20.8	41.5
Biogas consumption	(kg/h)	117.0	279.2	523.0
Average electrical power absorbed by the H_2 production system	(kW)	42	105	209
Average electrical power absorbed by the refuelling line	(kW)	16.8	42.4	83.1
SOFC installed size	(kW)	113.0	242.0	518.7
SOFC average electrical output	(kW)	58.8	147.4	292.1
Specific energy consumption	(kWh/kgH_2)	70.0	66.0	61.8
Specific biogas consumption	(kg/kgH_2)	14.3	13.4	12.6
LCOH	(€/kgH_2)	10.62	8.60	8.09
DPBP	(years)	20	14	8

A comparison of small, medium and large stations reveals clear scale effects on both technical and economic performance. As station capacity increases from 8.2 to 41.5 kgH_2/h, the specific energy consumption decreases from 70.0 to 61.8 kWh/kgH_2, while the specific biogas consumption is reduced from 14.3 to 12.6 kg/kgH_2. These improvements are reflected in the economic indicators, with the LCOH decreasing from 10.62 €/kgH_2 for the small station to 8.09 €/kgH_2 for the large one, and the discounted payback period shortening from about 20 years, indicating no economic attractiveness, to approximately 8 years. Overall, larger stations benefit from a more efficient utilisation of the SOFC system and the refuelling infrastructure, resulting in enhanced techno-economic performance.
These results demonstrate that the proposed refuelling station architecture, combining renewable feedstock with mature thermochemical conversion technologies, is both technically and economically viable for medium and large-scale plants, and represents a robust option for advancing low-carbon mobility.

Acknowledgements
This research was funded by the European Union - NextGenerationEU from the Italian Ministry of Environment and Energy Security, POR H2 AdP MEES/ENEA with involvement of CNR and RSE, PNRR-Mission 2, Component 2, Investment 3.5 "Ricerca e sviluppo sull'idrogeno" CUP: I83C22001170006.

References
[1] Caponi R., Bocci E., Del Zotto L., "On-site hydrogen refuelling station techno-economic model for a fleet of fuel cell buses", International Journal of Hydrogen Energy (Elsevier), 71 (2024), pp. 691-700
[2] SAE International, SAE J2601 – Fueling Protocols for Light Duty Gaseous Hydrogen Surface Vehicles, 2020.

Levelized Cost of Hydrogen from 1 MW Proton-Conducting Ceramic Electrolysis system: Techno-Economic Study in European scenario

***F. Romano*[1], *V. Cigolotti*[2], *and M. Minutillo*[1]**
[1] *Department of Industrial Engineering, University of Salerno, Fisciano, Italy*
[2] *ENEA - Italian National Agency for New Technologies, Energy and Sustainable Economic Development, Naples, Italy*
fabiana.romano001@studenti.uniparthenope.it

Rising global greenhouse gas emissions, driven by increasing energy demand, make rapid decarbonization essential, positioning green hydrogen, produced via renewable-powered water electrolysis, as a key energy carrier for achieving net-zero goals. Among the different water electrolysis technologies, particular interest is currently focused on the innovative Proton Conducting Ceramic Electrolyzer (PCCEL), which represents a promising solution still under development. PCCEL operates at intermediate temperatures (400-600°C), with high efficiency, low cell degradation and cheap stainless-steel materials for pressurized system [1, 2].
In this context, the present study performs a Techno-Economic Analysis (TEA) of a 1 MW PCCEL system, aiming to evaluate the Levelized Cost of Hydrogen (*LCOH*) and to assess its potential for sustainable hydrogen deployment within the European energy landscape.
To model the PCCEL system and assess the techno-economic feasibility, the analysis is performed by using a numerical approach based on a thermo-electrochemical model developed in Aspen Plus environment (Figure 1).

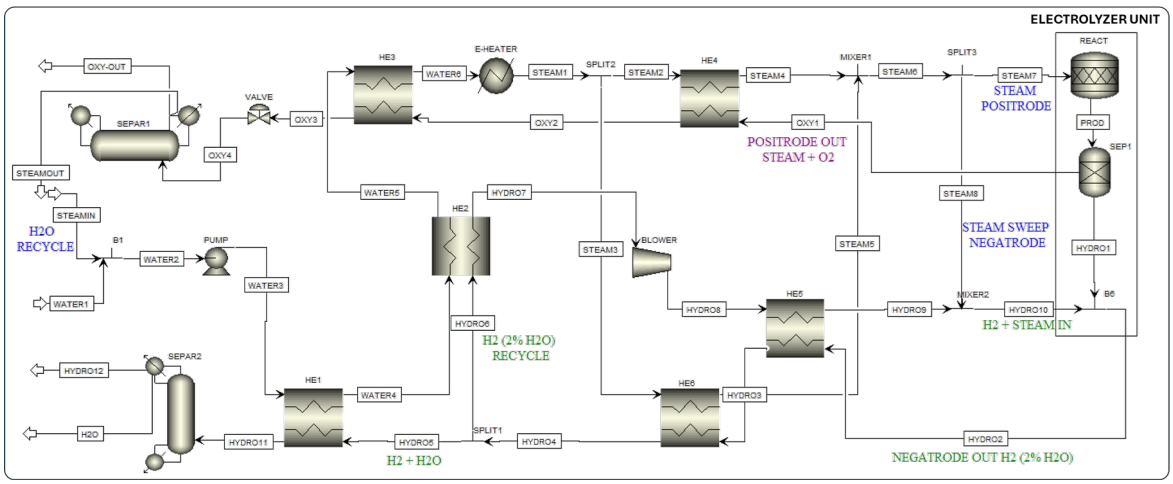

Figure 1. PCCEL system developed in the Aspen Plus environment.

This model calculates the operating conditions and sizing of each component, providing the necessary data to estimate system costs and the resulting LCOH. These main data are summarized in Table 1.

Table 1. Operating conditions and sizing of BoP components.

Operating conditions	**Units**	**Value**
Feed water mass flow rate	kg/h	298
Hydrogen mass flow rate	kg/h	26.2
Component duty and size	**Units**	**Value**
HE 1 (Duty/Size)	kW - m^2	32.5 - 18.6
HE 2 (Duty/Size)	kW - m^2	1.1 - 0.83
HE 3 (Duty/Size)	kW - m^2	45.5 - 71.8
HE 4 (Duty/Size)	kW - m^2	29.0 - 51.6
HE 5 (Duty/Size)	kW - m^2	2.45 - 1.38
HE 6 (Duty/Size)	kW - m^2	29.0 - 57.8

The *LCOH* is estimated by applying the following equation [3]:

$$LCOH = \frac{CRF \cdot [C_{FC,tot} + \sum_{n=0}^{N-1}(C_{O\&M,\,n,\,an} + C_{rep,\,n=t,an})]}{m_{H_2,year}} \quad (1)$$

where *CRF*, equal to 0.06, is the capital recovery factor: it is estimated based on the real interest rate I_r and the electrolysis system lifetime (*N*) equal to 20 years. $C_{FC,tot}$ is the total fixed capital cost. It is defined as the sum of the fixed capital costs of single component ($C_{FC,i}$) and is calculated as illustrated in Equation 2. $C_{FC,I}$ is determined considering the investment cost of single component ($CAPEX_i$) and the cost factors (f_{cost}), related to the installation of the technical and engineering equipment (Equation 3) [4].

$$C_{FC,tot} = \sum C_{FC,i} \quad (2)$$

$$C_{FC,i} = f_{cost} \cdot CAPEX_i \quad (3)$$

$C_{O\&M,n,an}$, and $C_{rep,n=t,an}$ are annual present values of the operating and maintenance costs, and replacement costs, respectively. To estimate these costs, the following Equations 4-5 are applied [3].

$$C_{O\&M,n,an} = \frac{C_{O\&M}}{(1+I_r)^n} \quad (4)$$

$$C_{rep,\mathrm{n=t,an}} = \frac{C_{rep}}{(1+I_r)^t} \quad (5)$$

$C_{O\&M,n,an}$ are calculated assuming the maintenance cost of 1.5% [5] and 2% [6] of CAPEX for the electrolyzer and BoP, respectively, feed water price and an average electricity cost in Europe of 75 €/MWh in 2024 [7]. $C_{rep,n=t,an}$ are defined considering t as the number of years in which the replacement of components is suggested.
Finally, $m_{H2,year}$ is the yearly hydrogen production through the PCCEL system. Assuming these parameters and applying this TEA methodology, the annual *LCOH* is equal to 5.44 €/kg of H_2.

Since the *LCOH* depends mainly on the average cost of electricity, a sensitivity analysis is also conducted to assess the effect of price changes on the *LCOH*. The LCOH is estimated considering both the electricity prices from various European countries in 2024 [7] and different time scenarios (100 €/MWh in 2023 and 40 €/MWh in 2030) [8,9]. The sensitivity analysis show LCOH ranging from 3.66 €/kg H_2 to 6.90 €/kg H_2 (without O_2 sales), underscoring the positive impact of renewables. By 2030, increased renewable penetration is expected reaching the target of the Hydrogen Europe SRIA of 3 €/kg H_2.
Although hydrogen production through electrolysis process is currently more expensive than alternative technologies (e.g., steam reforming of methane), it represents the most promising solution for significant emissions reductions in the medium to long term.

Acknowledgements
PROTOSTACK project has received support from the European Union's Horizon 2020 Research and Innovation Program, Hydrogen Europe and Hydrogen Europe Research.

References
[1] R. Martin, "GHG EMISSIONS OF ALL WORLD COUNTRIES JRC SCIENCE FOR POLICY REPORT," 2024. doi: 10.2760/0115360.
[2] F. Romano, E. Vøllestad, C. Denonville, A. Arrigoni, V. Cigolotti, and M. Minutillo, " Environmental impacts study of high temperature electrolyzers," Journal of Physics: Conference Series 3143 (2025) 012080 doi:10.1088/1742-6596/3143/1/012080
[3] A. Perna, E. Jannelli, S. Di Micco, F. Romano, and M. Minutillo, "Designing, sizing and economic feasibility of a green hydrogen supply chain for maritime transportation," Energy Convers Manag, vol. 278, Feb. 2023, doi: 10.1016/j.enconman.2023.116702.
[4] G. P. Towler and R. K. Sinnott, Chemical engineering design : principles, practice and economics of plant and process design. Butterworth-Heinemann is an imprint of Elsevier, 2022.
[5] E. Vartiainen et al., "True Cost of Solar Hydrogen," Solar RRL, vol. 6, no. 5, May 2022, doi: 10.1002/solr.202100487.
[6] D. Jang, J. Kim, D. Kim, W. B. Han, and S. Kang, "Techno-economic analysis and Monte Carlo simulation of green hydrogen production technology through various water electrolysis technologies," Energy Convers Manag, vol. 258, Apr. 2022, doi: 10.1016/j.enconman.2022.115499.
[7] Ffe - https://www.ffe.de/en/publications/european-day-ahead-electricity-prices-in-2024/
[8] Electricity prices in Europe in 2023 https://gmk.center/en/posts/electricity-prices-in-europe-fell-significantly-in-january-2023
[9] STATISTA - Average electricity wholesale price in 2025 -https://www.statista.com/statistics/1267548/italy-monthly-wholesale-electricity-price/#statisticContainer

Economic Assessment of Multi-Fuel Solid Oxide Fuel Cells System for Shipping Under Alternative Hydrogen, Methanol, and Ammonia Supply Pathways

S. Di Micco[1], A. Cappiello[1], and M. Minutillo[2]

[1] *Department of Engineering, University of Naples "Parthenope", Naples, Italy*
[2] *Department of Industrial Engineering, University of Salerno, Fisciano, Italy*
simona.dimicco@uniparthenope.it

Maritime transport emits about 1 billion tonnes of CO_2 annually (2.5% of global GHGs) and still relies mainly on HFO/MDO (>80%), with limited uptake of LNG (5–6%) and other alternatives [1]. Meeting EU Green Deal objectives and IMO targets requires technologies beyond today's state of the art.

Hydrogen and its carriers, together with fuel-cell propulsion, are key candidates for climate-neutral shipping. Ammonia and methanol are attractive due to liquid storage and decent volumetric energy density, but each brings major safety and integration constraints (toxicity/corrosion for NH_3, cryogenic storage for LH_2, low flash point and IGF Code compliance for methanol).

Techno-economic assessment (TEA) is a core tool to test the feasibility of alternative maritime power systems as shipping moves toward deep decarbonization. Long-range vessels, still largely powered by fossil-fuel internal combustion engines, face tighter regulation and operational constraints linked to emissions, fuel costs, and efficiency limits. In this context, solid oxide fuel cells (SOFCs) stand out for high electrical efficiency and fuel flexibility, with the potential to reduce both greenhouse gases and local pollutants.

This study focuses on the economic assessment of a small scale multi-fuel SOFC system (6 kW) for marine applications. Total investment costs as well as operating and maintenance costs are quantified. Different fuel-pathway scenarios have been analysed for fuel cost estimation (hydrogen from SMR, SMR+CCS, and renewable routes; fossil and green methanol; green ammonia). Moreover, key performance indicators such as Specific Fixed Capital (SFC), Specific Operating Cost (SOP), and Specific Net Present Cost (SNPC) have been derived to identify the main cost drivers and trade-offs.

The economic analysis draws on the technical results reported in a previous work [3], where the authors developed and validated a thermo-electrochemical model of a 6 kW unit to estimate operating conditions and overall system performance. The multifuel system is conceived as a system that can operate separately with different fuels, like ammonia (NH_3), methanol (CH_3OH), or hydrogen (H_2). The block diagram of the propulsion system is illustrated in Figure 1. The SOFC provides DC power for propulsion and onboard services; a DC–DC converter stabilizes and regulates the DC bus. Since the propulsion motor is AC, a DC/AC inverter feeds the motor, while an AC switchboard distributes power to other loads (transformers are assumed for all users except the motor). Motor speed is controlled via a frequency converter, and torque is transmitted to the propeller shaft through a gearbox.

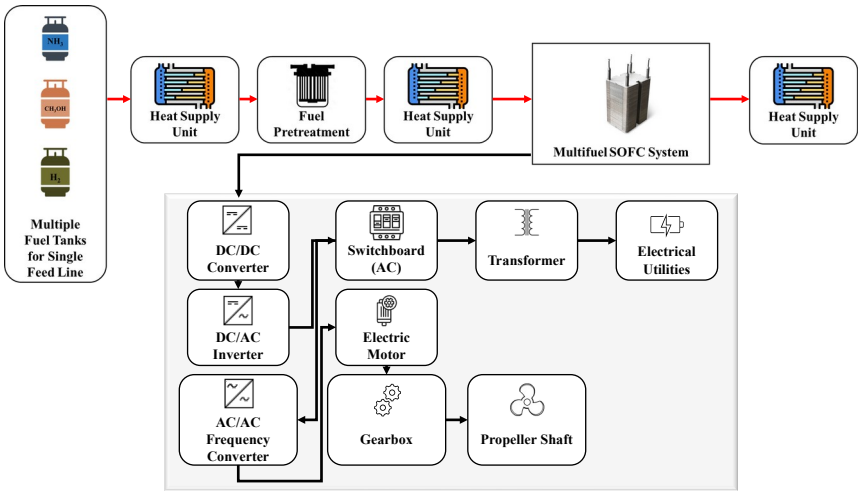

Figure 1: Block diagram configuration of the onboard multi-fuel SOFC system

The economic analysis has been performed by estimating, as previously mentioned, the total investment cost (CAPEX) and the main techno-economic KPIs—Specific Fixed Capital (SFC), Specific Operating Cost (SOP), and Specific Net Present Cost (SNPC) by using the following equations:

$$C_{inv,tot} = C_{PU} + C_{BoP} \quad (1)$$

Where C_{PU} and C_{BoP} represents the costs fort the SOFC power unit and the Balance of Plant, respectively. The total investment costs ($C_{inv,tot}$) has been calculated equal to 48,211€. Maintenance costs have been estimated at 2% (assumed on an annual basis) of the capital investment costs for the Power Unit system and the Balance of Plant (BoP). The operating costs have been estimated considering different fuel-pathway scenarios and, consequently, different costs: H_2 from SMR with a specific cost of 3.33 €/kg, H_2 from SMR with CCS with a specific cost of 4.12 €/kg, green H_2 at 6.71 €/kg, fossil and green CH_3OH with specific costs of 0.44 and 0.78 €/kg and, finally, NH_3 with a specific cost of 1 €/kg. The estimation of the total capital investment cost, together with the maintenance and the operating costs has allowed the calculation of the following Key Performance Indicators, taking into account different fuels pathways:

- **KPI₁: Specific Fixed Capital Cost (SFC)**, calculated as the ratio between the total fixed capital cost (C_{FC}) and the nominal power (P_n) of the propulsion system:

$$KPI_1 = S_{FC} = \frac{C_{FC}}{P_n} \left[\frac{€}{kW}\right] \quad (2)$$

- **KPI₂: Specific Operating Cost (SOP)**, calculated as the ratio between the operating costs during the plant lifetime ($C_{O,n}$) and the nominal power (P_n) of the propulsion system:

$$KPI_2 = S_{OP} = \frac{\sum_{n=0}^{N-1}(C_{O,n})}{P_n} \left[\frac{€}{kW}\right] \quad (3)$$

Where N represents the system lifetime.

- **KPI_3: Specific Net Present Cost (S_{NPC}),** calculated as the ratio between the net present cost (NPC) and the nominal power (P_n) of the propulsion system:

$$KPI_3 = S_{NPC} = \frac{NPC}{P_n} \left[\frac{€}{kW}\right] \quad (4)$$

The NPC is defined as the present value of all the costs of installing and operating the system's components (total fixed capital cost C_{FC}, operating costs C_O, maintenance costs C_M, and replacement costs C_{rep}) over the system lifetime (N), minus the present value of all the revenues (Rev), such as revenues due to the avoided CO_2 due to the use of hydrogen carriers, that it earns over the system lifetime; therefore, it is calculated as:

$$NPC = C_{FC} + \sum_{n=0}^{N-1} (C_{O,n} + C_{M,n} + C_{rep,n=t,} - Rev_{CO_{2_{av}},n}) \quad (5)$$

Table 1 shows the obtained results for the KPIs:

Table 1: KPIs results

	H_2 from SMR	**H_2 from SMR with CCS**	**Green H_2**	**Fossil CH_3OH**	**Green CH_3OH**	**Green NH_3**
KPI_1 (S_{FC}) [€]	8,035					
KPI_2 (S_{OP}) [€]	48,521	60,032	97,771	35,031	62,357	89,362
KPI_3 (S_{NPC}) [€]	92,523	104,034	141,773	79,033	106,359	133,364

Techno-economic evaluations like this are crucial to support the deployment of innovative maritime power systems. By linking performance-based system sizing with CAPEX/OPEX and key performance indicators, such assessments bridge the gap between modelled prototypes and bankable, commercially deployable SOFC solutions, accelerating the adoption of low-emission propulsion technologies.

Acknowledgements
This research has received funding from the European Union's Horizon 2020 Research and Innovation program under Grant Agreement N.101069828, project FuelSOME—Multifuel SOFC system with Maritime Energy vectors.

References
[1] IEA. International Shipping; IEA: Paris, France, 2021. Available online: https://www.iea.org/reports/international-shipping (accessed on 30/07/2025).
[3] Di Micco S, Sztrinko P, Cappiello A, Cigolotti V, Minutillo M. Multi-Fuel SOFC System Modeling for Ship Propulsion: Comparative Performance Analysis and Feasibility Assessment of Ammonia, Methanol and Hydrogen as Marine Fuels. J Mar Sci Eng 2025;13. https://doi.org/10.3390/jmse13101960.

Dynamics and Diversity of Light Harvesting

S. Seki, T. Miyata, K. Namba, R. Fujii, and G. Kurisu - Pigment structural diversity in light-harvesting complexes from eukaryotic photosynthetic organisms

A. Amelii, V. Gandolfi, Z. Guardini, A. Ghezzi, R. Caferri, A. Garcia Fleitas, G. N. Cerullo, L. Dall'Osto, C. D'Andrea, and R. Bassi – Tracking excited-state dynamics and quenching in vivo: a time-resolved analysis in light-harvesting antenna mutants

M.S. Rao, F.H. Ali, S.K. Penneru, G. Nagy, S.V. Pingali, G. Garab, H. O'Neill, B.D. Bruce – Adaptive Spatiotemporal Remodeling of Cyanobacterial Thylakoids Under Varying Growth Light Conditions

S. Shubhankar, D. Bina, L. Moravcová, E. Özcan, A. T. Paradzah, T. Polivka – Energy transfer and quenching in VCP under stress conditions

D-H. Li, A. Ruban, J.-P. Zhang, and J. Zheng – Excimer and non-photochemical quenching in LHCII

Pigment structural diversity in light-harvesting complexes from eukaryotic photosynthetic organisms

***S. Seki*[1], T. Miyata[2,3], K. Namba[2,3], R. Fujii[4], and G. Kurisu[1,3]**
[1] *Institute for Protein Research, UOsaka, Suita, Osaka, Japan.*
[2] *Grad. Sch. Frontier Biosci., UOsaka, Suita, Osaka, Japan.*
[3] *JEOL YOKOGUSHI Res. Alliance Labs., UOsaka, Suita, Osaka, Japan.*
[4] *Grad. Sch. Frontier Biosci., UOsaka, Suita, Osaka, Japan.*
[5] *ReCAP, Osaka Metropol. Univ., Osaka, Japan.*
s-seki@protein.osaka-u.ac.jp

Light-harvesting complexes (LHCs) are essential components for sunlight acquisition in photosynthetic processes, enabling both efficient solar energy capture and regulated dissipation of excess excitation energy [1]. Eukaryotic photosynthetic organisms exhibit extensive diversity in pigment composition and arrangement, including variations in chemical structures, three-dimensional conformations, and binding positions within protein scaffolds, allowing adaptation to diverse light environments on Earth [2]. However, the structural complexity of pigment-binding patterns has made it challenging to understand the mechanisms how individual pigments function and how their spatial organization is controlled by the protein matrix.

In recent years, our group has determined high-resolution cryo-electron microscopy structures of LHCs from multiple natural organisms, as well as from a recombinant system, providing structural bases for understanding spectral tuning and energy management in eukaryotic light-harvesting systems.

1.The green-light absorption mechanism in green algal LHCII was elucidated through cryo-electron microscopy structures from several green algae (Fig. 1a) [3]. Structural comparisons revealed partial pigment replacement, while spectroscopic analyses demonstrated systematic variation in absorption energies correlated with the number and identity of bound carbonyl carotenoids. Notably, the presence or absence of a specific carbonyl carotenoid enabled clarification of the molecular origin of green-light absorption in marine green algae.

2. The 1.94 Å cryo-EM structure of the prasinophyte-specific antenna Lhcp from *Ostreococcus tauri* was subsequently determined (Fig. 1b) [4]. Although Lhcp shares a conserved core architecture with plant-type LHCII, it exhibits a distinct pigment composition, including a cis-isomer of esterified antheraxanthin B that stabilizes its trimeric assembly. These structural features account for functional divergence and reflect adaptation during early eukaryotic photosynthetic evolution.

3. The near–far-red absorption mechanism of the red-shifted violaxanthin–chlorophyll protein (rVCP) from the eustigmatophyte Trachydiscus minutus was further elucidated (Fig. 1c) [5]. Cryo-EM analysis revealed a previously unrecognized heterodimeric tetrameric architecture and huge Chlorophyll (Chl)

a cluster formation through the hetero dimer. Quantum chemical calculations demonstrated that protein-regulated excitonic coupling among chlorophyll a pigments in the cluster, without pigment modification or charge-transfer contributions, gives rise to strong absorption around 700 nm.

4. Finally, the cryo-EM structure of in vitro reconstituted recombinant LHCII was determined, establishing structural equivalence to the native complex with minor differences in pigment occupancy [6]. This result validates recombinant LHCII as a robust platform for systematic manipulation of pigment composition and protein sequence in functional and design-oriented studies.

Collectively, these structural analyses define how protein scaffolds regulate pigment identity, positioning, and electronic coupling to achieve adaptive light harvesting. The mechanistic principles identified here provide a foundation for understanding natural photosynthetic systems and for the rational engineering of light-harvesting modules for future solar-energy and photosynthesis-inspired applications.

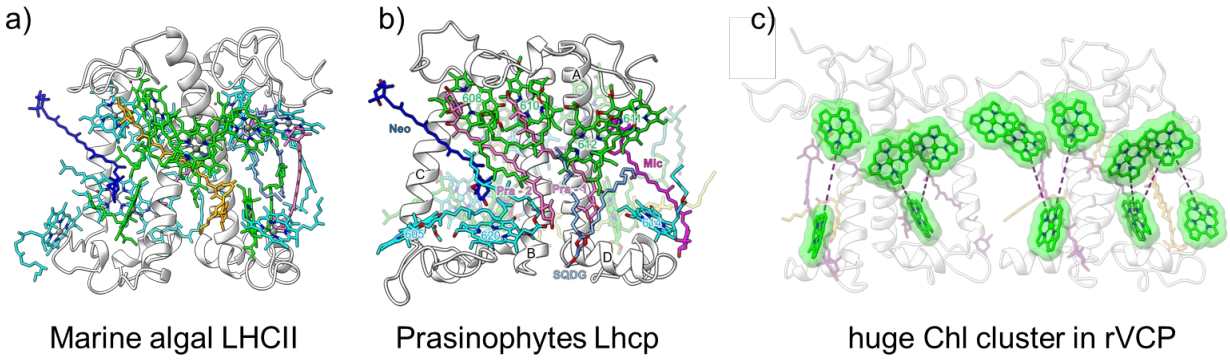

Figure 1: Cryo-EM structure of Marine algal LHCII (a), Prasinophytes Lhcp (b) and rVCP from eustigmatophytes (c).

References

[1] Croce, R. and van Amerongen H. "Light harvesting in oxygenic photosynthesis: Structural biology meets spectroscopy", Science, 369, 6506, 2020, aay2058.
[2] Iwai, M. et al. "Structural Diversity in Eukaryotic Photosynthetic Light Harvesting", Annual Review of Plant Biology, 75, 2024, 119-152.
[3] Seki, S. et al. "Structural insights into blue-green light utilization by marine green algal light harvesting complex II at 2.78 Å", BBA Adv., 2, 2022, 100064.
[4] Seki, S. et al. "Distinctive and functional pigment arrangements in Lhcp, a prasinophyte-specific photosynthetic light-harvesting complex", Commun. Biol., 8, 2025, 1586.
[5] Seki, S. et al. "Exciton Delocalization Promotes Far-Red Absorption in a Tetrameric Chlorophyll a Light-Harvesting Complex from Trachydiscus minutus", JACS, 147, 51, 2025, 47675-47689.

[6] Seki, S. et al. "Exciton Delocalization Promotes Far-Red Absorption in a Tetrameric Chlorophyll a Light-Harvesting Complex from Trachydiscus minutus", PNAS nexus, 3, 9, 2024, pgae405.

Tracking excited-state dynamics and quenching *in vivo*: a time-resolved analysis in light-harvesting antenna mutants

***Antonello Amelii*[1], Valerio Gandolfi[2], Zeno Guardini[1], Alberto Ghezzi[2], Roberto Caferri[1], Ariel Garcia Fleitas[2], Giulio N. Cerullo[2,3,4], Luca Dall'Osto[1], Cosimo D'Andrea[2,3], and Roberto Bassi[1,4,5]**

[1] *Università di Verona, Verona, Italy*
[2] *Politecnico di Milano, Milano, Italy*
[3] *Istituto Italiano di Tecnologia, Milano, Italy*
[4] *Accademia Nazionale dei Lincei, Rome, Italy*
[5] *Anton Dorhn Experimental Marine Station, Naples, Italy*
antonello.amelii@univr.it

The ability of plants to regulate light harvesting while safely dissipating excess energy is vital for survival under fluctuating light conditions. To prevent photodamage when light intensity exceeds their capacity for photosynthesis, they employ non-photochemical quenching (NPQ)—a multi-component process that harmlessly converts surplus excitation energy into heat, thereby safeguarding the photosynthetic apparatus from photoinhibition [1].
PAM fluorescence measurements have been invaluable for assessing NPQ at the whole-leaf level; however, they cannot unequivocally distinguish genuine energy dissipation from other factors that influence fluorescence yield, such as static quenching, photobleaching, or chloroplast rearrangements [2-4]. This limitation is particularly evident in antenna-deficient mutants, where changes in pigment composition and antenna size complicate data interpretation. To address these challenges, we employed time- and spectrally-resolved fluorescence lifetime snapshot measurements [2-4], in *Arabidopsis thaliana* and *Hordeum vulgare* mutant lines lacking specific pigment–protein complexes or NPQ regulatory proteins, enabling us to track the *in vivo* dynamics of excited chlorophyll states during NPQ induction and relaxation.
Combined with global analysis, measurements on control mutants lacking specific components of the photosynthetic apparatus allowed us to associate individual kinetic components with defined biochemical entities. This approach provides an intrinsic and quantitative measure of energy dissipation, resolving NPQ dynamics into spectrally and kinetically distinct elements. Analysis of decay-associated spectra enabled the identification of two nanosecond components, whose relative amplitudes and lifetimes change depending on the size of the PSII antenna system and upon light exposure, as well as a faster component originating from the PSI–LHCI complex. Upon exposure to saturating light, a dissipative response was observed in all genotypes, implying that each pigment-binding protein contributed to the overall NPQ activity. However, the dominant energy quenching component requires trimeric LHCII complexes, PsbS and zeaxanthin, whereas monomeric Lhcb subunits act as additional quenching sites and excitonic bridges that sustain PSII cooperativity [5]. Moreover, the absence of the outer antenna increases excitation energy transfer between PSII and PSI, suggesting PSII-to-PSI spillover becomes

relevant in LHC-deficient plants and further indicating that Lhcb complexes are crucial for preserving the structural organization that regulates energy balance between the photosystems. Collectively, these findings establish NPQ as a cooperative, multi-site process that links antenna architecture to photoprotective efficiency, offering new insight into how plants dynamically regulate energy flow under fluctuating light conditions.

Acknowledgements
This work was funded by European Research Council (ERC Advanced Grant 101053983-GrInSun).

References
[1] Bassi, R., & Dall'Osto, L. "Dissipation of light energy absorbed in excess: the molecular mechanisms", Annual review of plant biology, 72(1), 2021, 47-76.
[2] Amarnath, K., Zaks, J., Park, S. D., Niyogi, K. K., & Fleming, G. R. "Fluorescence lifetime snapshots reveal two rapidly reversible mechanisms of photoprotection in live cells of *Chlamydomonas reinhardtii*", Proceedings of the National Academy of Sciences, 109, 22, 2012, 8405-8410.
[3] Sylak-Glassman, E. J., Malnoë, A., De Re, E., Brooks, M. D., Fischer, A. L., Niyogi, K. K., & Fleming, G. R. "Distinct roles of the photosystem II protein PsbS and zeaxanthin in the regulation of light harvesting in plants revealed by fluorescence lifetime snapshots", Proceedings of the National Academy of Sciences, 111, 49, 2014, 17498-17503.
[4] Sylak-Glassman, E. J., Zaks, J., Amarnath, K., Leuenberger, M., & Fleming, G. R. "Characterizing non-photochemical quenching in leaves through fluorescence lifetime snapshots", Photosynthesis Research, *127*, 1, 2016, 69-76.
[5] Guardini, Z., Dall'Osto, L., Gomez, R. L., Caferri, R., Joliot, P., & Bassi, R. "Mapping light-harvesting and photoprotection responses in the Photosystem II antenna system of higher plants", Plant Physiology, *199*, 4, 2025.

Adaptive Spatiotemporal Remodeling of Cyanobacterial Thylakoids Under Varying Growth Light Conditions

Mahipal S. Rao[1], Fedaa H. Ali[2], Sree Kavya Penneru[1], Gergely Nagy[3], Sai Venkatesh Pingali[3], Győző Garab[4], Hugh O'Neill[3], Barry D. Bruce[1]

[1]BCMB Department, University of Tennessee, Knoxville, TN, USA; [2]Genome Science and Technology (GST) Program, University of Tennessee, Knoxville, TN, USA; [3]Neutron Scattering Division (Neutron Sciences Directorate), Oak Ridge National Laboratory, Oak Ridge, TN, USA; [4]Biological Research Centre, Szeged, Hungary
Corresponding author @ bbruce@utk.edu

Photosynthetic membranes are not static scaffolds: they are adaptive, mesoscale energy-conversion platforms that must continuously balance light harvesting, photoprotection, and electron transport as irradiance changes. Yet, despite decades of biochemical and structural work on photosystems, the in vivo spatiotemporal remodeling of thylakoid membranes during light acclimation remains poorly constrained, largely because most ultrastructural methods are destructive or provide limited access to dynamics in living cells. Here, we address this gap using the thermotolerant cyanobacterium *Chroococcidiopsis* sp. TS-821, which exhibits an unusual fascicular thylakoid arrangement with prominent spherical formations and undergoes a growth-light-dependent transition of photosystem I (PSI) from dimers to tetramers. Cryo-EM analysis of the PSI tetramer indicates a pronounced concavity and suggests that PSI structural dynamics upon tetramerization can generate a concave stromal surface in one of the two principal planes. Importantly, the cryo-EM geometry provides a clear structural basis for a propensity to induce membrane bending/curvature, particularly when considered alongside the very high local abundance of PSI tetramers in discrete regions of the thylakoid membrane under high-light growth, where collective packing effects could amplify curvature at the mesoscale. To test this coupling between photosystem organization and membrane architecture, we use non-destructive, high-resolution small-angle neutron scattering (SANS) on actively growing TS-821 cells to quantify changes in thylakoid organization across defined growth-light regimes. The SANS profiles show distinct, light-dependent signatures of thylakoid reorganization, consistent with remodeling of membrane periodicity/ordering rather than a simple change in cell morphology and align with independent evidence for PSI oligomeric-state shifts under high light. Ongoing work will correlate SANS-derived structural metrics with electron microscopy (including 3D ultrastructural analysis) to identify the specific membrane features (e.g., lamellar repeat spacing, domain organization, and curvature distributions) underlying the scattering transitions. Together, this multi-scale strategy links photosystem supramolecular plasticity to thylakoid morphodynamics in living cyanobacteria, offering a new framework for understanding light acclimation and photoprotection. We further hypothesize that increased thylakoid curvature and fascicularization may provide an optical/architectural "light-avoidance" advantage—reducing effective light load through self-shading or altered photon pathlengths—in a way that more strictly concentric or parietal thylakoid organizations cannot. If so, a relatively simple shift in membrane architecture driven by photosystem reorganization could represent an evolutionarily accessible route for cyanobacteria adapting to more intense

and/or rapidly fluctuating irradiance, including during transitions from aquatic to more exposed terrestrial or near-surface environments. Finally, we will extend this framework with cryo-electron tomography (cryo-ET) to directly visualize thylakoid ultrastructure and curvature distributions in 3D across light regimes, enabling quantitative links between SANS-derived structural metrics and membrane topology in intact cells. In parallel, we will perform comparative genomic analyses across cyanobacterial lineages spanning diverse thylakoid architectures to identify genetic signatures associated with PSI oligomeric propensity (e.g., determinants of dimer/tetramer equilibria and associated accessory factors) and to test whether predicted oligomerization capacity correlates with the evolution of reticulated, fascicular, concentric, or parietal membrane organizations. Together, these approaches will help establish a mechanistic and evolutionary map connecting PSI supramolecular plasticity to thylakoid architectural diversity and light adaptation.

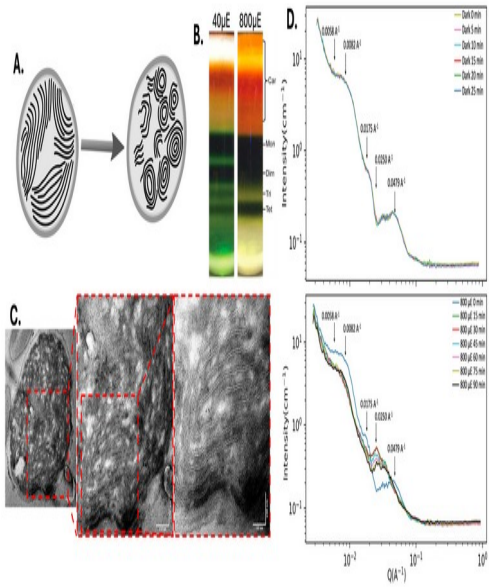

Figure 1: *Chroococcidiopsis* TS-821 thylakoid membranes undergo rapid dynamics when exposed to different light regimes to evade photodamage. A. Schematic of expected membrane organization after exposure to high light (adapted from [1]). B. TS-821 upregulates the production of carotenoids and the tetrameric form of PSI after exposure to high light (adapted from [2]). C. Initial TEM representative images supporting our hypothesis of increased thylakoid curving after exposure to increased light intensity. D. Small-angle Neutron Scattering data showing a time-series of membrane reorganization in dark-adapted and after TS-821 cells are exposed to high light (800µE) levels.

References

[1] Mareš J, Strunecký O, Bučinská L and Wiedermannová J "Evolutionary Patterns of Thylakoid Architecture in Cyanobacteria", Front. Microbiol. 10:277. doi: 10.3389/fmicb.2019.00277, 2019

[2] Dmitry A. Semchonok, Meng Li, Barry D. Bruce, Gert T. Oostergetel, Egbert J. Boekema "Cryo-EM structure of a tetrameric cyanobacterial photosystem I

complex reveals novel subunit interactions", Biochimica et Biophysica Acta (BBA) - Bioenergetics, Volume 1857, Issue 9, Pages 1619-1626, doi: 10.1016/j.bbabio.2016.06.012, 2016

Energy transfer and quenching in VCP under stress conditions

Shubhankar Shubhankar [1], ***David Bina*** [1,2], ***Lada Moravcová*** [1], ***Emrah Özcan*** [1], ***Alex T. Paradzah*** [1], ***Tomas Polivka*** [1]

[1] *Faculty of Science, University of South Bohemia, České Budějovice, Czech Republic*
[2] *Institute of Plant Molecular Biology, Biological Centre, Czech Academy of Sciences, České Budějovice, Czech Republic*

sshubhankar@prf.jcu.cz

As immobile organisms, plants, algae, and cyanobacteria are constantly exposed to harsh environmental conditions such as high light intensity and extreme temperatures. To survive, they rely on photoprotective mechanisms such as quenching, which safely dissipates excess absorbed light energy as heat to prevent photodamage [1]. When photosynthetic systems exceed their light saturation point, the risk of over-excitation increases, leading to photoinhibition and the formation of reactive oxygen species, which can severely impair photosynthesis [2]. In the absence of effective quenching mechanisms, excess excitation energy would cause irreversible damage to the photosynthetic apparatus, ultimately compromising organismal viability.

This underscores the critical importance of elucidating the molecular basis of energy dissipation pathways, which are associated with antenna proteins. One such antenna protein is the Violaxanthin–Chlorophyll-a protein (VCP) that represents a unique Chl-a-only member of the light-harvesting complex (LHC) superfamily. Unlike higher plant LHCII, which binds with Chl-a, Chl-b, and multiple carotenoids, VCP binds only ~~with~~ Chl-a together with three non-carbonyl carotenoids: violaxanthin (Vio), vaucheriaxanthin (Vau), and vaucheriaxanthin-ester. While spectroscopically very similar in solution, ~~These~~ these ~~pigments~~ carotenoids have distinct spectral signals in VCP~~, .~~ ~~with s~~Some studies ~~indicating~~ indicate ~~that carotenoids in VCP~~they give rise to absorption bands at ~485, 503, and 520-525 nm [3,5], which represent different protein-pigment interactions, hence contributing differently to the overall energy transfer landscape. Structural studies have shown that VCP shares the conserved pigment-binding nucleus typical of LHC proteins but deviates in its exclusive use of Chl-a and non-carbonyl carotenoids.

For this study, we focused on VCP from *Nannochloropsis*, a genus of eustigmatophyte microalgae known for its exceptionally high growth rates and biotechnological relevance. It has a wide range of biotechnological applications, including lipid production, oral delivery systems in aquaculture due to their robustness as well as rich carotenoid content, and as a nutrient-rich feed source for farm animals [3]. Their ability to thrive in high light marine environments makes them ideal models for understanding the interplay between light harvesting and photoprotection.

Earlier spectroscopic work has shown that carotenoid-to-chlorophyll energy transfer in VCP is highly efficient (~90%) [4], suggesting an important role of

quenching under stress conditions. This feature sets VCP apart from other LHC family members, such as LHCII, where violaxanthin participation in energy transfer is relatively low, and total efficiency of the ~~system~~ carotenoid-to-Chl energy transfer remains significantly lower. To better understand how VCP responds to protein-level stress, we subjected the isolated complex to increasing concentrations of urea, as well as elevated temperatures, and monitored structural and functional changes using time-resolved fluorescence and ultrafast transient absorption spectroscopy. These techniques allow us to probe pigment-specific excited state dynamics on femtosecond timescales; track population flow using ~~EADS~~ global fitting and assess how pigment-protein interactions reshape under perturbations.

Under stress, VCP displayed a consistent shortening of the Chl-a fluorescence lifetime, indicating enhanced quenching activity. This is consistent with stress-induced opening of dissipative channels, and it can be speculated that it is because of increased car-chl coupling or disordering of protein structure that can lead to alternating relaxation pathways.

In the carotenoid absorption bands, a blue-shift was observed under stress conditions, suggesting that the carotenoid binding to VCP was also affected. Interestingly, despite these changes, VCP still showed energy transfer from carotenoids to chlorophylls, although with lower efficiency (50%), highlighting that the protein is robust and resilient under stressful conditions. This resilience mirrors observations in related eustigmatophyte antennae, such as red-shifted rVCP, where efficient energy transfer persists even when excitonic structures or pigment interactions are altered by environmental stress [5]. Also, maintaining decent car-to-Chl energy transfer efficiency is a sign of light-harvesting, while the shorter Chl-a lifetime is a sign of stress-induced quenching. Thus, we can conclude that VCP optimizes the balance between light-harvesting and quenching.

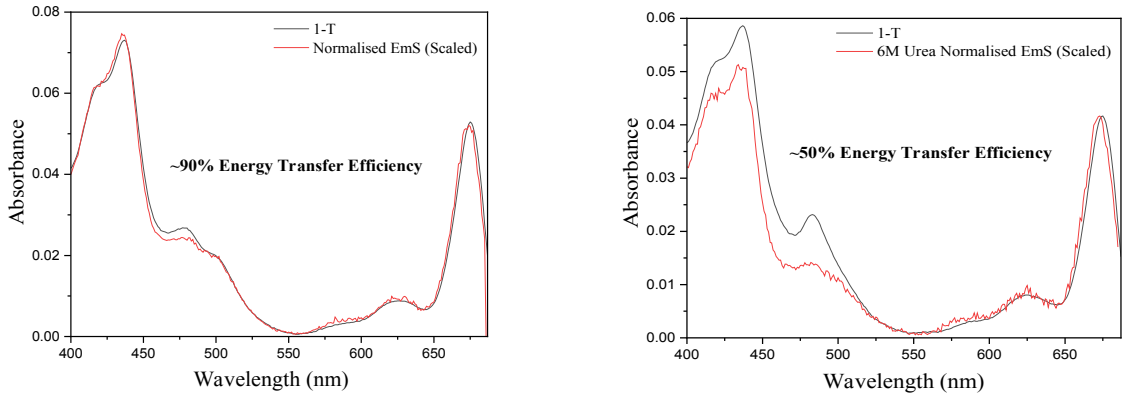

Fig 1. & 2. ~~Excitation fluorescence~~ Fluorescence excitation spectra of VCP detected ~~with a fixed emission of~~at 690 nm for control (left) ~~&~~ and 6M urea (right), respectively.

Acknowledgements
This work was supported by the P JAC project "Photomachines" Reg. No CZ.02.01.01/00/22_008/0004624.

References
[1] Govindjee, U, Barbara Demmig-Adams, Gyozo Garab, and William Adams. Non-photochemical quenching and energy dissipation in plants, algae and cyanobacteria. Dordrecht: Springer Netherlands, 2014.
[2] Al-Hoqani, U., Young, R., & Purton, S. The biotechnological potential of Nannochloropsis. Perspectives in Phycology. 1-15. 2017
[3] Keşan, G., Litvín, R., Bína, D., Durchan, M., Šlouf, V., & Polívka, T. Efficient light-harvesting using non-carbonyl carotenoids: Energy transfer dynamics in the VCP complex from Nannochloropsis oceanica. Biochimica et Biophysica Acta (BBA)-Bioenergetics. 370-379. 2016.
[4] Bína D., Durchan M., Kuznetsova V., Vácha F., Litvín R., Polívka T. "Energy transfer dynamics in a red-shifted violaxanthin–chlorophyll a light-harvesting complex." Biochimica et Biophysica Acta (BBA) – Bioenergetics 1860, 111–120 (2019).
[5] Llansola-Portolés M. J., Litvín R., Ilioaia C., Pascal A. A., Bína D., Robert B. "Pigment structure in the violaxanthin–chlorophyll-a-binding protein VCP." Photosynthesis Research 134, 51–58 (2017).

Excimer and non-photochemical quenching in LHCII

***D.-H. Li*[1], *A. Ruban*[1], *J.-P. Zhang*[2], *and J. Zheng*[3],**
[1] *Queen Mary University of London, London, United Kingdom*
[2] *Renmin University of China, Beijing, China*
[3] *Peking University, Beijing, China*
danhong.li@qmul.ac.uk

Photosynthesis initiates with light absorption, mainly by light-harvesting antenna complexes (LHC), primarily LHCII in higher plants. This energy is efficiently transferred to Photosystem II (PSII) reaction centers, driving primary photochemical reactions. LHCII thus balances light capture with dissipating excess energy under high light to prevent photodamage from accumulated ^{1}Chl* and reactive oxygen species (ROS). Plants use photoprotective mechanisms like energy-dependent quenching (qE), a key part of non-photochemical quenching (NPQ), to rapidly dissipate surplus ^{1}Chl* as heat, protecting photosynthetic machinery.

Our investigation focuses on the role of the chlorophyll (Chl) excimer, a photophysical intermediate recently identified in LHCII. The excimer-like intermediate has been observed under various environmental conditions, including in 70% glycerol-solubilized LHCII trimers, proteoliposomes, and detergent-free LHCII aggregates [1]. This Chl excimer is characterized by an unstructured broadband emission at approximately 730 nm at cryogenic temperatures. Crucially, the 730 nm fluorescence band observed in quenched LHCII (Q-F730) exhibits a positive correlation with the quenching efficiency of Chl fluorescence at 680 nm. This correlation strongly suggests that the Chl excimer directly mediates the quenching of ^{1}Chl* and plays a significant role in NPQ.

To elucidate the mechanism of ^{1}Chl* deactivation, we employed a combination of ultrafast transient absorption (fs-TA) and broadband two-dimensional electronic spectroscopy (2DES). These advanced spectroscopic techniques allowed us to compare the photophysical dynamics in quenched (Q-F730) and unquenched (U-F680) LHCII preparations. Our findings reveal a substantial reduction in the photoproduction of carotenoid triplet excitation (^{3}Car*) in Q-F730 compared to U-F680. This observation is a critical piece of evidence, implying that intersystem crossing is unlikely to be the major deactivation channel for ^{1}Chl* in the quenched state. Instead, our data are consistent with a mechanism where ^{1}Chl* deactivation proceeds via the formation of a Chl excimer, followed by the subsequent population of a Chl charge transfer (CT) state and Car S_1 state. This provides direct spectroscopic evidence linking the excimer to Chl singlet excitation quenching in LHCII, offering profound insights into the mechanistic basis of NPQ.

Further detailed analysis of the fs-TA kinetics revealed that the excimer in Q-F730 exhibits a much shorter lifetime compared to U-F680. The observed

transition from negative to positive signs in the fs-TA kinetics for Q-F730 suggests a transformation of the excimer into a different transient species. At room temperature, the excimer fluorescence in Q-F730 is drastically reduced compared to observations at 77 K. This temperature-dependent behaviour is attributed to energy barriers that promote the conversion of the excimer (E*) to CT states (E*-to-CT conversion) and excimer dissociation. This suggests a dynamic interplay between excimer and CT states, where thermal fluctuations at physiological temperatures facilitate the conversion to CT states, thereby reducing excimer fluorescence.

In Q-F730, we identified competing pathways for ^{1}Chl* deactivation. Energy transfer to the lutein S_1 state occurs with a rate constant of $(15.8\ ps)^{-1}$, while energy transfer to the excimer occurs with a rate constant of $(11.9\ ps)^{-1}$. This indicates that both pathways contribute significantly to the overall quenching process. The subsequent conversion of the excimer to CT states and to Car S_1 state further contributes to the efficient dissipation of excess energy.

Our research provides compelling spectroscopic evidence for the involvement of Chl excimers and subsequent CT states, as well as lutein S_1 state in the efficient deactivation of ^{1}Chl* within LHCII, particularly under conditions of excess light [2]. This mechanism offers a refined understanding of how photosynthetic organisms protect themselves from photodamage, highlighting the sophisticated energy transfer and dissipation strategies employed by nature.

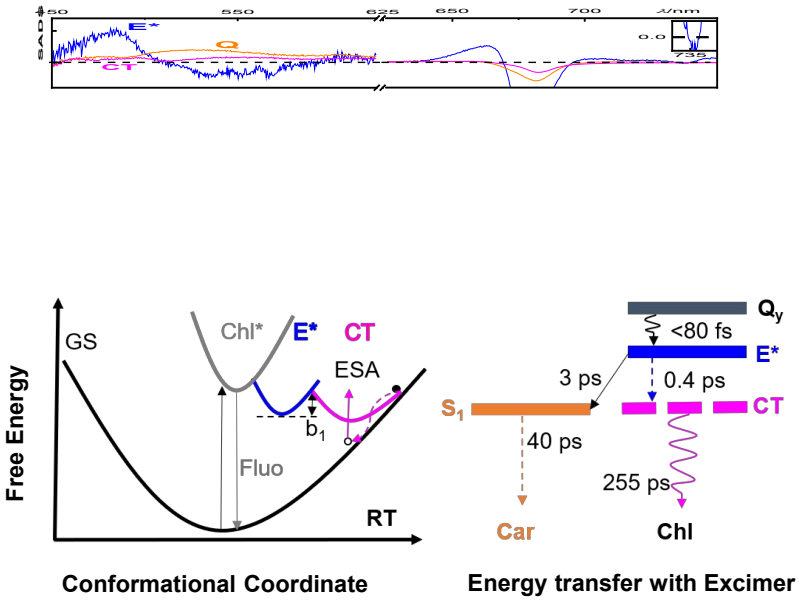

Figure 1: The energy transfer patten of excimer in the quenched state. Q stands for quencher, and E* represents the excimer species.

Acknowledgements
We acknowledge financial supports from the National Science Foundation of China. This work was supported by a China Scholarship Council Ph.D. studentship

References
[1] S. Wilson, D.-H. Li, and A. V. Ruban, "The structural and spectral features of light-harvesting complex II proteoliposomes mimic those of native thylakoid membranes," J. Phys. Chem. Lett. 13, 24, 2022, 5683–5691.
[2] J.-W. Zou[§], D.-H. Li[§], A. V. Ruban, J.-P. Zhang, J. Zheng et. al., "Excimer and non-photochemical quenching in LHCII," J. Chem. Phys. 163, 195104, 2025, 1–14.

Hydrogen Production II

C. Li, X. Shi, Z. Yang, H. Luo, B. Chen, Y. Cai, T. Yang, R. Chahine, J. Xiao - Machine learning Prediction and SHAP Analysis of Breakthrough Times on Pressure Swing Adsorption for Hydrogen Purification

D. Uner - Fast pyrolysis of biomass and downstream processing of the products using concentrated solar energy

A. Di Nardo, L. P. Di Bonito, A. Di Colandrea, A. Parisi, G. Ruoppolo, F. Di Natale, and G. Landi - Waste-derived platinum-based catalysts for raw glycerol valorization to hydrogen by Aqueous Phase Reforming

C. Ruocco, O. Muccioli, C. Falchetta, E. Meloni, V. Palma - Joule heating of Pd-Cu/CeO_2-Al_2O_3 foam catalysts for H_2 production via methanol steam reforming

G. Crescente, G. Baiardo, G. d'Ippolito, G. Squadrito - Design and development of a fermentation system for Bio-Hydrogen production by Thermotoga neapolitana

Machine learning Prediction and SHAP Analysis of Breakthrough Times on Pressure Swing Adsorption for Hydrogen Purification

Chenglong Li[1], Xinyang Shi[2], Ziyu Yang[2], Hao Luo[1], Ben Chen[3], Yonghua Cai[3], Tianqi Yang[3,*], Richard Chahine[4], Jinsheng Xiao[3,4]

[1] *School of Mechanical and Electrical Engineering, Wuhan Business University, Hubei 430056, China*
[2] *Wuhan Maritime Communication Research Institute, Hubei 430205, China*
[3] *School of Automotive Engineering, Wuhan University of Technology, Hubei 430070, China*
[4] *Hydrogen Research Institute, Université du Québec à Trois-Rivières, QC G8Z 4M3, Canada*
corresponding.author: tqyang@whut.edu.cn

Abstract
Accurate prediction of breakthrough behavior in adsorption beds is critical for opti-mizing hydrogen purification processes. In this study, a physical-mathematical model describing hydrogen mixture (H2/CO2/CH4/CO=76%/17%/3%/4%) adsorption on the Metal-organic framework (MOF) UTSA-16 was established and validated against ex-perimental breakthrough curves. The validated model demonstrated strong agreement with experimental data for breakthrough times, curve profiles and component separa-tion order, confirming its reliability in simulating multi-component transport behavior. The validated model was subsequently used to generate a representative dataset under systematically varied operating conditions, including feed flow rate, temperature and adsorption pressure. This dataset enabled the training and evaluation of four machine learning algorithms: decision tree (DT), random forest (RF), gradient boosting regres-sion tree (GBRT), and artificial neural network (ANN). A two-stage workflow, com-bining hyperparameter optimization with repeated K-fold cross-validation, was im-plemented to ensure fair model comparison and robust performance evaluation. Results showed that ANN consistently outperformed tree-based algorithms, achieving the lowest mean RMSE (10.86) with narrow confidence intervals and highly significant improvements ($p < 0.001$). Unlike tree models, which suffered from overfitting or lim-ited robustness, ANN demonstrated superior generalization and stability. To improve model interpretability, SHapley Additive exPlanations (SHAP) analysis was applied to quantify feature contributions to breakthrough time prediction. The results indicate that adsorption pressure is the most influential factor, followed by feed flow rate and tem-perature, consistent with the governing PSA transport and adsorption mechanisms. This work highlights the effectiveness of combining ANN with SHAP analysis for re-liable and interpretable breakthrough time prediction in hydrogen purification PSA systems.
Keywords: Machine learning, SHAP Analysis, UTSA-16, pressure swing adsorption, hydrogen purification, breakthrough time

Results

Figure 1 presents the comparison between simulated breakthrough curves and experimental data at 305 K and 16 bar, with total flowrates of 2.0 SLPM (Fig. 1a) and 1.0 SLPM (Fig. 1b). The breakthrough curves predicted by the physical model exhibit excellent agreement with the experimental data in terms of breakthrough time, curve shape, and peak positions, indicating that the physical-mathematical model can reliably capture the dynamic transport behavior of hydrogen mixtures in the UTSA-16 adsorption bed. The breakthrough curves show that breakthrough times follow the order: CO_2 > CH_4 > CO > H_2, consistent with the adsorption capacities of UTSA-16 for these gases [1]. In addition, an increase in the inlet flowrate leads to shorter breakthrough times, as higher flowrates reduce the gas residence time in the bed, thereby decreasing the contact time with the adsorbent and accelerating breakthrough. These validation results confirm that the physical model can generate high-quality breakthrough curve data, providing a solid foundation for subsequent machine learning-based training and prediction, and offering guidance for optimizing adsorption bed design and operating conditions.

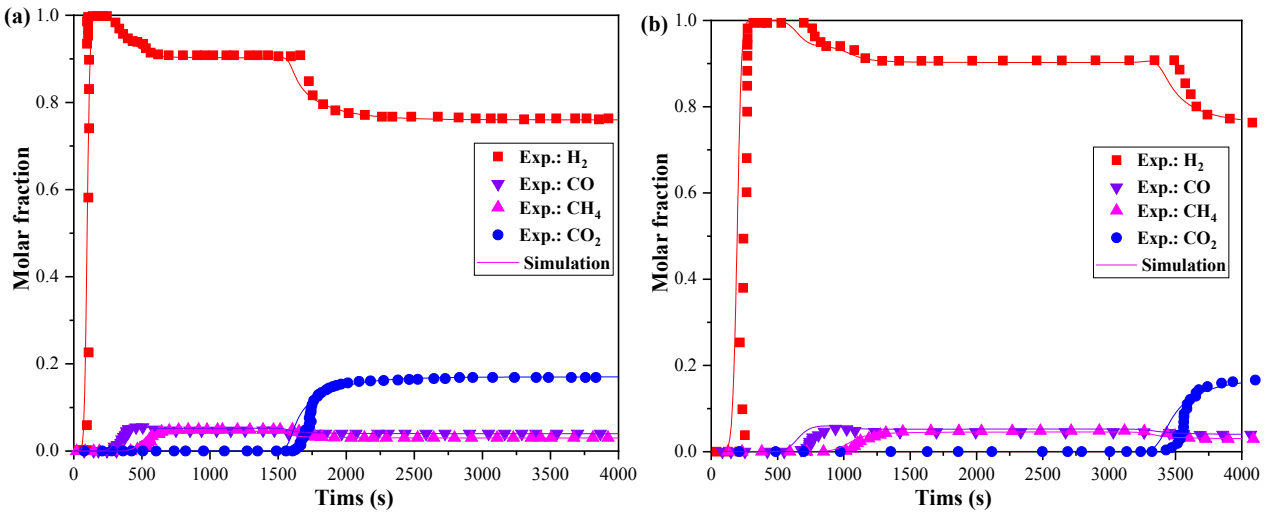

Figure 1. Comparison of the breakthrough curve between experimental data of Ref. [2] and simulation results on UTSA-16 at 16 bar and 305 K with a flowrate of 2.0 SLPM (a) and 1.0 SLPM (b).

Acknowledgements

This research is funded by the 2024 University-Industry-Research Innovation·Fund of·China (2024IT275).

References

[1] Li C, Luo H, Yuan Y, Tong L, Chen B, Yang T, et al. Equilibrium and dynamic adsorption characteristics of zeolite 5A, LiX, 13X and MOF UTSA-16 adsorbents for hydrogen purification. Int J Hydrogen Energy. 2025;140:889-99.

[2] Grande CA, Blom R, Andreassen KA, Stensrød RE. Experimental results of pressure swing adsorption (PSA) for pre-combustion CO_2 capture with metal organic frameworks. Energy Procedia. 2017;114:2265-70.

Fast pyrolysis of biomass and downstream processing of the products using concentrated solar energy

D. Uner
Chemical Engineering, Middle East Technical University, Ankara 06800 Turkiye
uner@metu.edu.tr

Photosynthesis, perfected through billions of years of evolutionary adaptation, will always be the best strategy of CO_2 mitigation and solar energy storage. The critical challenge is to develop chemical technologies to convert biomass to conventional fuels. An energy source is needed with sufficiently high flux and high enough temperatures to be useful to drive the endothermic bond breaking processes. Our proposed solution is to use concentrated solar energy, which can provide thermal energy at very high temperatures, T>2500 K. The challenges with solar energy include the intermittency as well as constructing a process around a moving energy source. Careful management of the transport of solids and collection of liquid and gaseous products are also additional problems to be solved for biomass processing.
We use a 70 cm OD concave mirror enabling us 300 W solar power at T>2500 K for biomass pyrolysis. The representative biomass compound is rice husk, with a manageable particle size and a morphology that enables us to monitor the process. Pyrolysis process was monitored by a batch unit, having a SiC foam at the focal point enabling the penetration of light. The effluent molecules were collected through a convergent chimney for gas analysis. Tar could be collected from the chimney walls also for analysis. Thermogravimetric analysis of the products enabled to determine the efficiency of the process.
The results of this study revealed that by adjusting the exposure time as well as the incident flux, processes ranging from drying to pyrolysis can be conducted. Biochar can be used as an industrial commodity or as a solid fuel. Gas phase and condensable products bear the potential for steam reforming. In addition to our most recent results of biomass pyrolysis, I will also present our earlier work of steam reforming powered by solar thermal energy[1-2].

Acknowledgements
The initial phase of this work was funded by TUBITAK under 1003 program under grant no 213M006. Financial support from SOCAR Turkiye is gratefully acknowledged.

References

[1] Calisan, A., Ogulgonen, C. G., Kincal, S., & Uner, D. (2019). Finding the optimum between volatility and cycle temperatures in solar thermochemical hydrogen production: Pb/PbO pair. *International Journal of Hydrogen Energy*, *44*(34). https://doi.org/10.1016/j.ijhydene.2018.12.189
[2] Calisan, A., Ogulgonen, C. G., Yilmaz, A., Uner, D., & Kincal, S. (2019). Steam methane reforming over structured reactors under concentrated solar irradiation. *International Journal of Hydrogen Energy*, *44*(34), 18682–18693. https://doi.org/10.1016/j.ijhydene.2019.04.033

Waste-derived platinum-based catalysts for raw glycerol valorization to hydrogen by Aqueous Phase Reforming

A. Di Nardo[1], L. P. Di Bonito[2], A. Di Colandrea[2], A. Parisi[2], G. Ruoppolo[1], F. Di Natale[2], and G. Landi [1]

[1] *Institute of Science and Technology for Sustainable Energy and Mobility, CNR, Naples, Italy*

[2] *Department of Chemical, Materials and Industrial Engineering, University of Naples Federico II, Naples, Italy*

gianluca.landi@cnr.it

Noble metals are widely recognised as the most effective catalytic materials due to their electronic structure, chemical inertness and high thermal stability, which enable mild operating conditions and long catalyst lifetimes. However, their high cost, limited availability and strong dependence on primary mining sources motivate the development of alternative approaches aimed at reducing noble metal consumption and improving resource efficiency [1].

In this context, increasing attention has been devoted to the recovery and valorisation of noble metals from secondary sources, such as exhausted sorbents, spent catalysts, industrial residues and electronic waste. Rather than being disposed of as waste, these materials can be reintegrated into catalytic applications through suitable recovery and re-functionalisation strategies. The transformation of noble-metal-containing wastes into waste-derived catalysts (WDCs) contributes to reducing reliance on virgin resources and supports the implementation of circular economy principles in heterogeneous catalysis [2].

Among renewable hydrogen production routes, the Aqueous Phase Reforming (APR) of glycerol represents a particularly attractive process. Raw glycerol is the main by-product of the biodiesel industry and is produced in large excess compared to the market demand, making it a low-cost and renewable feedstock. APR allows hydrogen production at relatively low temperatures (200 - 300 °C) and moderate pressures in liquid water, avoiding energy-intensive vaporisation steps and enabling direct integration with biomass-derived aqueous streams [3]. Nevertheless, the efficiency and selectivity of the process strongly depend on catalyst formulation, metal dispersion and metal-support interactions.

This work reports some results of the DURABLE project, funded within the Italian National Research Programme (PRIN 2022PNRR call). In particular, this work presents an investigation of carbon-supported platinum catalysts obtained through urban mining for hydrogen production via glycerol APR. A granular activated carbon (GCN) was employed both as a conventional support for platinum deposition by incipient wetness impregnation (IWI), used as a reference catalyst, and as a sorbent for platinum recovery from waste streams through a leaching/adsorption process, yielding a Waste-Derived Catalyst (WDC) [4]. The two preparation routes were designed to enable a direct comparison between traditionally synthesised and waste-derived catalytic systems, highlighting the impact of the metal recovery strategy on catalyst properties and performance.

Prior to catalytic testing, the fresh catalysts were characterised to investigate their structural, textural and physico-chemical properties. Nitrogen physisorption (BET) was employed to determine surface area and porosity, while inductively coupled plasma mass spectrometry (ICP-MS) and X-ray fluorescence (XRF) were used to quantify platinum loading and elemental composition. Temperature-programmed reduction with hydrogen (H_2-TPR) was carried out to evaluate the reducibility and redox behaviour of the catalysts, whereas NH_3-TPD and CO_2-TPD analyses were performed to assess the acidic and basic properties of the materials.
Catalytic APR experiments were carried out in a high-pressure batch reactor (Parr Instruments 4567 SGL, stainless steel, total volume 300 mL) operating at 290 °C and 10 bar_g, using an aqueous glycerol solution (5 wt.%). Operating conditions are summarised in Table 1. Gas and liquid products were analysed by an Agilent MicroGC 3000 and an Agilent 1100 HPLC, respectively. Yields to liquid products were negligible, and, thus, catalytic performance was evaluated in terms of glycerol conversion and gas-phase product yields.

Table 1: Operating conditions adopted for glycerol APR experiments performed in batch reactor.

Operating conditions	
P_{IN} (bar_g)	10
$V_{IN,\ SOL}$ (mL)	130
Gly (%wt.)	5
t_r (min)	170
Catalyst weight (mg)	500
T (°C)	290

As shown in Figure 1, the WDC catalyst exhibited a glycerol conversion comparable to that of the reference IWI catalyst, demonstrating the effectiveness of the platinum recovered from waste as an active phase for APR. However, differences in the gas-phase product distribution were observed. In particular, the WDC showed lower yields of H_2 and CO_2 and a higher CO yield, while CH_4 formation was similar for both catalysts. Characterisation results suggest that the waste-derived preparation route influences the nature of the active sites and metal-support interactions, thereby affecting reaction pathways and selectivity.
Overall, the results demonstrate the feasibility of employing waste-derived platinum catalysts for renewable hydrogen production from glycerol APR. This work highlights the potential of circular approaches in catalysis to reduce dependence on critical raw materials while enabling sustainable energy conversion processes.

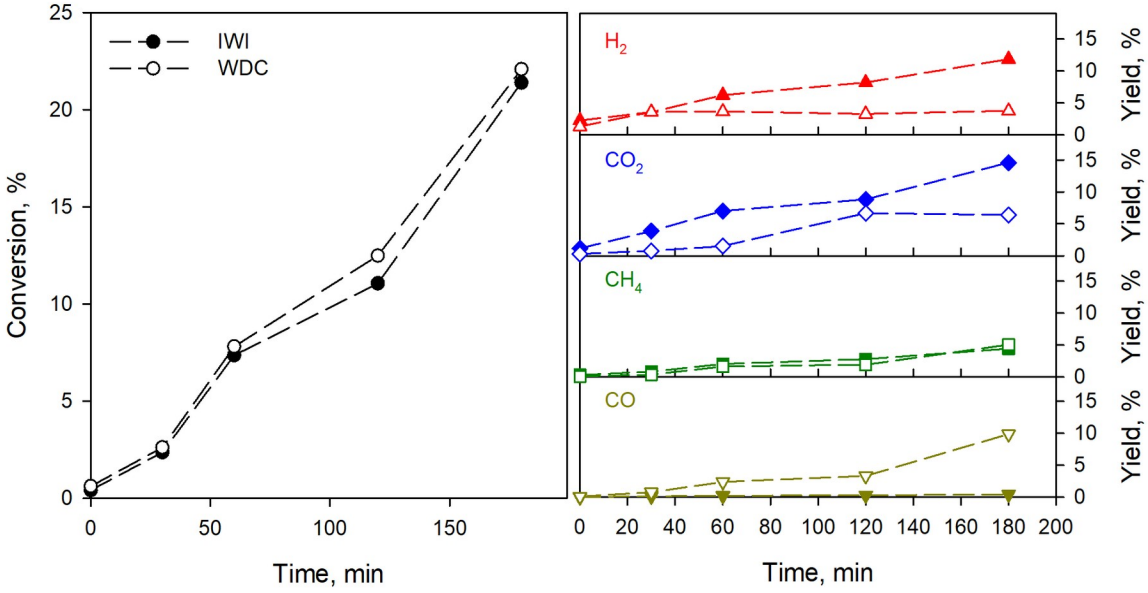

Figure 1: Glycerol conversion and gas-phase product yields (H_2, CO_2, CH_4 and CO) as a function of time during APR over IWI (reference) and WDC (waste-derived) Pt/GCN catalysts.

Acknowledgements
This work was funded by the European Union – Next Generation EU through the Italian Ministry of University and Research (MUR), within the National Research Programme and Projects of Relevant National Interest (PRIN), "Green and Sustainable Urban Mining of Noble Metals" (DURABLE project), Grant No. P2022RF4Z7; CUP E53D23017430001.

References
[1] M. Ryabicheva, et al. From lab to market: Economic viability of modern hydrogen evolution reaction catalysts, Fuel, 395, 2025, 135227
[2] K. Wink, I. Hartmann, "Recent Progress in Turning Waste into Catalysts for Green Syntheses" Sustainable Chemistry, *5*, 1, 2024, 27-39.
[3] J.P. Gujar, A. Verma, B. Modhera "Optimizing glycerol conversion to hydrogen: A critical review of catalytic reforming processes and catalyst design strategies", International Journal of Hydrogen Energy, 109, 2025, 823-850.
[4] L. P. Di Bonito, P. Kyriacou, A. Di Colandrea, T. Krasia-Christoforou, G. Ruoppolo and F. Di Natale, "New sorbents for the hydrometallurgic recovery of gold from electric and electronic wastes", Environ Sci Pollut Res, 2025, https://doi.org/10.1007/s11356-025-36712-w

Joule heating of Pd-Cu/CeO_2-Al_2O_3 foam catalysts for H_2 production via methanol steam reforming

***C. Ruocco*[1], *O. Muccioli*[1,2], *C. Falchetta*[1], *E. Meloni*[1] and V. Palma[1]**
1 Department of Industrial Engineering, University of Salerno, Fisciano, ITALY
2 Department of Chemical Engineering, 'La Sapienza' University of Rome, Rome, Italy
cruocco@unisa.it

Electrified reformers based on Joule heating are emerging as a promising renewable alternative to conventional furnace-based methanol steam reforming; however, thermal management within structured catalytic beds remains a critical challenge affecting process efficiency. Methanol produced from biomass, being easily stored and carried on-board, is a very attractive candidate for H_2 generation; however, the exploitation of electrified reformers in the field of methanol conversion has been scarcely investigated.
The present study aims to (i) analyse the catalytic and energetic performance of a Joule heated structured catalyst in a methanol steam reformer reactor (ii) verify the development of axial thermal gradients as a function of space velocity, and (iii) evaluate the role of inlet gas preheating in redistributing the enthalpy demand along the catalytic bed. In particular, four Pd-Cu/CeO_2-Al_2O_3 OB-SiC foam catalysts were wrapped by means of a Kanthal resistance, in turn connected to a power generator (direct current); three K-thermocouples were placed in the inlet T_{IN}, middle T_{MID} and outlet T_{OUT} section of the catalytic system to monitor the reaction temperatures in 3 axial positions (Figure 1) and an heating chamber was added to preheat the feeding stream at 400°C. The reactor performance was investigated under a 10%CH_3OH-15%H_20-75%Ar stream at atmospheric pressure in the 200-600°C range by varying the WHSV between 1 and 5 h^{-1}, with particular attention to the effect of inlet gas preheating on temperature profile and energetic efficiency.
The axial temperature profile along the catalytic bed was strongly affected by the space velocity in the configuration without preheating (Figure 1). For example, at WHSV=2 h^{-1}, the gap between middle and outlet temperatures exceeded 50°C, and the inlet temperature stabilized around 200°C for middle temperatures above 400°C. In fact, increasing WHSV intensifies the thermal gradient within the catalytic bed. This behaviour can be explained considering the coupled effect of convective heat demand and reaction endothermicity. At higher space velocities, the larger inlet flow rate increases the sensible heat required to raise the reactant temperature as well as the endothermic heat demand associated with methanol reforming. As a result, a pronounced quenching effect develops in the upstream section of the bed, where the local enthalpy sink is concentrated. Downstream, as the reactants progressively absorb heat and their temperature rises, the local thermal demand decreases, allowing the electrical heating to sustain similar or slightly higher outlet temperatures. Consequently, the amplification of the axial gradient with WHSV reflects a redistribution of the enthalpy load along the reactor axis.

These thermal effects must be considered when interpreting the efficiency trends: at 1 h^{-1}, the maximum energetic efficiency (E, calculated as reported by Zeng et al. [1]) of 28% was recorded at 1 h^{-1} and of 40% at 2 h^{-1} (400°C), while E values around 50% for outlet temperatures equal or higher than 500°C were measured at 3 h^{-1}. By fixing WHSV=4 h^{-1}, the gap between inlet and outlet sections was further increased also reaching 130 °C while a mean difference of 140°C was recorded at 5 h^{-1}; the corresponding energetic efficiency were attested to 56-57%.

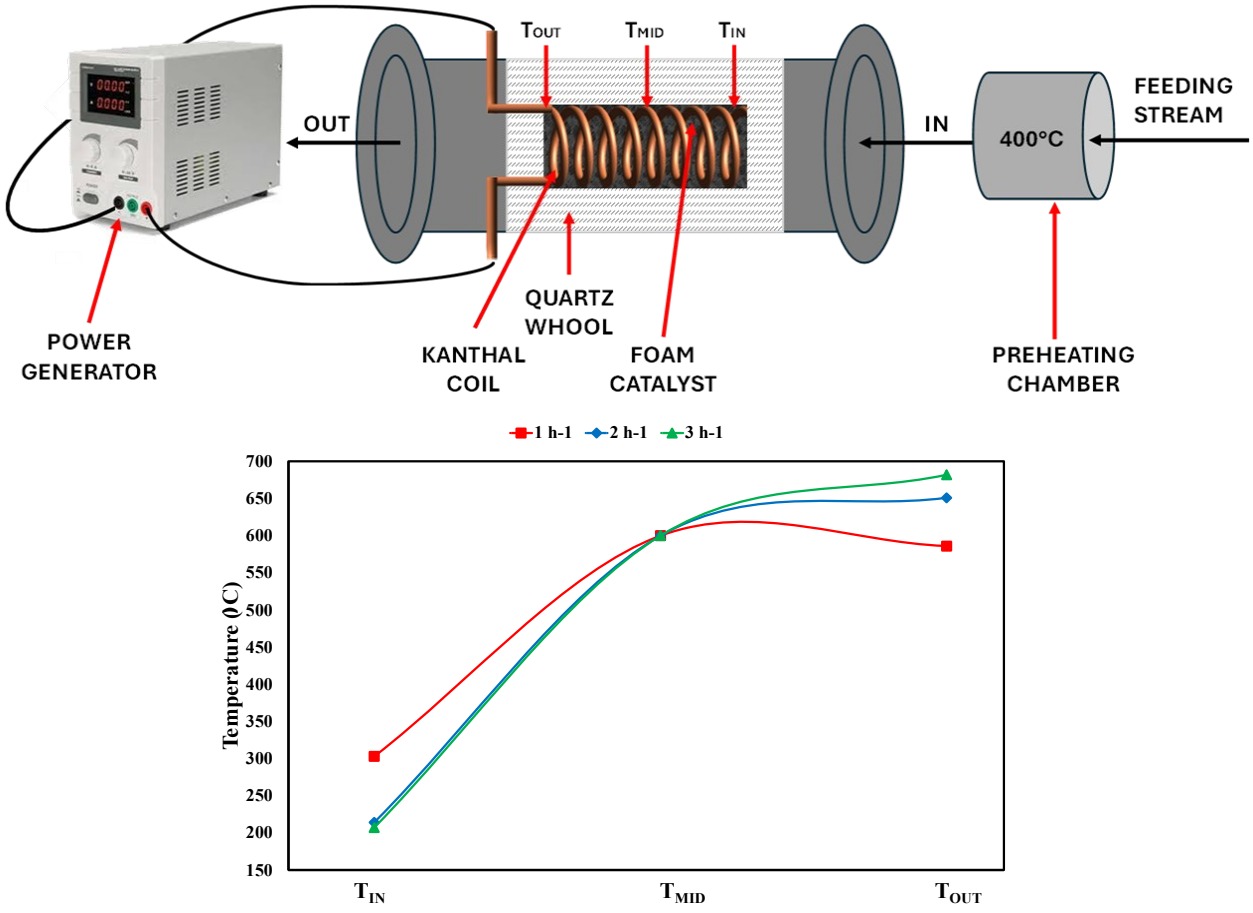

Figure 1: (Upper picture) Schematic representation of the reaction system and (Down picture) axial temperature profile at 600°C without preheating at different WHSVs.

On the other hand, the preheating of feeding stream strongly modified the temperature profiles across the catalytic bed. The introduction of inlet preheating effectively mitigated the quenching effect in the first section of the reactor, resulting in a more uniform temperature distribution and improved reactor thermal efficiency. In fact, the gap between middle and outlet temperatures was sensibly reduced and this phenomenon was more pronounced during the tests at high space velocities; moreover, the energy efficiency was improved for every selected contact time and, for a WHSV=5 h^{-1}, E passed from 56 to 65%. The comparison with data available in the recent

literature [2] demonstrates that the present research offers a valid energy-efficiency alternative in the field of electrified hydrogen production via the methanol steam reforming route.

Acknowledgements
This research was funded by PRIN - Bando 2022 Prot. 2022M7BHN7 "Liquid hydrogen carriers as sustainable fuels for innovative energy systems configurations in the maritime sector – LYRICA".

References
[1] L. Zheng, M. Ambrosetti, D. Marangoni, A. Beretta, G. Groppi, E. Tronconi, Electrified methane steam reforming on a washcoated SiSiC foam for low-carbon hydrogen production, AIChE Journal, 69 (2021) 1-9.
[2] H. Huang, S. Bai, K. Bai, Z. Xiao, A Joule Heating-Driven Flow-Through SiC Catalytic Membrane Microreactor for Hydrogen Production from Methanol Steam Reforming. Ind Eng Chem Res 64 (2025)11868–78.

Design and development of a fermentation system for Bio-Hydrogen production by *Thermotoga neapolitana*

Giulia Crescente*[ab], Giuseppe Baiardo[b], Giuliana d'Ippolito[c], Gaetano Squadrito[b]

[a] *Università di Messina (UNIME) – Dipartimento di Ingegneria, C.da Di Dio (Vill.S.Agata), Messina – 98158, Italia*

[b] *Consiglio Nazionale delle Ricerche – Istituto di tecnologie Avanzate per l'Energia "Nicola Giordano (CNR-ITAE), via S. Lucia sopra Contesse 5, 98126 Messina – Italia*

[c] *Consiglio Nazionale delle Ricerche - Istituto per i Polimeri, Compositi e Biomateriali (IPCB), via Campi Flegrei, 34, 80078 Pozzuoli NA - Italia*

**corresponding author: giulia.crescente@studenti.unime.it / giulia.crescente@itae.cnr.it*

Clean hydrogen is proposed as a widely used commodity both as fuel and as raw material. In the programs for de-carbonisation, it appears to be one of the keys to sustainable development [1]. In addition to the traditional hydrogen production technologies, the biological and bio-electrochemical production of hydrogen from biomasses has begun to be evaluated in a circular economy perspective, trying to valorize wastes. In these processes microorganisms convert biomass into hydrogen by catalytic activity of enzymes as hydrogenase and nitrogenase, and different strains of bacteria applied to a wide range of substrates and by different methods, such as dark fermentation, has been proposed for this purpose [2].

Within these strain, the hyper-thermophilic (living over 60°C) Thermotogales showed a good activity in hydrogen production. In particular, Thermotoga neapolitana (DSM 4359, ATCC 49049) was largely studied [3]. This bacterium is relatively easy to use in a single culture as the extreme temperature conditions reduce the risk of contamination by other strains. It has been reported that T. neapolitana reaches hydrogen yield values close to the theoretical 4 H_2 molecule per glucose molecule. These facts make T. neapolitana particularly promising for biotechnology and energy recovery, as well as for the sequestration of CO_2, while producing chemical compounds of industrial interest such as acetic acid and lactic acid, as well as biomass. Consequently, Thermotoga Neapolitana appears really interesting for scale up from laboratory to significant scale hydrogen production facility.

The objective of this work is the development of a prototype system for hydrogen production from waste water based on thermotoga strains. Here we report the first experimental results on a lab scale prototype running in continuous flow configuration.

Starting from literature experimental data about thermotoga neapolitana hydrogen production in different operative conditions, and previous research on the capacity of thermotogales to grow attached to solid supports [3-4], was designed a fermenter and the model plant using the design approach sketched in Figure 1.

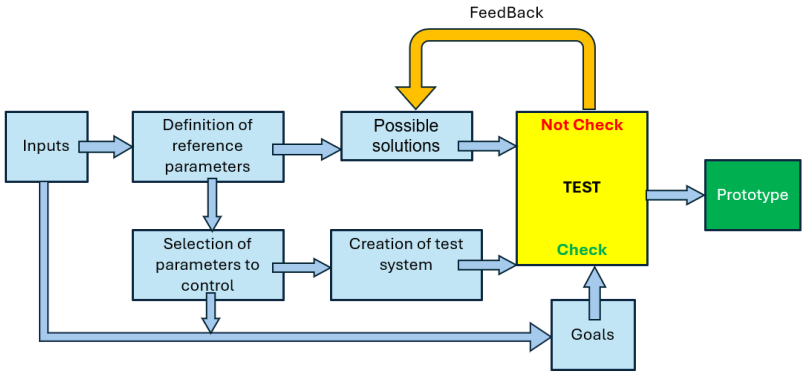

Figure 1 : *Operational cycle of prototype development*

Most of the experiments on Termotogales, including T. neapolitana, have been conducted in a batch configuration and on limited amounts of culture medium, usually between 100 mL and 1L. Moreover the nutrient concentrations reported in literature are relatively low (up to 10 g/L). Despite the good potential demonstrated by the batch approach, the scale-up is not easy both due to low production rate and the overall size of the system which is configured at low production density. One way to overcome this problem is to work with a higher concentration of bacteria and to achieve this an opportunity is done by moving from a batch configuration with floating bacteria to a configuration with supported bacteria and continuously flowing culture media. Because this allows to maintain a quite constant bacteria population and nutrients concentration optimising, in this way, the production rate of hydrogen and by-products. Among the various anaerobic fermentation systems proposed and implemented on an industrial scale, the internally circulating reactor (ICR) was identified in this work as the most suitable for working under continuous flow conditions, as shown in Figure 2, where the plant scheme is reported. Notably, in terms of the material used, stainless steel was chosen as the material for the construction of the bioreactor and whole plant because thermotogals have a low affinity for steel, ensuring easier maintenance of the plant, as well as for its excellent thermo-mechanical properties. Testing for evaluating the overall plant efficiency is running. Preliminary results are in line with literature data, and support confidence that these production rates could be excedeed by optimising the process operative conditions and controls.

In conclusion, the possibility to scale up hydrogen production using thermotoga neapolitana attached on solid supports and in continuous flow has been demonstrated. The result was possible by the design of a plant based on ICR reactor configuration and by using a proprietary fermenter design. Future work will be centred on plant management optimisation and alternate bacteria batch testing.

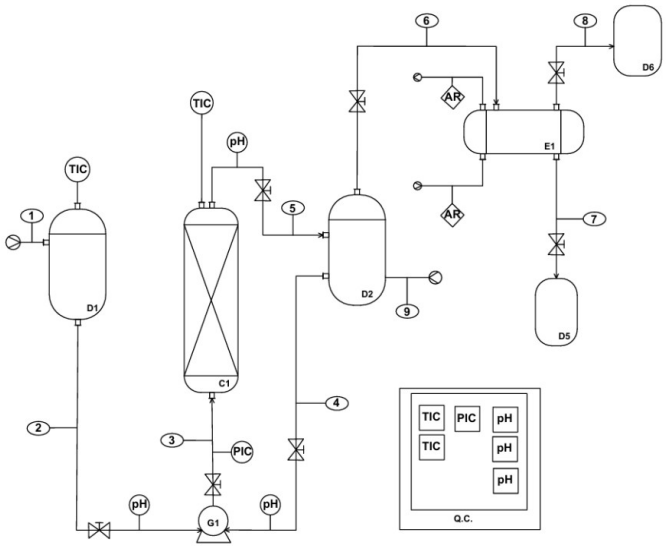

***Figure 2**: Prototype plant for bio-hydrogen production by bacteria T. Neapolitana (**Q.C.** Control panel, **TIC**, **PIC**, **pHC** are indicator and controller of T, P and pH, **AR** Cooling water, **C1** Bioreactor with filling, **D1** Thermostatted and insulated bacterial culture tank, **D2** Recirculation tank, **D3** Graduated tank for measuring hydrogen produced, **D4** Graduated free-flowing tank for measuring hydrogen produced, **D5** Condenser outlet , **D6** Hydrogen buffer, **E1** Condenser, **G1** Pump, **1** Input current, **2** Current input of T. Neapolitana bacteria, **3** Bioreactor power supply, **4** Recirculation current exiting the membrane reactor, **5** Outgoing current from the bioreactor, **6** Hydrogen saturated, **7** condensate, **8** Product hydrogen collection line, **9** Buffer solution supply to stabilize the pH of the bacterial solution)*

Acknowledgements

The activity here reported is supported by:

- *"This research was funded by the European Union – NextGeneration EU from the Italian Ministry of Environment and Energy Security POR H2 AdP MMES/ENEA with involvement of CNR and RSE, PNRR - Mission 2, Component 2, Investment 3.5 "Ricerca e sviluppo sull'idrogeno", CUP: B93C22000630006".*
- *"The European Union – Horizon Europe -Widera, project "Green Innovations in Hydrogen for Sustainable Energy Transition" (H2START), GA 101136692*

References

[1] Nicita A, Squadrito G, Maggio G – Int. J. Hydrogen Energy 44 (2019), pp 11371–84.

[2] Xianxian Xu, Quan Zhou, Dehai Yu - Int. J. Hydrogen Energy 47 (2022), 33677 - 33698.

[3] N Pradhan, L Dipasquale, G d'Ippolito, A Panico, P N L Lens, G Esposito and A Fontana- Int. J. Mol. Sci. 2015, 16, 12578-12600 ; doi :10.3390/ijms160612578

[4] G d'Ippolito, G Squadrito, M Tucci, N Esercizio, A Sardo, M Vastano, M Lanzilli, A Fontana, P Cristiani - Bioresource Technology 319 (2021) 124078

Phenotyping and In vivo Profiling

R. Ünnep, G. Nagy, G. Garab, O. Zsiros, K. Solymosi and L. Draskovits - Monitoring photosynthetic membrane structure in vivo: a small-angle neutron scattering approach

A. Das, M. Kovar, M. Barboricova, J. Ferencova, M. Brestic and M. Zivcak - High-throughput phenotyping reveals genotypic variation in photosynthetic responses of wheat to elevated nighttime temperatures

A. Herdean, L. Hoch, A. Willis, Z. Benedikty, R. Zunt, M. Trtilek, J. Trtilek and P.J. Ralph - High-Throughput Automated Phenotyping of Microalgae

M. Zivcak, M. Kovar, M. Barboricova, J. Ferencova, A. Das, P. Hauptvogel and M. Brestic - From noise to signal: Analyzing structural and functional changes in wheat PSII photochemistry under seasonal and meteorological drivers

Monitoring photosynthetic membrane structure *in vivo*: a small-angle neutron scattering approach

R. Ünnep[1], G. Nagy[2], G. Garab[3], O. Zsiros[3], K. Solymosi[4] and [1]L. Draskovits

[1]Budapest Neutron Centre, Institute for Energy Security and Environmental Safety HUN-REN Centre for Energy Research, Budapest, Hungary

[2]Neutron Scattering Division, Oak Ridge National Laboratory, Oak Ridge, Tennessee, USA
[3]Institute of Plant Biology, Biological Research Centre, HUN-REN Centre for Energy Research, Szeged, Hungary

[4]Department of Plant Anatomy, Institute of Biology, Faculty of Science, ELTE Eötvös Loránd University, Budapest, Hungary

unnep.renata@ek.hun-ren.hu

Climate change and its effects on agricultural crops, the rise in global population and thus food demand, as well as humanity's efforts to reduce dependence on fossil energy sources, increasingly highlight the importance of research on the mechanisms of light-energy conversion. Over recent decades, our knowledge advanced considerably regarding the structure and function of protein complexes that are key to oxygenic photosynthesis. In contrast, much less is known about the *in vivo* architecture, organization, and structural dynamics of photosynthetic membrane systems, i.e., the thylakoid membranes, in the mesoscopic size range.

In our investigations, we predominantly apply small-angle neutron scattering (SANS). Although the method offers great potential for studying intact systems (living unicellular organisms, whole intact plants), it is less well-known among researchers working on photosynthesis. SANS, a non-invasive technique, offers unique possibility for *in vivo* studies in mesoscopic range, via providing accurate structural information on large statistical population under physiological conditions - without artefacts caused by fixation and staining - with time resolutions of seconds or minutes. This is especially important in samples possessing structural flexibility and capable of membrane reorganizations. SANS typically carries information about the size, shape, orientation and relative spatial arrangement of scattering particles in the sample[1,2]. In the last 2-3 decades, we introduced several methodological innovations, enabling us to extend SANS measurements from isolated thylakoid membranes to intact leaves. In recent years, we have progressed even further, studying processes in whole, potted plants without any pretreatment.

In my presentation, I aim to demonstrate the advantages of the SANS method through our own research results. I will also address the protective mechanisms induced by changes in light intensity and spectral composition—energy-dependent non-photochemical quenching[3] and state transitions[4]—as well as drought stress[5–7].

We have shown for the first time *in vivo* using wild-type and mutant *Chlamydomonas reinhardtii* that the state transition in *C. reinhardtii* modifies the chloroplast thylakoid membrane ultrastructure, affecting the stacking and periodicity of the photosynthetic membranes[4]. We used SANS to follow structural changes of the thylakoid membrane system in leaves of *Monstera deliciosa*, under conditions that trigger non-photochemical quenching (NPQ). We observed that illumination which induces NPQ causes a marked decrease in the periodic order of the stacked grana thylakoid membranes — the characteristic SANS signal associated with regular lamellar stacking becomes significantly reduced. The kinetics of the membrane reorganization during light exposure and the subsequent recovery in the dark follow a time course very similar to the kinetics of NPQ. We have also showed that the light-induced membrane rearrangements are enable NPQ but are not caused by it directly[3]. Via investigating the pH-dependency of the SANS profiles of magnetically aligned isolated plant thylakoid membranes, our experiments allowed us to conclude that the observed low-pH induced smearing and broadening of the Bragg peak and the increased mosaicity of membranes reflect loosening in the periodic order of the thylakoid membranes, which evidently arises from some undulations and/or membrane bending[8].

In recent years, our research has increasingly focused on ultrastructural changes induced by drought-stress across various organisms: (i) The photosynthesis of the desiccation-tolerant desert cyanobacterium (*Leptolyngbya ohadii*) can fully recover upon predawn dew deposition, even though the organisms remain desiccated for most of the daytime. The thylakoid system in hydrated cells is multilamellar, whereas desiccated cells display no diffraction peak, only a broad shoulder. Based on these SANS results and other structural and functional measurements, a novel energy-dissipation mechanism has been proposed, relying on the aggregation state of the light-harvesting antenna complexes[9]. (ii) In the case of *Ctenanthe setosa (Roscoe) Eichler*—a species with exceptional drought tolerance—we demonstrated that even after 41–45 days without water, it can preserve the structure and function of its photosynthetic apparatus almost unchanged. Uniquely, we were able to follow the reversible structural changes over time in a living plant[7]. In addition, we participated in modeling salinity stress using NaCl treatment in wheat (*Triticum aestivum L.*)[6] and peppermint *Mentha spicata L. var. crispa "Moroccan"*[5].

Acknowledgements
OTKA PD 138540/National Research, Development and Innovation Office; HUN-REN Researcher Mobility Programme 2025; NKKP Advanced 153509

References

1. Nagy, G. & Garab, G. Neutron scattering in photosynthesis research: recent advances and perspectives for testing crop plants. *Photosynth. Res.* 150, 41–49 (2021).
2. Unnep, R., Nagy, G., Markó, M. & Garab, G. Monitoring thylakoid ultrastructural changes in vivo using small-angle neutron scattering. *Plant Physiol. Biochem. PPB* 81, 197–207 (2014).
3. Ünnep, R. *et al.* Thylakoid membrane reorganizations revealed by small-angle neutron scattering of Monstera deliciosa leaves associated with non-photochemical quenching. *Open Biol.* 10, 200144 (2020).
4. Nagy, G. *et al.* Chloroplast remodeling during state transitions in Chlamydomonas reinhardtii as revealed by noninvasive techniques in vivo. *Proc. Natl. Acad. Sci. U. S. A.* 111, 5042–5047 (2014).
5. Ounoki, R. *et al.* Salt Stress Affects Plastid Ultrastructure and Photosynthetic Activity but Not the Essential Oil Composition in Spearmint (Mentha spicata L. var. crispa 'Moroccan'). *Front. Plant Sci.* 12, 739467 (2021).
6. Ounoki, R. *et al.* Etioplasts are more susceptible to salinity stress than chloroplasts and photosynthetically active etio-chloroplasts of wheat (Triticum aestivum L.). *Physiol. Plant.* 175, e14100 (2023).
7. Hembrom, R., Ünnep, R., Sárvári, É., Nagy, G. & Solymosi, K. Dynamic in vivo monitoring of granum structural changes of Ctenanthe setosa (Roscoe) Eichler during drought stress and subsequent recovery. *Physiol. Plant.* 177, e14621 (2025).
8. Ünnep, R. *et al.* Low-pH induced reversible reorganizations of chloroplast thylakoid membranes - As revealed by small-angle neutron scattering. *Biochim. Biophys. Acta Bioenerg.* 1858, 360–365 (2017).
9. Bar Eyal, L. *et al.* Changes in aggregation states of light-harvesting complexes as a mechanism for modulating energy transfer in desert crust cyanobacteria. *Proc. Natl. Acad. Sci. U. S. A.* 114, 9481–9486 (2017).

High-throughput phenotyping reveals genotypic variation in photosynthetic responses of wheat to elevated nighttime temperatures

***A. Das*[1], M. Kovar[1], M. Barboricova[1], J. Ferencova[1], M. Brestic[1,2], and M. Zivcak[1]**

[1] *Institute of Plant and Environmental Sciences, Slovak University of Agriculture, Nitra, Slovakia*

[2] *Shandong Agricultural University, National Key Laboratory of Wheat Improvement, Taian, China*

e-mail: marek.zivcak@uniag.sk

Global climate models consistently project a distinct asymmetry in warming patterns, where minimum nighttime temperatures are rising at a considerably faster rate than daytime maximums across major cereal-producing regions [1]. That represents a pervasive and often underestimated threat to crop productivity, fundamentally differing from acute diurnal heat extremes. In C3 crops like wheat, elevated night temperatures primarily disrupt the plant's carbon economy by intensifying dark respiration rates, thereby depleting carbohydrate reserves accumulated during the photoperiod and reducing the assimilates available for grain filling [2]. Furthermore, supraoptimal nighttime temperatures impose cumulative physiological stress that influences leaf metabolism and overall integrity, affecting the function and structure of molecular components in chloroplasts, including photosynthetic enzymes and thylakoid membrane components [3, 4]. Despite the urgency of this problem, the intraspecific variation in thermal tolerance among high-yielding wheat genotypes remains poorly characterized, particularly regarding the long-term acclimation of the photosynthetic apparatus to warmer nights.

In our experiments, we used the high-throughput PlantScreen™ phenotyping platform to conduct a comprehensive, non-invasive assessment of responses of distinct wheat genotypes under fully controlled environmental conditions. By constructing a specialized temporary chamber within the facility, we simulated a nocturnal warming scenario of 3–4°C above ambient controls while strictly preserving identical daytime irradiance and temperature regimes, thereby isolating the specific physiological consequences of warmer nights from confounding diurnal variables. We applied sophisticated image-based phenotyping protocols with a primary emphasis on elucidating the functional status of the photosynthetic apparatus. Time-series chlorophyll fluorescence imaging was employed to continuously monitor the dynamics of maximum quantum efficiency, electron transport, and non-photochemical dissipation throughout the season. These functional parameters were interpreted alongside RGB-derived data quantifying structural canopy expansion and hyperspectral reflectance indices indicative of physiological stress, with automated datasets further validated by manual measurements.

The results revealed that elevated night temperatures acted as a driver of phenological acceleration, modifying the architecture of the photosynthetic apparatus by promoting rapid leaf area expansion. However, this developmental acceleration came at significant functional costs, particularly through shortening the vegetative period and accelerating senescence of individual leaf positions. Chlorophyll fluorescence analysis demonstrated that while plants subjected to nocturnal warming attained peak photosynthetic efficiency significantly earlier than control plants, they subsequently exhibited premature and rapid downregulation of overall photochemical activity. This accelerated senescence trajectory, characterized by a shortened duration of active photosynthesis, implies reduced capacity for carbon assimilation during critical grain-filling stages. Importantly, the study unveiled pronounced genotypic plasticity in thermal tolerance. Response patterns varied substantially across the screened germplasm, ranging from the relative stability observed in the bread wheat cultivar *T. aestivum* cv. Layagatli-80, which maintained moderate photochemical competence under stress, to the severe physiological sensitivity of the durum wheat *T. durum* cv. LD 222, which exhibited marked and rapid decline in photosynthetic performance. These findings highlight the efficiency of automated, image-based phenotyping in dissecting the complex interactions between structural development and functional photosynthetic integrity under thermal stress. The identified genotypic variation provides valuable information, emphasizing the need to introgress traits for sustained photosynthetic duration at high nighttime temperatures into breeding programs, thereby paving the way for future research into the mechanisms governing resilience of photosynthetic machinery under future warming scenarios.

Acknowledgements
The research work and presentation of the results was supported by the research projects APVV-22-0392 and the projects VEGA-1-0048-25 and VEGA 1-0639-26.

References
[1] Sillmann, J., Kharin, V. V., Zwiers, F. W., Zhang, X., Bronaugh, D. (2013). Climate extremes indices in the CMIP5 multimodel ensemble: Part 2. Future climate projections. Journal of Geophysical Research: Atmospheres, 118(6), 2473-2493.
[2] Sadok, W., Jagadish, S. K. (2020). The hidden costs of night-time warming on yields. Trends in Plant Science, 25(7), 644-651.
[3] Tombesi, S., Cincera, I., Frioni, T., Ughini, V., Gatti, M., Palliotti, A., & Poni, S. (2019). Relationship among night temperature, carbohydrate translocation and inhibition of grapevine leaf photosynthesis. Environmental and Experimental Botany, 157, 293-298.
[4] Shi, W., Muthurajan, R., Rahman, H., Selvam, J., Peng, S., Zou, Y., & Jagadish, K. S. (2013). Source–sink dynamics and proteomic reprogramming under elevated night temperature and their impact on rice yield and grain quality. New Phytologist, 197(3), 825-837.

High-Throughput Automated Phenotyping of Microalgae

A. Herdean[1], L. Hoch[1], A. Willis[2], Z. Benediktyova[3], R. Zunt[3], M. Trtilek[3], J. Trtilek[3] and P.J. Ralph[1]
[1] *University of Technology Sydney, Australia*
[2] *CSIRO, Australian National Algae Culture Collection, Australia*
[3] *Photon Systems Instruments, Czech Republic*
benedikty@psi.cz

Despite their small size, microalgae are photosynthetic organisms with broad practical applications in fuel production, nutrition, environmental remediation, and the production of high-value compounds. Their wider commercial deployment, however, is limited by the lack of scalable and standardized phenotyping approaches. To address this challenge, we developed PhenoSelect, an automated platform that combines robotics, spectroscopy, fluorometry, flow cytometry, and advanced data analytics to enable high-throughput, multi-parameter phenotyping of microalgae.

Using this system, five algal species including *Chlorella sorokiniana*, *Haematococcus pluvialis*, *Halospirulina tapeticola*, *Nannochloropsis australis*, and *Phaeodactylum tricornutum*, were analyzed across 96 environmental and chemical conditions. Key traits including photosynthetic performance, growth dynamics, and cell size were quantified with high reproducibility. Species-specific phenotypic plasticity was visualized using Ranked Spider Plots and heatmaps, while overall phenome breadth was assessed via convex hull volume. *H. pluvialis* displayed the largest phenotypic space, indicating high adaptability, whereas *N. australis* exhibited the smallest phenome, consistent with a more specialized ecological strategy. Optimal photosynthetic activity and growth conditions varied among species, with low light intensity and nutrient-rich environments generally promoting higher performance.

PhenoSelect is built on PSI's AlgaeScreen™ robotic platform and enables fully automated, daily measurements with minimal manual intervention, while allowing modular expansion through additional analytical instruments. This platform fills critical gaps in algal biotechnology by accelerating strain selection, enabling quantification of phenotypic drift, and supporting predictive modeling. By delivering reproducible, multi-trait phenotyping at scale, PhenoSelect represents a significant advance in algal research and bioprospecting, with direct relevance to sustainable industrial production systems.

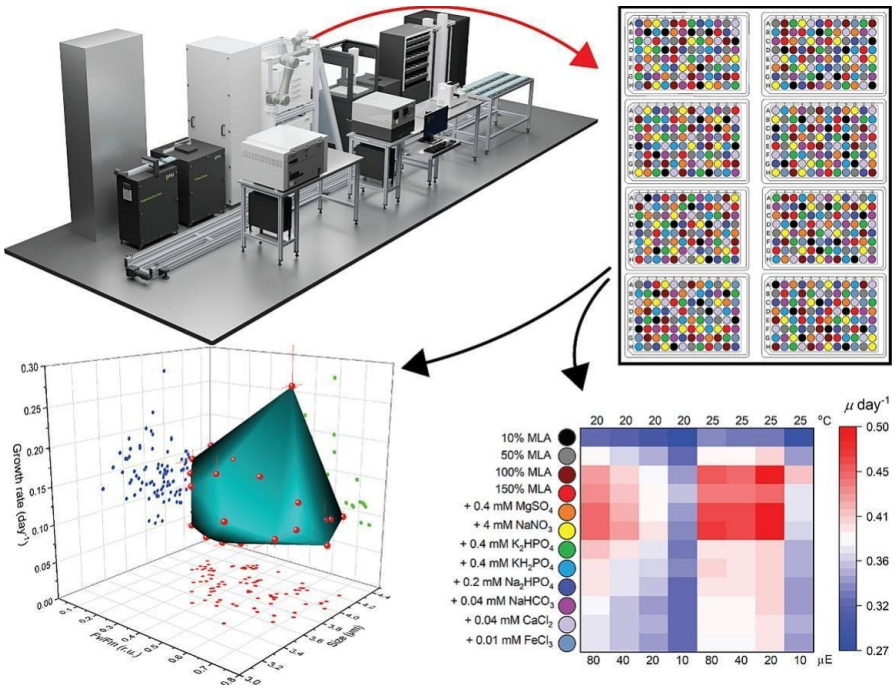

Figure: The high-throughput phenotyping workflow and resulting phenotypic landscape of *Chlorella sorokiniana* CS-903 exposed to 96 environmental and chemical conditions. The upper left panel shows the automated robotic phenotyping platform integrating cultivation, handling, and analytical modules. The upper right panel displays the experimental layout of 384-well microplates, with individual wells representing distinct treatment conditions.
The lower right panel presents a heatmap summarizing growth rate responses (μ day^{-1}) across selected environmental variables, including light intensity, temperature, and media composition. The lower left panel visualizes the multidimensional phenotypic space using a 3D scatter plot and convex hull, integrating growth rate, photosynthetic efficiency (F_v/F_m), and cell size to capture phenotypic variability and plasticity across all tested conditions.

Acknowledgements
The CSIRO Australian National Algae Culture Collection (ANACC) is acknowledged for providing the algal strains used in this research, including CS-903, CS-1030, CS-785/02, CS-416, and CS-786.

References
[1] A, Herdean. et al. "Automated phenotyping of microalgae: scalable solution for high-throughput analysis", *Bioresource Technology* 434, 2025, 132763.

From noise to signal: Analyzing structural and functional changes in wheat PSII photochemistry under seasonal and meteorological drivers

***M. Zivcak*[1], *M. Kovar*[1], *M. Barboricova*[1], *J. Ferencova*[1], *A. Das*[1], *P. Hauptvogel*[1] and *M. Brestic*[1,2]**

[1] *Institute of Plant and Environmental Sciences, Slovak University of Agriculture, Nitra, Slovakia*

[2] *National Agricultural and Food Centre, Research Institute of Plant Production, Piestany, Slovakia*

e-mail: marek.zivcak@uniag.sk

The analysis of the functionality and structural alterations of the photosynthetic apparatus via the measurement of rapid chlorophyll a fluorescence kinetics is currently widely established as a robust method for evaluating the effects of environmental constraints and stress factors on crops [1]. By recording the polyphasic rise of fluorescence induction (the O-J-I-P transient), this non-invasive technique allows for the precise detection of limitations in electron transport, the status of electron carriers, and specific damage or acclimation responses at the level of Photosystem II (PSII) and the entire electron transport chain in chloroplast thylakoids [2]. Advanced biophysical models applied to these rapid kinetics allow for the calculation of a vast array of parameters, including the quantum efficiencies of partial photochemical processes, probability-based variables, parameters characterizing the reaction center activity, and a series of phenomenological parameters defining energy fluxes per excited cross-section or per reaction centres [3,4]. However, the generation of such a large number of parameters creates a significant analytical challenge regarding the correct selection of variables relevant to specific research objectives. This complexity often leads to a dichotomy in usage: researchers either restrict themselves to very basic parameters, thereby failing to exploit the diagnostic potential of the method, or they overuse a large number of variables, resulting in data redundancy and a loss of focus on the biological essence of the problem.

To resolve this issue, it might be very helpful to provide users with specific information on how individual parameters behave in relation to seasonality, changing environmental conditions, and specific genotype differences. In the present study, we addressed this by analyzing an extensive dataset of in situ measurements of fast chlorophyll fluorescence kinetics records taken on a broad collection of winter wheat (*Triticum* sp.) genotypes. The experimental material included various botanical taxa and a wide range of geographical origins, encompassing both old regional varieties and modern cultivars, grown in regular field trials within a gene bank of Research Institute of Plant Production in Piestany (Slovakia) in a typical production area of Central Europe. This robust dataset, linked to environmental conditions and parameters derived from basic methods characterizing plant condition and

functional leaf area, allowed for a comprehensive evaluation of photosynthetic performance under realistic field conditions. The aim was to identify seasonal trends, fluctuations caused by immediate environmental drivers, and genotype-dependent differences across the full spectrum of parameters derived from rapid fluorescence kinetics.

Using multivariate statistical analyses, we successfully classified groups of parameters based on their response patterns, providing a physiological and photochemical interpretation of their variability. We specifically defined a subset of parameters that primarily reflect seasonal changes, correlating with the ontogenetic development and senescence of the leaf tissue. Distinct from these were parameters that are less variable seasonally but serve as highly sensitive indicators of current environmental conditions, reflecting acute acclimation and the dynamic regulation of electron flow. Furthermore, the analysis identified specific parameters that best reflected the intrinsic differences between the studied genotypes, remaining robust against environmental noise. This classification makes it possible to define specific photochemical phenomena that drive seasonality versus those that define environmental plasticity in plants. The results obtained provide a baseline information for the correct selection of parameters, offering users of the technique clear guidance. Ultimately, this serves to refine the application of chlorophyll fluorescence in both laboratory conditions and field trials, enhancing its value in applied research and wheat breeding programs aimed at improving crop sustainability and stabilizing photosynthesis under future climate scenarios.

Acknowledgements

The research work and presentation of the results was supported by the research projects APVV-22-0392 and the projects VEGA-1-0048-25 and VEGA 1-0639-26.

References

[1] Kalaji H.M., Jajoo A., Oukarroum A. et al.: Chlorophyll a fluorescence as a tool to monitor physiological status of plants under abiotic stress conditions. – Acta Physiol. Plant. 38: 102, 2016.

[2] Stirbet, A., Lazár, D., Kromdijk, J., Govindjee. (2018). Chlorophyll a fluorescence induction: can just a one-second measurement be used to quantify abiotic stress responses? Photosynthetica, 56(1), 86-104.

[3] Strasser R.J., Tsimilli-Michael M., Srivastava A.: Analysis of the chlorophyll a fluorescence transient. – In: Papageorgiou G.C., Govindjee (ed.): Chlorophyll a Fluorescence: A Signature of Photosynthesis, Advances in Photosynthesis and Respiration, Vol. 19. Pp. 321-362. Springer, Dordrecht 2004.

[4] Stirbet A., Govindjee: Chlorophyll a fluorescence induction: a personal perspective of the thermal phase, the J-I-P rise. Photosynth. Res. 113: 15-61, 2012.

Poster Session

D. Mlynarikova Vysoka, M. Kovar, M. Zivcak, M. Barboricova, J. Ferencova, H. Ghaffari, A. Shomali, A. Das, X. Yang, M. Brestic – Acclimation of primary photochemical reactions in lettuce leaves to UV-B radiation

M. Kovar, M. Barboricova, M. Zivcak, D. Mlynarikova Vysoka, J. Ferencova, H. Ghaffari, A. Shomali, A. Das, X. Yang, M. Brestic – Silicon modulated photosynthetic performance during drought of buckwheat plants

M. Barboricova, M. Kovar, M. Zivcak, D. Mlynarikova-Vysoka, A. Das, H. Ghaffari and M. Brestic - Non-Invasive Screening Methods for Wheat Photosynthetic Performance Under Combined Drought and Heat Stress

G. Rankelytė, J. Chmeliov, A. Gelzinis, and L. Valkunas – Protein-Controlled Electronic Energy Transfer in Photosynthetic Complexes

M. Vítová, V. Jílková, M. Čížková, J. Thabet, J. Kvíderová, J. Elster and J. Frouz – Photosynthetic activity of cyanobacteria growing on phytotoxic substrates

M. Ballestriero, E. Marrocchino, L. Sansone, R. Carraro, N. Govoni and L. Ferroni - Photosynthesis in Vitis vinifera cv. Fortana, a historic ungrafted grape variety of the sandy coast of Emilia-Romagna (Northern Italy)

S. Penneru, S. Tiruvadi-Krishnan, R. Lamichhane and B. Bruce – Beyond Static Structures: Single-Molecule FRET Resolves Mobile GTPase Domains in Chloroplast Protein Import

P. Suresh, S. Tiruvadi-Krishnan, J. Kolape, A. Joshi, R. Lamichhane and B. D. Bruce - Real-Time TOC Receptor Mobility Reveals Dynamic Import Microdomains in Isolated Pisum sativum Chloroplasts

E. Pykhova, M. Kozuleva, D. Vilyanen, A. Ashikhmin, A. Nikolaev, and M. Borisova-Mubarakshina – Modulatory Effects of Plastoquinone C on Photosynthesis: From Molecular Docking to In Vivo Stress Acclimation

A. Nikolaev, N. Rudenko, N. Novichkova, D. Vetoshkina and M. Borisova-Mubarakshina – Plastoquinone-dependent H_2O_2 signaling controls PS II antenna size via a chloroplast serine protease

R.A. Voloshin, S.K Zharmukhamedov, and S.I. Allakhverdiev - Electrogenic properties of thylakoid membrane at distinct applied voltage

M. Goncharova, E. Zadneprovskaya, R. Voloshin, D. Gabrielyan, N. Lobus, S. Allakhverdiev - CO_2 content affects the photosynthetic and biochemical profile of the green microalga Desmodesmus armatus ARC06

J. Manoyan, L. Hakobyan, and L. Gabrielyan - Biohydrogen photoproduction by Chlorella vulgaris cultivated on distiller's grains, brewer’s spent grains and potato peel waste

M. Musone, F. Migliardini, A. Basco, A. Di Nardo, and G. Landi - Development and Validation of a Simplified Kinetic Model for Ni-Ru/CeO2 Catalysts in Low-Temperature Steam Methane Reforming and as a Basis for Integrated Power-to-Gas Systems

M. Ahlhaus – Upgrading of biomass to fuels and green Carbon as Reductant for Metallurgy

O. Muccioli, C. Maffei, C. Ruocco, E. Meloni, V. Palma - Decarbonizing propylene production: high selectivity and low energy consumption using Joule-heated PtSn-based structured catalysts

A. Cappiello, S. Di Micco, R. Nastro, M. Minutillo - Design and testing of single-chamber air-cathode Microbial Fuel Cells Fed with Organic Residues

M. Minutillo, G. D'Andrea, E. Jannelli, M. Della Pietra - Pilot-Scale Demonstration of Green Hydrogen Production via 25 kW SOEC System

I. Papallo, G. de Alteriis, R. Schiano Lo Moriello – Mechanical and thermal measurements towards the development of additive manufactured products with tailored structural/functional properties

V. Spinelli, V. Gallicchio, R. Di Bernardo, M. Martorelli, A. Gloria - Cellular automata and metamaterials for the design of advanced smart products

M. Murolo, I. Papallo, V. Gallicchio, V. Spinelli, R. Di Bernardo, M. Martorelli, A. Gloria - Generative design for additive manufacturing and a new paradigm for the development of sustainable functional systems

Acclimation of primary photochemical reactions in lettuce leaves to UV-B radiation

***D. Mlynarikova Vysoka*[1], M. Kovar[1], M. Zivcak[1], M. Barboricova[1], J. Ferencova[1], H. Ghaffari[2,3], A. Shomali[1], A. Das[1], X. Yang[3], M. Brestic[1,3]**

[1] *Institute of Plant and Environmental Sciences, Slovak University of Agriculture, Nitra, Slovakia*

[2] *Agrobiotech Research Centre, Slovak University of Agriculture, Nitra, Slovakia*

[3] *State Key Laboratory for Wheat Improvement, Shandong Agricultural University, Taian, China*

dominika.vysoka@uniag.sk

The photosynthetic activity of plants is light wavelength dependent. Ultraviolet-B radiation (UV-B) in range 280–315 nm is a relatively minor component of sunlight, but it has a significant effect on the plants due to the high energy of quanta. The UV-B is an important component of the environment acting as an eco-physiological factor with the potential to alter plant growth and photosynthesis. However, the effects of UV-B radiation on biological processes are highly dependent on plant species, further on the doses of the radiation, and the acclimation level of the plants [1]. Photosystem 2 (PSII) is one of the most sensitive cellular elements under various environmental stressful factors The main reason for the harmful effects of UV-B radiation is initiations of photochemical reactions, including production of reactive oxygen species (ROS), which damages biologically active molecules [2].

The objective of this study was to evaluate how UV-B radiation influences antenna-dependent photosynthetic acclimation reactions, resulting in modulation of primary photochemical reactions. cell antioxidant status and overall morphology of both green- and red-leaf lettuce plants (*Lactuca sativa* L., cvs. Lento and Rosemary). Using comprehensive assessment of biophysical (JIP test), biochemical (contents of MDA, photosynthetic pigments, anthocyanins and polyphenols), physiological and morphological (dry matter, leaf area) traits as well as full plant scale chlorophyll *a* fluorescence imaging (FluorCam) and hyperspectral reflectance connected to PlantScreen™ phenotyping platform were analysed effects of stress acclimation and level of UV-B induce photodamage. In series of experiments were used four intensities of UV-B irradiance supplementation (0, 26, 53 and 141 mW/m^2). Dose-dependent UV-B radiation increased the content of flavonoids but not anthocyanins. The production of cellular ROS and also the oxidative damage marker MDA also increased. It has been previously documented that a higher concentration of H_2O_2 may have stimulated both polyphenols and anthocyanin synthesis [3]. ROS can damage the structural components of photosystem II, such as D1, D2, CP43, LHCII, and PsbH proteins present in thylakoid membranes, resulting in observed decline of maximum quantum yield of PSII photochemistry (Fv/Fm).The red genotype showed higher resistance to the increasing intensity of UV-B radiation, mainly by maintaining a higher efficiency of primary photosynthetic reactions. This trait significantly corelates

with both anthocyanins and flavonoids content, as well as with the activity of antioxidant enzymes. The results confirmed the assumption that the UV-B irradiance influenced physiological responses both at the level of functional and structural parameters of the photosynthetic apparatus, at the level of growth and morphological signs, as well as selected biochemical indicators.

Acknowledgements
The study was supported by the national grants APVV-22-0392, APVV-24-0586, VEGA-1-0425-23 and VEGA-1-0048-25.

References
[1] Brestic, M. et al. Acclimation of Photosynthetic Apparatus to UV-B Radiation. In: Kataria, S., Singh, V.P. (eds) UV-B Radiation and Crop Growth. Plant Life and Environment Dynamics. Springer, Singapore, 2022.
[2] Campos, F.G. et al. UV-B Radiation in the Acclimatization Mechanism of Psidium guajava in Sunlight. Horticulturae 2023, 9, 1291
[3] Liu, M. et al. Acetylated Proteomics of UV-B Stress-Responsive in Photosystem II of Rhododendron chrysanthum. Cells 2023, 12, 478

Silicon modulated photosynthetic performance during drought of buckwheat plants

***M. Kovar*[1], *M. Barboricova*[1], *M. Zivcak*[1], *D. Mlynarikova Vysoka*[1], *J. Ferencova*[1], *H. Ghaffari*[2,3], *A. Shomali*[1], *A. Das*[1], *X. Yang*[3], *M. Brestic*[1,3]**

[1] *Institute of Plant and Environmental Sciences, Slovak University of Agriculture, Nitra, Slovakia*

[2] *AgroBioTech Research Centre, Slovak University of Agriculture, Nitra, Slovakia*

[3] *State Key Laboratory for Wheat Improvement, Shandong Agricultural University, Taian, China*

marek.kovar@uniag.sk

Buckwheat (Fagopyrum spp.), a pseudocereal, is increasingly recognized as a functional food due to its high content of essential amino acids, vitamins, and phenolic compounds (1). However, plants are continuously exposed to a range of environmental stresses, among which drought stress is one of the most complex and detrimental abiotic factors. It significantly disrupts plant metabolic processes, impairs crop quality and yield, and affects morphological, physiological, and molecular responses (2). Drought stress disrupts key functions such as photosynthetic pigment synthesis, photosynthesis and respiration, nutrient uptake, ROS homeostasis, and leaf gas exchange in plants (3). To mitigate the detrimental effects of drought stress, various strategies have been adopted, including the application of growth regulators, mineral nutrients, and signalling molecules. Among these, silicon (Si) has garnered increasing attention over the past two decades due to its multifunctional role in enhancing plant resilience against a wide array of abiotic stresses, including drought (4).

This study aimed at investigating the protective role of silicon (Si; concentration 0, 1, 3, 5 and 7 mM) in mitigating drought-induced damage of photosynthetic performance in common buckwheat plants (*Fagopyrum esculentum* L., cv. Panda). Using comprehensive assessment of biophysical (JIP test), biochemical (MDA content, photosynthetic pigments, antioxidant enzymatic activity), physiological and morphological (dry matter, leaf area) traits were analysed effects of foliar applied Si in stabilization of biological processes of buckwheat plants under progressive drought. Drought stress caused a substantial reduction in stem diameter, shoot length, fresh weight and dry weight in buckwheat plants. The foliar application of Si enhanced several morphological traits in plants under drought conditions. Reduction of stomatal conductance (g_S) after foliar-applied Si in well-watered conditions was observed in dose-manner dependence. Conversely, during dehydration, silicon delayed stomatal closure. We also observed that drought induced production of cell H_2O_2, increased MDA content and chlorophyll content decreased. Si application mitigated these undesirable effects.

The influence of foliar-applied Si on the primary photosynthetic machinery (donor and acceptor sides of PSII) under drought was investigated using fast chlorophyll a fluorescence kinetics (JIP-test). Maximal photochemical

PSII efficiency (Fv/Fm) was relative stable under drought. Si-treated plants exhibited mainly a marked increase in fluorescence intensity in the I-P phase relative to control plants. Analyse

Foliar-applied Si at concentration 5 mM mitigate drought-induced by damage maintenance of chlorophyll content, preserving thylakoid membrane integrity, and optimizing energy fluxes at chloroplast electron-transport chain, and modulated stomatal behaviour. Finally, these findings highlight the protective role of Si in improving plant stress tolerance.

Acknowledgements
The study was supported by the national grants APVV-22-0392, APVV-24-0586, VEGA-1-0425-23 and VEGA-1-0048-25.

References
[1] Cheng, A. Shaping a sustainable food future by rediscovering long-forgotten ancient grains. Plant Science, 2018, 269, 136-142.
[2] Aubert, L. Different drought resistance mechanisms between two buckwheat species *Fagopyrum esculentum* and *Fagopyrum tataricum*. Physiologia plantarum, 2021, 172, 577-586.
[3] Rastogi, A. et al. Does silicon really matter for the photosynthetic machinery in plants…? Plant Physiology and Biochemistry, 2021, 169, 40-48.
[4] Liu, B. Mechanisms of silicon-mediated amelioration of salt stress in plants. Plants, 2019, 307.

Non-Invasive Screening Methods for Wheat Photosynthetic Performance Under Combined Drought and Heat Stress

***M. Barboricova*[1], *M. Kovar*[1], *M. Zivcak*[1], *D. Mlynarikova-Vysoka*[1], *A. Das*[1], *H. Ghaffari*[1] and *M. Brestic*[1]**

[1] *Institute of Plant and Environmental Sciences, Slovak University of Agriculture, Nitra, Slovakia*

e-mail: barboricovamaria332@gmail.com

Wheat is one of the most important agricultural species for ensuring global food security; however, its production is increasingly threatened by environmental stresses, such as drought and high temperatures, during growth and development. Current climate model predictions indicate increased frequency and intensity of these stress factors, which individually and in combination significantly reduce photosynthetic activity, growth, and final yield of wheat—more so than individual stresses alone [1]. It was also demonstrated that combined drought and high-temperature stress causes a more significant decrease in key morphological and physiological parameters than either stress separately, emphasizing the need to understand the adaptation mechanisms of different varieties [2,3,4]. Therefore, identifying and characterizing varietal differences in tolerance to combined abiotic stresses is crucial for developing more resilient wheat varieties under climatically variable conditions.

We employed a comprehensive suite of non-invasive methods to assess photosynthetic performance and water status in wheat genotypes grown in pots in greenhouse conditions. Chlorophyll fluorescence parameters were measured to characterize the structure and functionality of photosystem II (PSII) using a Handy PEA fluorometer (Hansatech, GB). Additionally, we utilized a MultispeQ device (PhotosynQ, USA) to simultaneously evaluate both PSII and photosystem I (PSI) activity, along with other parameters. Plant water status was determined by measuring relative water content (RWC), while direct photosynthetic rates and stomatal conductance were quantified using an open gas exchange system (LI-6400, Li-Cor, Lincoln, NE, USA). This integrated approach allowed comprehensive evaluation of the photosynthetic responses of individual wheat varieties under drought and high-temperature conditions.

The measured results confirm that a sudden period of extremely high temperatures (up to 36°C) in connection with drought (relative water content, RWC, below 70%) led to a pronounced decrease in net photosynthesis (Aco_2) and stomatal conductance (g_s) in stressed plants. The effects were most severe in photosynthetic mutants deficient in chlorophyll *b*, which were associated with insufficient photoprotection, emphasizing the importance of regulatory mechanisms for stable photosynthesis. In addition to recognizing differences between varieties, another goal was to verify the usefulness of individual parameters obtained by MultispeQ through comparison with datasets obtained using standard gas exchange and fluorescence methods. While the correlation

between CO_2 assimilation and electron transport rate, measured by a simultaneous gas exchange and fluorescence system, was only moderate, the results showed high correlation between parameters obtained by MultispeQ measured in light-exposed samples and Handy PEA measurements under dark-adapted conditions. Thus, MultispeQ data reflect structural and functional impairment of the photosynthetic apparatus by stress and non-stomatal effects, rather than a decrease in actual photosynthesis and electron transport rate caused predominantly by stomatal closure. The dataset obtained in our experiments provided essential information needed for correct interpretation of MultispeQ data, and this knowledge is applicable both in future research and in practical applications for screening crop stress effects.

Acknowledgements
The research work and presentation of the results was supported by the research projects APVV-22-0392 and the projects VEGA-1-0048-25 and VEGA 1-0639-26.

References
[1] Asseng, S. et al.: Uncertainty in simulating wheat yields under climate change. Nature Climate Change. 3 : 827–832, 2013.
[2] Barboricova, M. et al.: Sensitivity of fast chlorophyll fluorescence parameters to combined heat and drought stress in wheat genotypes. Plant, Soil and Environment. 68(7): 309–316, 2022.
[3] Brestic, M., Zivcak M. PSII fluorescence techniques for measurement of drought and high temperature stress signal in crop plants: protocols and applications. Molecular stress physiology of plants. Springer. Pp. 87–131, 2013.
[4] Kalaji H.M., Jajoo A., Oukarroum A. et al.: Chlorophyll a fluorescence as a tool to monitor physiological status of plants under abiotic stress conditions. – Acta Physiol. Plant. 38: 102, 2016.

Protein-Controlled Electronic Energy Transfer in Photosynthetic Complexes

***G. Rankelytė*[1], *J. Chmeliov*[1,2], *A. Gelzinis*[1,2], *and L. Valkunas*[1,2]**
[1]*Department of Molecular Compound Physics, Centre for Physical Sciences and Technology, Vilnius, Lithuania*
[2] *Institute of Chemical Physics, Faculty of Physics, Vilnius University, Lithuania*
gabriele.rankelyte@ftmc.lt

Photosystem I (PSI), located in the thylakoid membrane of chloroplasts, is the most efficient light-to-energy conversion apparatus. In order to reach and maintain high quantum yield, all processes in PSI, including electronic energy transfer (EET) between the pigments, must be exceptionally rapid.

After the absorption of photon and excitation of a single pigment, excitation energy can be transferred to the nearby pigment over a relatively short distance (tens of angstroms). Such excitation dynamics is determined by pigment-pigment couplings J_{mn} [1], described in terms of the electronic transition densities. Using the well-known approach (TrEsp method) electronic transition densities can be replaced by the atomic transition charges [2].

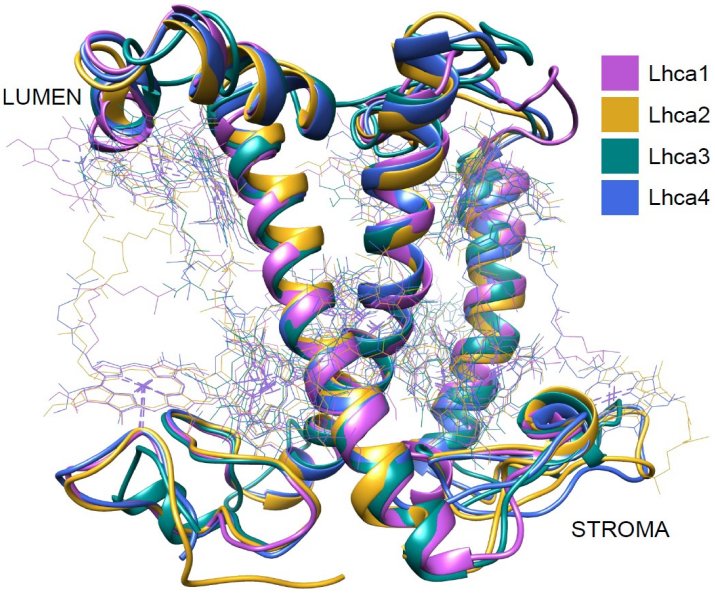

Figure 1: Lhca1-4 complex structures mapped on top of each other. Chlorophylls are depicted in wire representation, carotenoids are not shown.

In our work we have investigated the excitation dynamics in four Lhca complexes of PSI light-harvesting antenna LHCI (see Figure 1). The structure of the antenna was obtained from the PDB (PDB ID: 5L8R) [3]. We used the aforementioned approach to obtain the chlorophyll-chlorophyll coupling energies in vacuum and in protein environment (with protein chain and other pigments present). For accounting for the protein environment, we used similar approach to our previous research [4]. We have also accounted for the

solvent screening effect [5] and compared the properties of exciton dynamics with the effects of protein and solvent and without (vacuum) (see Figure 2 for example of chlorophyll transition dipole moment comparison).

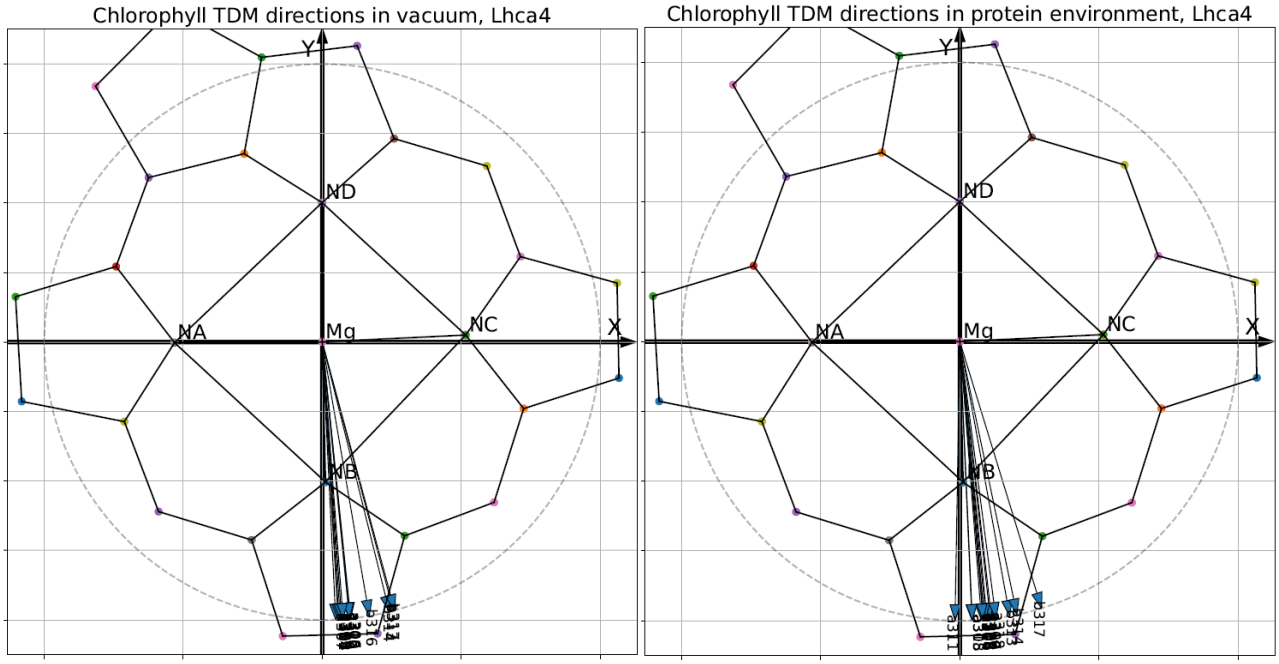

Figure 2: Directions of chlorophyll Q_y transition dipole moment calculated from transition charges for all chlorophylls in Lhca4. Results are given in vacuum (left) and in protein environment (right).

Acknowledgements
Computations were performed using the resources of the High Performance Computing Center "HPC Sauletekis" at Faculty of Physics, Vilnius University.

References

[1] G. D. Scholes "Long-range resonance energy transfer in molecular systems", Annual Review of Physical Chemistry, 54, 1, 2003, 57-87.
[2] M. E. Madjet, A. Abdurahman, T. Renger "Intermolecular Coulomb couplings from ab initio electrostatic potentials: application to optical transitions of strongly coupled pigments in photosynthetic antennae and reaction centers," Journal of Physical Chemistry B, 110, 34, 2006, 17268-17281.
[3] Y. Mazor, A. Borovikova, I. Caspy, N. Nelson "Structure of the plant photosystem I supercomplex at 2.6 Å resolution", Nature plants, 3, 3, 2017, 1-9.
[4] G. Rankelytė, A. Gelzinis, B. Robert, L. Valkunas, J. Chmeliov "Environment-dependent chlorophyll–chlorophyll charge transfer states in Lhca4 pigment–protein complex", Frontiers in Plant Science, 15, 2024, 1412750.
[5] G. D. Scholes, C. Curutchet, B. Mennucci, R. Cammi, J. Tomasi "How solvent controls electronic energy transfer and light harvesting", Journal of Physical Chemistry B, 111, 25, 2007, 6978-6982.

Photosynthetic activity of cyanobacteria growing on phytotoxic substrates

***M. Vítová*[1], V. Jílková[2], M. Čížková, J. Thabet, J. Kvíderová, J. Elster and J. Frouz[1]**

[1]*Institute of Botany, Czech Academy of Sciences, Department of Phycology, Třeboň, Czech Republic*

[2]*Biological Centre, Czech Academy of Sciences, Institute of Soil Biology and Biogeochemistry, České Budějovice, Czech Republic*

milada.vitova@gmail.com

Biological crusts (biocrusts) are soil communities formed by living organisms that live immediately below or above the soil surface [1,2]. Biocrusts are often found in arid or barren regions, where they cover the surface where other vascular plants do not occur. They can act as a natural prevention of wind and water erosion and prepare the site for settlement by other organisms [3]. Microalgae as an integral part of biocrusts can contribute to the initial stages of reclamation thanks to their ability to photosynthesize and rapidly colonize new substrates. They not only initiate the process of soil formation but also ensure its long-term stability. Microalgae facilitate the accumulation of organic matter, improve soil structure and create favorable conditions for subsequent colonization by bacteria, fungi and higher plants [4-6].

The goal of this study was to design and apply biotechnologies for the revival of phytotoxic soils (e.g. post-mining dumps) based on the use of cyanobacteria. Reclamation of dumps and restoration of ecosystems can be achieved either through spontaneous primary succession or controlled secondary succession [7,8]. Microalgal strains isolated from biocrusts from the Lítov post-mining dump (Northern Czechia) [9] and others coming from algal collections were tested in laboratory experiments for a grow on soils (Fig. 1). Measurement of the effective quantum yield (ΦPSII) using a fluorometer showed that the strains can still perform photosynthesis although with reduced efficiency (Fig. 2). The observed Qmax values 0.3–0.5 align with typical stress-influenced efficiencies reported for cyanobacteria in polluted environments.

Desmonostoc mucorum was selected for following greenhouse experiments. The environmental conditions of cultivation (air temperature, air humidity and irradiance/photosynthetically active radiation) were monitored, which were characterized by high variability even within a single day. Fluorometric measurement of the effective quantum yield (ΦPSII), as an indicator of physiological state and photosynthetic activity, demonstrated a relatively good physiological state during cultivation. The regular decrease in ΦPSII during the day was caused by irradiance, the lowest values, indicating strongly stressful conditions, were achieved at low temperatures below 0 °C. After increasing the temperature, a rapid recovery of photosynthetic activity was observed, therefore *Desmonostoc mucorum* can be considered well adapted to variable

environmental conditions. The possibility of long-term monitoring of physiological state and photosynthetic activity by measuring variable chlorophyll fluorescence on biological soil crusts was also verified and demonstrated.

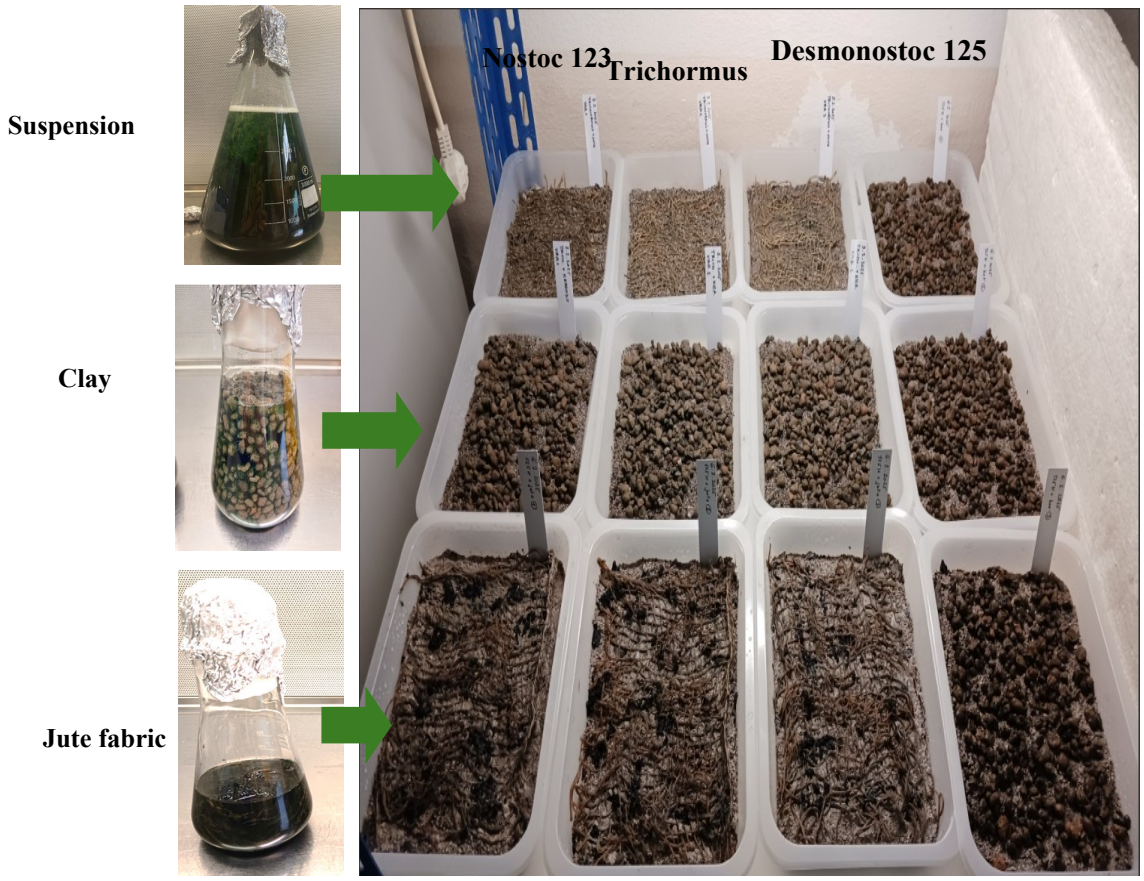

Figure 1: Cyanobacteria growing on phytotoxic substrates. Different ways of application using suspension, clay or jute fabric.

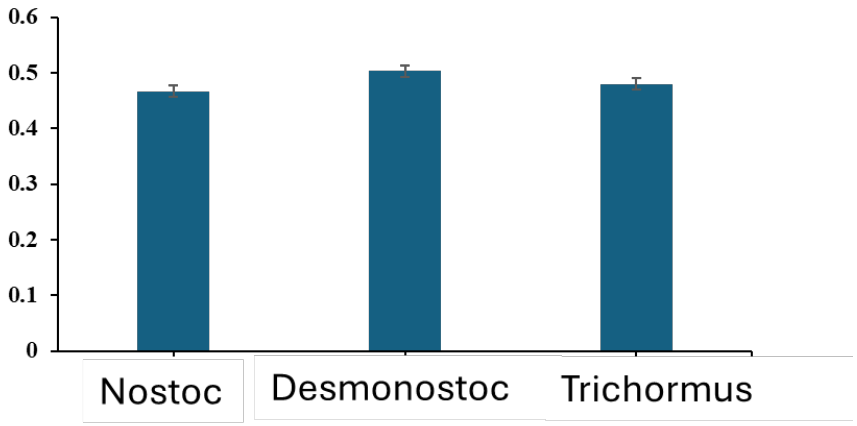

Figure 2: Effective quantum yield (ΦPSII) of cyanobacteria growing on phytotoxic substrates determined fluorometrically.

Acknowledgements

Project SS07020063 is co-financed from the state budget by the Technology agency of the Czech Republic and Ministry of the Environment under the Program Environment For Life. The project is financed in the frame of National Recovery Plan from European Recovery and Resilience Instrument.

References

[1] J. Belnap "The world at your feet: desert biological soil crusts", Frontiers in Ecology and the Environment, 1, 2003, 181-189.
[2] B. Weber et al. "What is a biocrust? A refined, contemporary definition for broadening research community", Biological Reviews, 2022, 10.1111/brv.12862.
[3] J. Belnap "The potential roles of biological soil crust in dryland hydrologic cycles", Hydrological Processes, 20, 2006, 3159-3178.
[4] X. Song et al. "Potential applications for multifunctional microalgae in soil improvement", Frontiers in Environmental Science, 2022, 10:1035332.
[5] B. Ramakrishnan, N.J. Maddela, K. Venkateswarlu, M. Megharaj "Potential of microalgae and cyanobacteria to improve soil health and agricultural productivity: a critical view", Environmental Science: Advances, 2, 2023, 586-611.
[6] L. Saini, H. Upadhyay, A. Chakraborty "Application of microphytes for soil reclamation", 2024, 10.1016/B978-0-443-13993-2.00026-8.
[7] K. Coradini, J. Krejčová, J. Frouz "Potential of vegetation and woodland cover recovery during primary and secondary succession, a global quantitative review", Land Degradation & Development, 33, 2022, 512-526.
[8] Y. Guan, J. Wang, W. Zhou, Z. Bai, Y. Cao "Delimiting supervision zones to inform the revision of land reclamation management modes in coal mining areas: A perspective from the succession characteristics of rehabilitated vegetation", Land Use Policy, 131, 2023, 106729.
[9] E. Enkhtaivan, O. Vacek, P. Vokurková, M. Spasić, R. Vašát, O. Drábek "Temporal changes of soil characteristics on Lítov spoil heap, Czech Republic", Soil & Water Research, 2024, 19(3), 133-143.

Photosynthesis in *Vitis vinifera* cv. Fortana, a historic ungrafted grape variety of the sandy coast of Emilia-Romagna (Northern Italy)

M. Ballestriero[1], E. Marrocchino[1], L. Sansone[2], R. Carraro[2], N. Govoni[1] and L. Ferroni[1]

[1] *Department of Environmental and Prevention Sciences, University of Ferrara, Ferrara, Italy*

[2] *Council of Agricultural Research and Economics, Research Centre for Viticulture and Enology, Conegliano (Treviso), Italy*

lorenzo.ferroni@unife.it

Vitis vinifera L. is one of the most important crops in the world for its products and cultural value. Its long breeding history across a wide geographic area selected a characteristic adaptability to different environments. After the crisis of viticulture brought about by phylloxera (*Daktulosphaira vitifoliae*) infestation in Europe in the mid of 19th century, almost all grapevines have been grafted onto resistant American rootstocks not to succumb to the pest. Only a few of grapevine varieties are still cultivated ungrafted, i.e., on their own root system, but this is not due to some kind of genetic resistance but rather to the soil in which they grow, which is inhospitable to phylloxera. On the eastern coast of Emilia-Romagna region (Italy), the grapevine variety named "Fortana" has historically been cultivated without grafting on a sandy soil. Local farmers describe Fortana as resistant to drought, which is a favourable trait in sandy soil characterized by high drainage. However, there are examples of plants growing just a few hundred metres from the Adriatic coast, where soils are prone to salinisation. We hypothesized that long-term cultivation in slightly saline soils may have selected or maintained a form of salinity tolerance in Fortana grapevines, i.e, maintaining a high photosynthetic efficiency when cultivated close to the seacoast.

This study aims at verifying the salinity tolerance of Fortana grapevine through an infield comparative analysis of some photosynthetic parameters in relation to distance of plants from the coast. The study took place in a vineyard near the Adriatic Sea in Comacchio (Ferrara, Italy) in July 2025. The vineyard comprises ungrafted Fortana vines that are around 60 years old. The analysed plants were 640 m, 540 m and 400 m from the coast. Analyses of fast chlorophyll *a* fluorescence were carried out with a Handy-PEA fluorometer, gas exchange measurements with a CIRAS2 Portable Photosynthesis System, stem water potential (Ψ_{stem}) with a Scholander pressure chamber. Fluorometric analyses were performed in the morning, at noon and in the afternoon to evidence differences in PSII photoinhibition. Fluorescence transients were treated according to JIP test parameters [1-3].

Maximum quantum yield of PSII (F_v/F_m), efficiency of the water-splitting complex on the donor side of PSII (F_v/F_o) and total performance index on absorption basis (PI_{tot}) resulted significantly higher in plants closer to the

coast, suggesting an overall healthier state. Electron flow probabilities, ΨETo and ΨREo, were also higher in plants at 400 m than at 640 and 540 m, while the normalized area above the OJIP transient, *Sm*, was slightly higher at 400 m than at 640 m, suggesting more capacitive electron carrier pools in the former. Since δRE did not show any difference, the increase in the pool of transporters was probably not specific to the plastoquinone pool or the final carriers but generalized of the entire PSII-PSI transport chain. The apparent PSII antenna size, represented by ABS/RC was larger in plants farther from the coast, possibly due to a lower concentration of photosynthetically active units. For all parameters, no relevant differences were found in relation to the time of the day. Gas exchange analyses revealed no differences among the three plant groups with respect to net photosynthesis P_N and stomatal conductance g_s. Ψ_{stem} also showed non-significant differences. Differently, transpiration was markedly higher in plants at 400 m from the coast, leading to a much lower intrinsic water use efficiency (*iWUE*) than in more distant plants. Quite surprisingly, these last parameters indicate a higher water availability in plants closer to the sea, so that leaves can afford to transpire more water, while being characterised by the same g_s and Ψ_{stem} as the others. In fact, in sandy soils near the coast, moderate salinity can reduce the osmotic potential of the soil, decreasing water availability for plants [4]. However, tolerant plants are known to induce acclimative responses to allow water uptake and transpiration; because, in this case, transpiration is higher, it is very likely that in response to highly draining and slightly saline conditions, the plants developed a deeper root system and, therefore, achieved a more efficient water supply. Effective leaf cooling by more intense transpiration is in line with the superior preservation of PSII function in these plants. These findings suggest that Fortana is not merely tolerant but may actually benefit from moderate coastal salinity conditions. This highlights its potential as a resilient cultivar for viticulture in marginal and climate-stressed coastal areas.

References

[1] Tsmilli-Michael, M. « Revisiting JIP-test: An educative review on concepts, assumptions, approximations, definitions and terminology », Photosynthetica, 58, SI, 2020,275-292.
[2] Stirbet, A. & Govindjee « On the relation between the Kautsky effect (chlorophyll a fluorescence induction) and Photosystem II: Basics and applications of the OJIP fluorescence transient », Journal of Photochemistry and Photobiology B : Biology, 104, 1–2, 2011, 236-257.
[3] Strasser, R.J., Tsimilli-Michael, M., Srivastava, A. « Analysis of the Chlorophyll a Fluorescence Transient. In: Papageorgiou, G.C., Govindjee (eds) Chlorophyll a Fluorescence », Advances in Photosynthesis and Respiration, 19, 2004, 321–362.
[4] Negrão, S., Schmöckel, S. M., & Tester, M. « Evaluating physiological responses of plants to salinity stress », Annals of Botany, 119, 1, 2016, 1-11.

Acknowledgements

This research was funded by the Ministry of Research of Italy through the project PRI2022 « Soil, water, sun: Exploring Ungrafted indigenous Italian *Vitis vinifera* L. varieties as a resilient resource against the effects of global climate change (EU-vitis) » (CUP F53C2400120).

Beyond Static Structures: Single-Molecule FRET Resolves Mobile GTPase Domains in Chloroplast Protein Import

***S. Penneru*[1], *S. Tiruvadi-Krishnan*[1], *R. Lamichhane*[1] *and B. Bruce*[1]**
[1] *Biochemistry and Cellular & Molecular Biology, University of Tennessee, Knoxville, Tennessee 37916, USA*
bbruce@utk.edu

Abstract: Photosynthetic capacity depends on rapid, selective assembly of a largely nuclear-encoded chloroplast proteome. Because most photosynthetic proteins are synthesized in the cytosol, regulated import across the chloroplast envelope is a key control point in chloroplast biogenesis and light acclimation (1). Import is initiated by the Translocon at the Outer Chloroplast membrane (TOC), where receptor GTPases are proposed to couple transit-peptide recognition to productive engagement of the translocation pathway (2). Although the overall structural architecture of TOC has advanced, the dynamic molecular logic that governs receptor switching, precursor handoff, and translocon activation remains poorly defined.

We investigate this regulatory layer by focusing on the TOC receptor GTPases Toc34 and Toc159/Toc120, using single-molecule photobleaching stoichiometry, single-molecule FRET, and chemical cross-linking to quantify ligand-dependent oligomerization and conformational ensembles. Using the fully monomeric fluorescent protein Green Lantern/mEGFP (3) as a robust single-molecule reporter, photobleaching shows that Toc34 populates a predominantly dimeric basal state, but dimerization is destabilized by the RuBisCO small subunit transit peptide and by nonhydrolyzable GTP analogs (GMP–PNP, GTPγS), consistent with a ligand-gated transition coupled to the GTPase cycle. Complementary FRET on GDP-bound Toc34 resolves three conformational populations with distinct transfer efficiencies, whereas transit peptide and/or GTP-analog binding eliminates detectable FRET, indicating a shift toward increased conformational mobility, larger inter-protomer separation, and/or monomerization. Cross-linking independently supports this nucleotide- and substrate-dependent oligomeric transition.

To convert these state changes into mechanistic interaction maps, we are expanding to inter-receptor FRET between labeled Toc34 and the Toc159/Toc120 G-domain, enabling direct measurement of nucleotide- and substrate-dependent heterotypic pairing and switching kinetics. We are also implementing systematic single-cysteine scanning across Toc34 and Toc159/Toc120(G) to generate defined labeling sites for distance-resolved FRET constraints, and developing single-cysteine, site-specifically labeled transit peptides to quantify precursor docking geometries and receptor–precursor dynamics in real time. Notably, existing cryo-EM reconstructions of TOC generally fail to resolve the GTPase domains of Toc34 and Toc159/Toc120, strongly suggesting that these functional modules are highly mobile and conformationally heterogeneous—precisely the regime where single-molecule and chemical-constraint approaches are most informative.

Significance: The TOC–TIC system imports thousands of nuclear-encoded proteins required for photosynthesis and plant growth, yet the most

functionally critical steps—precursor capture, receptor switching, and handoff—are driven by transient, dynamic interactions that are difficult to infer from static structures. By integrating single-molecule stoichiometry with multi-distance FRET (Toc34–Toc34, Toc34–Toc159/Toc120(G), and transit peptide–receptor) and orthogonal cross-linking constraints, this work provides a quantitative framework for how nucleotide state and precursor engagement reshape TOC receptor assemblies to tune import efficiency and fidelity. These in vitro mechanistic maps establish a foundation for next-stage experiments in more native contexts, including reconstituted and isolated TOC-containing complexes and ultimately in vivo validation of receptor switching models that underlie chloroplast biogenesis.

Acknowledgements
Research in the Lamichhane lab is supported by the NIH grant R35GM142946 (RL). The authors also acknowledge financial support from the Charles P. Postelle Distinguished Professorship of Biotechnology and the NSF Grant IOS-2233695 (BDB).

References

(1) Martin, W. 2003. Gene transfer from organelles to the nucleus: frequent and in big chunks. *Proc Natl Acad Sci U S A*. 100(15):8612-8614, doi: 10.1073/pnas.1633606100.
(2) Schleiff, E., J. Soll, M. Kuchler, W. Kuhlbrandt, and R. Harrer. 2003. Characterization of the translocon of the outer envelope of chloroplasts. *J Cell Biol*. 160(4):541-551, doi: 10.1083/jcb.200210060.
(3) Campbell, B. C., E. M. Nabel, M. H. Murdock, C. Lao-Peregrin, P. Tsoulfas, M. G. Blackmore, F. S. Lee, C. Liston, H. Morishita, and G. A. Petsko. 2020. mGreenLantern: a bright monomeric fluorescent protein with rapid expression and cell filling properties for neuronal imaging. *Proc Natl Acad Sci U S A*. 117(48):30710-30721, doi: 10.1073/pnas.2000942117.

Real-Time TOC Receptor Mobility Reveals Dynamic Import Microdomains in Isolated *Pisum sativum* Chloroplasts

P. Suresh[1], S. Tiruvadi-Krishnan[1], J. Kolape[2], A. Joshi[1,3], R. Lamichhane[1,3] and B. D. Bruce[1,3]

[1] *Department of Biochemistry & Cellular and Molecular Biology, University of Tennessee, Knoxville, USA*

[2] *Advanced Microscopy and Imaging Center, University of Tennessee, Knoxville, USA*

[3] *Graduate School of Genome Science and Technology, University of Tennessee, Knoxville, USA*

bbruce@utk.edu

Chloroplast biogenesis and photosynthetic performance require the targeted import of ~2,700 nuclear-encoded proteins from the cytosol. This trafficking is mediated by the TOC/TIC translocon system, which must deliver high throughput while maintaining selectivity across the chloroplast double membrane. Although core TOC components (e.g., Toc75, Toc34, Toc159) and key regulatory inputs (ATP/GTP, transit peptides, receptor interactions, and proteolytic remodeling) have been identified, how the import machinery is organized in space and time in intact plastids remains unclear. Most mechanistic models derive from in vitro assays or partially solubilized components, leaving a gap in understanding whether TOC/TIC behaves as uniformly distributed channels or as a spatially compartmentalized, dynamically assembling system coordinated at envelope microdomains and contact sites.

Here we interrogate TOC organization and dynamics in intact, isolated *Pisum sativum* chloroplasts, focusing on the receptor GTPase Toc34 as an entry point for mapping import-site behavior. Using Laser scan and Airy scan immunofluorescence confocal microscopy and immunogold electron microscopy, we observe Toc34 concentrated in discrete punctate envelope sites, consistent with specialized translocon microdomains and potential contact regions that could organize TOC/TIC coupling. We further examine Toc34 co-localization with Toc159 and Toc75 across plastid maturation, revealing patterns consistent with developmentally regulated remodeling of import-site composition or abundance. To connect localization to function, we apply single-particle tracking by TIRF microscopy, resolving two Toc34 mobility states: a faster, freely diffusing population and a slower, confined-yet-dynamic population. This switching is consistent with Toc34 cycling between an unengaged diffusion mode and a transiently stabilized state associated with receptor clustering, precursor engagement, and/or coupling to translocation.

Future directions will build a mechanistic bridge from these in situ observations to import function. We will test whether Toc34 confinement correlates with active import by adding defined precursors/transit peptides and manipulating nucleotide state (ATP/GTP/GDP analogs) while quantifying mobility shifts and microdomain stability. We will expand multiplex imaging to additional TOC/TIC

markers and candidate contact-site factors to determine whether puncta represent TOC–TIC hubs or modular receptor assemblies, and will examine how import-site number, composition, and dynamics scale across controlled plastid maturation stages. Finally, we will pursue correlative super-resolution/EM approaches to link single-molecule dynamics to ultrastructural context at defined envelope regions.

Significance: These results provide direct evidence that TOC receptors are spatially organized and dynamically mobile in intact chloroplasts**,** moving the field beyond detergent-solubilized snapshots toward a native-state description of how import is executed at the envelope. Importantly, TOC behavior is unlikely to be independent: receptor clustering and mobility states should reflect—at least in part—coupling to TIC and downstream biogenesis demands**,** including the changing requirements for stromal proteome assembly and thylakoid development during chloroplast maturation. By quantifying TOC organization and Toc34 single-molecule dynamics in chloroplasts isolated from tissues at distinct developmental/maturity states**,** this work provides a practical route to connect envelope translocon behavior with the physiological progression of greening, offering measurable structural and dynamic readouts that can be integrated with precursor import assays and ultrastructural analyses. More broadly, these approaches establish a framework for understanding how plastids tune protein trafficking capacity during developmental transitions and environmental light shifts across the plastid family.

Modulatory Effects of Plastoquinone C on Photosynthesis: From Molecular Docking to In Vivo Stress Acclimation

***E. Pykhova*[1*], *M. Kozuleva*[1], *D. Vilyanen*[1], *A. Ashikhmin*[1], *A. Nikolaev*[1], *and M. Borisova-Mubarakshina*[1]**

[1]*Institute of Basic Biological Problems, RAS, Pushchino, Russia*

**Corresponding author. Fax: +7(9125)51-86-85, E-mail: katkapw@yandex.ru*

Plastoquinone A (PQ A) is a mobile electron carrier of the photosynthetic electron transfer chain in the thylakoid membrane. Under excess light conditions, interaction of plastoquinone with reactive oxygen species can lead to generation of modified plastoquinone derivatives, notably hydroxyplastoquinone (PQ C). Although PQ C has traditionally been regarded as a marker of oxidative damage, we propose that its accumulation may play a regulatory role in photosynthetic responses to stress.

This study integrated molecular docking, *in vitro*, and *in vivo* approaches to assess the functional consequences of PQ C accumulation. Molecular docking was used to analyze the interaction of PQ A and PQ C with major plastoquinone-interacting sites of the photosynthetic electron transfer chain. Docking simulations revealed that PQ C binds more weakly than PQ A to the Q_A site of photosystem II (PS II), whereas at the Q_B site PQ-C exhibited more favorable binding energies compared to PQ A, likely reflecting differences in the hydrophobic microenvironment of these sites.

In vitro experiments were conducted using PS II-enriched membranes isolated from *Spinacia oleracea*. Purified PQ A and PQ C were incorporated into liposomes, and their effects were evaluated by Clark-type electrode measurements of oxygen evolution and OJIP fluorescence induction. These experiments demonstrated that PQ C inhibits PS II catalytic activity at concentrations above ~10–15 μM, whereas PQ A did not exhibit inhibitory effects across a broad concentration range.

In vivo analyses were performed on *Arabidopsis thaliana abc1k1* mutants, which display impaired mobilization of plastoquinone from plastoglobuli to the thylakoid membrane. Under high light, these mutants showed an approximately twofold reduction in CO_2 assimilation and a pronounced decrease in proton-motive force (pmf), concomitant with a marked increase in the PQ C/PQ A ratio. Accumulation of PQ C in *abc1k1* mutants was associated with very strong upregulation (reported here up to ~700-fold) of several genes involved in retrograde signaling and stress-related regulation (*PTM*, *ABI4*, *AOX2*).

Taken together, these data suggest that accumulation of PQ C may act as a signal contributing to the activation of plastid-to-nucleus signaling pathways

involved in the protection of the photosynthetic electron transport chain and the prevention of photodamage under excess light. Our findings highlight the qualitative composition of the plastoquinone pool as an important regulatory factor in photosynthetic performance under stress conditions.

This work was supported by the Russian Science Foundation (Grant No. 23-14-00396).

Plastoquinone-dependent H_2O_2 signaling controls PS II antenna size via a chloroplast serine protease

***A. Nikolaev*, N. Rudenko, N. Novichkova, D. Vetoshkina and M. Borisova-Mubarakshina**
Institute of Basic Biological Problems RAS, Federal Research Center Pushchino Scientific Center for Biological Research of RAS, 142290 Pushchino, Moscow Region, Russia
nikolaevtolya@list.ru

Chloroplast-to-nucleus ROS retrograde signaling is essential for acclimation of the photosynthetic apparatus to environmental stresses. One of the key mechanisms is the regulation of the photosystem II (PS II) antenna size depending on light conditions and other environmental factors. The PS II antenna size has been shown to be regulated by the redox state of the plastoquinone pool (PQ pool)[1]. However, the components linking chloroplast redox status to nuclear gene regulation remain poorly defined.

In the present work we demonstrate that the coupling of the signaling pathway initiated in chloroplasts at the level of the PQ pool with the signaling pathway in the cell cytoplasm for the regulation of gene expression encoding PS II antenna proteins (Lhcb proteins) occurs through the activation of chloroplast membrane serine protease by hydrogen peroxide. As it is known, the protease activity leads to the processing of the chloroplast envelope-bound transcription factor PTM, enabling its relocation to the nucleus, where it induces ABI4 expression. ABI4, in turn, represses transcription of *lhcb* genes, resulting in downsizing of the PS II antenna. We show that H_2O_2 at physiologically relevant concentrations specifically stimulates the activity of chloroplast envelope proteases, since this activation is inhibited by PMSF (phenylmethylsulfonyl fluoride), a selective serine protease inhibitor. Gene expression analysis confirms the coordinated upregulation of *ABI4*, and *PTM*, as well as serine *SPPA1* envelope protease in high light. Therefore, we conclude that serine proteases, presumably *SPPA1* protease, are involved in retrograde signaling from chloroplasts to the nucleus.

Our recent studies demonstrated that the PQ pool components are significantly involved in H_2O_2 formation in chloroplasts, with the high rate under high light conditions [for review see 2]. On the basis of these and above-decribed data we suggest that H_2O_2, formed by chloroplast components in light, including components of the PQ pool, can alter the activity of serine protease when diffusing through chloroplast envelope, which in turn affects the conversion of the chloroplast envelope-associated transcription factor PTM into a soluble form. Therefore, our findings indicate a link between redox changes in the PQ and the H_2O_2 level in chloroplasts with protease-mediated signaling cascades in cytoplasms. In general, the obtained data reveal the connection between chloroplast and nuclear control of photosynthetic light harvesting, highlighting a signaling strategy for the PS II antenna size regulation in higher

plants. The hypothetical mechanism of this retrograde signaling pathway is presented in Fig. 1 and it is published in [4].

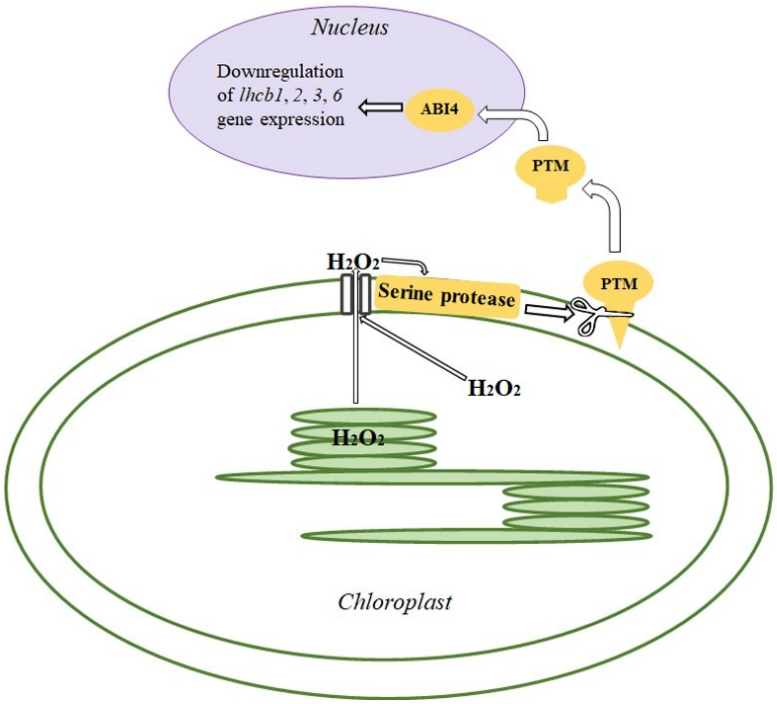

Figure 1: The hypothetical mechanism of the retrograde signaling proceeding for PS II antenna size downsizing.

Acknowledgements

This work was supported by the Russian Science Foundation, grant number 23-14-00396 (extension), https://rscf.ru/project/23-14-00396/.

References

1. Yang, D.-H.; Andersson, B.; Aro, E.-M.; Ohad, I. The Redox State of the Plastoquinone Pool Controls the Level of the Light-Harvesting Chlorophyll a/b Binding Protein Complex II (LHC II) during Photoacclimation. *Photosynthesis Research* 2001, *68*, 163–174, doi:10.1023/A:1011849919438.
2. Borisova-Mubarakshina M.M. (2025) Networking of plastoquinone pool and reactive oxygen species in higher plant signaling. Russian Journal of Plant Physiology, 72(247).
3. Nikolaev, A.A.; Rudenko, N.N.; Novichkova, N.S.; Vetoshkina, D.V.; Borisova-Mubarakshina, M.M. (2025) Revealing Missing Links in the Downsizing of the Photosystem II Antenna in Higher Plants Under Stress Conditions. Antioxidants, 14, 1505. doi: 10.3390/antiox14121505.

Electrogenic properties of thylakoid membrane at distinct applied voltage

R.A. Voloshin[1], S.K Zharmukhamedov[2], and S.I. Allakhverdiev[1,2]
[1] *K.A. Timiryazev Institute of Plant Physiology, Russian Academy of Sciences, Botanicheskaya Street 35, Moscow 127276, Russia*
[2] *Institute of Basic Biological Problems, Russian Academy of Sciences, Pushchino, Moscow Region 142290, Russia*
voloshinra@gmail.com

Previous studies have shown that thylakoid membranes are capable of generating photocurrent in photoelectrochemical cells [1]. Our previous work demonstrated the necessity of a natural oxygen-evolving complex (OEC) or external electron donors for thylakoid-stimulated photoelectric activity [2]. However, further studies are required to better understand the mechanisms of reduction of oxidized biological sensitizer in a photoelectrochemical cell.
In this study, we examine the influence of several factors known to affect the activity of the OEC (high temperature, pre-irradiation, incubation with an exogenous donor) on the photosynthetic and electrogenic properties of thylakoid membranes.
We demonstrated that treatment of thylakoids with hydroxylamine (20 mM, 30 minutes) and heat treatment (50°C, 1 hour) lead to similar changes in the OJIP curve shape: a signal drop after the J-peak and the absence of the J-P growth stage. Fluorescence curves after two hours of treatment at 45°C and after 30 minutes of incubation at 50°C have the same shape.
Thylakoid membranes subjected to prolonged heat treatment or treatment with hydroxylamine failed to generate current in a photoelectrochemical cell. However, the addition of hydroxylamine at low concentrations or treatment at a temperature of about 30 degrees does not affect or has a slight enhancing effect on photoelectrogenic activity.

Acknowledgements
This work was supported by the Russian Science Foundation (24-14-00033), and in particular (25-74-31001) and by the state contract of the Ministry of Science and Higher Education of the Russian Federation (theme No. 122050400128-1).

References
[1] E. Musazade, R. Voloshin, N. Brady, J. Mondal, S. Atashova, S. Zharmukhamedov, I. Huseynova, S. Ramakrishna, M. Najafpour, J. Shen, B. Bruce, S. Allakhverdiev. "Biohybrid solar cells: Fundamentals, progress, and challenges", Journal of Photochemistry and Photobiology C: Photochemistry Reviews, 35, 134-156.
[2] R. Voloshin, M. Goncharova, S. Zharmukhamedov, B. Bruce, S. Allakhverdiev. "In vitro photocurrents from spinach thylakoids following Mn depletion and Mn-cluster reconstitution", Biochimica et Biophysica Acta - Bioenergetics, 1866, 1, 2025, 149523.

CO_2 content affects the photosynthetic and biochemical profile of the green microalga *Desmodesmus armatus* ARC06

***M. Goncharova*[1], E. Zadneprovskaya[1], R. Voloshin[1], D. Gabrielyan[1], N. Lobus[1], S. Allakhverdiev[1,2]**
[1] *K.A. Timiryazev Institute of Plant Physiology, Russian Academy of Sciences, Botanicheskaya Street 35, Moscow 127276, Russia*
[2] *Institute of Basic Biological Problems, Russian Academy of Sciences, Pushchino, Moscow Region 142290, Russia*
gon.mary.sweet@gmail.com

Some members of the genus *Desmodesmus*, including *Desmodesmus armatus*, are remarkably efficient at CO_2 fixation, opening the possibility of using them to clean industrial gas emissions [1]. More efficient and cost-effective use of these microalgae in bioremediation systems requires a deeper understanding of the adaptive mechanisms they activate in conditions of elevated carbon dioxide levels. This study compares the photosynthetic efficiency and biochemical composition of *D. armatus* ARC06 cells depending on the carbon dioxide content in the medium. We grew the cells in a laboratory intensive culture system [2] with two aeration conditions: a CO_2-enriched air-gas mixture (1.5-2%) or sterile air.

With elevated CO_2 levels, the maximum starch content of 439 mg/g dry weight was recorded on the sixth day of the experiment, while with air bubbling it was half this value. Conversely, the highest protein yield was observed on the third day of cultivation under air bubbling conditions: 218 mg/g dry weight. Cells growing at high CO_2 levels demonstrated the most efficient photosystem II (PSII) function on the second day, then a gradual decline occurred. In cells grown in air, PSII efficiency significantly decreases on the third day, then increases by the sixth. Different adaptive strategies are reflected in both the metabolomic profile and photosynthetic activity.

Acknowledgements
This work was supported by the Russian Science Foundation (24-14-00033), and in particular (25-74-31001) and by the state contract of the Ministry of Science and Higher Education of the Russian Federation (theme No. 122050400128-1).

References
[1] Y. Wang et al. "Isolation and Whole-genome analysis of Desmodesmus sp. SZ-1: Novel acid-tolerant carbon-fixing microalga", Bioresource Technology, 414, 2024, 131572.
[2] D. Gabrielyan et al. "Laboratory System for Intensive Cultivation of Microalgae and Cyanobacteria", Russian Journal of Plant Physiology, 70, 2023, 202–213.

Biohydrogen photoproduction by *Chlorella vulgaris* cultivated on distiller's grains, brewer's spent grains and potato peel waste

***J. Manoyan*, L. Hakobyan, and L. Gabrielyan**
Yerevan State University, Yerevan, Armenia

jmanoyan@ysu.am

Green algae have great potential for waste utilization, as they can efficiently harness sunlight energy, making them promising for large-scale applications in green biotechnology [1]. Using green algae for waste management not only helps reduce waste but also supports algal biomass production for green energy generation [1,2]. This dual benefit enhances their value, especially in addressing current global environmental challenges.

Hydrogen (H_2) is an eco-friendly fuel that burns without causing pollution. In green algae H_2 production is linked to photosynthetic electron transfer and is catalyzed by [Fe]-hydrogenase [2,3].

This study aimed to investigate H_2 photoproduction by *Chlorella vulgaris* Pa-023 cultivated on various types of waste, including distiller's grains (DG), brewer's spent grains (BSG), and potato peel waste (PPW) (Fig 1). DG and BSG, by-products of alcohol production, are rich in proteins, sugars, organic acids, vitamins, and other compounds [1]. PPW, a by-product of the food industry, contains carbohydrates, starch, proteins, unsaturated fatty acids, and various phytochemicals [4]. Given their high carbon content, these wastes can serve as effective media for cultivating green algae.

Culture of green alga *Chlorella vulgaris* Pa-023 (Algae Collection, Microbial Depository Center, NAS, Armenia) were cultivated under aerobic conditions on standard Tamiya medium upon illumination [5]. The growth of *C. vulgaris* was monitored by changes in optical density at 680 nm. For H_2 production assay, culture of *C. vulgaris* was transferred to fresh standard Tamiya and various waste-containing media. H_2 production assay was performed under anaerobic conditions and continuous illumination (Climate chamber ICH110L, Memmert, USA), and was monitored by standard gas chromatography techniques (GC 7820A, Agilent Technologies, USA) [5]. The effect of PS II inhibitor, diuron, on H_2 production by *C. vulgaris* Pa-023 was also determined. BSG and DG were obtained from the "Kilikia" beer factory and "Alex Grig" Alcohol Plant Co (Yerevan, Armenia), respectively. Assays were conducted using both undiluted and diluted wastes. The pH of the wastes was adjusted to 7.5 [5].

In this study, three different types of waste were evaluated to determine the most suitable substrate for maximizing H_2 yield in *C. vulgaris* Pa-023. H_2 photoproduction in *C. vulgaris* cultivated on various types of waste began after 24 h. The highest H_2 yield was observed in *C. vulgaris* grown on two-fold diluted BSG after 48-72 h, which was three times higher than the H_2 yield in the control culture cultivated in standard Tamiya medium. Meanwhile, cultivation on undiluted PPW and five-fold diluted DG resulted in ~2 times

higher H_2 yield compared to the control culture. However, no H_2 production was detected in *C. vulgaris* cultivated in undiluted BSG and DG, likely due to the high concentration of organic compounds in these wastes. These findings highlight the importance of waste dilution in optimizing substrate composition to facilitate H_2 production in *C. vulgaris*.

It is well established that green algae utilize both PS II-dependent and PS II-independent pathways for H_2 generation [3,5]. To evaluate the mechanisms of H_2 production by *C. vulgaris* cultivated on various wastes, the effect of the PS II inhibitor, diuron, on H_2 yield was analyzed. Diuron inhibited H_2 production by 70% in *C. vulgaris* grown in two-fold diluted BSG and 5-fold diluted DG, highlighting the crucial role of PS II as the major electron donor in H_2 generation. In *C. vulgaris* cultivated in PPW, diuron suppressed H_2 yield by 60%, indicating that 60% of the electrons for H_2 production are derived from the PS II-dependent pathway, whereas the remaining 40% of electrons are supplied via the PS II-independent pathway.

Thus, tested waste are efficiently utilized by *C. vulgaris* Pa-023, providing a more cost-effective alternative source for H_2 production compared to traditional media.

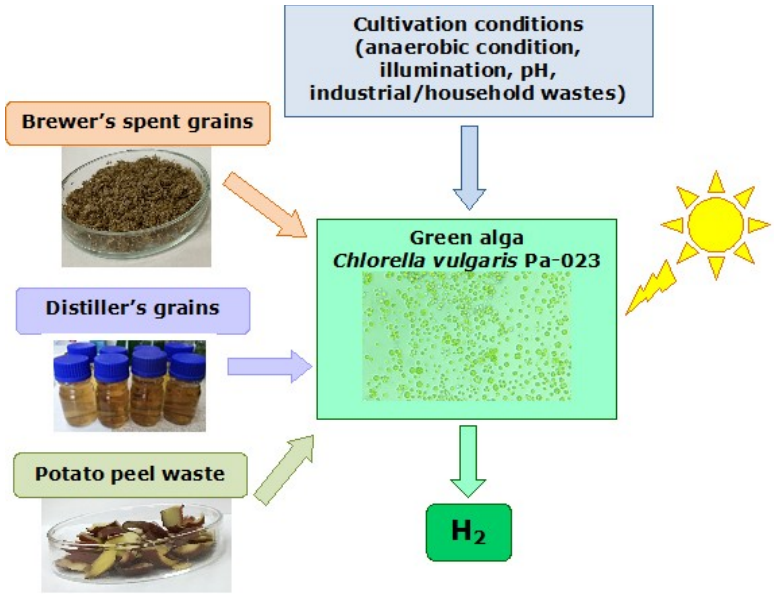

Figure 1: Schematic illustration of H_2 photoproduction by *C. vulgaris* Pa-023 cultivated on brewer's spent grains, distiller's grains and potato peel waste.

Acknowledgements
This work was supported by the Higher Education and Science Committee of Armenia, in the frames of the research project 25RG-1F098 (to L.G.).

References

[1] L. Hakobyan, L. Gabrielyan. Phototrophic microorganisms as the future of green biotechnology. In: Microbial essentialism: An industrial perspective. Singh et al. (eds.). Elsevier: Academic Press, 2024, 181-205, ISBN: 978-0-443-13932-1.

[2] PC. Hallenbeck, LC. Zampol, E. Sagir. Photosynthesis and hydrogen from photosynthetic microorganisms. In: Microalgal Hydrogen Production. Seibert, Torzillo (eds.). R. Soc. Chem., 2018, 1-30, ISBN: 978-1849736725.
[3] EV. Petrova, GP. Kukarshikh, TE. Krendeleva, TK. Antal. The mechanisms and role of photosynthetic hydrogen formation by green microalgae. Microbiol 89, 2020, 259–275.
[4] O. Awogbemi, DVV. Kallon, AO. Owoputi. Biofuel generation from potato peel waste: current state and prospects. Recycling 7, 2022, 23.
[5] J. Manoyan, L. Hakobyan, T. Samovich, N. Kozel, N. Sahakyan, H. Muravitskaya, V. Demidchik, L. Gabrielyan. Comparison of sulfur and nitrogen deprivation effects on photosynthetic pigments, polyphenols, photosystems activity and H_2 generation in *Chlorella vulgaris* and *Parachlorella kessleri.* Int. J. Hydrogen Energy 59, 2024, 408-418.

Development and Validation of a Simplified Kinetic Model for Ni-Ru/CeO_2 Catalysts in Low-Temperature Steam Methane Reforming and as a Basis for Integrated Power-to-Gas Systems

M. Musone[1], F. Migliardini[1], A. Basco[1], A. Di Nardo[1], and G. Landi[1]
[1] *CNR-STEMS, Naples, Italy*
gianluca.landi@stems.cnr.it

Nickel-based catalysts represent the industrial standard for steam methane reforming (SMR) due to their favorable balance of activity, selectivity, and cost-effectiveness. Nevertheless, pure Ni catalysts often suffer from rapid deactivation and limited low-temperature activity [1–3]. To overcome these limitations, bimetallic catalysts incorporating noble metals supported on cerium oxide (CeO_2) have attracted significant attention. In a recent study by Sorbino et al. [4], Ni–Ru/CeO_2 catalysts (7 wt% Ni, 1 wt% Ru) were synthesized by wet impregnation and evaluated under low-temperature SMR conditions (<600 °C). The formulation exhibited high methane conversion, hydrogen yield, and stability, with CeO_2 providing oxygen storage capacity and Ru enhancing activity via Ni site modification and cooperative H_2O/CH_4 activation on dual nanoparticles—ideal for 450-600 °C operation with membrane reactors.

Beyond hydrogen production, such catalytic systems are also highly relevant for Power-to-Gas (PtG) applications, where the efficient conversion of renewable hydrogen into synthetic methane, through CO_2 methanation, is a key enabling technology. Hydrogen, the primary energy carrier in PtG schemes, faces challenges in storage, transport, and large-scale integration [5, 6]. Methanation provides a viable alternative by increasing energy density and ensuring compatibility with existing gas grid infrastructures [7, 8].

In this context, the development of a simplified kinetic model capable of accurately describing both low-temperature SMR and CO_2 methanation represents a valuable tool for improving the understanding and predictive capability of these catalytic systems; although SMR is not directly part of PtG schemes, its combined investigation with CO_2 methanation enables the formulation of a unified kinetic model capable of describing chemically opposite conversion pathways between CH_4 and H_2 over similar catalytic systems, with direct relevance for future PtG applications.

Experimental studies were performed in a Micromeritics FR-100 fixed-bed reactor under kinetically controlled conditions (400–550 °C, 2–5 bar). Contact times were chosen to avoid thermodynamic equilibrium, enabling intrinsic kinetic measurements. SMR and WGS reactions were investigated independently by varying feed composition, temperature, and pressure. Additional DoE campaigns expanded the dataset and systematically evaluated the impact of key operating parameters.

Consistent trends were observed, as shown in Figure 1, with SMR conversion increasing with temperature and decreasing with pressure, while WGS conversion was enhanced at higher pressures.

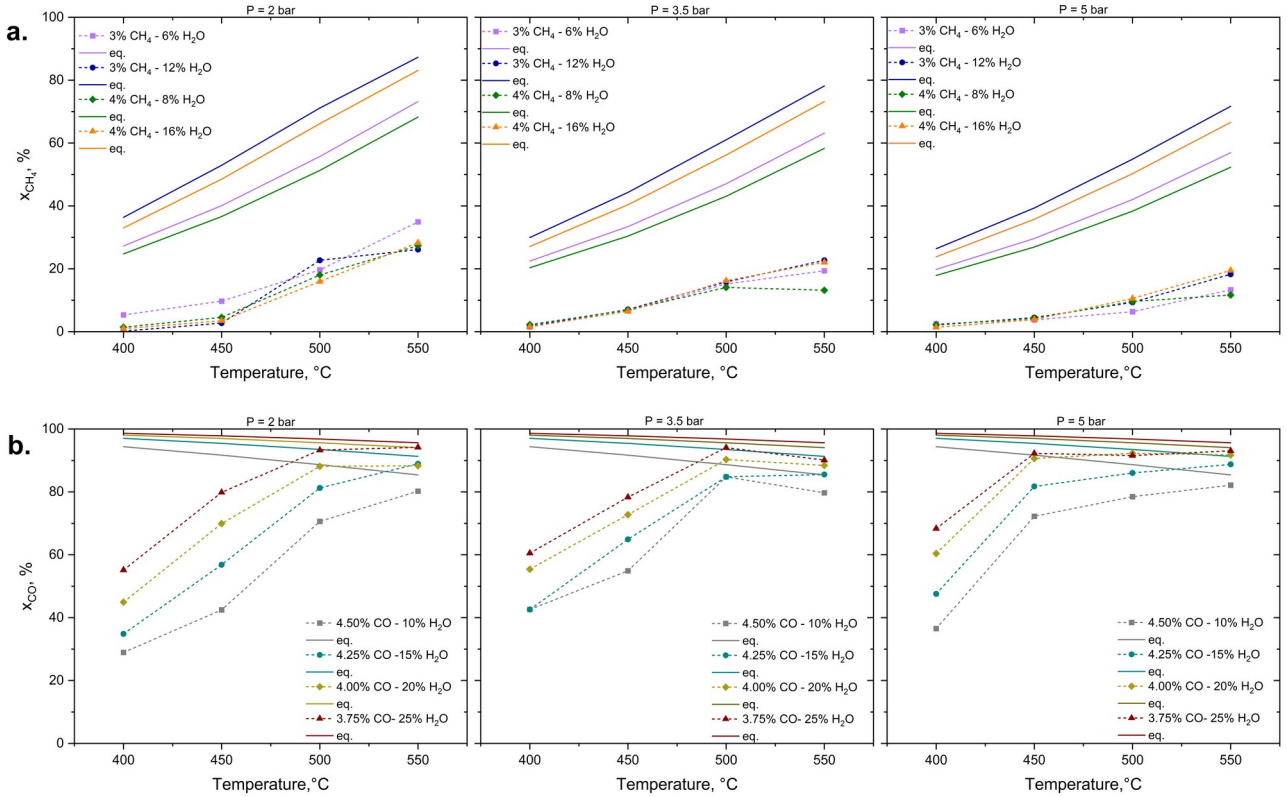

Figure 1: Conversion trends for (a.) SMR and (b.) WGS as a function of temperature and pressure.

As illustrated in Figure 2, the presence of CO_2 in the feed showed a negligible effect on methane conversion, supporting its exclusion from adsorption terms, in agreement with literature results [9].

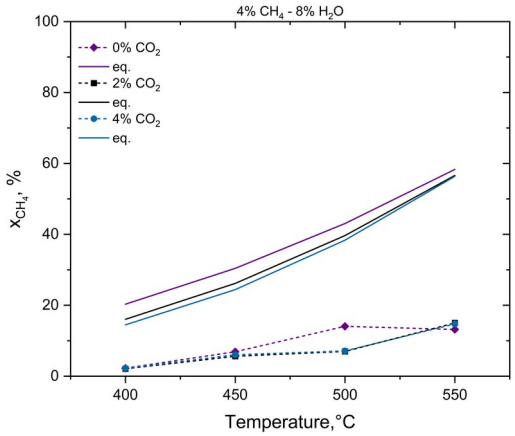

Figure 2: Effect of CO_2 partial pressure in the feed on methane conversion during SMR.

Three Langmuir–Hinshelwood–Hougen–Watson (LHHW) kinetic expressions for the WGS reaction were evaluated using optimisation routines implemented in MATLAB. The models differed in their description of hydrogen adsorption and desorption mechanisms. Results indicate that formulations based on molecular hydrogen desorption provide the best agreement with the experimental data, whereas the model assuming dissociative hydrogen desorption does not adequately reproduce the observed trends. The resulting SMR–WGS kinetic framework was implemented for subsequent model validation, reactor simulations, and system-level modelling of intensified hydrogen production and integrated Power-to-Gas configurations. Results showed a good fit to experimental results, thus suggesting a good prediction of SMR and CO_2 methanation by implementing the proposed kinetics in modelling applications.

Acknowledgements
This work was carried out within the PNRR project "Hydrogen Research and Development", funded by the European Union – NextGenerationEU.

References

[1] E. Meloni, M. Martino, V. Palma, "A short review on Ni based catalysts and related engineering issues for methane steam reforming", Catalysts, 10, 2020, 352.
[2] S.D. Angeli, G. Monteleone, A. Giaconia, A.A. Lemonidou, "State-of-the-art catalysts for CH4 steam reforming at low temperature", International Journal of Hydrogen Energy, 39, 2014, 1979–1997.
[3] J.O. Ighalo, P.B. Amama, "Recent advances in the catalysis of steam reforming of methane (SRM)", International Journal of Hydrogen Energy, 51, 2024, 688–700.
[4] G. Sorbino, A. Di Benedetto, C. Italiano, M. Thomas, A. Vita, G. Ruoppolo et al., "Novel Ni–Ru/CeO2 catalysts for low-temperature steam reforming of methane", International Journal of Hydrogen Energy, 137, 2025, 961–975.
[5] P. Deiana, L. Colelli, C. Bassano, Y. De Pra, G. Testa, N. Verdone et al., "Power-to-gas pilot plant for CO2 methanation with a Ni-based catalyst", Industrial & Engineering Chemistry Research, 64, 2025, 3886–3901.
[6] J.J. Ríos, J. Ancheyta, A. Mantilla, A. Elyshev, A. Zagoruiko, "Enhancing the prediction capability of a literature COx methanation kinetic model", Fuel, 410, 2026, 137834.
[7] L. Colelli, C. Bassano, N. Verdone, V. Segneri, G. Vilardi, "Power-to-gas: process analysis and control strategies for dynamic catalytic methanation systems", Energy Conversion and Management, 305, 2024, 118257.
[8] S.H. Wai, Y. Ota, K. Nishioka, "Performance analysis of Sabatier reaction on direct hydrogen inlet rates based on solar-to-gas conversion systems", International Journal of Hydrogen Energy, 46, 2021, 26801–26808.
[9] C. D. Don-Pedro, R. R. Ratnakar, S. Chenna, V. Balakotaiah, "Comprehensive thermodynamic analysis and simulation of electrified modular reactors for bi-reforming of methane", Chem Eng Sci, 306, 2025, 121229

Upgrading of biomass to fuels and green Carbon as Reductant for Metallurgy

M. Ahlhaus
Hochschule Stralsund University of Applied Sciences, Stralsund, Germany
matthias.ahlhaus@hochschule-stralsund.de

Nature is producing biomass via photosynthesis as the basis of life by providing organic compounds containing carbon, hydrogen and oxygen as well as stored sun energy. That biomass can further be upgraded to fuels and chemicals in a wide range from hydrogen over carbohydrates or oxygenates to carbon.
Conversion of biomass needs processing by two main chemical routes:

I. **Biochemical** conversion of wet and green biomass via fermentation to produce ethanol or biogas that can be further upgraded to biomethane.
II. **Thermochemical** conversion of lignocellulosic biomass under high temperature via
    1. Pyrolysis without additional reactants to produce solid charcoal as well as combustible gases and condensable biocrude oil that needs further upgrading.
    2. Gasification with substoichiometric air forming producer gas as a mixture of carbon-containing gases like CO_2, CO, CH_4 as well as Bio-H_2. The gas composition can offer the quality of synthesis-gas for further production of carbonaceous bio-fuels and chemicals by
    methanation to synthetic bio-SNG (=CH_4) or by
    liquefaction via Fischer-Tropsch-synthesis to advanced biofuels as well as alcohol and oxygenates.

Complementary to bio-H_2 and bio-fuels the bio-carbon becomes even more important:
For the green energy sector bio-CO_2 as the green carbon-source is inevitable for further upgrading of electrolytic hydrogen e-H_2 from other renewable energies to synthetic green e-fuels.
But besides the energy sector there are multiple emerging opportunities and markets for bio-carbon in the green chemical sector as

- gaseous bio-CO_2 for synthesis of e-chemicals together with electrolytic e-H2 and for
- solid bio-coal (or bio-char, activated carbon, green coal /coke) as a reductant for ore in metallurgical processes and steel industry.

In cooperation with steel industry different bio-coals produced from various bioresources in industrial as well as in demonstration plants under a wide range of pyrolytic conditions have been collected.
These bio-coals have been analysed at Stralsund University of Applied Sciences (HOST) in order to compare their suitability as reductant for metallurgy.
Ash and fixed carbon C_{fix} remain solid during thermo-gravimetric analysis (TGA; figure 1) after high temperature treatment up to 700°C (definition of tau=1) and further up to 900°C under inert atmosphere before oxidation with air follows at tau=4.5.

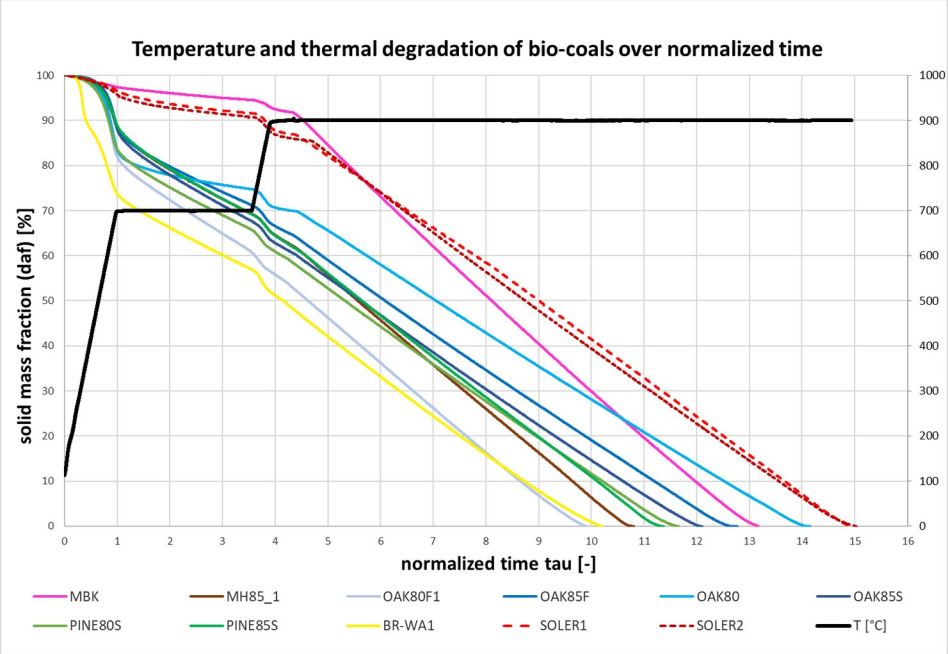

Figure 1: Temperature and thermal degradation of bio-coals over normalized time during Thermo-Gravimetric Analysis (TGA)

High temperature during pyrolysis is the main reason of splitting volatile matter from the solid bio-coals; the remaining solid bio-char contains ash and high yields of fixed carbon.
The analytic results of the bio-coals show a spread of ash-contents from more than 7% to values lower than 1% on the dry basis (figure 2). These remarkable differences of ash content in the bio-coals result from unequal content of mineral matter in the basic bio material and is collateral affected by different pyrolytic conditions during thermo-chemical production of the bio-coals.

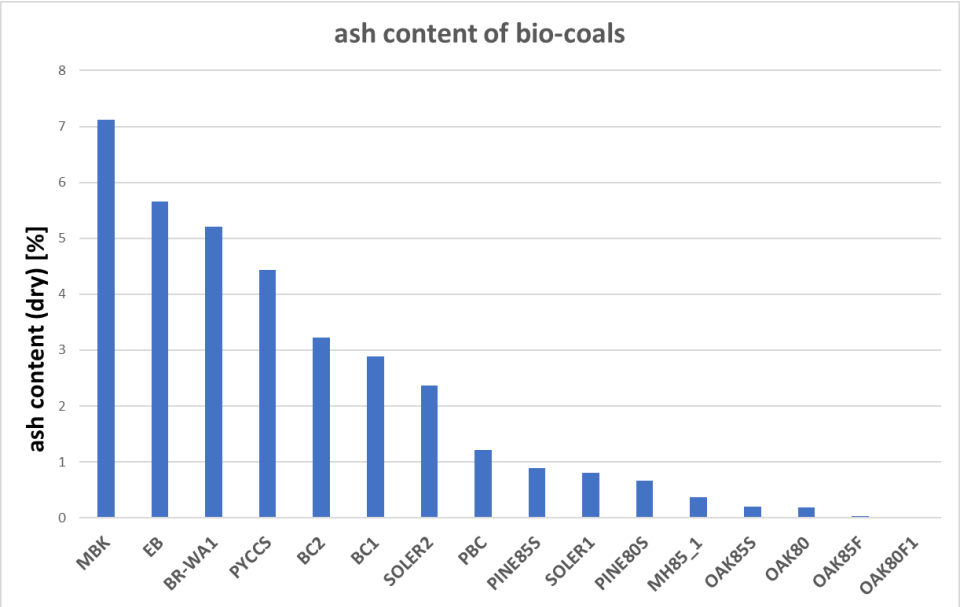

Figure 2: Ash content (dry basis) of bio-coals

But the ash content is of minor significance for final use of these bio-coals in metallurgy. More important for metallurgical processes is the content of fixed carbon as the chemical element that is reducing the ore to metals.

During TGA the splitting of solid Bio-coal and subsequent formation of volatile matter is increased with higher temperature and results in reducing the yield of remaining fixed carbon. TGA of bio-coals show contents of Fixed Carbon (figure 3) in a wide range between 54% and 91%(dry basis) at 700°C; these yields are diminished to values between 45% and 85% by intensification of thermal decomposition of the remaining solid compounds by temperatures up to 900°.

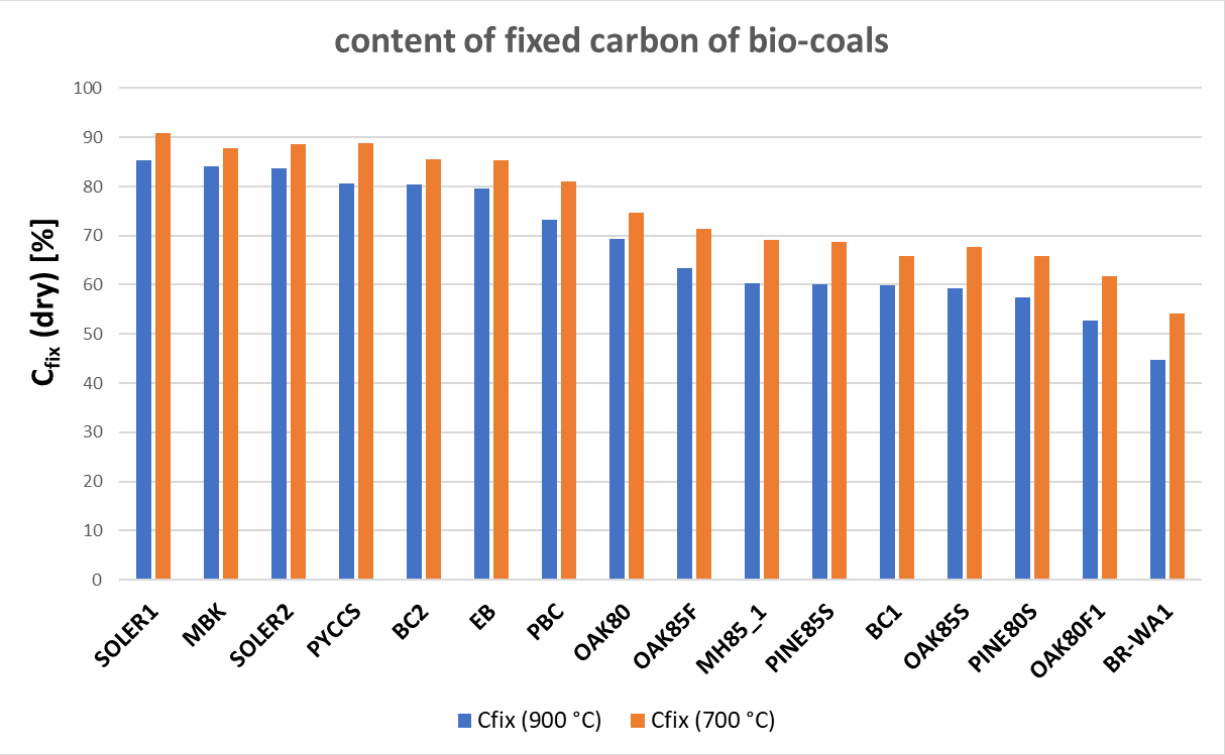

Figure 3: Content of fixed carbon (dry basis) in different bio-coals

Preliminary analyses of bio-coals produced from various origin biomass under different pyrolytic conditions show a wide range of ash content and fixed carbon. Further ongoing research is focused on mechanical quality characteristics of pellets from these bio-coals and examination of their chemical reactivity as a reducing agent for metallurgy.

Decarbonizing propylene production: high selectivity and low energy consumption using Joule-heated PtSn-based structured catalysts

***O. Muccioli*[1,2], C. Maffei[1], C. Ruocco[1], E. Meloni[1], V. Palma[1]**
[1] *University of Salerno, Fisciano, Italy*
[2] *'La Sapienza' University of Rome, Rome, Italy*
omuccioli@unisa.it

To address the limited propylene selectivity, the rapid deactivation of the catalyst, and the high energy demand challenges of the propane dehydrogenation (PDH) reaction, this study explores the electrification of the process via Joule heating. Traditional PDH reactors rely on an external heating mode, typically through fossil fuel combustion, to achieve the required temperatures in the catalyst. It results in an inefficient radial thermal gradient with hotter regions near the reactor wall that further promote the homogeneous side reactions [1]. In this work, Pt-Sn/MgAlO catalytic formulation was deposited over SiSiC periodic open cell structures (POCS), simultaneously acting as resistive heating elements. The structured catalysts were electrified through ring-shaped nickel-plated copper connections, and tested for the PDH reaction under both conventional external heating and Joule heating modes. The axial thermal profile was recorded by using K-type thermocouples inserted into a quartz tube, which was placed inside a channel excavated along the axial direction of the catalyst. This configuration enabled temperature measurements at the inlet, middle, and outlet of the monolith while electrically insulating the sensors. The electrified reactor configuration reverses the heat flux direction, providing the heat rapidly and selectively to the catalyst. This enables rapid and uniform heating of the catalyst while maintaining lower the reactor wall temperature, thereby suppressing undesired gas-phase reactions and mitigating coke formation [2]. As a result (Fig. 1), enhanced propylene selectivity was achieved (>99% at 570 °C). Despite of the comparable propane conversion values, the electrified catalytic system assured higher propylene selectivity with respect to the conventional one, in the whole temperature range investigated, confirming the beneficial effect of the innovative heating method.
Furthermore, the catalytic system was tested under severe reaction conditions (80 vol% C_3H_8 in He) in a compact purpose-designed steel reactor integrated with a power supply unit (Fig. 1). This setup overcomes the limitations of traditional laboratory quartz reactors, representing a significant advancement in the study of the electrified catalytic processes.
The energy analysis was also conducted, evaluating the electrical power consumption and the overall energy efficiency. Although the Joule-heated PDH are not experimentally explored in the current literature, existing research, including our previous work [2], has highlighted the advantages of microwaves electrification. Nevertheless, the low intrinsic efficiency of magnetrons undermines the energy competitiveness of the microwaves as electrified

heating method. In contrast, the results of this study confirmed that Joule heating provides more efficient alternative, even employing the same catalytic system under the same reaction conditions (from 20% to 48% energy efficiency).
Following these findings, the electrified catalyst was scaled up implementing a dual-foam system in series within the same reactor. This configuration allowed to achieve a reduction of the specific energy consumption and an improvement of the energy efficiency.

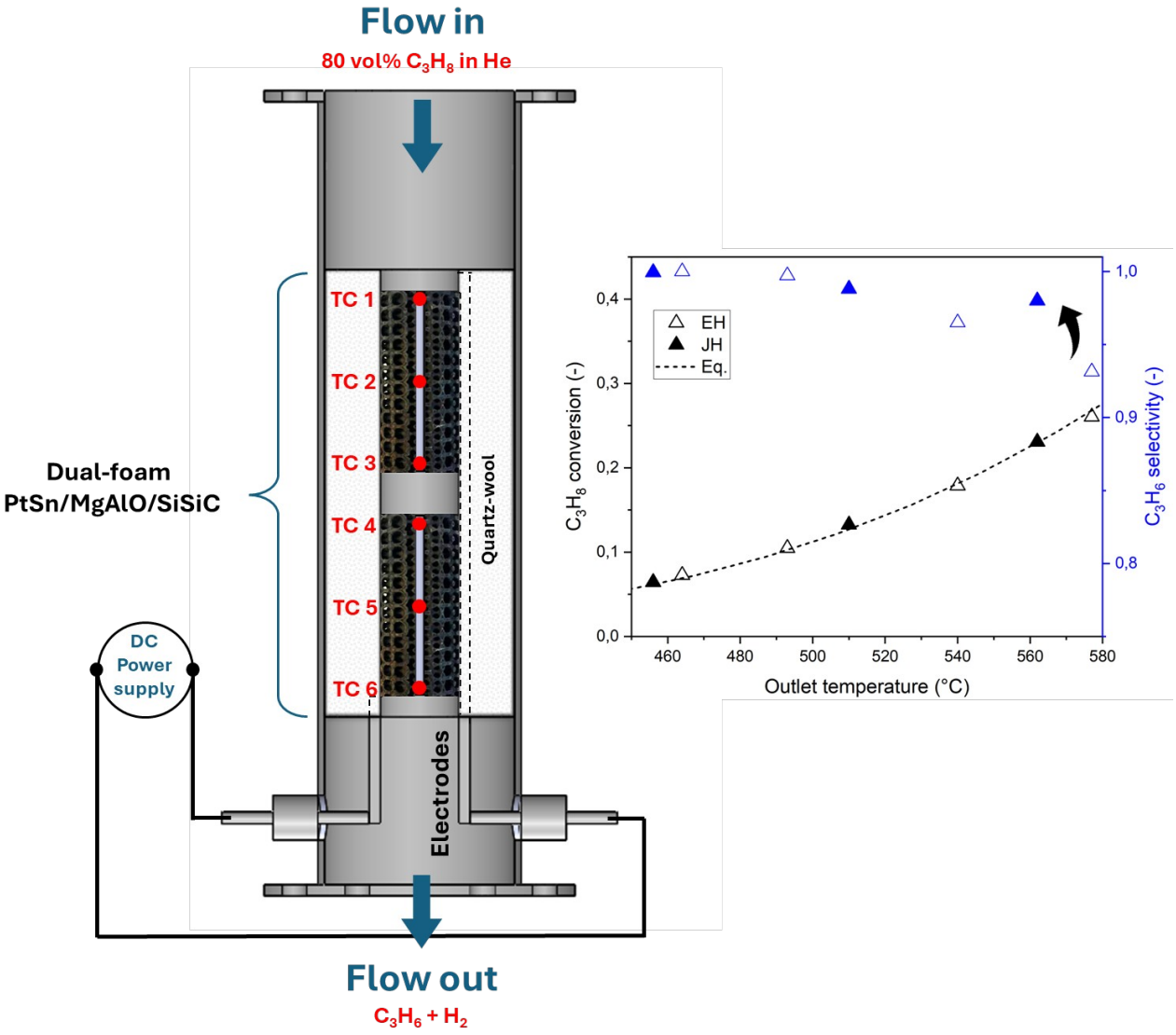

Figure 1: Scheme of the Joule-heated dual-foam catalytic reactor (on the left); results of the PDH activity tests in with both Joule and traditional external heating in terms of C_3H_8 conversion and C_3H_6 selectivity (7 h^{-1} WHSV, 80 vol% C_3H_8 in He, 1 atm)

References

[1] A. Ramirez, J. L. Hueso, R. Mallada, and J. Santamaria, "MW-activated structured reactors to maximize propylene selectivity in the oxidative dehydrogenation of propane," Chemical Engineering Journal, vol. 393, Aug. 2020.
[2] O. Muccioli, E. Meloni and V. Palma, "Microwave-susceptible structured catalysts for highly selective dehydrogenation of propane to propylene", Chemical Engineering Journal, 2025, 520, 166082.
[3] Y. Kwak, C. Wang, C. A. Kavale, K. Yu, E. Selvam, R. Mallada,J. Santamaria, I. Julian, J. M. Catala-Civera, H. Goyal, W. Zheng,D. G. Vlachos, "Microwave-assisted, performance-advantaged
electrification of propane dehydrogenation", Science advances, 2023, 9,eadi8219.

Design and testing of single-chamber air-cathode Microbial Fuel Cells Fed with Organic Residues

A. Cappiello[1,2], S. Di Micco[1,2], R. Nastro [1], M. Minutillo[2,3]
[1] *Department of Engineering, University of Naples "Parthenope", Naples, Italy*
[2] *Atena SCARL, Naples, Italy*
[3] *Department of Industrial Engineering, University of Salerno, Fisciano, Italy*
aniello.cappiello001@studenti.unipathenope.it

Driven by the transition toward sustainable energy and circular economy, this study explores Microbial Fuel Cells (MFCs) as a dual solution for waste valorization and energy recovery. By leveraging microbial metabolism to convert organic matter directly into electricity, this research specifically focuses on the performance of MFCs using real organic substrates [1-2].
The study illustrates a standardized methodology to test and analyze the behavior of single-chamber air-cathode MFCs that use fennel, celery, and olive pomace as substrates. This framework, covering reactor design and building, electrode preparation, and biofilm development, aims to assure the reproducibility and flexibility in experimental activities, in order to optimize system operating conditions and, as a consequence, the performance.
The reactors (154 mL working volume) were designed using CAD with a parallelepiped external structure and a cylindrical internal chamber. Moreover, they were fabricated via Fused Deposition Modeling (FDM) using Polylactic acid (PLA), a material selected for its sustainability and biocompatibility. This additive manufacturing approach ensured rapid prototyping and high geometric repeatability across all units [3].

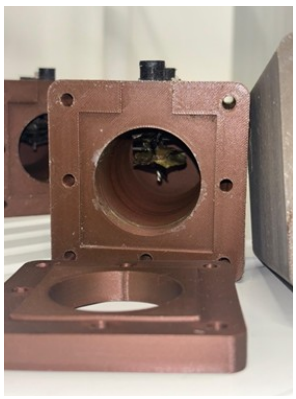

Figure 1: 3D-printed single-chamber MFC reactor with installed anode.

Each reactor was equipped with a carbon fiber brush anode and an air-breathing activated carbon cathode. The anodic electrode, characterized by high porosity and large specific surface area, was selected to promote biofilm adhesion and electron transfer. The cathode consists of activated carbon coated with polytetrafluoroethylene (PTFE) and coupled with a nickel mesh acting as current collector [4].

Electrodes were positioned facing each other within the reactor to limit internal resistance while preserving adequate substrate distribution and mass transfer.
The anodic biofilm was developed using endogenous bacterial communities extracted from compost, including microorganisms belonging to the Bacillus, Geobacillus, and Brevibacillus genera. Prior to inoculation, anodes were chemically pretreated in a 0.5 M hydrochloric acid solution to enhance surface properties.
Biofilm incubation was carried out in a mineral medium with sodium acetate under controlled anodic polarization. After assembly, the reactors were conditioned to stabilize electrochemical behavior. Fennel, celery, and olive pomace were prepared as substrates at different concentrations, as reported in Table 1.

Table 1: Substrates prepared for experimental activities

Organic Substance	**Substrate Composition**
Fennel 1	50 %wt Fennel – 50%wt Mineral Solution [5]
Fennel 2	
Fennel 3	70 %wt Fennel – 30 %wt Mineral Solution [5]
Olive Pomace 1	30 %wt Olive Pomace – 70 %wt Mineral Solution [5]
Olive Pomace 2	
Cellery 1	50 %wt Cellery – 50%wt Mineral Solution [5]
Cellery 2	
Cellery 3	70 %wt Cellery – 30 %wt Mineral Solution [5]

During the experimental testing pH was checked in order to maintain it within the optimal range for microbial activity (6.5–7.5).
Electrochemical testing activities were performed using a multichannel biopotentiostat, Corrtest Instruments CS310X, allowing parallel operation and monitoring of multiple MFC reactors (figure 2).
The experimental protocol includes open-circuit potential monitoring and polarization curve acquisition through staircase voltammetry.
The definition of a standardized testing procedure represents a key outcome of the present research activities, providing a consistent basis for subsequent performance analysis and comparison among different substrate configurations [6-7].
These activities aim to establish a controlled and reproducible experimental framework for MFCs operating with real organic residues.
The combined use of additive manufacturing, systematic biofilm development, and standardized electrochemical protocols provides the basis for future quantitative performance evaluation, substrate comparison, and scalability assessment in renewable and hybrid energy applications.

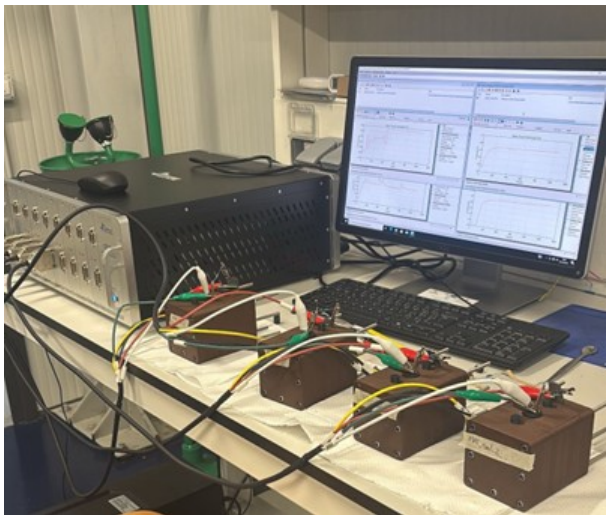

Figure 2: *Experimental setup for electrochemical testing with multichannel biopotentiostat.*

Aknowledgments

This work was supported by the AGRITECH National Research Centre for Agricultural Technologies, funded by the Italian Ministry of University and Research (MUR) under the Next Generation EU – PNRR Mission 4, Component 2 programme. The authors acknowledge the contribution of all partners involved in the AGRITECH project.

References

[1] Minutillo, M., Di Micco, S., Di Giorgio, P., Erme, G., Jannelli, E., Investigating air-cathode microbial fuel cells performance under different serially and parallelly connected configurations, Energies, 2021;14(16): 5116.
[2] Ahn, Y.; Logan, B.E. A multi-electrode continuous flow microbial fuel cell with separator electrode assembly design. Appl. Microbiol. Biotechnol. 2012, 93, 2241–2248.
[3] Ford, S.; Despeisse, M. Additive manufacturing and sustainability: An exploratory study of the advantages and challenges. J. Clean. Prod. 2016, 137, 1573–1587.
[4] Minutillo, M.; Nastro, R.A.; Di Micco, S.; Jannelli, E.; Cioffi, R.; Di Giuseppe, M. Performance assessment of multi-electrodes reactors for scaling-up microbial fuel cells. E3S Web Conf. 2020, 197, 08020.
[5] Logan, B.; Cheng, S.; Watson, V.; Estadt, G. Graphite fiber brush anodes for increased power production in air-cathode microbial fuel cells. Environ. Sci. Technol. 2007, 41, 3341–3346.
[6] Corrtest Instruments Multichannel potentiostat (8-CH,EIS*1)CS310X(Opt.C), online: https://www.corrtest.com.cn/en/ - Accessed 19/12/2025.

Pilot-Scale Demonstration of Green Hydrogen Production via 25 kW SOEC System

***M. Minutillo*[1], *G. D'Andrea*[2], E. Jannelli[2], M. Della Pietra[3]**
[1] *Department of Industrial Engineering, University of Salerno, Fisciano, Italy*
[2] *Department of Engineering, University of Naples "Parthenope", Naples, Italy*
[3] ENEA, Italian National Agency for New Technologies, Energy and Sustainable Economic Development, Casaccia Research Centre, Rome, Italy
gianpaolo.dandrea001@studenti.uniparthenope.it

In recent years, the growing focus on decarbonization has positioned green hydrogen as a strategic energy vector for a sustainable future. Solid Oxide Electrolyzer Cells (SOECs) represent an advanced technology for hydrogen production, due to their high electrical efficiency and potential for reducing operational costs, making them particularly promising for large-scale applications. To demonstrate the potential of SOECs in sustainable hydrogen production, the PROMETEO project aims to develop a pilot plant for green hydrogen generation based on a 25 kW SOEC, integrated with photovoltaic (PV) and concentrated solar thermal (CST) systems. The system was implemented by integrating commercially available components, selected through a careful analysis based on technical performance and cost-effectiveness, with particular attention to component compatibility and compliance with operational and safety requirements.
The Balance of Plant (BoP), schematically shown in Figure 1, is distributed across two 10-foot skids, divided into a hot section and a cold section.

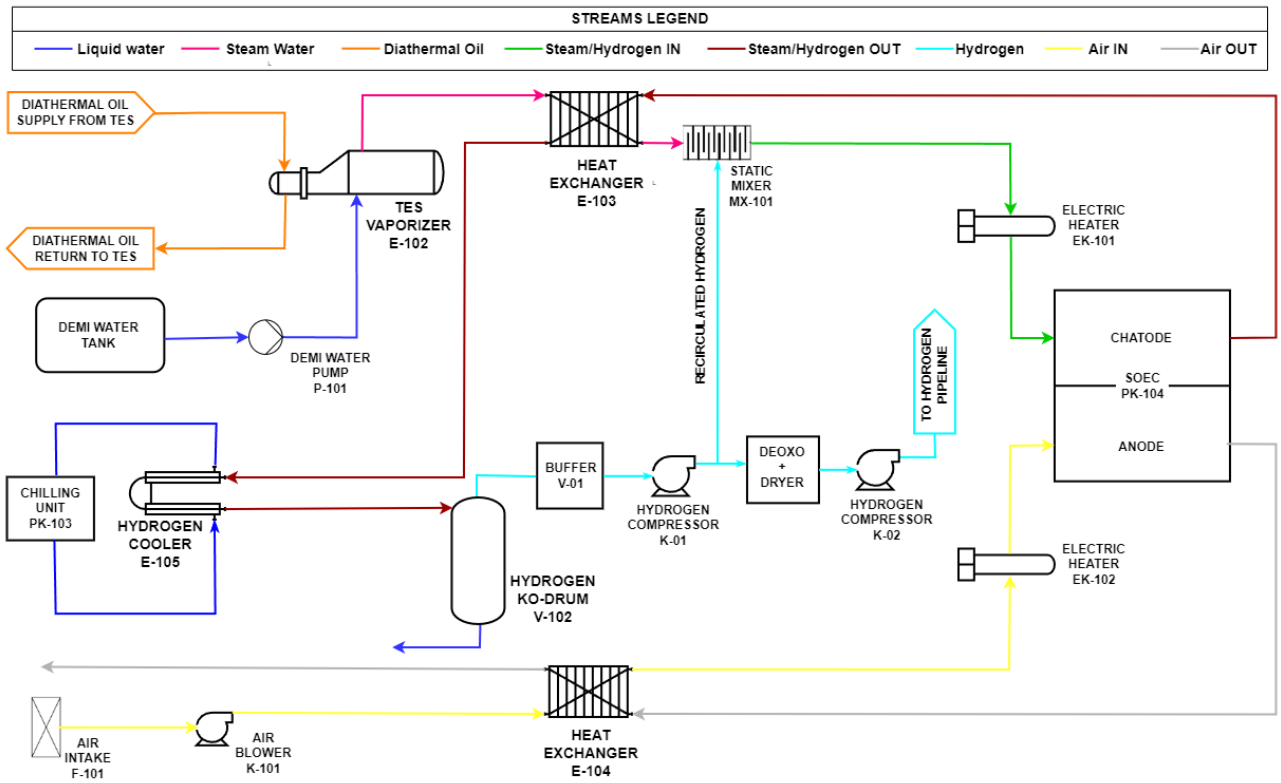

Figure 1. BoP PROMETEO

From a process perspective, the system can be described by distinguishing between the anodic and cathodic lines.
The anodic line handles the process air via an air blower and an air-to-air heat exchanger, which recovers thermal energy from the hot anodic exhaust gases to preheat the incoming airflow. This heat exchanger (Figure 2a) allows the recovery of approximately 4.5 kW of thermal power, significantly improving the overall system efficiency. Downstream, an electric heater (about 1.5 kW under nominal steady-state conditions) raises the air temperature to 733 °C before entering the stack. Particular attention was given to the design of the air line and the selection of high-temperature-resistant materials, in order to prevent critical conditions related to chromium release at elevated temperatures.
The cathodic line integrates the TES vaporizer, designed to vaporize the feed water using thermal energy supplied by the concentrated solar tower (CST) heat transfer oil [1]. To ensure continuous operation even in the absence of solar irradiation, the vaporizer is equipped with an additional 5.5 kW electric heater. The produced steam is mixed with hydrogen at 10 mol % in a static mixer and subsequently preheated in a second heat exchanger (Figure 2b), which recovers approximately 2.3 kW from the cathodic exhaust gases. A final electric heater (about 1.2 kW under nominal steady-state conditions) ensures the required inlet temperature (733 °C) to the stack. The produced hydrogen is then cooled with chilled water (from 198 °C to 11 °C) in a dedicated heat exchanger (Figure 2c), purified via a knock-out drum, and finally routed to storage.
All process lines were designed using materials selected to ensure high-temperature compatibility, chemical compatibility, and adherence to pressure specifications defined during the design phase.


a)


b)


c)

Figure 2 heat exchangers:
a) E-104 air to air b) E-103 steam to steam/H2 c) E-105 Hydrogen cooler

Table 1 reports the main operating conditions of the heat exchangers used in the process, indicating the inlet and outlet flows on both the hot and cold sides, their corresponding temperatures, and the calculated heat duty for each unit. The data include both heating and partial vaporization, where applicable.

Table 1 Heat duty and operating conditions of heat exchangers.

TAG	SERVICE	COLD SIDE			HOT SIDE			Heat Duty [kW]
		Stream	T In [°C]	T Out [°C]	Stream	T In [°C]	T Out [°C]	
E-102	TES VAPORIZER	Demi Water	20	125	Diathermal Oil	200	182.5	6.3
E-103	CATHODE FEED EFFLUENT HEAT EXCHANGER	Steam/H2 in	125	656	Steam/H2 out	715	198	2.3
E-104	ANODE FEED EFFLUENT HEAT EXCHANGER	Air in	125	577	Air out	715	540	4.5
E-105	HYDROGEN COOLER	Cooled water	5	12	Steam/H2 out	198	11	2.8

A key aspect is the control system, which is based on three pillars: hierarchical architecture, state machine, and control loops.
Operational control is separated from safety control: a non-safety PLC (NSR) manages the state machine and the loops, while a safety PLC (SR) or dedicated hardware loops intervene in the event of faults or hazards. The plant operates in states such as Off, Ready, Hot Standby, Night Mode, Partial Load, and Full Load—modes identified and tested in experimental campaigns by E. Crespi et al. [2] and in the modeling analysis by Minutillo et al. [3]. Alarms, ranging from Level 1 to 4, trigger actions from warnings to emergency shutdown (ESD). Eleven loops control flow rates, temperatures, and pressures. The main loop (CL1) uses voltage-based logic to optimize stack efficiency, adjusting hydrogen production via steam flow or temperature. Other loops manage steam flow (CL2), evaporator pressure (CL3), air/hydrogen flows (CL5, CL6), and cathode/anode temperatures (CL7, CL8).
The PROMETEO plant is designed to achieve a hydrogen production rate exceeding 15 kg/h, with a specific system energy consumption below 40 kWh per kilogram of hydrogen produced.

Acknowledgements

This project has received funding from the Fuel Cells and Hydrogen 2 Joint Undertaking (now Clean Hydrogen Partnership) under Grant Agreement No 101007194. This Joint Undertaking receives support from the European Union's Horizon 2020 Research and Innovation program, Hydrogen Europe and Hydrogen Europe Research.

References

[1] Barreto, G., Romero, M., González-Aguilar, J., Giaconia, A., & Testi, M. (2025). Design point, part load and annual performance analysis of a 100 kW SOEC system integrating a solar steamer under electrolyser operational constraints. *Renewable Energy*, 124340.
[2] Crespi, E., Ragaglia, D., Panaccione, F., & Testi, M. (2023, June). Control of a Solid Oxide Electrolysis system for hydrogen generation from solar power and thermal energy storage. In *2023 International Conference on Clean Electrical Power (ICCEP)* (pp. 765-774). IEEE.
[3] Minutillo, M., Jannelli, E., Giaconia, A., Altomonte, A., & D'Andrea, G. (2025). *High-Efficiency SOEC System Coupled with Renewable Sources: Modeling and Energy Analysis at Operating modes variation* [Poster presentation]. European Fuel Cells and Hydrogen PIERO LUNGHI CONFERENCE.

Mechanical and thermal measurements towards the development of additive manufactured products with tailored structural/functional properties

***I. Papallo*[1], G. de Alteriis[1], R. Schiano Lo Moriello[1]**
[1] *Department of Industrial Engineering, University of Naples Federico II, Naples, Italy*

ida.papallo@unina.it

The increasing applications of Additive Manufacturing (AM) technologies in industrial production have currently led to product reimagination from a new standpoint. AM techniques enable the creation of complex shapes, thus improving the performance of critical components in several fields (i.e., from aerospace and automotive to biomedical applications) [1-4].

It is frequently stressed how the relationship among the process parameters, microstructure and mechanical properties may result crucial in different areas, also involving novel and conventional fabrication techniques [1-4]. As reported in the literature, several cellular structures were already analysed in order to obtain a wide range of functional and mechanical properties. Over the past years, many researchers have already focused on the mechanical performance of diamond, body-centered-cubic and octet-truss lattice. In this context, several kinds of porous and semi-porous devices were also proposed and suitably investigated [1].

In the product development process, the first step should be to perform a critical analysis of commercially available devices and related fabrication processes. The mechanical and functional requirements should be properly identified to re-define design as well as manufacturing guidelines for the development of next generation components [2]. Further technical considerations should be made on the role of advanced measurement methods and design strategies supporting the ideation process through the development of technical alternatives according to the structural and functional criteria [2]. The role of the mechanical and thermal measurements towards smart design for AM of innovative products with tailored properties was stressed, also focusing on technical features and differences in terms of solutions for the given design problem. The mechanical and thermal measurements supported the creative design methods, demonstrating the process efficiency and real effectiveness.

Acknowledgments
The research was also partially carried out in the framework of the INVITALIA R&D&I Project NEMESI "New Engineering & Manufacturing Enhanced System Innovation", CUP C67G22000420008.

References

[1] I. Papallo, A. Gloria, M. Martorelli, "Design of Additive Manufactured Devices with Tailored Properties: Tackling Biomedical Challenges", Lecture Notes in Mechanical Engineering 2024, https://doi.org/10.1007/978-3-031-52075-4_10.
[2] I. Papallo, M. Martorelli, F. Lamonaca, A. Gloria, "Generative design and insights in strategies for the development of innovative products with tailored mechanical and/or functional properties", Acta IMEKO, 12(4), 2023. https://doi.org/10.21014/actaimeko.v12i4.1716.
[3] R. De Santis, T. Russo T, J.V. Rau, I. Papallo, M. Martorelli, A. Gloria, "Design of 3D Additively Manufactured Hybrid Structures for Cranioplasty", Materials 2021, 14(1):181. https://doi.org/10.3390/ma1401018.
[4] I. Papallo et al., "Preoperative definition and new concept design of 3D printed buttress model to seal skull base after endoscopic endonasal surgery", Rapid Prototyping Journal 2024, 30(9). https://doi.org/10.1108/RPJ-08-2023-0280.

Cellular automata and metamaterials for the design of advanced smart products

***V. Spinelli*[1], *V. Gallicchio*[1], *R. Di Bernardo*[1], *M. Martorelli*[2], *A. Gloria*[2]**
[1] *CeSMA, University of Naples Federico II, Italy*
[2] *Department of Industrial Engineering, University of Naples Federico II, Naples, Italy*

vincenzo.spinelli@unina.it

Over the past years, the attention has been focused on the design of a new generation of computationally capable intelligent materials, benefiting from multistable metamaterials. Several material properties (e.g., shape reconfigurability, multistability, reprogrammable modulus, programmable stiffness) have been frequently considered for functional flexibility [1].

Currently, the incorporation of computing power into materials may also represent a revolutionary feature which should allow the integration of mechanical properties with information processing.

Accordingly, the attention was focused on the design for additive manufacturing [2-4] and development of advanced, architected materials consisting of a grid of discrete cells which are able to switch between stable states benefiting from local, rule-based interactions, similar to computational cellular automata models [1].

The idea should be to develop materials by means local interaction rules for achieving a global behaviour, however providing information processing, mechanical computation, and shape-morphing capabilities.

Concerning structure and design, the developed metamaterials consisted of a regular grid of unit cells, where each cell may exist in a finite number of stable configurations. The state of each cell can be updated on the basis of its previous state and the states of its neighbouring cells [1].

Such materials may perform several computational tasks, thus highlighting high mechanical intelligence.

The research stressed key applications including several technical features and smart materials/structures with tailored functional properties.

Acknowledgments
The research was partially carried out in the framework of the INVITALIA R&D&I Project NEMESI "New Engineering & Manufacturing Enhanced System Innovation", CUP C67G22000420008. The research was also partially supported by the European Research Executive Agency (REA) project SENS4CORN No 101086364.

References

[1] Z.Liu, H.Fang, J.Xu, K.-W.Wang, "Cellular Automata Inspired Multistable Origami Metamaterials for Mechanical Learning". Adv. Sci.2023, 10, 2305146. https://doi.org/10.1002/advs.202305146.
[2] I. Papallo, A. Gloria, M. Martorelli, "Design of Additive Manufactured Devices with Tailored Properties: Tackling Biomedical Challenges", Lecture Notes in Mechanical Engineering 2024, https://doi.org/10.1007/978-3-031-52075-4_10.
[3] I. Papallo, M. Martorelli, F. Lamonaca, A. Gloria, "Generative design and insights in strategies for the development of innovative products with tailored mechanical and/or functional properties", Acta IMEKO, 12(4), 2023. https://doi.org/10.21014/actaimeko.v12i4.1716.
[4] I. Papallo et al., "Preoperative definition and new concept design of 3D printed buttress model to seal skull base after endoscopic endonasal surgery", Rapid Prototyping Journal 2024, 30(9). https://doi.org/10.1108/RPJ-08-2023-0280.

Generative design for additive manufacturing and a new paradigm for the development of sustainable functional systems

***M. Murolo*[1], *I. Papallo*[1], *V. Gallicchio*[2], *V. Spinelli*[2], *R. Di Bernardo*[2], *M. Martorelli*[1], *A. Gloria*[1]**

[1] *Department of Industrial Engineering, University of Naples Federico II, Naples, Italy*
[2] *CeSMA, University of Naples Federico II, Italy*

miriam.murolo@unina.it

Innovation plays a crucial role for small businesses driving sustainability, growth and competitiveness.
Due to the dynamic feature of today's market, small businesses must be able to continuously adapt and innovate, with the aim of satisfying evolving customer needs, thus staying competitive [1].
In this scenario, generative design for additive manufacturing is an AI-driven, iterative design process that employs algorithms to create lightweight, high-performance, and complex geometries optimized for 3D printing.
By defining parameters like material, load, and constraints, this methodology creates specific shapes and material distribution that reduce mass while enhancing performance and speeding up product development [2].
Such methodological approach is able to complement "free complexity" advantage of additive manufacturing, as generative design enables the development of devices that are generally tailored for layer-by-layer production rather than subtractive methods.
Primary benefits of generative design for additive manufacturing clearly include performance improvement (e.g., enhanced strength-to-weight ratios and functional optimization), rapid development (e.g., significant reduction of the time spent on manual design iterations and simulation), and cost reduction (e.g., material waste reduction and supply chain simplification).
Accordingly, generative design may be considered as a “collaborative partner” for the designer.
It supports designers through the generation of multiple alternatives fitting the predefined criteria [2].
The research highlighted a shift in the designer's role from manually creating products to selecting the most suitable option from a wide range of high-performance solutions generated during the design process.
Innovative, lightweight and sustainable structures with tailored properties were designed spanning from aerospace applications to hydrogen storage systems.

Acknowledgments
The research was partially carried out in the framework of the INVITALIA R&D&I Project NEMESI "New Engineering & Manufacturing Enhanced System Innovation", CUP C67G22000420008. The research was also partially supported by the European Research Executive Agency (REA) project SENS4CORN No 101086364.

References

[1] K. Mirkovski, P. Williams, L. Liu, H. Liu, and M. Indulska, "An AI-Assisted Framework for Improving Innovativeness in Small Businesses: A Human–AI Collaboration Perspective", Information Systems Journal, 35 (6), 1603–1629, 2025. https://doi.org/10.1111/isj.12597.
[2] I. Papallo, M. Martorelli, F. Lamonaca, A. Gloria, "Generative design and insights in strategies for the development of innovative products with tailored mechanical and/or functional properties", Acta IMEKO, 12(4), 2023. https://doi.org/10.21014/actaimeko.v12i4.1716.